PLACE IN RETURN BOX to remove this checkout from your record.
TO AVOID FINES return on or before date due.
MAY BE RECALLED with earlier due date if requested.

DATE DUE	DATE DUE	DATE DUE

MECHANISTIC EVALUATION AND SUBSTRATE SPECIFICITY
ANALYSIS OF A PHENYLALANINE AMINOMUTASE

By

Washington Mutatu

A DISSERTATION

Submitted to
Michigan State University
in partial fulfillment of the requirements for
the degree of

DOCTOR OF PHILISOPHY

Chemistry

2010

ABSTRACT

MECHANISTIC EVALUATION AND SUBSTRATE SPECIFICITY ANALYSIS OF A PHENYLALANINE AMINOMUTASE

By

Washington Mutatu

Phenylalanine aminomutase (PAM) derived from *Taxus* is a multifunctional enzyme that catalyzes the reversible vicinal exchange of the amino group and the pro-(3*S*) hydrogen of various (2*S*)-α-arylalanines to make the corresponding (3*R*)-β-arylalanines, with *trans*-cinnamic acid as a major by-product. A combination of ^{1}H- and ^{2}H-NMR experiments were employed to analyze the stereochemistry at C2 of the β-phenylalanine product catalyzed by PAM. [3,3-^{2}H$_2$]-(2*S*)-α-phenylalanine was incubated with PAM, and the biosynthetically-derived ^{2}H-labeled β-phenylalanine derivatized as the *N*-acetyl methyl ester, revealed deuterium chemical shift values consistent with those of [2,3-^{2}H$_2$]-(2*S*,3*R*)-and (2*R*,3*S*)-β-phenylalanine racemate. Considering that chiral GC-MS analysis confirmed the β-product to be the (3*R*)-enantiomer, and that an earlier study showed that the amino group migrates with retention of configuration at its terminus, the mutase was therefore shown to stereospecifically shuttle the *pro*-(3*S*) hydrogen to C2 with retention of configuration.

The deuterium kinetic isotope effect on V_{max}/K_M is 2.0 ± 0.2, indicating that C$_\beta$-H bond cleavage is rate limiting. The migratory deuterium of [^{2}H$_8$]-(2*S*)-α-phenylalanine was shown to dynamically exchange (up to 70 %) with

protons from the solvent during the isomerization. The equilibrium constant of the enzyme for the natural substrate is 1.1 at 30 °C.

The PAM reaction does not require an external cofactors but involves a post transcriptionally and autocatalytically synthesized 3,5 -dihydro-5-methylidene-$4H$-imidazolone (MIO) moiety which is believed to assist in shuttling the amino group between the α and β positions of the substrate. The presence of the catalytic motif in PAM was confirmed by mutagenesis. Mutants S176A, S176G and S176T were used as blanks against wild-type enzyme in difference UV-visible spectroscopy with monitoring of the signature peak at 308 nm as observed in similar experiments with tyrosine aminomutase that also contain an MIO. The presence of the MIO in PAM was further confirmed by inhibition with cysteine at pH 10.5 under both aerobic and anaerobic conditions. An absorbance peak at 338 nm was observed which is typical of the formation of a cysteine-MIO complex as seen for the ammonia lyases. This absorbance maximum was absent when PAM mutants S176A, G and T were analyzed analogously. The PAM mutants (S176A, G T) converted 4'-nitro- and 4'-flourophenylalanines to their β-isomers. Likely, the MIO, at least in part functions to reduce the pKa of the β-hydrogens to facilitate the removal of the pro-3S hydrogen by a general base within the active site.

When *E. coli* transinfected with a plasmid carrying the *pam* gene is grown under light illumination it has a higher level of endogenously synthesized β phenylalanine compared to non-illuminating conditions.

I dedicate this work to my wife Jane, my daughter Vongaishe, and sons, Trinity, Rangariro, and Farai. I hope they will be inspired to work hard in all their endeavors.

ACKNOWLEDGEMENTS

run the QToff mass spectrometer and analyze the results. Thanks also goes Doug Whitten for carrying out PAM peptide sequencing; the results were useful in confirming phosphorylation of the enzyme. I would also like to acknowledge Dr. Mitch Smith for allowing working in his lab, wherein I acquire skills to synthesized small molecules and running NMR experiments.

Many thanks goes to my family: Jane for being supportive and checking on my progress regularly, Trinity for setting a good example to his siblings, Rangariro for his desire to pursue Engineering, Farai for the energy and sportsmanship, and Vongai for keeping me busy whenever I was not working on my research. I also thank my friend Gasseller and his wife Pauline for encouraging me to play tennis, which kept me energized. Dr. Edward Mazhangara and his family assisted me in settling in East Lansing during the initial days of my program, and for this, I am most thankful. Pastor Dave Williams of Mt. Hope church provided me with spiritual encouragement, which made my life more meaningful.

PREFACE

Chapter 1 covers a detailed investigation on the stereochemistry of the migratory hydrogen on the C2 position of the Beta product. Chapter 2 includes an evaluation of the substrate specificity of PAM and the discussion on the effects of electronic and inductive effects on the reactivity of the substrate. Chapter 3 covers the general characterization of PAM, in terms of the kinetics, growth, overexpression and purification optimization and general assay techniques. Chapter 3 also covers mutagenetic investigation of the role of the MIO cofactor on the activity and functionality of PAM and an investigation into the role of a general base during the PAM catalysis is also described. Chapter 4 is the investigation of the effect of light on the activity of PAM as measured by the amount of endogenous β phenylalanine. Chapter 5 was an attempt to establish the mechanism of the reaction by utilizing ^{13}C and ^{15}N NMR and analyzed the intermediates and transient states formed during the reaction.

TABLE OF CONTENTS

CHAPTER 5
AN ATTEMPT TO DECIPHER THE MECHANISM OF PHENYLALANINE AMINOMUTASE (PAM) USING AN ISOTOPICALLY ENRICHED

LIST OF TABLES

LIST OF FIGURES

is the proposed nucleophilic attack on the aromatic ring on the methylidene of the MIO, followed by (ii) the collapse of the sigma complex and elimination of NH_3, and step (iii) the rebound of the NH_3 at the C3 position. Step (iv) is the sigma complex formation and (v) is the NH_3 elimination as proposed for the PAL

LIST OF ABBREVIATIONS

PAM . . . . .phenylalanine aminomutase

PAL. . . . . phenylalanine ammonia lyase

TAL . . . . .tyrosine ammonia lyase

HAL . . . . .histidine ammonia lyase

TAM . . . . .tyrosine aminomutase

LAM . . . . lysine aminomutase

MIO 3,5-dihyro-5-methylidene-4*H*-imidazol-4-one

E.coli . . . . *Escherichia coli*

IPTG . . . . Isopropyl galactopyranoside

SDS . . . . sodium dodecyl sulfate

PAGE . . . . polyacrylamide gel electrophoresis

ASG . . . . alanine-serine-glycine triad

GC/EI-MS . . . . coupled gas chromatography and electron- impact mass spectrometry

E1cb . . . . first order elimination reaction that proceeds via a carbanion intermediate.

S176C, A, T and G . . . . .mutant of PAM where serine-176 has been replaced by cysteine, alanine, threonine and glycine.

Y322F, H. . . . . mutant of PAM where tyrosine-322 has been replaced by penylalanine or histidine

C107A, H. . . . . mutant of PAM where cysteine-107 has been replaced by alanine or histidine

ATP . . . . adenosine triphosphate

EtOAc . . . . ethyl acetate

^{1}H- and ^{2}H-NMR . . . . proton- and deuterium-nuclear magnetic resonance,

kDa . . . . kilodaltons

k.i.e. . . . . kinetic isotope effect

LB . . . . Luria-Bertani medium

MWCO . . . . .molecular weight cut-off

α . . . . .alpha

β . . . . .beta

μ . . . . .micro

mL . . . . milliliters

μL . . . . .microliters

μg . . . . .microgram

δ . . . . .delta

ppm . . . . parts per million

W . . . . watt

Nm . . . . nanometer

mm . . . . millimeter

cm . . . . .centimeter

h . . . . hour

s . . . . .second

PCR . . . . polymerase chain reaction

dNTP . . . . deoxynucleotide triphosphate

MQ H_2O . . . . .milliquire water

Sg . . . . *S*treptomyces globisporous

T. brevifolia . . . . *brevifolia* . . . .*Taxus brevifolia*

2'-Ado . . . . 2'-adenosine

SAM . . . .*S*-adenosine methionine

PLP . . . . pyridoxal pyrophosphate

GTP . . . . guanidine triphosphate

Δ . G. . . . . .Gibbs energy change

V_{max} . . . . maximum velocity

K_M . . . .Michael-Menten constant

K_{cat} . . . . .catalytic turnover

Vrel . . . . .relative velocity

Vo . . . . .initial velocity

FW . . . . formulae weight

UV . . . . .ultraviolet

MHz . . . . .megahetz

Ni-NTA . . . . nickel nitrilotriacetic acid

RIPL . . . . .arginine Isoleucine proline lysine

mM . . . . millimolar

μ .M . . . . micromolar

CHAPTER 1

Assessment of the Cryptic Stereochemistry of Phenylalanine Aminomutase: Retention of Configuration at the Migration Termini.

1.1 INTRODUCTION

Aminomutase enzymes typically catalyze the isomerization of α-amino acids to β-amino acids; however, there are a few that catalyze the migration of a terminal amino group position at the δ- and ε- carbon of appropriate amino acids. Of the seven aminomutases identified so far there are five distinct proposed mechanisms. The first class include D-lysine-5,6-aminomutase, D-ornithine-5,4-aminomutase and leucine-2,3-aminomutase which utilize adenosylcobalamin and pyridoxal phosphate (PLP) as cofactors and involve the cleavage of the C-Co to generate a radical.[1-8] Another mechanistic class of aminomutases is represented by lysine-2,3-aminomutase[9-54] from *Clostridium subterminale*,[55-60] which belongs to a group S-adenosylmethionine (SAM)-dependent enzymes which carry an iron-sulfur (4Fe-4S) cluster and also require PLP; a 5'-deoxyadenosyl radical is generated during the reaction.[60-77] A third class uses only PLP without generation of radicals. For example, glutamate-1-semialdehyde aminomutase catalyzes the conversion of glutamate-1-semialdehyde to δ-aminolevulinic acid,[78] which is the universal precursor for the biosynthesis of heme, chlorophyll, and other pyrroles.[79-83] A fourth class includes tyrosine-2,3-aminomutase[84-88] from *Bacillus brevis* that only requires ATP as a cofactor. The final mechanistic class

1

includes tyrosine-2,3-aminomutase from *Streptomyces globisporous* (SgTAM) and phenylalanine aminomutase (PAM) from *Taxus*.

The stereochemical course of the lysine-2,3-, tyrosine-2,3-, arginine-2,3-, and the α-lysine-5,6- aminomutase reactions have been evaluated.[89,90] The vicinal transfer of the amino group of each substrate was shown to invert the configuration at the receiving carbon, replacing one of the diastereotopic hydrogens formerly at this position. Of these isomerases, the stereoselectivity of the reciprocal hydrogen transfer is known for only the arginine-2,3- and lysine-2,3- aminomutase reactions, wherein the configuration at the receiving prochiral carbon is inverted. The stereochemistry of the arginine-2,3-isomerase reaction was assessed *in vivo* in *Streptomyces griseochromogenes* by feeding stereoisomers $[2,3,3-^2H_3]$-,$[3,3-^2H_2]$-, and $[2-^2H]$-arginines.[91] The results revealed the complete retention of the original δ-hydrogens with migration of one to the α-position, as well as partial loss of the original α-hydrogen presumably due to arginine racemase activity. (*3R*)- $[3-^2H]$-and (*3S*)-$[3-^2H]$-arginines were synthesized unambiguously and used to determine that the *pro-3R* hydrogen of α-arginine migrates to the α-position (C-2).

The cofactor requirements of arginine-2,3-aminomutase (AAM) from *Streptomyces* have been empirically determined to be (*S*)-adenosylmethionine and pyridoxal phosphate. However, the catalytic mechanism likely involves homolysis and free-radical coupling processes that initiate the removal of relatively non-acidic alkyl hydrogen ($pK_a \geq 45$) at C_β from the arginine substrate. Arginine is structurally similar (from C_α to C_δ) to the α-ornithine and α-lysine

2

substrates of their respective aminomutases, whose mechanisms are radical mediated. Furthermore, α-arginine lacks electronic stabilization, which could be achieved by the presence of, for example, an adjacent aromatic or allylic group that would increase the acidity of the hydrogen at C_β in a heterolytic reaction. A series of ^{15}N, ^{13}C-labeled α-arginines were fed to the *Streptomyces* in order to examine the mechanism of L-β-arginine formation in the biosynthesis of the antibiotic blasticidin S. Analysis of the derived antibiotic by ^{13}C NMR spectroscopy revealed intramolecular migration of the amino group from the α- to the β-carbon, revealing the presence of an arginine-2,3-aminomutase.

The multifunctional phenylalanine aminomutase (PAM) from *Taxus* catalyzes the vicinal exchange of the amino group and the *pro*-(3*S*) hydrogen of (2*S*)-α-phenylalanine to produce (3*R*)-β-phenylalanine.[92-101] While the migration of the amino group from C2 to C3 of the product was already known to proceed intramolecularly with retention of configuration,[98-100] the stereochemistry of the hydrogen transfer remained unknown. The stereochemistry of the amine group at the C3 position was established as *R* by incubating PAM with (*S*)-[U-^{14}C]-phenylalanine, then converting the product to the 1-(*S*)-camphanate methyl ester, and finally comparing its retention time to that of authentic *N*-[(1'-*S*)-campanoyl]-(3*R*)-β-phenylalanine methyl ester on radio-HPLC. The *R* configuration of the β-phenylalanine catalyzed by the aminomutase on the paclitaxel synthetic pathway is consistent with the configuration of the amino group found in paclitaxel. This supports the premise that β-phenylalanine is indeed an intermediate on the

paclitaxel pathway. Use of (S)-[2-^{15}N, ring-$^{2}H_5$]-phenylalanine demonstrated that the amine group is transferred intramolecularly during the course of PAM catalysis. When $(2S,3S)$-[ring, $2,3$-$^{2}H_7$]-phenylalanine was used as a substrate, no deuterium was detected at the C3 position, but a 2,2-dideuterio β-product was confirmed by GC/MS analysis suggesting that only the $(3S)$-deuterium migrated from the C3 to the C2 position (Figure 1.1B).

Not only is the retention of stereochemistry at the migration termini of the amino group an uncommon characteristic of all the aminomutase mechanisms described, but the stereochemistry of the product is opposite that of the $(3S)$-product made initially in the mechanistically-related TAM reaction.[86] However, despite this apparent divergence in stereochemistry between the aryl amino acid aminomutases, both the lack of cofactor dependency and similarity of the amino acid sequences between PAM and TAM (from *Streptomyces*) (56% amino acid similarity) reveal that these enzymes belong to the same family, which includes several ammonia lyases (Figure 1.3). The lyases share a characteristic active site motif, ASG (also present in the aminomutases) that autocatalytically rearranges to form a functional 3,5-dihydro-5-methylidene-4-*H*-imidazol-4-one(MIO) prosthesis. The MIO facilitates the elimination of NH_3 group and H^+ from the arylalanine substrate to form an aryl acrylate product in the lyase reaction. The MIO moiety purportedly couples with the substrate by electrophilic attack on the *ortho*-carbon of the aromatic ring or by direct electrophilic capture of the amino group (Figure 1.2). Similar MIO involvement is proposed in the

4

aminomutase reaction mechanism where, instead, the vicinal NH_3 and H^+ interchange intramolecularly and rebound to the phenylpropanoid to complete the reaction cycle forming the β-amino acid product (Figure 1.1A).

(S)-α-phenylalanine   (R)-β-phenylalanine
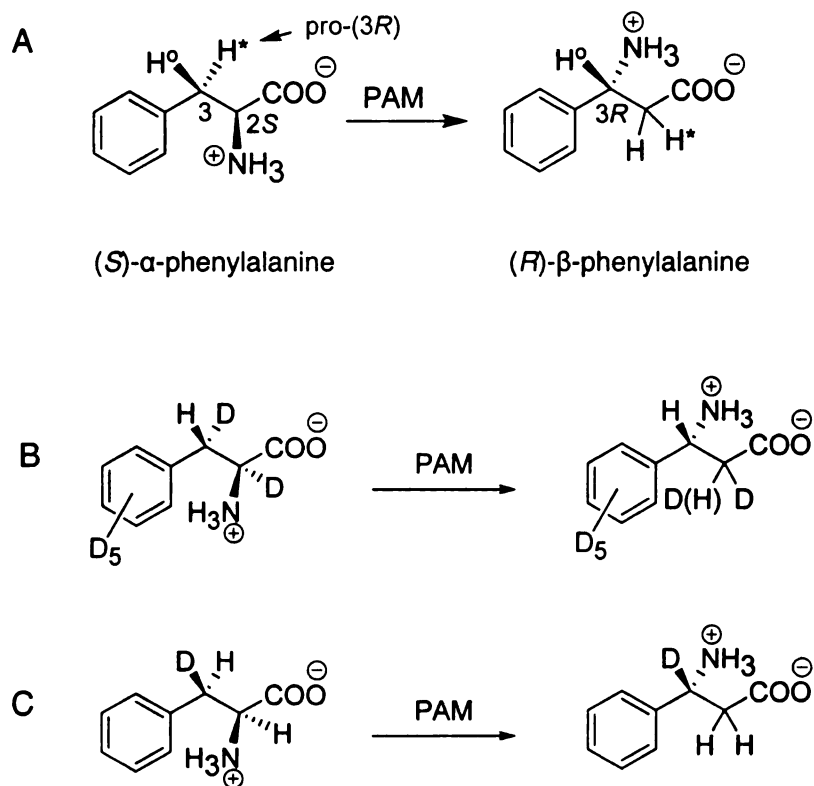
Figure 1.1 The reaction of PAM with α-phenylalanine showing the retention of configuration of the NH_2 group migrating from C2 to C3 (A), confirming that only the pro-(3R)-hydrogen migrates to the C2 position (B and C).

σ-complex with MIO

amino group activation by MIO
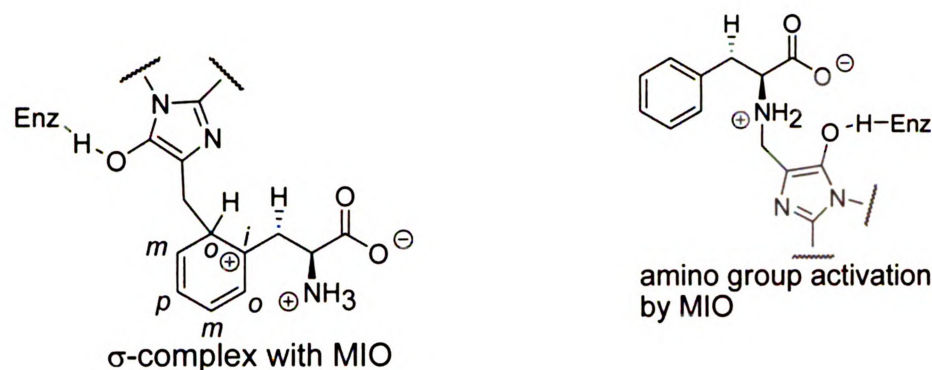
Figure 1.2 The proposed mechanism of PAM involving the aromatic ring as nucleophile (left) or the amine as nucleophile (right).


```
                140         *          160         *          180         *          200
PAM_T.cana : CSSRRTN--QLSELQESLIRCLLAGVFTKGCASSVD------ELPATATRSAMLLRLNSFTYGCSGI
PAM_T.chin : CSSRRTN--QLSELQESLIRCLLAGVFTKGCASSVD------ELPATVTRSAMLLRLNSFTYGCSGI
PAL_G.bilo : TSHRRTS--QGVELQKELIRFLNAGVFGS-CEGN-------VLPEATTRAAMLVRTNTLPQGYSGI
PAL_P.sylv : TSHRRTN--QGAELQKELIRFLNAGVLGK-CPEN-------VLSEDTTRAAMLVRTNTLLQGYSGI
PAL_A.thal : TSHRRTK--NGTALQTELIRFLNAGIFGN-TKETCH-----TLPQSATRAAMLVRVNTLLQGYSGI
PAL_R.toru : SADTRTE--DAISLQKALLEHQLCGVLPSSFDSFRLGRGLENSLPLEVVRGAMTIRVNSLTRGHSAV
TAM_S.glob : MIYMQVDKSKEVELQTNLVRSHSAGVGPL------------FAEDEARAIVAARLNTLAKGHSAV
HAL_P.puti : LASTRIASHDLENLQRSLVLSHAAGIGAP------------LDDDLVRLIMVLKINSLSRGFSGI
TAL_R.spha : LANRLISGENVRTLQANLVHFLASGVGPV------------LDWTTARAMVLARLVSIAQGASGA
              LQ   L6      G6                          l    R  6  4 n3   G S

               *          220         *          240         *          260
PAM_T.cana : RWEVMEALEKLLNSNVSPKVPLRGSVSASGDLIPLAYIAGLLIGKPSVVARIGDDVE---VPAPEAL
PAM_T.chin : RWEVMEALEKLLNSNVSPKVPLRGSVSASGDLIPLAYIAGLLIGKPSVIARIGDDVE---VPAPEAL
PAL_G.bilo : RWALLETIEKLLNAGITPKLPLRGTITASGDLVPLSYIAGLLTGRPNSKVRTRDGTE---MSGLEAL
PAL_P.sylv : RWDILETVEKLLNAGLTPKLPLRGTITASGDLVPLSYIAGLLTGRPNSRVRSRDGIE---MSGAEAL
PAL_A.thal : RFEILEAITSLLNHNISPSLPLRGTITASGDLVPLSYIAGLLTGRPNSKATGPDGES---LTAKEAF
PAL_R.toru : RLVVLEALTNFLNHGITPIVPLRGTISASGDLSPLSYIAAAISGHPDSKVHVVHEGKEKILYAREAM
TAM_S.glob : RPIILERLAQYLNEGITPAIPEIGSLGASGDLAPLSHVASTLIGEG---YVLRDGRP---VETAQVL
HAL_P.puti : RRKVIDALIALVNAEVYPHIPLKGSVGASGDLAPLAHMSLVILGEG---KARYKGQW---LSATEAL
TAL_R.spha : SEGTIARLIDLLNSELABAVESRGTVGX--DLTPLAHMVLCLQGRGD--FLDRDGTR---LDGAEGL
              r   6  6    6N  6 P 6P   G36 asgDL PL  6   6 G             6  2

               *          280         *          300         *          320         *
PAM_T.cana : SRVGLRP--FKLQAKEGLALVNGTSFATALASTVMYDANVLLLLVETLCGMFCEVIFGRE-EDAHPL
PAM_T.chin : SRVGLRP--FKLQAKEGLALVNGTSFATALASTVMYDANVLLLLVETLCGMFCEVIFGRE-EDAHPL
PAL_G.bilo : KQVGLEK-PFELQPKEGLAIVNGTSVGAALASIVCFDANVLAVLSEVVSAMFCEVMNGKP-EFTDPL
PAL_P.sylv : KKVGLEK-PFELQPKEGLAIVNGTSVGAALASIVCFDANVLALLSEVISAMFCEVMNGKP-EFTDPL
PAL_A.thal : EKAGISTGFFDLQPKEGLALVNGTAVGSGMASMVLFEANVQAVLAEVISAIFAEVMSGKP-EFTDHL
PAL_R.toru : ALFNLEP--VVLGPKEGLGLVNGTAVSASMATLALHDAHMLSLLSQSLTAMTVEAMVGHAGSFHPFL
TAM_S.glob : AERGIEP--LELRFKEGLALINGTSGMTGLGSLVVGRALEQAQQAEIVTALLIEAVRGSTSPELAEG
HAL_P.puti : AVAGLEP--LTLAAKEGLALLNGTQASTAYALRGLFYAEDLYAAAIACGGLSVEAVLGSRSPEDARI
TAL_R.spha : RRGRLQP--LDLSHRDALALVNGTSAMTGIALVNAHACRHLGNWAVALTALLAECLRGRTEAMAAAL
```

Figure 1.3 A partial sequence alignment of PAM_*T. canadensis* with other MIO carrying enzymes PAM_*T. chinensis*, PAL_*G. biloba*, PAL_*sylvestris*, PAL_*A. thaliana*, PAL_*R. toruloides*, TAM_*S. globisporous*, HAL_*P. putida* and TAL_*R. sphaeroides*.

On the surface, the net vicinal rearrangement reactions of the 2,3-aminomutases appear similar. However, there is clear mechanistic diversity among the β-isomerases. Therefore, unveiling the complete stereochemistry of the reaction mechanisms will help to identify the determinants that sort the aminomutases into coherent sub classes. In this study, the cryptic stereochemistry of the PAM reaction involving the hydrogen transfer from C3 to C2 of the phenylpropanoid substrate is defined. A deuterium label tracer method is described for the measurement of the overall kinetic isotope effect of the C_β-H bond cleavage. The exchange of the transient hydrogen with protons from an alternative source was also investigated in deuterium-labeling studies, and the equilibrium constant of the PAM reaction was measured to assess the difference in free energy between the reactant and the product.

1.2 RESULTS AND DISCUSSION

1.2.1 *Hydrogen Exchange at C2 of the PAM Reaction Product.*

The hydrogen exchange in the PAM reaction was tracked as a function of time to further evaluate cryptic aspects of the mechanism. [ring, 2,3,3-^{2}H$_8$]-(2S)-α-Phenylalanine, at saturation (500 µM), was incubated with PAM ($K_M \approx$ 45 µM) in buffer dissolved in H$_2$O over a period of 50 h. After 0.25 h, 0.2 mol% (0.5 nmol) of the substrate had converted to β-phenylalanine that was comprised of ~57% D$_7$-isotopomer and ~43% of D$_8$-isotopomer (Figure 1.3) as determined by GC/EI-MS analysis. The D$_7$ species contained the intact phenylpropanoid fragment ion (m/z 185), and a fragment ion derived from C2-C3 bond fissure m/z 154 (a D$_6$ species, no D$_5$ species were identified) indicated that the deuterium resided at the phenyl (D$_5$) and benzylic (D$_1$) carbons (Table 1.1B). Thus, the H- for D-replacement was confirmed to have occurred at C2, and not at C3, nor in the aromatic ring. During the period from 0.25 to ~2 h, the isotope exchange rate constant was at 0.52 h^{-1} while the product abundance increased from 0.2 mol% to 0.8 mol% relative to substrate (Figure 1.3). The H/D exchange rate decreased and finally reached equilibrium (~75 % H- for D- replacement) at longer incubation times, while the product increased from 0.8 mol% to 10 mol% relative to substrate between 2 and 50 h.

The origin of the proton source in the exchange experiment was ascertained through a reciprocal experiment conducted by incubating PAM with unlabeled α-phenylalanine in buffer, wherein the H$_2$O was replaced by D$_2$O. After

8

a 12 h incubation, the derivatized β-phenylalanine product isolated from this enzyme-catalyzed reaction was comprised of ~70% D_1- and ~30% D_0- isotopomers and confirmed the extent of hydrogen replacement observed in the previous experiment with unlabeled solvent (Table 1.1C). Evaluation of the β-amino acid isotopomers by GC/EI-MS fragmentation confirmed that the deuterium in the D_1-species was at C2 (Table 1.1C). Furthermore, if the deuterium exchange described above resulted from the in situ chemical N-acetylating and methyl esterification steps used to derivatize the amino acids, then complete replacement of deuterium by hydrogen would have been anticipated, particularly for samples in which the β-amino acid product was least abundant; yet, this was not observed.
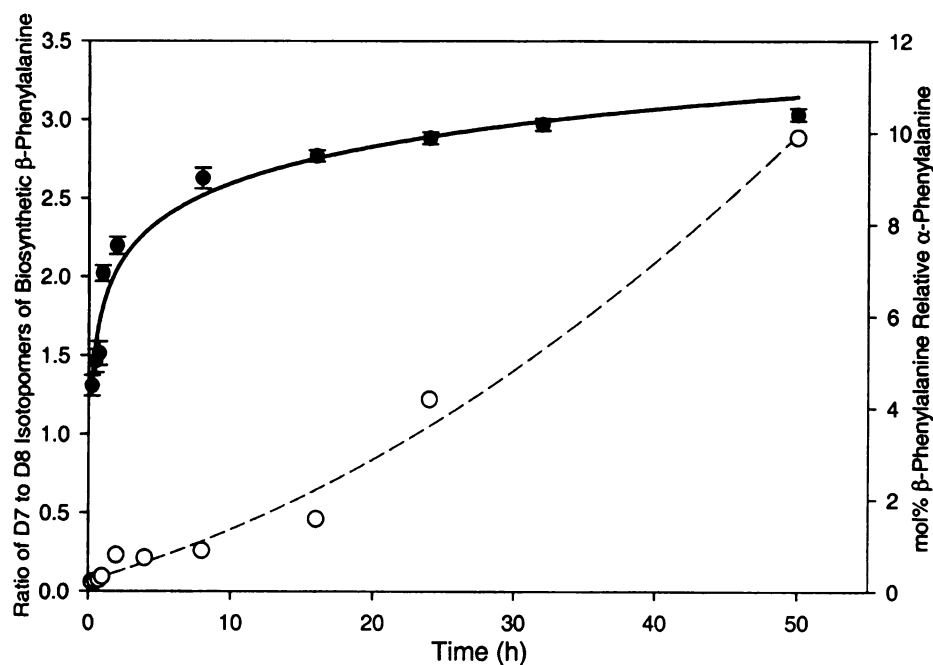
Figure 1.4 Hydrogen exchange at the C2 position

Table 1.1 A summary of the H/D exchange during the PAM reaction. Diagnostic ions resulting from electron impact-mass spectrometry fragmentation. Shown are mass spectral fragments after bond fissure at sites 'a' and 'b', yielding diagnostic ions of the corresponding N-acetyl-α-phenylalanine methyl ester.
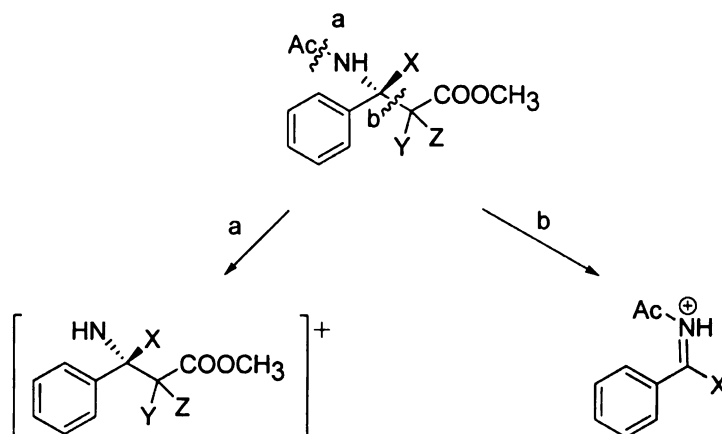
2-(*S*)-α-phenylalanine	Ion (*m/z*) observed by EI-MS analysis	
	m/z 178 (Do), X,Z,Y = H	*m/z* 148 (Do) X= H
	m/z 185 (D$_7$) X, Z = D, Y = H, ring = D$_5$ *m/z* 186 (D$_0$), X, Y, Z = D ring = D$_5$	*m/z* 154 (D$_6$)
	m/z 178 (D0) X, Y, Z = H *m/z* 179 (D1) X, Y = H, Z = D	*m/z* 148 (D0) X = H
	m/z 179 (D1): X, Y, Z = H *m/z* 180 (D2): X, Z = D, Y = H	*m/z* 149 (D1) X = D

10

1.2.2 *Complete Stereochemistry of the PAM Reaction.*

The ^{1}H-NMR chemical shift values of the diagnostic protons at C2 of β-phenylalanine were measured and observed at δ = 5.43 (doublet of doublets), for $C_\beta H$NH, and at δ = 2.92 (doublet of doublets) and 2.82 (doublets of doublet) for $C_\alpha HH$ (Figure 1.5B). The diagnostic protons at $C_\alpha H_2$ in a mixture of unlabeled authentic *N*-acetyl (3*R*)-β- and (2*S*)-α-phenylalanine methyl esters (each at ~200 µM) dissolved in [$^2H_8$]-ethyl acetate, and were found to be well-resolved (by Δδ 0.24) from the chemical shifts signals of the protons at C3 (i.e., the diastereotopic benzylic protons ($C_\beta H_2$) of α-phenylalanine at δ = 3.08 (doublet of doublets) and 3.15 (doublet of doublets) (Figure 1.5C). The resolution between the α- and β-phenylalanine proton chemical shift signals indicated that the signals for both compounds could be measured simultaneously. Therefore, the need to chromatographically-separate the [^2H]-labeled α- (substrate) and β-(biosynthetic product) amino acids in the biosynthetic assay prior to assessing the stereochemistry of the C2 deuterium in the [^2H]-labeled biosynthetic product by ^{2}H-NMR was precluded. The relative configuration of the prochiral hydrogens at C2 of β-phenylalanine were assigned by employing the racemate of *N*-acetyl (2*S*,3*R*)- and (2*R*,3*S*)-[2,3-$^2H_2$]-α-phenylalanine methyl ester that was synthesized by stereo specific reduction (palladium/D_2 gas) of an *N*-acetyl *trans*-enamine methyl ester (Figure 1.12); the (2*S*)- and (2*R*)-deuteriums in the enantiomeric pair are spectroscopically equivalent. ^{2}H-NMR analysis of the synthetic dideuterio product, dissolved in ethyl acetate, revealed chemical shift

11

resonances at δ = 5.42 (C$_\beta$DNH, singlet) and at 2.82 (C$_\alpha$DH, singlet); the latter signal corresponds to the deuterium at the (2S)- and (2R)-positions of the enantiomeric mixture (Figure 1.6).
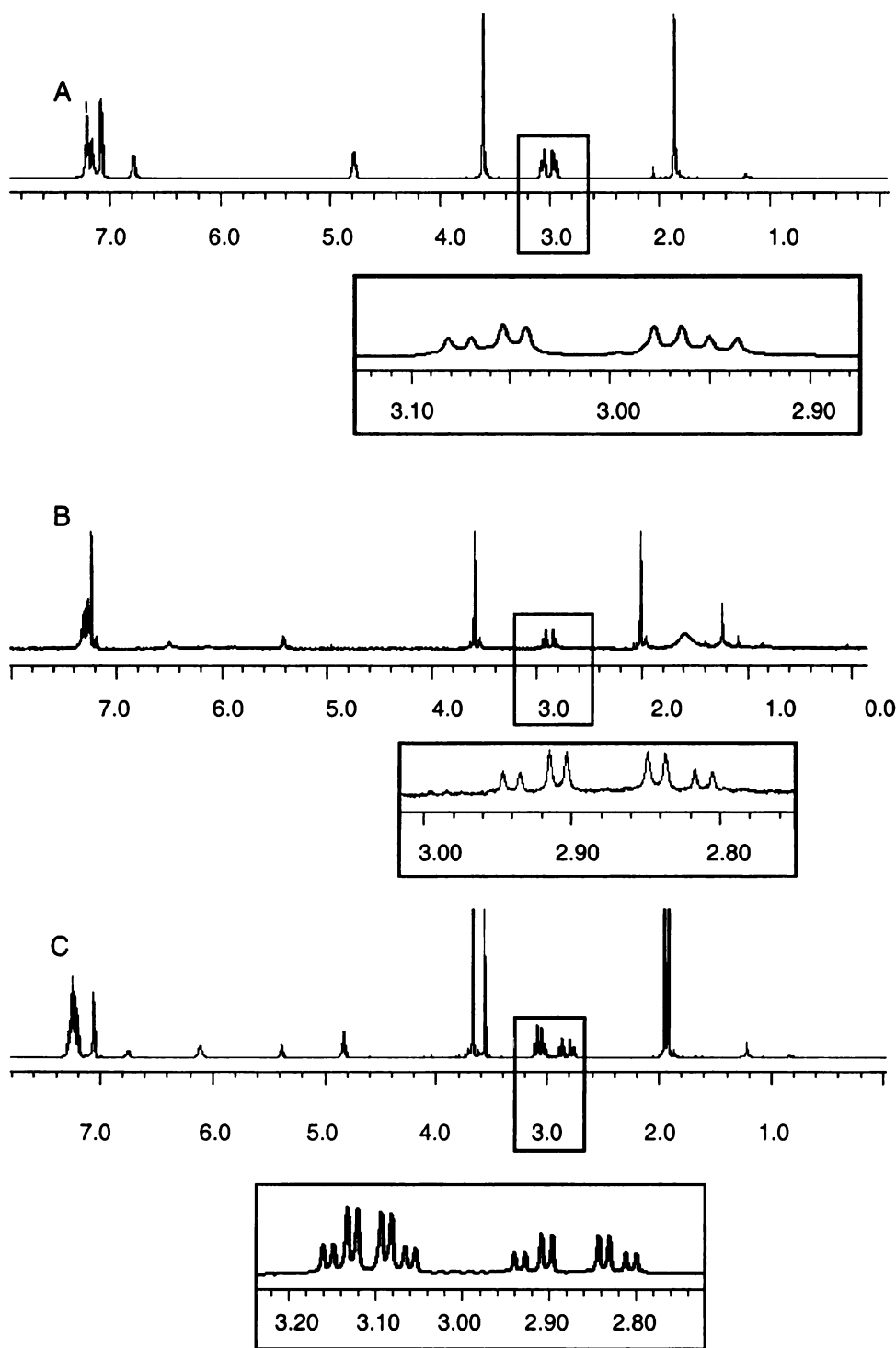
Figure 1.5 ^{1}H NMR for α-phenylalanine (A), β-phenylalanine (B) and α- and β-phenylalanine, the amino acids were derivatized to their mixture of N-acetylated methyl esters. The expanded regions showing the splitting patterns are shown in the inserts below the full spectra.

13
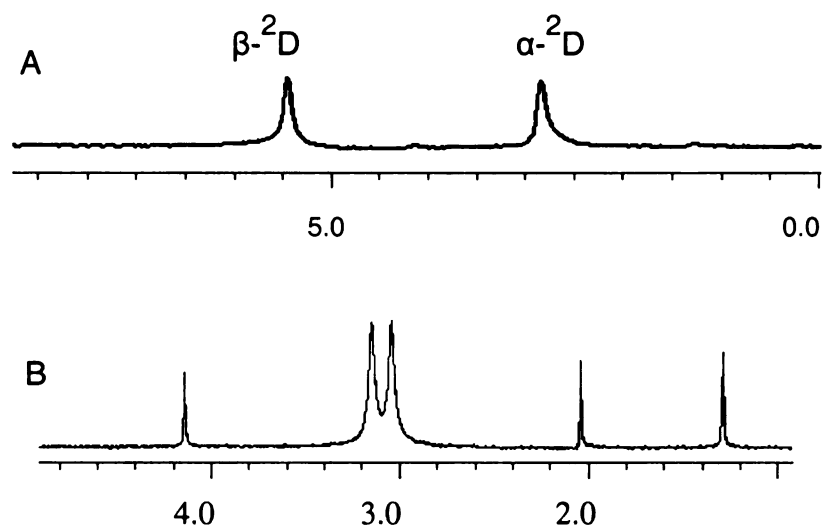
Figure 1.6 A. ^{2}H-NMR for an enantiomeric mixture of [2,3-^{2}H2]-(2S,3R)- and (2R,3S)-β-phenylalanine as N-acetylated methyl esters. The peaks are observed at δ = 2.82 and 5.32 ppm for α- and β- ^{2}D respectively. B. The ^{2}H-NMR of [3,3-^{2}H2]-α-phenylalanine derivatized as the N-acetylated methyl ester.

Figure 1.7 The Newman projects of diastereoisomers (2S,3R)-, (2R, 3S)-[2-,3-^{2}H2]-N-acetyl-phenylalanine methyl ester.

14
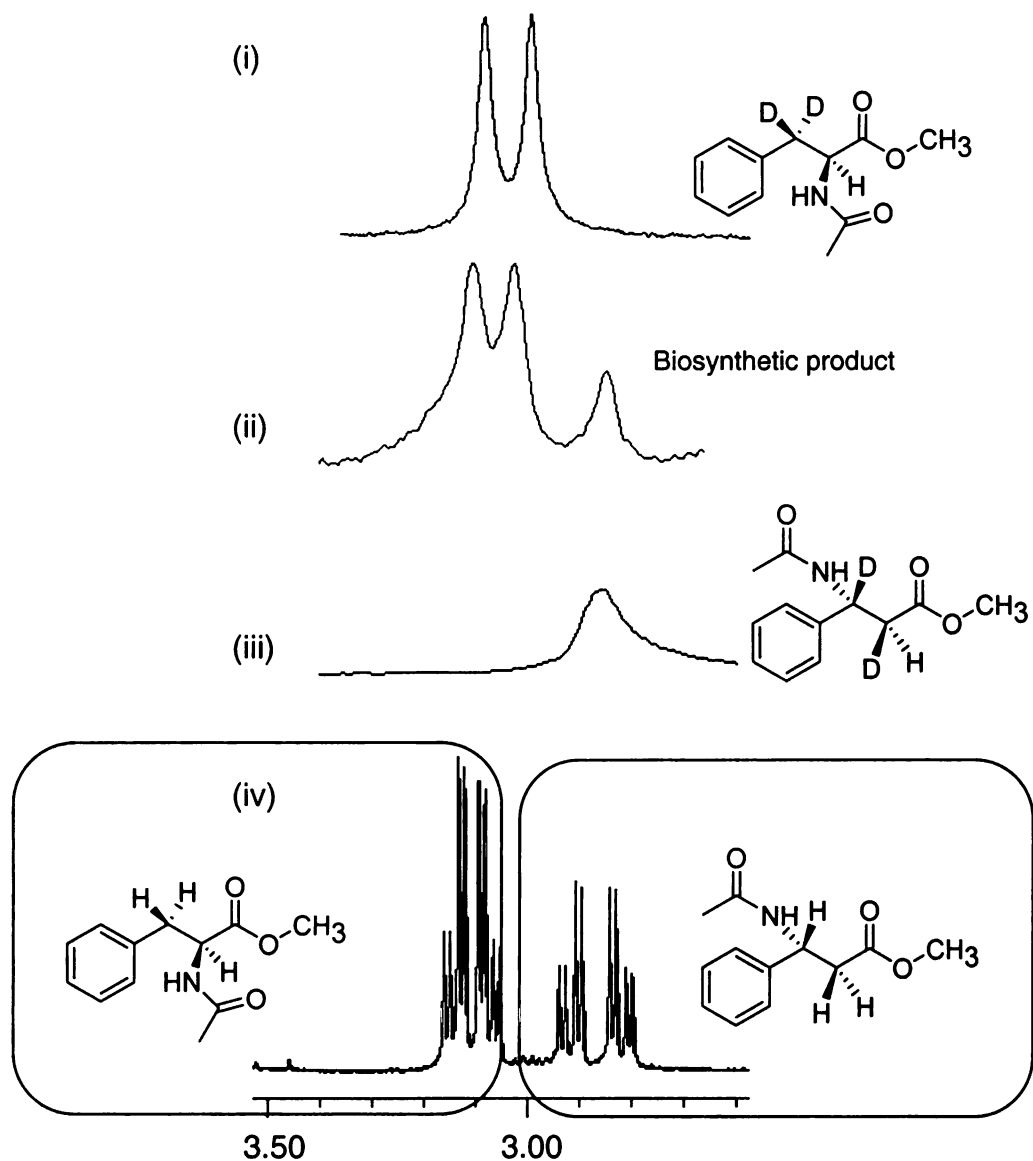
Figure 1.8 Study of the complete stereochemistry at the C2 position of the β-product with reference to the migratory hydrogen from the C3 position. (i) [3,3-^{2}H$_2$]-phenylalanine as substrate, (ii) the biosynthetic product, (iii) the aunthentic [2,3-^{2}H$_2$]-phenylalanine and mixture of natural α- and β-phenylalanine. All the amino acids were derivatized to their methyl esters.

A ^{2}H-NMR spectrum of the [3, 3-^{2}H$_2$]-labeled substrate was acquired for referencing the chemical shift signals of the unused substrate in the enzyme assay to examine the stereochemistry (Figure 1.6B). The labeled α-amino acid was incubated for 10 h in assay buffer without PAM, and derivatized and isolated

15

like the amino acids in the catalytic assays. The derivatized amino acid showed deuterium chemical shift resonances at δ 3.09 and 3.15 for the diastereotopic deuteriums (Figure 1.8.i) in the ^{2}H-NMR spectrum; the chemical shifts were identical to those of the unlabeled isotopomer that was analyzed by ^{1}H NMR (Figure 1.8.iv). Incidentally, D-D spin couplings are about 40 times smaller than H-H spin couplings; therefore, the resolution of peak splitting caused by this coupling is not observed in ^{2}H-NMR, and the deuterium signals appear as singlets.

[3,3-^{2}H$_2$]-(2S)-α-phenylalanine (5mM) was incubated for 10 h with 50-fold more PAM enzyme than used in general assays. The reaction progress of the enzyme assay was monitored by GC/MS-EI for this investigation, and the reaction was stopped when it was estimated that sufficient product had been made and was comprised of enough [2,3-^{2}H]-β-phenylalanine isotopomer for ^{2}H-NMR detection. These conditions were met just as equilibrium was reached, i.e., the abundance of substrate and product were near 50:50. Had this reaction continue any longer at equilibrium, all of the migrating deuterio group will have been washed out (Figure 1.9). ^{2}H-NMR analysis of the [^{2}H]-labeled β-phenylalanine isotopomer derivatized and isolated after incubation revealed chemical shifts at δ = 5.43 (HNC$_β$D) and at δ = 2.82 (HC$_α$D) (Figure 1.8.iii). These signals were identical to those of the authentic deuterated racemic β-phenylalanine synthesized earlier (Figure 1.6A). This NMR data coupled with the known, exclusive (3R)-stereochemistry of the biosynthetically-derived [^{2}H]-β-

16

phenylalanine product, establishes the biosynthetic product as the (2*S*, 3*R*)-enantiomer.

Further analysis of the ^{2}H-NMR spectrum of the derivatized biosynthetic product (Figure 1.8.iii) showed that when the integral of the peak area for the resonance signal at δ = 5.43 (C$_\beta$*D*) was set to the expected value of 1.0 deuterium, the relative abundance of deuterium at C2 was a fraction (~0.30) of its expected value of 1.0 (Figure 1.9). This fractional loss of deuterium supports the level of hydrogen exchange observed in the isotope replacement assays conducted earlier. This isotopic ratio was confirmed by GC/EI-MS analysis (Table 1.1D) of the product; the relative diagnostic ion abundances were at 100% (D$_1$ species) and 28% (D$_2$ species) (Table 1.1D), after correcting for the mass contributions of natural abundance ^{13}C.

A peak area of 1.8 was assigned to the chemical shift signals corresponding to the two diastereotopic deuteriums at C3 of the remaining [3,3-^{2}H$_2$]-labeled substrate in the enzyme assay, above. Comparing the integral of 1.8 to the integral of the signal (set at 1.0), in the same spectrum, that corresponds to the peak area of the signal corresponding to the one deuterium at C3 (C$_\beta$DN) of the biosynthetic β-amino acid, indicates an approximate substrate to product ratio of 48:52 (Figure 1.10). Importantly, if the D- for H- exchange observed in biosynthetic product, resulted from the chemical derivatization of the amino acids, then racemization at C$_\alpha$ of β-phenylalanine would have been highly

anticipated. This effect, however was not observed in the ^{2}H-NMR spectrum of

the biosynthesized [^{2}H]-β-phenylalanine derivative (Figure 1.8.ii).
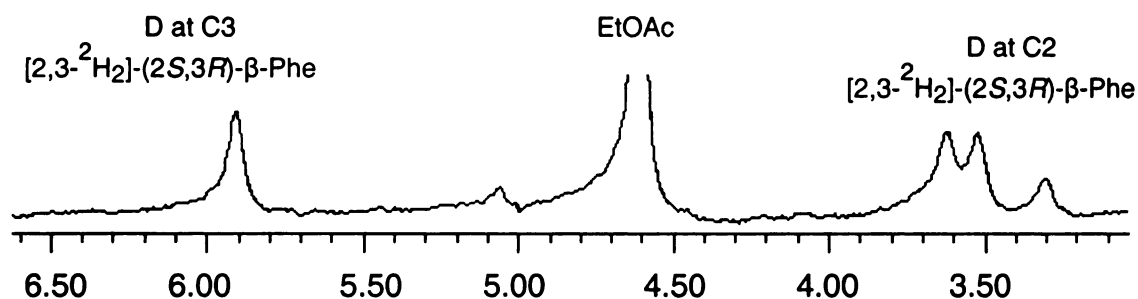
Figure 1.9 Assessment of the equilibrium conditions of the PAM with respect to the unreacted substrate and product. Dideteurated α-phenylalanine was incubated with PAM at 30 °C until the reaction reached equilibrium (17 h).

1.2.3 The Rate Determining Step on the Isomerization Pathway.

An equal mixture of unlabeled- and perdeuterio-(2S)-α-phenylalanines (at saturation) was incubated for 3 h with PAM under typical conditions, and the reaction was processed for analysis as described previously. The resulting biosynthetically-derived β-phenylalanine isotopomers (~0.7 mol% relative to substrate) were comprised of 66 mol% of D_0 product and 34 mol% of a mixture of D_7 and D_8 product. This suggests a primary isotope effect on V_{max}/K_M of approximately 2.0 ± 0.2 for the removal of the *pro*-3S hydrogen, which is likely a rate-determining step of the catalytic cycle. Notably, no D_1-labeled β-

phenylalanine was detected, indicating that intermolecular deuterium crossover from the $[^2H_8]$-α-phenylalanine to the D_0 β-isomer was below detection limits.

1.2.5 Equilibrium constant measurements

The equilibrium of the PAM reaction was measured by incubating PAM (100 µg) with α-phenylalanine (100 µM) in 10 mL of 50 mM sodium phosphate buffer pH 8.5 at 31 °C. Samples (1mL) were collected at time intervals ranging from 15 min to 24 h. The mol% of substrate and the β-phenylalanine product derivatized as their N-acetyl methyl esters were monitored by GC/MS analysis (Figure 1.9). An equilibrium (Keq) of 1.1 favoring the β-isomer was assessed.
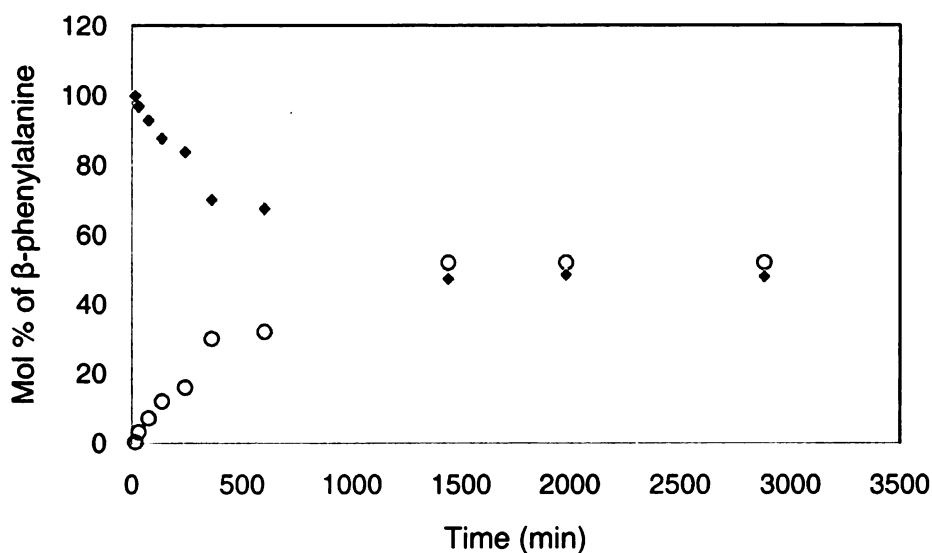
Figure 1.10 Measurement of the equilibrium constant of the PAM reaction with the natural substrate. PAM (100 µg) was incubated with 100 µM substrate and samples were at set time points and assayed as above. The α-substrate change over time is shown in black squars and the β-product in open circles.

1.3 DISCUSSION

1.3.1 Hydrogen Washout during Isomerization Chemistry.

The mechanism of the phenylalanine aminomutase reaction is considered to proceed, in part, similar to that proposed for the reaction of the related ammonia lyases, as mentioned previously. In terms of reaction chemistry and substrate specificity, the phenylalanine ammonia lyase (PAL) provides a practical model upon which to base the PAM reaction. The ASG amino acid sequence motif of PAL is proposed to form an MIO moiety in the active site that provides a similar function as a Lewis acid to promote the elimination of ammonia from the phenylpropanoid (Figure 1.11). This elimination process begins by removal of the *pro*-(3*S*) hydrogen by putatively a [137]His residue of PAL from *Rhodosporidium toruloides*[102] (Figure 1.11.iv), followed by $E1_{cb}$-type displacement of ammonia from the substrate to form *trans*-cinnamate[103,104] (Figure 1.11.vii). The mode of MIO-substrate coupling via the aryl ring in the PAL reaction (and other aryl amino acid lyase reactions) has been widely studied and is strongly supported empirically, and, therefore, is incorporated in the proposed mechanism for the aminomutase reaction. Thus, by analogy, the ASG sequence of the phenylalanine aminomutase from *Taxus* (50% sequence similarity to PAL from *R. toruloides*, (Figure 1.2) is proposed to also form a functional MIO that assists the isomerization reaction.[100] However, removal of the *pro*-3*S* hydrogen in PAM is likely initiated by the conserved [107]Cys residue (see Figure 1.2) that aligns with

sequence aligns with [137]His of PAL from *R. toruloides* (see Figure 1.2).
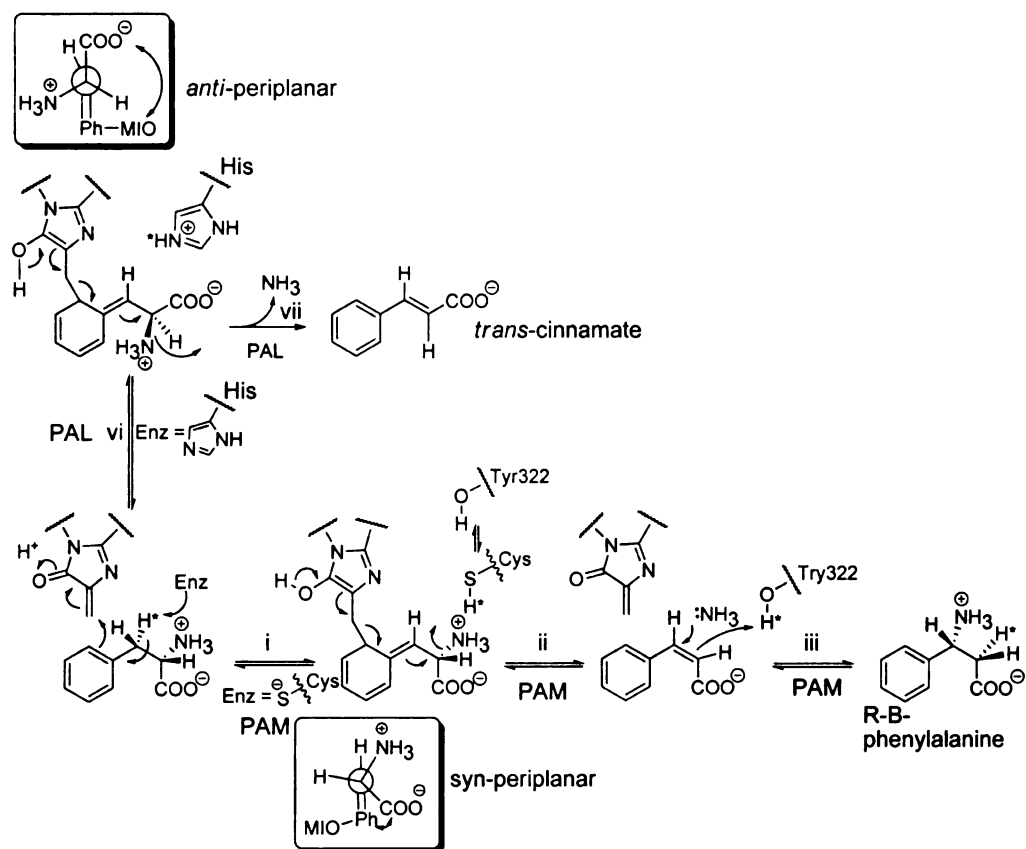
Figure 1.11 The mechanism of PAL *R. toluroides* (steps vi and v)and the proposed mechanism of phenylalanine aminomutase (PAM) (steps i-iii). Step (i) is the proposed nucleophilic attack on the aromatic ring on the methylidene of the MIO, followed by (ii) the collapse of the sigma complex and elimination of NH_3 , and step (iii) the rebound of the NH_3 at the C3 position. Step (iv) is the sigma complex formation and (v) is the NH_3 elimination as proposed for the PAL mechanism.

Deuterium-labeling studies incorporating GC/MS analysis confirmed that the *pro*-(3S) hydrogen of phenylalanine is partially intermolecularly exchanged with protons from water (pH 8.0) as it migrates to C_α of the product during the

isomerization reaction. There are likely two major pathways responsible for the observed proton dynamics that include H-exchange between 1) substrate and enzyme and 2) between enzyme and solvent.[105] Thus, the extent of deuterium exchange in the β-amino acid product formed by the PAM reaction from [^{2}H$_8$]-α-phenylalanine was evaluated. The substrate remained at saturation (up to 50 h, <10 mol% product made) to prevent dynamic equilibrium during the time course of the experiment, and thus minimized contributions from the reverse reaction (K_{eq} = 1.1). No loss of deuterium was detected in the substrate after 50 h by GC/EI-MS analysis (data not shown), thus confirming that the commitment to the forward reaction was maintained during the course of the investigation.

Therefore, the ^{2}H-labeled substrate likely transfers the pro-(3S) deuteron to a proposed general base (tyrosine residue) in the PAM active site. This now-labeled catalytic residue is either directly accessible by bulk water, and the D- for -H exchange takes place between tyrosine and the hydrogens of the solvent, or the tyrosine residue transfers the deuteron to proximate H-exchangeable amino acids or backbone amides that are reachable by solvent water[105]. Either of these transfer events, likely among others, are necessary to account for the H- for D-substitution that occurs prior to D-rebound since the level of exchange occurs to a large extent (60-75%) prior to product formation. Hence, the D-rebound to form substrate must be slower than the rate at which equilibrium is established between the deuterons transferred from the substrate to PAM than the H- for D-exchange between the enzyme and bulk water.

These aforementioned considerations provide one scenario wherein the ionizable hydroxyl hydrogen of tyrosine could exchange directly with the protons of bulk solvent, e.g., solvent has direct access to the active site tyrosine. Thus, the extent of H- for D- replacement would be expected to be time-independent. That is, once a deuterium from [^{2}H]-labeled substrate transfers to the active site tyrosine, the H- for D- exchange with solvent would ultimately equilibrate faster than the slower D/H-rebound. Consequently, an H : D ratio reflective of the two processes (exchange and rebound) would be established at the start of the reaction and the ratio of "unlabeled" to "labeled" product^2 would partition roughly according to this ratio; this ratio would be time-independent for the duration of the reaction.

However, a transient time-dependent deuterium exchange was observed early in the PAM reaction (Figure 1.4). Time-dependent hydrogen exchange in proteins is common and has been described for various proteins,[106,107] and the H/D exchange dynamics have been investigated using ^{2}H-labeling and electrospray ionization mass spectrometry to probe the rate at which backbone amide protons undergo chemical exchange with the protons of water.[108] Although amide N-H bonds are covalent and are often well-protected by their hydrogen-bonding interactions, they, however, engage in continuous exchange with the hydrogens of water.[106]

In the deuterium exchange assay with PAM and [^{2}H$_8$]-labeled substrate, D-rebound occurs at ~40% at 15 min, as evidenced by the 3:2 (mol/mol) ratio of "unlabeled" to "labeled" β-phenylalanine products at 0.2 mol% abundance

23

relative to substrate (Figure 1.4). After several hours, the D-rebound was comparatively lower at ~25%, and the extent of H- for D- exchange increased and stabilized at 75%, indicating a 3:1 (mol/mol) mixture of "unlabeled" to "labeled" β-phenylalanine products at ~10 mol% abundance relative to substrate (Figure 1.3). This observation is consistent with an initial deuterium "burst," after the first few round of catalysis that deposits deuterons from the substrate to active site locations upon isomerization of [^{2}H$_8$]-α-phenylalanine. The deuteron transfer from the substrate to the putative active site tyrosine was assessed to be the slow step in the isomerization reaction, and was based on the primary kinetic isotope effect on V_{max}/K_m of 2.0, which was calculated in a competitive assay with ^{2}H- and ^{1}H-labeled substrates. However, once a deuteron is removed from the substrate, plausible transfer of this deuteron to other proximate amino acid residues and backbone amides in the active site is likely[105]. Displacement of H- for D- at these sites on the enzyme would perturb the proton equilibrium between enzyme and solvent. Conceivably, very early in the reaction, the deuteron that is shuttled away from the catalytic tyrosine can reasonably be shuttled back part of the time and rebound to the product, before ultimate dilution with protons from the solvent. Thus, early in the PAM reaction, relatively less deuterium is lost in the PAM reaction compared to much later (Figure 1.9). After 2 h, the initial deuteron "burst" probably approaches dynamic equilibrium with bulk solvent protons and the rate of deuteron-load onto PAM by the substrate matches the rate of H/D-exchange on the enzyme. The observed 3:1, H/D-product ratio observed at later times (Figure 1.9) is likely a best approximation for the relative

24

rates between the H- for D- exchange and D-rebound. The abundance of β-phenylalanine increased steadily during this exchange process, indicating that the hydrogen exchange rate stabilized as a consequence of dynamic equilibration with active PAM enzyme, and not as a result of compromised enzyme activity. This observed exchange of substrate protons with bulk solvent protons contrasts the process in the radical-mediated lysine 2,3-aminomutase reaction where proton exchange between solvent and substrate is not observed.[2]

Penetration of bulk phase H_2O into the tertiary structure of proteins forming the active site has been demonstrated,[109] whereupon H- for -D exchange occurs. Therefore, the H- for -D exchange observed between [^{2}H]-labeled substrate and H_2O in the PAM reaction (Table 1.1) suggest that the access of protons of solvent water to the PAM active site is transiently time-dependent, and that the exchange rate is fast enough to see significant washout of label from the substrate.

1.3.2. *Stereochemical Fate of the PAM Reaction.*

The PAM enzyme catalyzes the conversion of [3,3-^{2}H$_2$]-α-phenylalanine substrate to a single (3R)-β-phenylalanine isomer as established by a Chiral GC method,[93] (data not shown), ^{2}H-NMR analysis of the [^{2}H]-labeled biosynthetic product and comparison to authentic stereospecifically deuterium-labeled β-phenylalanine analyzed by identical methods revealed the product had (2S,3R)-stereochemistry. This stereochemical outcome indicated that during the course of
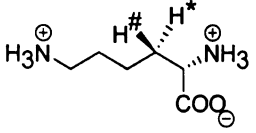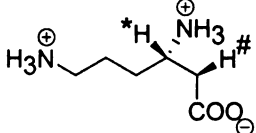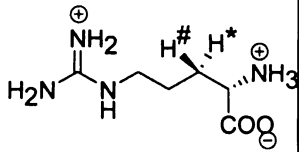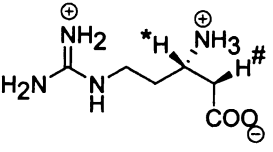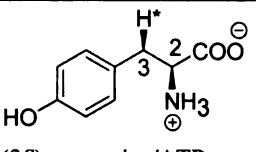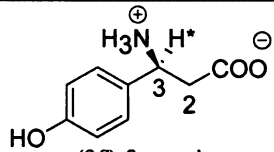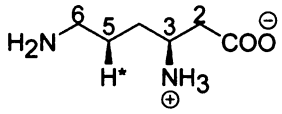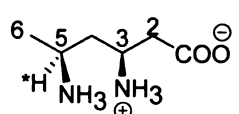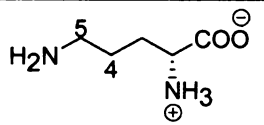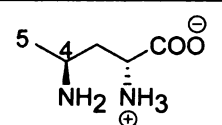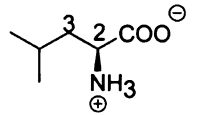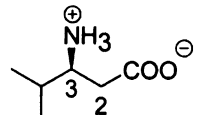
the catalytic reaction, the amino group formerly at the (2S)-position was replaced by the pro-(3S) deuterium, which migrated from C3, consequently proceeding with retention of configuration at C2. Reciprocally the amino group migration also proceeds with retention of configuration at the C3 terminus. The retention of configuration at both C2 and C3 during the isomerization is a unique mode of interchange among all of the aminomutases studied (c.f Table 1.2). To conform to the stereochemistry observed in the PAM-catalyzed product, the substrate may bind in the PAM active site with the carboxylate and phenyl ring of a putative intermediate in a syn-periplanar orientation (Figure 1.10). This orientation positions the migrating NH_3 and H groups of the α-phenylalanine on the same side of the molecule within the active site for facile exchange that results in retention of configuration at both receiving carbons (Figure 1.10). The "cisoid" orientation proposed here is distinctive relative to the anti-periplanar docking orientation of the α-phenylalanine substrate in the mechanistically-related phenylalanine ammonia lyases[110] (Figure 1.10) and, accordingly, this conformational difference in binding may likely contribute to the selectivity of the mutase and lyase reactions.

Notably, although PAM (from a plant) and the tyrosine aminomutase (from bacteria) originate from disparate sources, these described aminomutases have 56% amino acid similarity (Figure 1.2), and the presence of a signature active site motif (ASG), present in both, indicates that an MIO prosthetic group is formed and assists catalysis like in the reactions of the homologous ammonia lyases. However, these arylalanines aminomutase mechanisms have distinct

26

stereochemical differences at the carbon accepting the amino group. The phenylalanine aminomutase produces exclusively (3*R*)-β-phenylalanine, even after several days of catalysis,[85] while in contrast, the tyrosine aminomutase initially catalyzes the conversion of (2*S*)-α-tyrosine to (3*S*)-β-tyrosine, then produces the product racemate over time. Therefore, the phenylalanine aminomutase likely binds its substrate differently than the tyrosine aminomutase, and/or possibly the catalytic residues of PAM are positioned with an asymmetric bias that precludes racemization.

Moreover, the hydrogen/deuterium exchange dynamics between deuterium labeled substrate and product, described in this investigation, apparently do not epimerize the stereochemistry at C2 during the course of the reaction. The ^{2}H-NMR spectrum of the [^{2}H]-labeled product showed a deuterium signal at δ = 2.82, exclusively, which corresponded to a signal in the ^{1}H-NMR spectrum for one of prochiral hydrogens at C2 of derivatized authentic unlabeled (3*R*)-β-phenylalanine (cf. Figure 1.6), the other signal in this spectrum was distinctly at δ = 2.92. No coincident signal at δ = 2.92 was observed in the ^{2}H-NMR spectrum of the labeled biosynthetic product (cf. Figure 1.8.iii).

Table 1.2 Summary of the source, substrates, products, cofactor requirement and the stereochemistry of the products of various aminomutases.

Aminomutase Source	Substrate/ Cofactors	Product	Stereochemistry at carbon accepting NH3(H)
Lysine-2,3 *Clostridium*	(2S)-α-lysine/Ado Met,PLP	(3S)-β-lysine	Inverted (inverted)
Arginine-2,3 *Streptomyces*	(2S)-α-arginine	(3S)-β-arginine	Inverted (inverted)
Tyrosine-2,3- *Bacillus*	(2S)-α-tyrosine/ATP	(3S)-β-tyrosine	Inverted (unknown)
Tyrosine-2,3- *Streptomyces*	No cofactors		Unknown (unknown)
Lysine-5,6- *Clostridium*	(3S)-α-lysine	(3S, 5S)-diaminohexanoate	Inverted (unknown)
Ornithine-2,3- *Clostridium*	(2R)-α-ornithine/AdoCbl, PLP	(2R, 4S)-diamino-pentanoate	Unknown (unknown)
Leucine-2,3- *Andrographis*	(2S)-α-leucine	(3S)-α-leucine	Unknown (unknown)

28

1.3.3 *Substrate/Product Distribution at Equilibrium.*

A general property considered of all amino acids is the greater strength of the C_β-N bond over the C_α-N bond, as observed for the lysine-2, 3-aminomutase reaction. The free energy ($\Delta G^\circ \approx$ −1.4 kcal•mol^{-1}) was calculated to be considerably less than zero, and the forward reaction was assessed to be largely enthalpy-driven.[22] However, in the PAM isomerization reaction, the product to substrate ratio of nearly 1.0 (Figure 1.9) suggests that the equilibrium is not principally governed by the difference in C-N bond strength between the α- and β-isomers; apparently, the presence of the aromatic ring of β-phenylalanine minimizes the difference in C_β-N and C_α-N bond energy.

1.3.3 CONCLUSIONS

The results of the isotopic labeling studies begin to define the boundaries of an acceptable mechanism for the PAM reaction processes (Figure 1.8). The use of isotopically-labeled substrates in this investigation established that the amino group at C2 and the vicinal *pro*-(3*S*) hydrogen are interchanged by PAM reaction chemistry with *retention* of configuration at *both* migration termini, which is an uncommon pathway for aminomutases (Table 1.2). The removal of the hydrogen, which likely initiates the rearrangement, appears to be involved in the rate determining step of catalysis (primary K.I.E ≈ 2.0). Enzyme assays in which D_2O replaced H_2O in the bulk solvent, indicated that there is significant, but fleeting time-dependent exchange between solvent hydrogens and the α-phenylalanine during the aminomutase reaction when the substrate was at apparent saturation. This mechanism is patently different from the radical-mediated lysine-2,3- and arginine-2,3-aminomutase mechanisms, wherein exchange of hydrogen on the substrate with those of solvent is excluded.

Exploring the subtleties of the PAM mechanism is vital toward understanding how this enzyme, involved in secondary metabolism, may direct product selectivity and retain ammonia after vicinal isomerization compared to the homologous and mechanistically-related phenylalanine ammonia lyases that eliminates ammonia from the same substrate and provides compounds to primary metabolic pathways. Furthermore, as β-peptides, comprised of β-amino acids continue to become more conventional in the development of synthetic, mimics of natural proteins antibiotics, PAM catalysis potentially provides an

30

alternative, tractable method toward the production of novel, stereospecific β-aryl

α-amino acid precursors for this application.

1.3 MATERIALS AND METHODS

1.3.1 *Chemicals and Reagents*

Deuterium gas, [ring, 2,3,3-$^2H_8$]- and [3,3-$^2H_2$]-β-phenylalanines, and D_2O (each at > 98% isotope enrichment) were purchased from Cambridge Isotope Laboratories (Andover, MA). Ethyl benzoylacetate (90%) and [$^2H_8$]-ethyl acetate (> 98% isotope enrichment) were purchased from Aldrich (St. Louis, MO). All other reagents were purchased from or Sigma- Aldrich, unless otherwise noted, and used without further purification.

EXPERIMENTAL PROCEDURES

1.3.2. *NMR Spectra Measurements*

All NMR measurements performed on a Varian UnityPlus500 and 1H NMR spectra were acquired at 500 MHz. The proton-decoupled ^2H-NMR experiments were performed at 76.77 MHz.

1.3.3 *GC/EI-MS Measurements*

A gas chromatograph (model 6890N, Agilent, Palo Alto, CA) coupled to a mass selective detector (model 5973 *inert®*, Agilent) was used for the analysis of derivatized products isolated from enzyme assays that were loaded onto a 5HS GC column (0.25 mm inner diameter × 30 m, 0.25-μm film thickness) mounted in a GC oven. The MS conditions were set with an ion scan mode from 100 – 300 atomic mass units at 70 eV ionization voltage. The GC conditions were as follows: column temperature was programmed from 70 °C (3 min hold) to 320 °C

at 10 °C/min and then a 3 min hold at 320 °C, splitless injection was selected, and helium was used as the carrier gas (1.2 mL/min).

1.3.4 *Heterologous Expression and Purification of PAM.*

For the following procedures minimal growth media (MGM) (1 L contained 12.8 g $Na_2HPO_4 \cdot 7H_2O$, 3 g KH_2PO_4, 0.5 g NaCl, 1.0 g NH_4Cl, 2 mL 1 M $MgSO_4$, 100 µL 1 M $CaCl_2$, 10 mL 100X βME Vitamin solution, and 20 ml-20% D-glucose solution) with ampicillin selection was employed instead of the previously used LB to propagate the bacterial cells expressing the *pam* clone because α-phenylalanine is an abundant ingredient in the LB media. The exogenous α-phenylalanine was converted to β-phenylalanine *in vivo* during the over expression of the *pam* gene in the transformed bacterial cells, and these amino acids were co-extracted in considerable quantity (~0.3 mM) from the cells during the clarification of the soluble enzyme fraction. The removal of these metabolites prior to conducting kinetic analysis in the previous study required repetitive anion exchange chromatography, with dialysis between reloading to remove sodium chloride, followed by Ni-affinity purification chromatography, then final dialysis to dilute 250 mM concentrations of imidazole to <1 µM. These manipulations drastically reduced enzyme activity, making this an impractical approach for the present investigation where significant quantities of biosynthetic α-phenylalanine are required for detection by low-sensitivity ^{2}H-NMR analysis. (2*S*)-phenylalanine is a minor component in the MGM used, and accordingly, the levels of α- and β-amino acids in the soluble fraction of the bacterial extract were reduced by ~50-

fold. Therefore, the numerous purification steps to remove background amino acids were avoided.

1.3.5 *Optimization of PAM purification*

In order to improve the purification of PAM using the Ni-NTA method the polyhistidine tag was switched from the N-terminal to the C-terminal as follows. By a cohesive-end PCR method, *pam* cDNA was subcloned from expression vector pET1981His into pET14b to place the poly-His epitope tag at the C-terminus (designated pET14-1981His). Preliminary purification of small-scale preparations of PAM protein expressed from pET1981His and from pET14b vector in *E. coli* BL21(DE3) indicated that the N-terminal-tagged protein bound to Ni-affinity column matrix 8-fold better than the C-terminal-tagged protein (<10% binding).[100] The oligonucleotide primers for this sub cloning procedure have been described previously.[100] *E. coli* BL21(DE3) cells transformed with pET14-1981His were grown for 16 h in 50 mL of MGM. These bacteria were used to inoculate 6 L of MGM containing 100 µg/mL ampicillin. The cell cultures were grown at 37 °C until OD_{600} = 0.6, over expression was induced by the addition of 1 mM of isopropyl-β-D-1thiogalactopyranoside, and the cultures were grown at 18 °C for 18 h. The remaining steps were conducted at 4 °C, unless otherwise noted. The cells were harvested by centrifugation at 5,000 × g (20 min), diluted in 100 mL of resuspension buffer (50 mM potassium phosphate, pH 8.0), and lysed by brief sonication (five 20-s bursts at 50% power (Misonix sonicator, Farmingdale, NY)) followed by removal of cellular debris by centrifugation at

34

15,000 × g (30 min). Residual light membrane debris was removed by centrifugation at 45,000 rpm (2 h). The clarified crude supernatant was partially purified by anion exchange (primarily to remove small molecules) and HIS-Select (Sigma-Aldrich) Ni-affinity gel chromatography (PAM eluted in 150 to 200 mM imidazole). The fractions containing soluble PAM (~76 kDa) were combined (10 mL total), and subjected to iterative concentration-dilution cycles on size-exclusion centrifugal filtration (Centriprep® Centrifugal Filter Units 30,000 MWCO, Millipore, Billerica, MA) to concentrate the protein solution to 3 mL and dilute imidazole concentration to <1 μM. Low imidazole concentrations would not confound the efficiency of our in situ amino acid derivatization chemistry nor contaminate the GC column used routinely in these analyses. However, only 60% of the enzyme activity remained in the retentate compared to the activity before removing the imidazole; no significant activity was found in the flow-through, indicating that PAM either was being denatured in this step or was being compacted unrecoverably into the filtration mesh during the >6 h centrifugation. Therefore, to avoid further loss of enzyme activity while attempting to maximize protein purity and dilute the imidazole concentration, the batch of protein at this stage was used as the working stock in subsequent assays. The quantity of concentrated enzyme (~50 μg/mL) was assessed by SDS-PAGE and Coomassie Blue staining as described elsewhere, and this enzyme preparation was judged to be ~70% pure.[100] The modest protein purity of PAM obtained after two chromatography steps was attributed to the abundant total protein isolated from the large-scale (6 L) bacteria cell culture expressing *pam*. The protein milieu,

even after anion exchange chromatography, contained significant protein that bound non-specifically to the affinity gel along with the His$_6$-tagged PAM. No improvement in column selectivity was gained by varying the imidazole concentration and increasing the salt concentrations in the wash solutions, as suggested by the manufacturer, to reduce non specific binding.

1.3.6 General PAM Assay.

(2S)-α-Phenylalanine (~500 μM) was added to 1 mL of 50 mM phosphate buffer (pH 8.0) containing partially purified PAM (~1 μg) and incubated at 30 °C for 2 h, and the production of (3R)-β-phenylalanine was evaluated. The assay buffer was carefully basified (0.1 M sodium hydroxide) until pH ≥ 11, treated with acetic anhydride (2 × 300 μL for 20 min between each addition), and the reaction was quenched by acidifying to pH 2 with 1 M HCl. The N-acetyl amino acids were extracted with ethyl acetate (3 × 1 mL), the organic fractions were combined, and the carboxylic acids were methyl-esterified by diazomethane treatment. The solvent was removed *in vacuo*, and the derivatized amino acid mixture was dissolved in 300 μL ethyl acetate, and 1 μL of this solution was analyzed by coupled GC/EI-MS.

1.3.7 Assessment of Hydrogen Exchange during the PAM Reaction.

PAM enzyme (1 μg/mL) was incubated with [ring,2,3,3-^{2}H$_8$]-(2S)-α-phenylalanine (250 μM) in 12 mL of 50 mM phosphate buffer (pH 8.0) at 30 °C, and a 1-mL aliquot of sample was removed initially every 15 min up to 1 h, then

at various time intervals up to 50 h. A complementary experiment was conducted wherein the water (H$_2$O) of a 50 mM phosphate buffer solution (2 mL, pH 8.0) was removed *in vacuo*, the remaining phosphate salts were re-dissolved in D$_2$O (2 mL), and the deuterated solvent was evaporated. The sample was again diluted with 2 mL of D$_2$O, and to this volume was added PAM enzyme (1 μg) solvated by 100 μL of protio-labeled buffer and 100 μL of a 5 mM solution (in D$_2$O) of unlabeled α-phenylalanine; this reaction was incubated to a single stop-time of 17 h. The isolated α-phenylalanine isotopomers were converted to N-acetyl methyl esters as described previously and subjected to mass spectrometric analysis to assess the deuterium content.

1.3.8 *Synthesis of N-Acetyl (2S,3R)- and (2R,3S)-[2,3-^{2}H$_2$]-Phenylalanine Methyl Ester Racemate.*

Ethylbenzoylacetate

1. MeOH, H$^+$
2. NH$_4$OAc, MeOH
   reflux, 5 h, 90%
3. Acetyl Chloride, pyridine
   0 °C to 25 °C, 18 h, 95%

(Z)-Methyl-3-acetamido-3-phenylacrylate

D$_2$ (gas), 30 psi
10 % wt, Pd/C, MeOH: 98%

(2S, 3R)-, (2R, 3S)-N-acetyl-β-methyl ester racemate
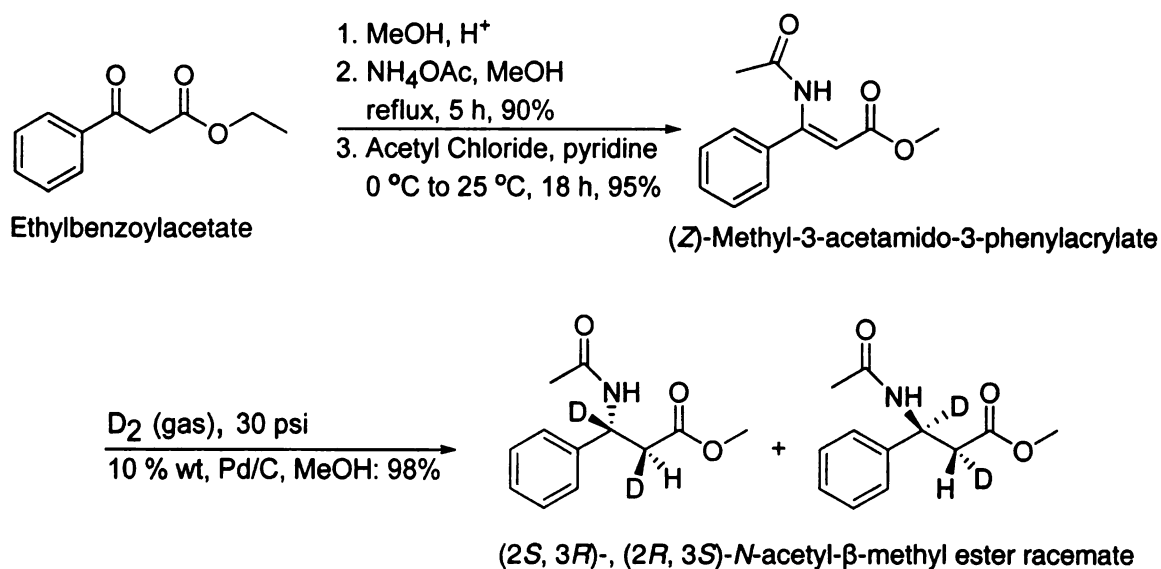
Scheme 1.12 Synthesis of (2S, 3R)-, (2R, 3S)-N-acetyl-β-methyl ester racemate.

The following synthesis procedure (Figure 1.12) is an adaptation of an established method.[111] To a stirred solution of ethyl benzoylacetate (57 mmol, 11 mL) dissolved in methanol was added concentrated sulfuric acid solution (0.5 mL). After 20 h, the solvent was evaporated and the resulting oil was partitioned between dichloromethane and water. The organic layer was collected and evaporated to yield methyl benzoylacetate, and used in the next step without further purification. The oil was dissolved in methanol (150 mL) and excess ammonium acetate (20 g) was added, and the solution was refluxed for 5 h. The reaction was cooled and the resulting crystals were removed by vacuum filtration. The solvent was then evaporated to yield the desired (Z)-methyl-3-amino-3-phenylacrylate enamine as an oil, which was purified over silica using 9:1 hexanes/ethyl acetate, v/v. A yield of 90% was obtained based on the ethyl benzoylacetate (9.0 g, 51 mmol). ^{1}H-NMR (300 MHz, CDCl$_3$): δ 3.70 (OCH_3), 4.98 (HC=C-), 7.48-7.60 (phenyl-H). GC/EI-MS: m/z 177 [M$^+$], 146 [M - OCH$_3$]$^+$.

1.3.10 Synthesis of (Z)-methyl -3-acetamido-3-phenylacrylate

To the purified enamine (11.3 mmol, 2 mL) in dry THF (50 mL) was added freshly distilled pyridine (10 mL), and the solution was cooled to 0 °C. Freshly distilled acetyl chloride (84.8 mmol, 7.5 eq., 6 mL) was added drop wise, and the reaction was warmed to room temperature and stirred overnight. Reaction progress was monitored by TLC, and additional acetyl chloride was added drop wise to complete the reaction. The sample was quenched by dilution with brine (50 mL) and extracted with chloroform (3 x 25 mL). The solvent was evaporated

and the *N*-acetyl enamine methyl ester was purified by silica gel (85:15 hexanes/ethyl acetate, (v/v)). The solvent was evaporated and the desired (*Z*)-methyl-3-acetamido-3-phenylacrylate was obtained quantitatively. 95% yield (2.3 g, 11 mmol). ^{1}H-NMR (300 MHz, CDCl$_3$): δ = 2.14 (s, C*H*$_3$C=O), 3.70 (s, OC*H*$_3$), 4.98 (s, C=C*H*), 7.48-7.60 (phenyl-*H*). GC/EI-MS: *m/z* 219 [M$^+$], 177 [M$^+$ - CH$_3$OH], 160 [M - CO$_2$CH$_3$ or M$^+$ - HNC(O)CH$_3$]$^+$.

1.3.11 *Synthesis of Dideuterio N-acetyl-(2S,3R)-, and -(2R,3S)-β-Phenylalanine Methyl Esters*

To the (*Z*)-acrylate (6.0 mmol, 1.3 g) dissolved in methanol (30 mL) in a Parr flask was added 10% w/w Pd/C (25 mg). The chamber was pressurized with deuterium gas at 30 psi to stereospecifically reduce the substrate by *syn*-addition. The reaction was shaken on a Parr Hydrogenator® for 24 h then filtered through Celite overlaying a short (~2 cm) column of silica to remove the catalyst. The methanol was evaporated to provide a racemic mixture of dideuterio *N*-acetyl-(2*S*,3*R*)- and (2*R*,3*S*)-β-phenylalanine methyl esters (> 98 % yield, 1.2 g). Proton-decoupled ^{2}H-NMR (79.77 MHz, ethyl acetate): δ = 2.82 (^{2}H at C2), 5.41 (^{2}H at C3). GC/EI-MS: *m/z* 223 [M$^+$], 180 [M$^+$ - CH$_3$C (O)], 100%), 149 [M$^+$ - HC(D)C(O)OCH$_3$], 20%). This compound was used to evaluate the stereochemistry of the hydrogen migration from C3 to C2 of the phenylpropanoid substrate in the PAM reaction. Since authentic β-phenylalanine specifically deuterium-labeled at C2 was not available, this synthetically-derived [^{2}H]-labeled

compound was also used to assess the extent of D- for H-exchange at C2 under the same basic and acidic conditions during the derivatization of the α- and β-phenylalanines to their *N*-acetyl methyl esters. Approximately 500 µM of the dideuterio *N*-acetyl amino acid ester was suspended in 1 ml of H_2O which was adjusted to pH 11 (0.1 M NaOH) in a 10 mL glass screw-capped tube and shaken vigorously (Vortex) for 1 min. The solution was then acidified (pH 2) with dropwise addition of 1 M HCl, and shaken for 1 minute. The suspension was extracted with ethyl acetate (300 µL), and the organic fraction was dried by passage through a column of sodium sulfate powder. A 1 µL aliquot of the eluant was analyzed by GC-EI/MS, and the diagnostic ion fragments revealed that the isotopic abundance of the base/acid-treated analyte was identical to that of the starting material, which was at 98% deuterium isotope enrichment, indicating that no H/D exchange occurred at C2 under the conditions outlined above.

1.3.12 *Evaluation of the Stereochemistry of the Hydrogen Migration in the PAM Reaction.*

^{1}H-NMR analysis of unlabeled (2*S*)-α- and (3*R*)-β-phenylalanines, at 200 µM each, dissolved in perdeuterio-ethyl acetate, was conducted to assess if the relative chemical shifts of the protons at C3 of the α-isomer and those at C2 of the β-isomer were well-resolved (Figure 1.8.4). Once the peak resolution was observed to be sufficient at 0.24 ppm, [3,3-^{2}H$_2$]-(2*S*)-α-phenylalanine (5 mM) was incubated with PAM (~ 50 µg) in each of two 1 mL samples (10 µmol substrate total) in phosphate buffer (pH 8.0) at 30 °C. The reaction progress and deuterium

40

distribution in the product were tracked by GC/MS analysis at regular intervals after the start of the reaction by removing aliquots (1 mL) from each sample, and the amino acids were derivatized as described earlier. Under these assay conditions, where 50-fold more protein was used than in a routine assay, the reaction was halfway to equilibrium at 6 h. Thus, the reaction was terminated at 10 h by careful basification to pH 10 (0.1 M sodium hydroxide solution), and the isotopomeric amino acids were derivatized as before, except that 20 µmol acetic acid was used. An estimated 830 µg of product (5 µmol, ~50 mol% conversion of substrate to product) was made, which was sufficient for analysis by ^{2}H NMR. The biosynthesized dideuterio-β-phenylalanine isotopomer was present at ~30% (~330 µg, 1.5 µmol) compared to the monodeuterio-β-isotopomer as judged by GC/EI-MS analysis. Diagnostic fragment ions were found at *m/z* 179 [PhC$_\alpha$D(NH)C$_\beta$H$_2$CO$_2$CH$_3^+$, 100%], 180 [PhC$_\alpha$D(NH)C$_\beta$DHCO$_2$CH$_3^+$, 28%], and 149 ([PhC(D)=NHAc$^+$], 20%). The dried mixture of derivatized deuterium-labeled α- and β-amino acids extracted from the aqueous assay solution was dissolved in 300 µL ethyl acetate and analyzed by proton-decoupled ^{2}H-NMR, with overnight scanning. The chemical shifts corresponding to the deuterium of the labeled β-phenylalanine in the sample were compared to those of the authentic (2*S*, 3*R*)- and (2*R*, 3S)-[2, 3-^{2}H$_2$]-*N*-acetyl β-phenylalanine methyl ester racemate dissolved in ethyl acetate to assess the stereochemistry at C2 of the biosynthetically-derived product. For reference, the [3,3-^{2}H$_2$]-(2*S*)-α-phenylalanine substrate (5 mM) was isolated from 1 mL of assay buffer (50 mM

phosphate buffer, pH 8.0) without PAM enzyme after a 12 h incubation at 30 °C. The substrate was derivatized to its *N*-acetyl methyl ester by described methods, dissolved in 300 μL ethyl acetate and analyzed by ^{2}H NMR.

1.3.13 *Assessment of the Kinetic Isotope Effect.*

PAM and an equal mixture of [ring, 2,3,3-^{2}H$_8$] - and unlabeled-(2S)-α-phenylalanine (500 μM of each) were incubated for 3 h until ~ 0.2% conversion of α- to β-phenylalanine (2.3 nmol) was observed under standard assay conditions. The amino acids were converted to their *N*-acetyl methyl esters as described previously, and the relative amounts of product derived from labeled and unlabeled substrate were compared. The isotopomers generated diagnostic base peak fragment ions in the mass spectrometer at *m/z* 178 (unlabeled product) (Table 1.1A), and at 185 and 186 (D$_7$ and D$_8$-labeled product, respectively) (Table 1.1B); the deuterium originating at C3 in the labeled substrate is partially lost during its transfer to C2 in the isomerization reaction. The ratio of the peak area for ion *m/z* 178 to the combined areas of ions *m/z* 185 and 186 was used to calculate the kinetic isotope effect on V_{max}/K_M in this competitive assay.[112]

1.3.14 *Measurement of the Equilibrium Constant*

To assess the equilibrium between product and substrate in the PAM reaction at 30 °C, α-phenylalanine at 100 μM was added to 10 mL of PAM (at ~25 μg/mL instead of 1 μg/mL used for routine assays) in 50 mM phosphate buffer (pH 8.0). Aliquots (1 mL) were withdrawn from the reaction at various time

42

points between 0.25-50 h. The reaction in each aliquot was stopped by careful addition of 0.1 M sodium hydroxide, and the amino acids were derivatized and analyzed by GC/EI-MS, as described above. The relative amounts of product and reactant at equilibrium were determined by linear regression analysis of the area of the base peak fragment ion of the derivatized α- or β-phenylalanines (m/z 162 and 178, respectively). Peak area was converted to concentration-of-product (or -substrate) by solving the corresponding linear equation, which was derived by plotting the area of the signature base peak ion, produced by the corresponding authentic N-acetyl-amino acid methyl ester standard, against the concentration of each standard in a dilution series ranging from 0 - 30 μM, at 5 μM intervals.

1.5 REFERENCES

1. Chen, H. P.; Wu, S. H.; Lin, Y. L.; Chen, C. M.; Tsay, S. S., Cloning, sequencing, heterologous expression, purification, and characterization of adenosylcobalamin-dependent D-ornithine aminomutase from *Clostridium sticklandii*. *J. Bio. Chem.* **2001,** *276*, (48), 44744-44750.

2. Frey, P. A.; Chang, C. H., Aminomutases. In *Chemistry and Biochemistry of B12*, ed.; Banerjee, R., John Wiley & Sons, Inc.: Hoboken, **1999**, 835-857.

3. Morley, C. G. D.; Stadtman, T. C., Fermentation of D-a-lysine. Purification and properties of an adenosine triphosphate regulated B12-coenzyme-dependent D-a-lysine mutase complex from *Clostridium sticklandii*. *Biochemistry* **1970,** *9*, (25), 4890-900.

4. Shinners, E. N.; Catlin, B. W., Arginine biosynthesis in Neisseria gonorrhoeae: enzymes catalyzing the formation of ornithine and citrulline. *J. Bacteriol.* **1978,** *136*, (1), 131-135.

5. Tsuda, Y.; Friedmann, H. C., Oxidation of Ornithine to 2-Amino-4-ketopentanoic Acid via 2,4-Diaminopentanoic Acid; Participation of B12 Coenzyme, Pyridoxal Phosphate, and Pyridine Nucleotide. *J. Biol. Chem.* **1970,** *245*, (22), 5914-5926.

6. Wolthers, K. R.; Rigby, S. E. J.; Scrutton, N. S., Mechanism of Radical-based Catalysis in the Reaction Catalyzed by Adenosylcobalamin-dependent Ornithine 4,5-Aminomutase. *J. Biol. Chem.* **2008,** *283*, (50), 34615-34625.

7. Aberhart, D. J.; Lin, H. J.; Weiller, B. H., Stereochemistry of lysine-2,3-aminomutase. *J. Am. Chem. Soc.* **1981,** *103*, (22), 6750.

8. Aberhart, D. J.; Gould, S. J.; Lin, H. J.; Thiruvengadam, T. K.; Weiller, B. H., Stereochemistry of lysine 2,3-aminomutase isolated from *Clostridium subterminale* strain SB4. *J. Am. Chem. Soc* **1983,** *105*, (16), 5461-5470.

9. Aberhart, D. J., Separation by high-performance liquid chromatography of a- and β-amino acids: application to assays of lysine 2,3-aminomutase and leucine 2,3-aminomutase. *Anal. Biochem.* **1988,** *169*, (2), 350.

10. Aberhart, D. J., Studies on the mechanism of lysine 2,3-aminomutase. *J. Chem. Soc., Perkin Transactions 1* **1988,** *2*, 343.

11. Aberhart, D. J.; Cotting, J. A., Mechanistic studies on lysine 2,3-aminomutase: Carbon-13-deuterium crossover experiments. *J. Chem. Soc., Perkin Transactions 1* **1988**, *8*, 2119-2122.

12. Baker, J. J.; Van der Drift, C.; Stadtman, T. C., Purification and properties of β-lysine mutase , a pyridoxal phosphate and B12 coenzyme dependent enzyme. *Biochemistry* **1973**, *12*, (6), 1054-1063.

13. Ballinger, M. D.; Frey, P. A.; Reed, G. H., Structure of a substrate radical intermediate in the reaction of lysine 2,3-aminomutase. *Biochemistry* **1992**, *31*, (44), 10782-10789.

14. Ballinger, M. D.; Reed, G. H.; Frey, P. A., An organic radical in the lysine 2,3-aminomutase reaction. *Biochemistry* **1992**, *31*, (4), 949-953.

15. Ballinger, M. D., Characterization of a substrate radical intermediate in the lysine-2,3-aminomutase reaction. **1993**, (DA9408546), 101.

16. Ballinger, M. D.; Frey, P. A.; Reed, G. H.; LoBrutto, R., Pulsed electron paramagnetic resonance studies of the lysine 2,3-aminomutase substrate radical: Evidence for participation of pyridoxal 5'-phosphate in a radical rearrangement. *Biochemistry* **1995**, *34*, (31), 10086-10093.

17. Baraniak, J.; Moss, M. L.; Frey, P. A., Lysine 2,3-aminomutase. Support for a mechanism of hydrogen transfer involving S-adenosylmethionine. *J. Biol. Chem.* **1989**, *264*, (3), 1357-1360.

18. Carroll, J.; Jonsson, E. N.; Ebel, R.; Hartman, M. S.; Holman, T. R.; Crews, P., Probing Sponge-Derived Terpenoids for Human 15-Lipoxygenase Inhibitors. *J. Org. Chem.* **2001**, *66*, (21), 6847-6851.

19. Chang, C. H.; Ballinger, M. D.; Reed, G. H.; Frey, P. A., Lysine-2,3-Aminomutase: Rapid Mix-Quench Electron Paramagnetic Resonance Studies Establishing the Kinetic Competence of a Substrate-Based Radical Intermediate. *Biochemistry* **1996**, *35*, (34), 11081-11084.

20. Chen, D.; Tanem, J.; Frey, P. A., Basis for the equilibrium constant in the interconversion of L-lysine and L-β-lysine by lysine 2,3-aminomutase. *Biochimica et Biophysica Acta - Proteins & Proteomics* **2007**, *1774*, (2), 297-302.

21. Chirpich, T. P.; Zappia, V.; Costilow, R. N.; Barker, H. A., Lysine 2,3-aminomutase. Purification and properties of a pyridoxal phosphate and S-adenosylmethionine-activated enzyme. *J. Biol. Chem.* **1970**, *245*, (7), 1778-1789.

22. Chirpich, T. P.; Barker, H. A., Lysine-2,3-aminomutase (Clostridium). In *Methods Enzymol.*, ed.; Colowick, S. P., Academic: New York, N. Y., **1971**; 17 (Pt. B), 215-222.

23. Cooper, A. J. L., Metal cofactor of lysine-2,3-aminomutase. *Chemtracts: Biochem. Mol. Biol.* **1991**, *2*, (5), 333-336.

24. Frey, P. A.; Moss, M. L., S-Adenosylmethionine and the mechanism of hydrogen transfer in the lysine 2,3-aminomutase reaction. *Cold Spring Harbor Symp. Quant. Biol.* **1987**, *52*, (Evol. Catal. Funct.), 571-577.

25. Frey, P. A.; Moss, M.; Petrovich, R.; Baraniak, J., The roles of S-adenosylmethionine and pyridoxal phosphate in the lysine 2,3-aminomutase reaction. *Ann. N. Y. Acad. Sci.* **1990**, *585*, (Vitamin B6), 368-378.

26. Frey, P. A., Lysine-2,3-aminomutase: is adenosylmethionine a poor man's adenosylcobalamin? *Faseb J.* **1993**, *7*, (8), 662-670.

27. Frey, P. A.; Reed, G. H., Lysine 2,3-aminomutase and the Mechanism of the Interconversion of Lysine and β-Lysine. In *Advances in Enzymology and Related Areas of Mol. Bio.*, ed.; **1993**; *66*, 1-39.

28. Frey, P. A.; Reed, G. H.; Moss, M. L.; Petrovich, R. M.; Ballinger, M. D.; Lieder, K. W.; Wu, W.; Chang, C. H.; Bandarian, V.; Ruzicka, F. J.; LoBrutto, R.; Beinert, H. In *The role of S-adenosylmethionine as a poor man's adenosylcobalamin in the reaction of lysine-2,3-aminomutase*, 1998; Kraeutler, B.; Arigoni, D.; Golding, B. T., Wiley-VCH Verlag GmbH, Weinheim, Germany.: 1998; **1996**, 435-446.

29. Frey, P. A.; Reed, G. H., Radical mechanisms in adenosylmethionine- and adenosylcobalamin-dependent enzymatic reactions. *Arch. Biochem. Biophys.* **2000**, 382, (1), 6-14.

30. Frost, J. W., Catalysis in a world with no petroleum. *Abstracts of Papers, 229th ACS National Meeting, San Diego, CA, United States, March 13-17,* **2005**.

31. Gould, S. J.; Thiruvengadam, T. K., Studies of nitrogen metabolism using C-13 NMR spectroscopy. 3. Synthesis of DL-[3-13C,2-15N]-lysine and its incorporation into streptothricin F1. *J. Am. Chem. Soc.* **1981**, *103*, (22), 6752-6754.

32. Jaffe, E. K.; Markham, G. D.; Rajagopalan, J. S., ^{15}N and ^{13}C NMR studies of ligands bound to the 280,000-dalton protein porphobilinogen synthase

elucidate the structures of enzyme-bound product and a Schiff base intermediate. *Biochemistry* **1990**, *29*, (36), 8345-8350.

33. James, C. L.; Viola, R. E., Production and Characterization of Bifunctional Enzymes. Domain Swapping To Produce New Bifunctional Enzymes in the Aspartate Pathway. *Biochemistry* **2002**, *41*, (11), 3720-3725.

34. Kilgore, J. L.; Aberhart, D. J., Lysine 2,3-aminomutase: role of S-adenosyl-L-methionine in the mechanism. Demonstration of tritium transfer from (2RS,3RS)-[3-3H]lysine to *S*-adenosyl-L-methionine. *J. Chem. Soc., Perkin Trans. 1* **1991**, (1), 79-84.

35. Kim, Y.-T.; Kurita, R.; Kojima, M.; Nishii, W.; Tanokura, M.; Muramatsu, T.; Ito, H.; Takahashi, K., Identification of arginine residues important for the activity of Escherichia coli signal peptidase I. *Bio. Chem* **2004**, *385*, (5), 381-388.

36. Kunz, F.; Retey, J.; Arigoni, D.; Tsai, L.; Stadtman, T. C., Absolute configuration of 3,5-diaminohexanoic acid from the β-lysine mutase reaction. *Helv. Chim. Acta* **1978**, *61*, (3), 1139-1145.

37. Lu, Z.; Nagata, S.; McPhie, P.; Miles, E. W., Lysine 87 in the b subunit of tryptophan synthase that forms an internal aldimine with pyridoxal phosphate serves critical roles in transimination, catalysis, and product release. *J. Bio. Chem.* **1993**, *268*, (12), 8727-8734.

38. Merkel, D.; Retey, J., Further insight into the mechanism of the irreversible inhibition of histidine ammonia-lyase by L-cysteine and dioxygen. *Helv. Chim. Acta* **2000**, *83*, (6), 1151-1160.

39. Morley, C. G. D.; Stadtman, T. C., Fermentation of D-.alpha.-lysine. Purification and properties of an adenosine triphosphate regulated B12-coenzyme-dependent D-.alpha.-lysine mutase complex from Clostridium sticklandii. *Biochemistry* **1970**, *9*, (25), 4890-900.

40. Morley, C. G. D.; Stadtman, T. C., Role of pyridoxal phosphate in the B12 coenzyme-dependent D-α-lysine mutase reaction. *Biochemistry* **1972**, *11*, (4), 600-605.

41. Moss, M.; Frey, P. A., The role of S-adenosylmethionine in the lysine 2,3-aminomutase reaction. *J. Biol. Chem.* **1987**, *262*, (31), 14859-14862.

42. Moss, M. L., The role of *S*-adenosylmethionine in the lysine-2,3-aminomutase reaction. **1989**, (DA8916438), 3974-3975.

43. Moss, M. L.; Frey, P. A., Activation of lysine 2,3-aminomutase by S-adenosylmethionine. *J. Biol. Chem.* **1990,** *265,* (30), 18112-18115.

44. Petrovich, R. M.; Ruzicka, F. J.; Reed, G. H.; Frey, P. A., Metal cofactors of lysine-2,3-aminomutase. *J. Biol. Chem.* **1991,** *266,* (12), 7656-7660.

45. Petrovich, R. M., Metal cofactors of lysine-2,3-aminomutase. **1992,** (DA9304174), 798.

46. Petrovich, R. M.; Ruzicka, F. J.; Reed, G. H.; Frey, P. A., Characterization of iron-sulfur clusters in lysine 2,3-aminomutase by electron paramagnetic resonance spectroscopy. *Biochemistry* **1992,** *31,* (44), 10774-10781.

47. Reed, G. H.; Ballinger, M. D., Characterization of a radical intermediate in the lysine 2,3-aminomutase reaction. *Methods Enzymol.* **1995,** *258,* 362-379.

48. Rétey, J.; Kunz, F.; Stadtman, T. C.; Arigoni, D., Mechanism of the . beta .-lysine - mutase reaction. *Experientia* **1969,** *25,* (8), 801-802.

49. Rétey, J.; Kunz, F.; Arigoni, D.; Stadtman, T. C., Studies on the b-lysine mutase reaction: Mechanism and steric course. *Helv. Chim. Acta* **1978,** *61,* (8), 2989-2998.

50. Ruzicka, F. J.; Lieder, K. W.; Frey, P. A., Lysine 2,3-aminomutase from Clostridium subterminale SB4: mass spectral characterization of cyanogen bromide-treated peptides and cloning, sequencing, and expression of the gene kamA in *Escherichia coli. J. Bacteriol.* **2000,** *182,* (2), 469-476.

51. Schmidt-Dannert, C.; De Boer, A. L.; Kwon, S. J. Genetically engineered bacteria for production of porphyrins. WO 2005012498, 2005.

52. Beatrix, B.; Zelder, O.; Linder, D.; Buckel, W., Cloning, sequencing and expression of the gene encoding the coenzyme B12-dependent 2-methyleneglutarate mutase from *Clostridium barkeri* in *Escherichia coli. Eur. J. Biochem.* **1994,** *221,* (1), 101-109.

53. Edwards, C. H.; Golding, B. T.; Kroll, F.; Beatrix, B.; Broker, G.; Buckel, W., Rotation of the exo-Methylene Group of 2-Methyleneglutarate Catalyzed by Coenzyme B12-dependent 2-Methyleneglutarate Mutase from Clostridium barkeri. *J. Am. Chem. Soc.* **1996,** *118,* (17), 4192-4193.

54. Forst, C. V.; Schulten, K., Phylogenetic Analysis of Metabolic Pathways. *J. Mol. Evol.* **2001,** *52,* (6), 471-489.

55. Hartrampf, G.; Buckel, W., On the steric course of the adenosylcobalamin-dependent 2-methyleneglutarate mutase reaction in *Clostridium barkeri*. *Eur. J. Biochem.* **1986,** *156*, (2), 301-304.

56. Kapatral, V.; Anderson, I.; Ivanova, N.; Reznik, G.; Los, T.; Lykidis, A.; Bhattacharyya, A.; Bartman, A.; Gardner, W.; Grechkin, G.; Zhu, L.; Vasieva, O.; Chu, L.; Kogan, Y.; Chaga, O.; Goltsman, E.; Bernal, A.; Larsen, N.; D'Souza, M.; Walunas, T.; Pusch, G.; Haselkorn, R.; Fonstein, M.; Kyrpides, N.; Overbeek, R., Genome Sequence and Analysis of the Oral Bacterium Fusobacterium nucleatum Strain ATCC 25586. *J. Bacteriol.* **2002,** *184*, (7), 2005-2018.

57. Kaplan, B. H.; Stadtman, E. R. In *Ethanolamine deaminase (Clostridium species)*, Methods Enzymol., 1971; Colowick, S. P., Academic, New York, N. Y.: **1971**; Issue Pt. B, 818-24.

58. Karlsson, S.; Lindberg, A.; Norin, E.; Burman, L. G.; Akerlund, T., Toxins, Butyric Acid, and Other Short-Chain Fatty Acids Are Coordinately Expressed and Down-Regulated by Cysteine in *Clostridium difficile*. *Infect. Immun.* **2000,** *68*, (10), 5881-5888.

59. Michel, C.; Hartrampf, G.; Buckel, W., Assay and purification of the adenosylcobalamin-dependent 2-methyleneglutarate mutase from *Clostridium barkeri*. *Eur. J. Biochem.* **1989,** *184*, (1), 103-107.

60. Michel, C.; Buckel, W.; Linder, D., Purification of the coenzyme B12-containing 2- methyleneglutarate mutase from Clostridium barkeri by high-performance liquid chromatography. *J. Chromatogr.* **1991,** *587*, (1), 93-9.

61. Michel, C.; Buckel, W., Coenzyme B12-dependent 2- methyleneglutarate mutase from Clostridium barkeri. Protection by the substrate from inactivation by light. *FEBS Lett.* **1991,** *281*, (1-2), 108-110.

62. Michel, C.; Albracht, S. P. J.; Buckel, W., Adenosylcobalamin and cob(II)alamin as prosthetic groups of 2- methyleneglutarate mutase from *Clostridium barkeri*. *Eur. J. Biochem.* **1992,** *205*, (2), 767-773.

63. Stadtman, T. C.; Renz, P., Anaerobic degradation of lysine. V. Properties of the cobamide coenzyme-dependent . beta .- lysine mutase of *Clostridium sticklandii*. *Arch. Biochem. Biophys.* **1968,** *125*, (1), 226-239.

64. Stadtman, T. C.; Grant, M. A. In *D-α-Lysine mutase (Clostridium)*, Methods Enzymol., 1971; Colowick, S. P., Academic, New York, N. Y.: **1971**; Pt. B, 211-215.

65. Stadtman, T. C.; Grant, M. A. In *L-β-Lysine mutase (Clostridium sticklandii)*, Methods Enzymol., 1971; Colowick, S. P., Academic, New York, N. Y.: **1971**; Pt. B, 206-211.

66. Valentin, H. E.; Mitsky, T. A.; Mahadeo, D. A.; Tran, M.; Gruys, K. J., Application of a Propionyl Coenzyme A Synthetase for Poly(3-Hydroxypropionate-co-3-Hydroxybutyrate). Accumulation in Recombinant Escherichia coli. *Appl. Environ. Microbiol.* **2000**, *66*, (12), 5253-5258.

67. Zelder, O.; Buckel, W., On the role of two different cobalt(II) species in coenzyme B12-dependent 2-methyleneglutarate mutase from *Clostridium barkeri. Biol. Chem. Hoppe-Seyler* **1993**, *374*, (1), 85-90.

68. Zelder, O.; Beatrix, B.; Leutbecher, U.; Buckel, W., Characterization of the coenzyme-B12-dependent glutamate mutase from Clostridium cochlearium produced in *Escherichia coli. Eur. J. Biochem.* **1994**, *226*, (2), 577-585.

69. Kozarich, J. W., S-Adenosylmethionine-dependent enzyme activation. *BioFactors* **1988**, *1*, (2), 123-128.

70. Sofia, H. J.; Chen, G.; Hetzler, B. G.; Reyes-Spindola, J. F.; Miller, N. E., Radical SAM, a novel protein superfamily linking unresolved steps in familiar biosynthetic pathways with radical mechanisms: functional characterization using new analysis and information visualization methods. *Nucl. Acids Res.* **2001**, *29*, (5), 1097-1106.

71. Krasotkina, J.; Walters, T.; Maruya, K. A.; Ragsdale, S. W., Characterization of the B-12- and iron-sulfur-containing reductive dehalogenase from *Desulfitobacterium chlororespirans. J. Bio. Chem.* **2001**, *276*, (44), 40991-40997.

72. Maillard, J.; Schumacher, W.; Vazquez, F.; Regeard, C.; Hagen, W. R.; Holliger, C., Characterization of the corrinoid iron-sulfur protein tetrachloroethene reductive dehalogenase of *Dehalobacter restrictus. Appl. Environm. Microbio.* **2003**, *69*, (8), 4628-4638.

73. Schumacher, W.; Holliger, C.; Zehnder, A. J. B.; Hagen, W. R., Redox chemistry of cobalamin and iron-sulfur cofactors in the tetrachloroethene reductase of *Dehalobacter restrictus. Febs Lett.* **1997**, *409*, (3), 421-425.

74. Thibodeau, J.; Gauthier, A.; Duguay, M.; Villemur, R.; Lepine, F.; Juteau, P.; Beaudet, R., Purification, cloning, and sequencing of a 3,5-dichlorophenol reductive dehalogenase from *Desulfitobacterium frappieri* PCP-1. *Appl. Environ. Microbio.* **2004**, *70*, (8), 4532-4537.

75. Murakami, K.; Hashimoto, Y.; Murooka, Y., Cloning and characterization of the gene encoding glutamate 1 - semialdehyde 2 , 1 - aminomutase , which is involved in .delta.-aminolevulinic acid synthesis in *Propionibacterium freudenreichii. Appl. Environ. Microbiol.* **1993,** *59,* (1), 347-350.

76. Contestabile, R.; Jenn, T.; Akhtar, M.; Gani, D.; John, R. A., Reactions of Glutamate 1-Semialdehyde Aminomutase with R- and S-Enantiomers of a Novel, Mechanism-Based Inhibitor, 2,3-Diaminopropyl Sulfate. *Biochemistry* **2000,** *39,* (11), 3091-3096.

77. Ilag, L. L., Genes in *Escherichia coli* and *Arabidopsis thaliana* that encode glutamate -1-semialdehyde 2 , 1-aminomutase , an enzyme in tetrapyrrole biosynthesis. **1993,** (DA9329357), 2901-2902.

78. Jordan, P. M., Highlights in haem biosynthesis. *Curr. Opin. struct. biol.* **1994,** *4,* (6), 902-911.

79. Singh, M. P.; Mroczenski-Wildey, M. J.; Steinberg, D. A.; Andersen, R. J.; Maiese, W. M.; Greenstein, M., Biological activity and mechanistic studies of *andrimid. J. Antibiot.* **1997,** *50,* (3), 270-273.

80. Yu, X. P.; Zhu, J. L.; Yao, X. P.; He, S. C.; Huang, H. N.; Chen, W. L.; Hu, Y. H.; Li, D. B., Identification of anrF gene, a homology of admM of andrimid biosynthetic gene cluster related to the antagonistic activity of *Enterobacter cloacae* B8. *World J. Gastroenterol.* **2005,** *11,* (39), 6152-6258.

81. Christenson, S. D.; Liu, W.; Toney, M. D.; Shen, B., A novel 4-methylideneimidazole-5-one-containing tyrosine aminomutase in enediyne antitumor antibiotic C-1027 biosynthesis. *J. Am. Chem. Soc.* **2003,** *125,* (20), 6062-6063.

82. Christenson, S. D.; Wu, W.; Spies, M. A.; Shen, B.; Toney, M. D., Kinetic analysis of the 4-methylideneimidazole-5-one-containing tyrosine aminomutase in enediyne antitumor antibiotic C-1027 biosynthesis. *Biochemistry* **2003,** *42,* (43), 12708-12718.

83. Montavon, T. J.; Christianson, C. V.; Festin, G. M.; Shen, B.; Bruner, S. D., Design and characterization of mechanism-based inhibitors for the tyrosine aminomutase *Sg*TAM. *Bioorg. Med. Chem. Lett.* **2008,** *18,* (10), 3099-102.

84. Parry, R. J.; Kurylo-Borowska, Z., Biosynthesis of amino acids. Investigation of the mechanism of β-tyrosine formation. *J. Am. Chem. Soc.* **1980,** *102,* (2), 836-837.

85. Prabhakaran, P. C.; Woo, N.-T.; Yorgey, P. S.; Gould, S. J., Biosynthesis of blasticidin S from L-α-arginine. Stereochemistry in the arginine-2,3-aminomutase reaction. *J. Am. Chem. Soc.* **1988,** *110,* 5785-5791.

86. Klettke, K. L.; Sanyal, S.; Mutatu, W.; Walker, K. D., β-Styryl- and β-aryl-β-alanine products of phenylalanine aminomutase catalysis. *J. Am. Chem. Soc.* **2007,** *129,* (22), 6988-6989.

87. Mutatu, W.; Klettke, K. L.; Foster, C.; Walker, K. D., Unusual Mechanism for an Aminomutase Rearrangement: Retention of Configuration at the Migration Termini. *Biochemistry* **2007,** *46,* (34), 9785-9794.

88. Steele, C. L.; Chen, Y.; Dougherty, B. A.; Hofstead, S.; Lam, K. S.; Li, W.; Xing, Z. *Taxus* Phenylalanine Aminomutase and Methods to Improve Taxol Production. Patent: WO 03/066871 A2, February 10, 2003.

89. Steele, C. L.; Chen, Y.; Dougherty, B. A.; Li, W.; Hofstead, S.; Lam, K. S.; Xing, Z.; Chiang, S.-J., Purification, cloning, and functional expression of phenylalanine aminomutase: the first committed step in Taxol side-chain. biosynthesis. *Arch. Biochem. Biophys.* **2005,** *438,* (1), 1-10.

90. Walker, K. D.; Floss, H. G., Detection of a phenylalanine aminomutase in cell-free extracts of *Taxus brevifolia* and preliminary characterization of its reaction. *J. Am. Chem. Soc.* **1998,** *120,* (21), 5333-5334.

91. Walker, K. D.; Klettke, K.; Akiyama, T.; Croteau, R., Cloning, heterologous expression, and characterization of a phenylalanine aminomutase involved in Taxol biosynthesis. *J. Bio. Chem.* **2004,** *279,* (52), 53947-53954.

92. Wu, B.; Szymanski, W.; Wietzes, P.; de Wildeman, S.; Poelarends, G. J.; Feringa, B. L.; Janssen, D. B., Enzymatic Synthesis of Enantiopure α- and β-Amino Acids by Phenylalanine Aminomutase-Catalysed Amination of Cinnamic Acid Derivatives. *Chembiochem* **2009,** *10,* (2), 338-344.

93. Calabrese, J. C.; Jordan, D. B.; Boodhoo, A.; Sariaslani, S.; Vannelli, T., Crystal structure of phenylalanine ammonia lyase: Multiple helix dipoles implicated in catalysis. *Biochemistry* **2004,** *43,* (36), 11403-11416.

94. Asano, Y.; Endo, K., Amino-Acid Racemase with Broad Substrate-Specificity, Its Properties and Use in Phenylalanine Racemization. *Appl. Microbiol. Biotechn.* **1988,** *29,* (6), 523-527.

95. Asano, Y.; Kato, Y.; Levy, C.; Baker, P.; Rice, D., Structure and function of amino acid ammonia-lyases. *Biocatal. Biotransform.* **2004,** *22,* (2), 133-138.

96. Hoofnagle, A. N.; Resing, K. A.; Ahn, N. G., Protein analysis by hydrogen exchange mass spectrometry. *Ann. Rev. Biophys. Biomol. Struct.* **2003,** *32,* 1-25.

97. Englander, S. W., Hydrogen exchange and mass spectrometry: A historical perspective. *J. Am. Soc. Mass Spectrometry* **2006,** *17,* (11), 1481-1489.

98. Wales, T. E.; Engen, J. R., Hydrogen exchange mass spectrometry for the analysis of protein dynamics. *Mass Spectr. Rev.* **2006,** *25,* (1), 158-170.

99. Maier, C. S.; Deinzer, M. L., Protein conformations, interactions, and H/D exchange. *Methods in Enzymology* **2005,** 402, (Biological Mass Spectrometry), 312-360.

100. Woodward, C.; Simon, I.; Tuechsen, E., Hydrogen exchange and the dynamic structure of proteins. *Mol. Cell. Biochem.* **1982,** *48,* (3), 135-160.

101. Gloge, A.; Zon, J.; Kövári, Á.; Poppe, L.; Rétey, J., Phenylalanine ammonia-lyase: The use of its broad substrate specificity for mechanistic investigations and biocatalysis-synthesis of L-arylalanines. *Chemistry - A Eur. J.* **2000,** *6,* (18), 3386-3390.

102. Holz, J.; Monsees, A.; Jiao, H.; You, J.; Komarov, I. V.; Fischer, C.; Drauz, K.; Borner, A., Synthesis of a new chiral bisphospholane ligand for the Rh(I)-catalyzed enantioselective hydrogenation of isomeric b-acylamido acrylates. *J. Organic Chem.* **2003,** *68,* (5), 1701-1707.

103. Northrop, D. B., Deuterium and tritium kinetic isotope effects on initial rates. *Method. Enzymol.* **1982,** *87,* (Enzyme Kinet. Mech., Pt. C), 607-625.

CHAPTER 2

Analysis of the Substrate Specificity of Phenylalanine Aminomutase (PAM)

2.1 INTRODUCTION

β-Amino Acid-Based Natural Product Pharmaceuticals

β-amino acids in general are constituents of several antibiotics and pharmaceutically-active natural products, such as januvia, blasticidin and taxol.

Januvia (sitagliptin phosphate) (Figure 2.1) is a first in a class of new oral medication which has been approved by the U.S. Food and Drug Administration for management of Type 2 diabetes.[1] It is in the category of drugs called (DPP-4) dipeptidyl-peptidase 4 inhibitors. DPP-4 is responsible for breaking down the proteins that stimulate insulin producing cells after a meal. If DPP-4 is inhibited, then the proteins can activate the release of insulin for a longer period of time, thereby lowering the glucose level in the blood. It is prescribed for Type 2 diabetes only.

Blasticidin S (Figure 2.4) is an antibiotic used to prevent the growth of both eukaryotic and prokaryotic cells, and functions by inhibiting peptide bond formation with the ribosome.[2]

Taxol (Figure 2.1) is a taxane diterpenoid[3-13] used to treat several cancers including ovarian,[14-31] metastatic breast (anthracycline-resistant), non-small cell lung cancer, small-cell lung cancer, squamous cancers of the head and neck and AIDS-related Kaposi's sarcoma[32-34] and some leukemias.[35-38] Cancer is the second cause of mortality in the USA and is responsible for one in four deaths.

The annual sale of Taxol[®] in 2006 reached 3 billion USA dollars. It is currently under investigation for the potential treatment of several other diseases including polycystic kidney diseases,[39] coronary retenosis[40-42] and Alzheimer's.[43-51] Although Taxol is a promising drug, there remain the challenges of drug resistance that is commonly observed with most antibiotics. Therefore, the development of alternative or next generation analogues of an existing drug becomes paramount. Biocatalysis offers the most flexible synthetic method of accessing second generation Taxols, which requires the optimization of selected enzymes found in the biosynthetic pathway of paclitaxel.

Other drugs that contain β-amino acids in their structures include the amino peptidase inhibitor bestatin[52] from *Streptomyces globisporous,* the anti-type II diabetes drug januvia,[53-58] myomycin, viomycin,[59] roseothricin, geomycin and tuberactinomycin.[59] Single β-aryl-β-alanines have been shown to have anti-epileptogenesis activity,[60] while other amino acids have been used as building blocks toward the synthesis of complex bioactive molecules, including β-lactams and β-peptides as mimics of α-peptide hormones and as antimicrobial compounds.[61]
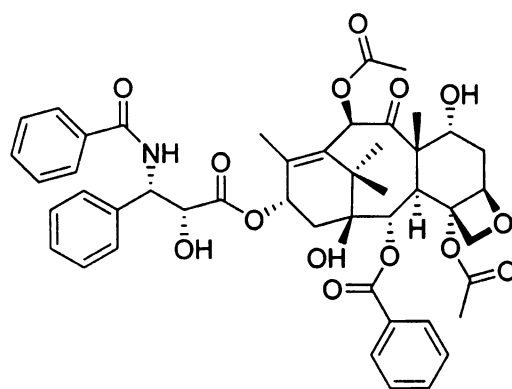
Paclitaxel (Taxol®)
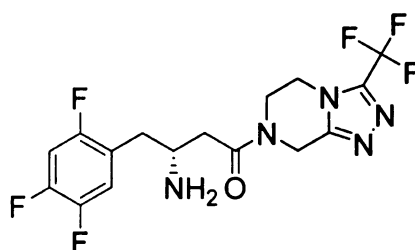
Januvia

Figure 2.1 Structure of taxol and januvia

Current sources of Paclitaxel

A semi-synthetic method was developed as a viable approach to address the supply issue.[6,62-68] This process involves extracting an advanced Taxol precursor, baccatin III, from the leaves of the European Yew *Taxus baccatta,* and from *T. wallichiana or T. cuspidata.* This precursor is protected at C7 position and coupled with an *N*-benzoyl phenylisoserine side chain precursor, as a synthesized β-lactam (Scheme 2.2). This is a relatively efficient process wherein a kilogram of either 10-deacetylbaccatin III or baccatin III can be converted into about 0.6 to 0.7 kg Taxol.[66,69]

R$_1$, R$_2$ = H: 10-Deacetylbaccatin III

R$_1$ = H, R$_2$ = Ac: Baccatin III

R$_1$ = SiEt$_3$, R$_2$ = Ac :7-TES-baccatin III
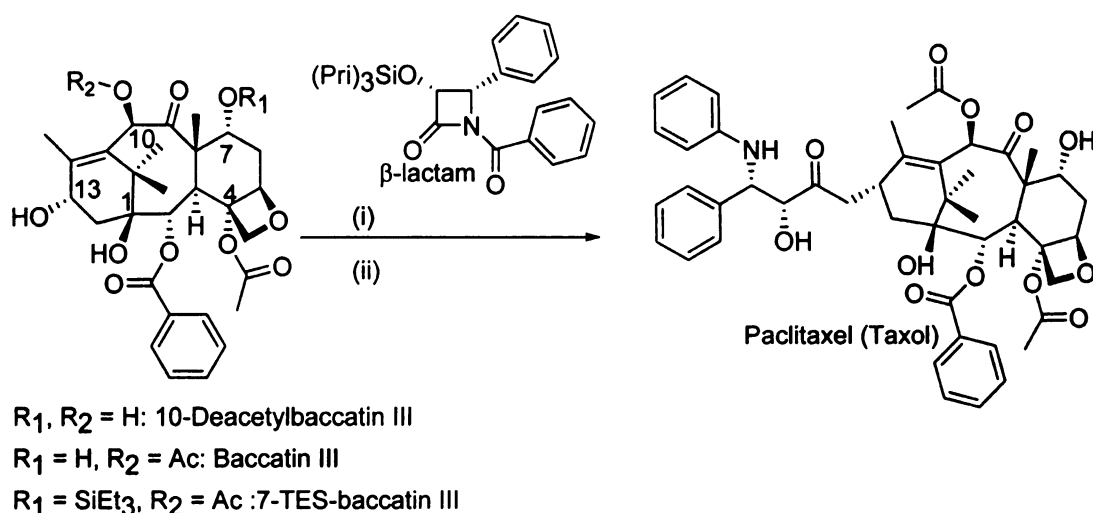
Scheme 2.2 Coupling of baccatin III with a β-lactam produces Taxol in two steps; (i) NaH, THF, β-lactam and (ii) HF, pyridine. The β-lactam was synthesized in seven steps.

Recently, Bristol-Myers Squibb collaborated with Phyton to develop a plant tissue culture technique i.e. a plant cell fermentation (PCF) technology[70-82] to produce paclitaxel. In this biosynthetic process, calli cultures of a specific *Taxus* cell line are propagated in aqueous medium in large fermentation tanks. The cell cultures are treated with methyl jasmonate to induce paclitaxel production, and paclitaxel is then extracted directly from cell cultures. The *Taxus* plant cell culture fermentation improved the sustainability and titers of the paclitaxel supply.[80,83] While the plant cell culture technique offers a sustainable resource, it does not offer the flexibility to produce modified paclitaxels with greater efficacy in terms of solubility, cytotoxicity, or targeted delivery, hence the

need to continue to explore better methods of synthesis by optimizing some enzymatic steps involved in the biosynthesis of this important drug.

Taxol Biosynthesis

In *Taxus* plants paclitaxel biosynthesis is initiated from the metabolism of methylerythritol phosphate (MEP)[84] pathway, which stems from the glyceraldehydes and pyruvate.[85-91] MEP is isomerized to isopentyl diphosphate and dimethylallyl phosphate.[92-94] Three IPP and two DMAP molecules condense to form the diterpenoid progenitor geranylgeranyl diphosphate (GGPP)[95] by action of a geranylgeranyl diphosphate synthase (GGPPS). Taxadiene synthase (TS) then cyclizes GGPP to form the tricyclic taxa-4(20),11(12)-diene. Eight cytochrome P450 mediated hydroxylation,[96-122] three acyl/aroyl CoA dependent transferases [taxadiene-5α-ol-*O*-acetyl transferase (TAT), 2α-*O*-benzoyltransferase (TBT) and 10-deacetylbaccatin-10-acetyl transferase (DBAT)], and a presumed rearrangement of an acetoxy oxirane to an oxetane formation) (Scheme 2.3)[100] results in the formation of baccatin III.

The biosynthesis and attachment of the C13 side chain for the baccatin III moiety involves 5 steps. First, is the conversion of (*S*)-α-phenylalanine to (*R*)-β-phenylalanine by a phenylalanine aminomutase, secondly the β-amino acid is coupled to coenzyme A by a putative ligase,[123-128] and the third step involves the transfer of the phenylpropanoid to the baccatin III core by a phenylpropanoyltransferase to form *N*-debenzoyl-2'-deoxypaclitaxel.[129]

Hydroxylation at the 2' position by a P450 is the penultimate step followed by benzoylation by a *N*-benzoyltransferase utilizing benzoyl CoA as a substrate.[130,131]
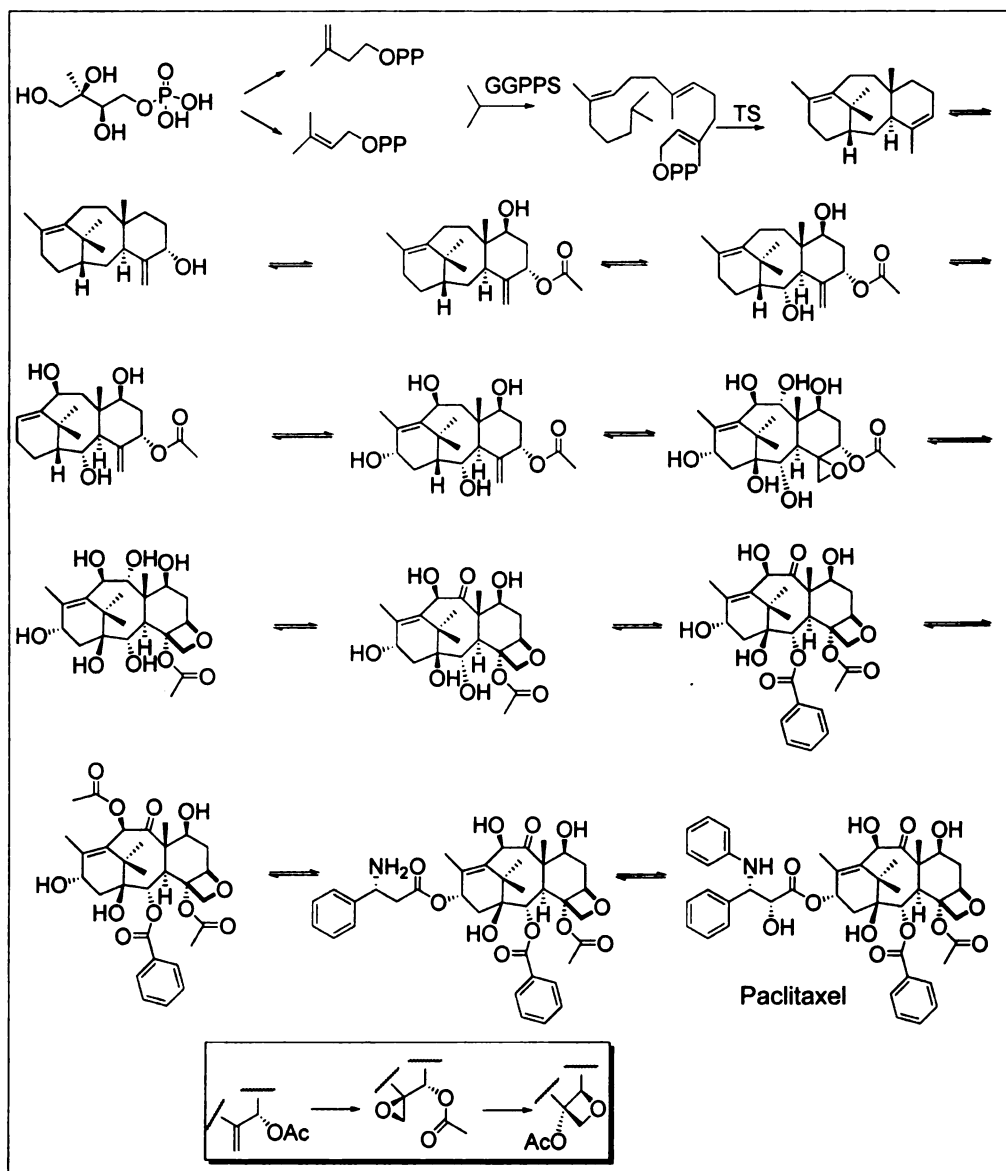
Scheme 2.3 Biosynthesis of paclitaxel. The proposed mechanism for the oxetane ring formation is shown in the inset.

Strategies for synthesizing β amino acids

Several strategies have been used for the synthesis of various substituted

β-amino-β-arylpropionic acids that include multi-step processes, and one pot

procedures such as the Knoevenagel condensation of benzaldehyde and malonic acid in the presence of an amine source (e.g. NH_4OAC).[132] Recently,

Node and co-workers reported a method of synthesizing β-amino acids through a Michael addition of a chiral amine to α,β- unsaturated esters, and the stereoselectivity was inverted by changing the solvent from diethyl ether to tetrahydrofuran (THF) when α,β-esters having an aromatic ring at the β-position were employed.[133] Good yields of β-amino acids with an enantiomeric excess of 82-99% have been reported, but the starting materials are protected as N-methoxycarbamates and the reaction is catalyzed and stereocontrolled by chiral pyrrolidines derivatives, which are difficult to access.[177] Recently, Parra reported a new approach to β-amino acids synthesis, which is based on the addition of dianions of carboxylic acids to isocyanates under acidic conditions.[134] The dianions are generated using lithium cyclohexylisopropylamide as base at -78 °C.

All the chemical methods reported so far use solvents which are toxic to the environment. However, there are presently no reports on biosynthetic strategies toward the production of asymmetric β-aryl-β-alanines from the corresponding α-isomers which are greener in nature. Tyrosine aminomutase (TAM) from *Streptomyces globisporous* is involved in the biosynthesis of enediyne C-1027 anti-tumor agent, TAM also has broad substrate specificity and is able to accept ring-chlorinated tyrosines as substrates.[135,136]

The *Taxus* phenylalanine aminomutase (PAM) (Scheme 2.11) provides a potential alternative route toward scalable production of novel β–amino acids as

drug intermediates. This isomerase shows high amino acid sequence homology (56% similarity) to a family of ammonia lyases that have broad substrate specificities with derivatives of aromatic amino acids.[137] Despite the wealth of information on the substrate specificity of the MIO-based reactions of the ammonia lyase family, there remains a paucity of investigation on the scope of the substrate specificity of the PAM enzyme. The potential of the mutase enzyme to biocatalyze the production of novel β-amino acids prompted a survey of several commercially-available *S*-α-amino arylpropanoic acids as substrates to examine specificity.
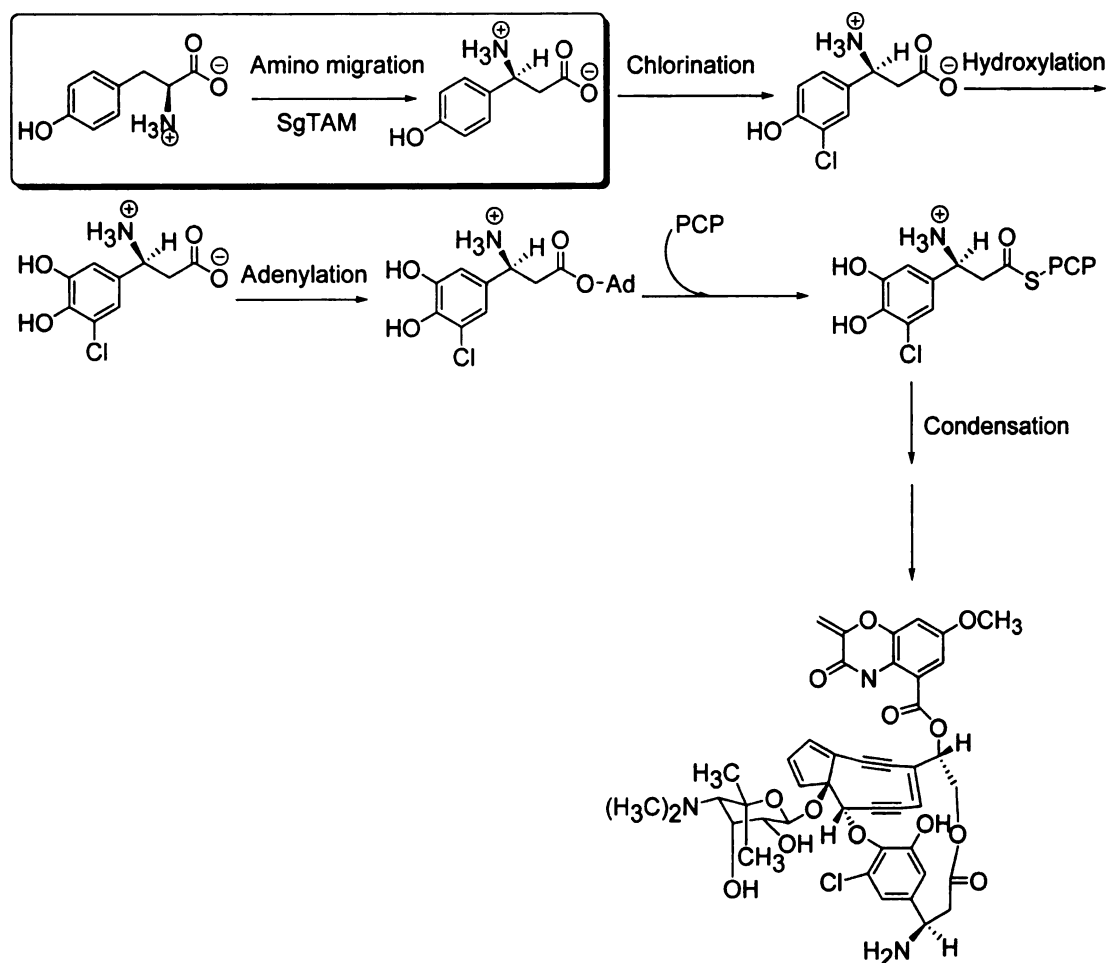
Scheme 2.4 Biosynthesis of C-1027 an antibiotic and antitumor agent isolated from *Streptomyces globisporous*. The first step of one of the biosynthetic branches to C-1027 is catalyzed by tyrosine aminomutase which converts α-tyrosine to β-tyrosine (inset)

2.2 RESULTS AND DISCUSSION

2.2.2 RESULTS

2.2.2.1 Substrate specificity evaluation

Enzyme assays were conducted with 25-50 µg/mL (> 70% pure) PAM of enzyme at 31 °C, over 3 h and the productive substrates are shown in Table 2.1. For poor substrates such as 4'-t-butyl-α-phenylalanine and (2S)-styrylalanine the reactions were incubated with 500 µg/mL enzyme for 3 h in order to increase the product yield at steady-state.

Table 2.1 Kinetic Parameters of PAM with various substrates. The V_{rel} is the ratio of V_{MAX} for a particular substrate and V_{MAX} of phenylalanine. The standard deviations are indicated in parenthesis.
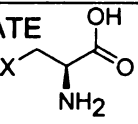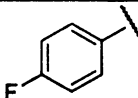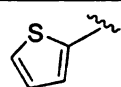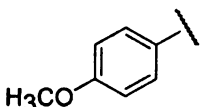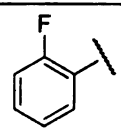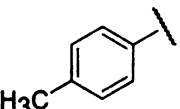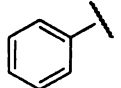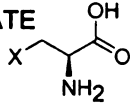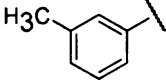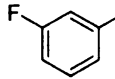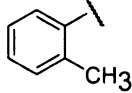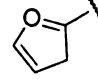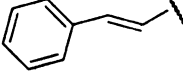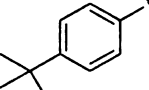
SUBSTRATE	K_M (µM)	V_{MAX} (nmol•h^{-1})	V_{MAX}/K_M (nmol• h^{-1}•µM^{-1})	V_{rel}
1	75 (17)	180 (10)	2.4 (0.6)	95 (7)
2	35 (8)	26 (1)	0.74 (0.17)	14 (1)
3	410 (46)	48 (1)	0.12 (0.01)	25 (1)
4	330 (65)	14 (1)	0.042 (0.01)	7.4 (<1)
5	160 (39)	4.4 (0.1)	0.028 (0.007)	2.3 (0.1)
6	97 (6)	1.9 (0.1)	0.020 (0.002)	1.0 (0.1)

Table 2.1 (continued)

SUBSTRATE	K_M (μM)	V_{MAX} (nmol·h^{-1})	V_{MAX}/K_M (nmol·h^{-1}·μM^{-1})	V_{rel}
7 (H3C-phenyl)	944 (100)	17 (0.15)	0.018 (0.0012)	8.9 (0.75)
8 (F-phenyl)	560 (60)	3.2 (0.30)	0.0057 (5.2 x 10^{-4})	1.7 (0.15)
9 (ortho-CH3 phenyl)	50 (5)	0.11 (0.01)	2.2 x 10^{-3} (3.0x10^{-4})	0.058 (0.006)
10 (furan)	410 (60)	0.03 (0.001)	7.3x10^{-5} (1.0x10^{-5})	0.016 (0.001)
11 (styryl)	780 (71)	0.078 (0.001)	1.0x10^{-4} (1.0x10^{-5})	0.041 (0.002)
12 (tert-butyl phenyl)	~10^{3}	<0.01	<<10^{-5}	<<0.001

β-amino acids were commercially-available for use as reference products, in derivatized form, except styryl-β-alanine which was synthesized as described below. Given the strict stereospecificity of PAM for S-phenylalanine and stereoselectivity for the production of R-β-isomer it was conceived that all of the unnatural β-amino acids made biosynthetically were also R. A chiral column however was used to establish the stereochemistry of the β-products by GC/MS analysis.

2.2.2 *Stereochemistry of the β-amino acids*

The catalytic efficiency at ~0.02 $nmol \cdot h^{-1} \cdot \mu M^{-1}$ of PAM for the 3'- and 4'-methyl-α-phenylalanine substrate (**7** and **5**, respectively) is nearly equal to the value for the natural substrate (**6**) (Table 2.1). However, noticeably higher V_{rel} values of 8.9 and 2.3 for the **7** and **5**, respectively, were observed (Table 2.1), while a V_{rel} at 0.05 and catalytic efficiency at 0.0022 $nmol \cdot h^{-1} \cdot \mu M^{-1}$ for the isomerization of the 2'-methyl regioisomer (**9**) was substantially lower. This apparent rate decrease is likely related to steric interactions of the *ortho*-methyl group (in place of H at one of the two *ortho*-carbons) (Figure 2.6) with active site residues, or the MIO, resulting in non-productive binding.

The V_{max} of PAM for 4'-*t*-butyl-α-phenylalanine (**12**) was slower ($V_{rel} <$ 0.001) than **6**; however, the modest isomerization of **12** reveals that the PAM active site can occupy a relatively bulky, aliphatic substituent at the *para*-position of the substrate (Figure 2.7). However, the nine —C—C—H bond extensions of the *t*-butyl group likely places **12** near the steric limits of the active site compared to the smaller 4'-methyl homolog **5**.
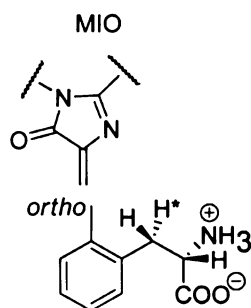
Figure 2.6 The aromatic ring attack on the terminal double of the catalytic MIO could be blocked by the presence of a methyl group at the *ortho-* position of the substrate L-phenylalanine leading to lower reactivity compared with the natural substrate.

Phenylalanine analogs bearing electron-withdrawing or electron-donating groups on the aromatic ring were used to investigate the effects of electron induction on PAM at steady-state. The catalytic efficiency of PAM catalysis for the 4'-fluoro-α-regioisomer (**1**) at 2.4 nmol•h^{-1}•μM^{-1} was greatest of all of the substrates tested. The 2'-fluoro isomer (**4**) was less efficiently catalyzed (0.027 nmol•h^{-1}•μM^{-1}) by ~60-fold compared to **1**, while the 3'-fluoro isomer (**8**) was even less efficiently isomerized (0.0057 nmol•h^{-1}•μM) by ~400-fold (Table 2.1). The turnover of each fluorinated substrate was greater than for phenylalanine. In general an electron-withdrawing flouro on the ring of the substrate may increase the acidity of the β_H of the substrate (Figure 2.8), thus increasing the overall reaction rate.
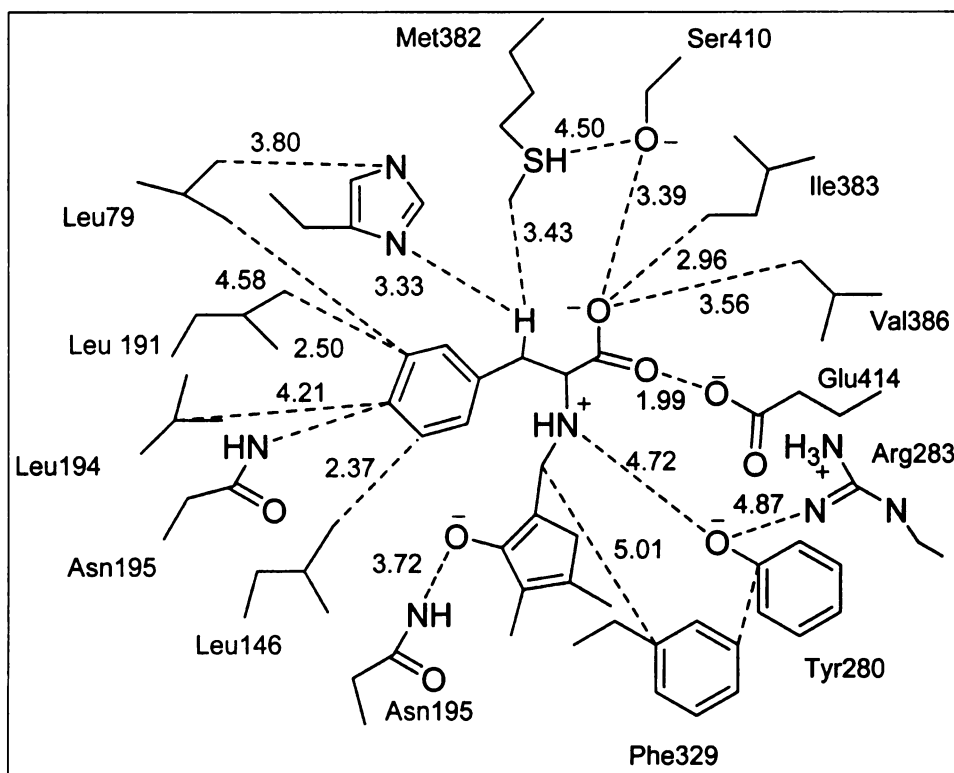
Figure 2.7 Shows a model of phenylalanine anchored in the active site of PAM with the phenyl ring interacting with hydrophobic residues. The approximate interaction distances between the substrate and the active site residues are indicated (Å).

The 4'-methoxy-α-phenylalanine substrate (**3**) also demonstrated greater efficiency (0.12 nmol•h^{-1}•μM^{-1}) and superior turnover (V_{rel} = 25) compared to **6** (Table 2.1). The 3'-methoxy regioisomer was surprisingly not a productive substrate, especially considering that the 3'-methyl substrate was converted to its β-isomer nearly 4 times faster than the 4'-methyl isomer. Perhaps steric

interactions are more significant with the larger -OCH$_3$ group, thus precluding proper active site binding.

Heteroaryl-β-phenylalanines, furan-2-yl- (**10**) and thioen-2-yl-*S*-α-phenylalanines (**2**), were tested as substrates of PAM at steady state, and **2** was found to produce β-amino acid product much faster (V_{rel} = 14) than **10** (V_{rel} = 0.02) (Table 2.1). The efficiency of PAM with **2** was second only to that of the 4'-fluoro species **1**, and was also isomerized ~40 times more efficiently than **6**. (*S*)-Styrylalanine (**11**) was found to be a productive substrate of PAM with a V_{rel} = 0.04 compared to **6** (Table 2.1); although, the catalytic efficiency (V_{MAX}/K_M ≈ 0.0001 nmol•h^{-1}•µM^{-1}) was comparatively much lower. Notably, PAM was unable to convert the saturated styrylalanine analog ((*S*)-2-amino-5-phenylpentanoic acid) to its β-isomer, suggesting that an extended conjugated allyl π-system next to the α-carbon, bearing the migrating amino group, is required for isomerization.

Allylglycine was found to be a non-productive substrate of PAM based on the expected retention time and fragmentation pattern of the β-*N*-acetyl allylglycine methyl ester standard. The lack of conversion could be due to improper binding of the substrate within the active, which probably confirms to aromatic amino acids by interaction with the hydrophobic leucine and isoleucine residues that are conserved among enzymes belonging to the MIO family (Figure 2.7). The other possibility could be that after the elimination of the amine a conjugated allyl system is formed and the rebounding amine could add to the γ- or δ- positions of the resulting polyunsaturated pentenoic acid. So, instead of the

expected β-allylglycine other compounds could be formed such *trans*-4-aminopent-2-enoic acid or *trans*-5-aminopent-3-enoic acid (Figure 2.8). Both compounds were synthesized, and no signal corresponding to the *N*-acetyl methyl ester derivatives of the amino acids was observed by GC/MS. These negative results suggested that the phenyl ring may be required for binding to the active site (Figure 2.7).
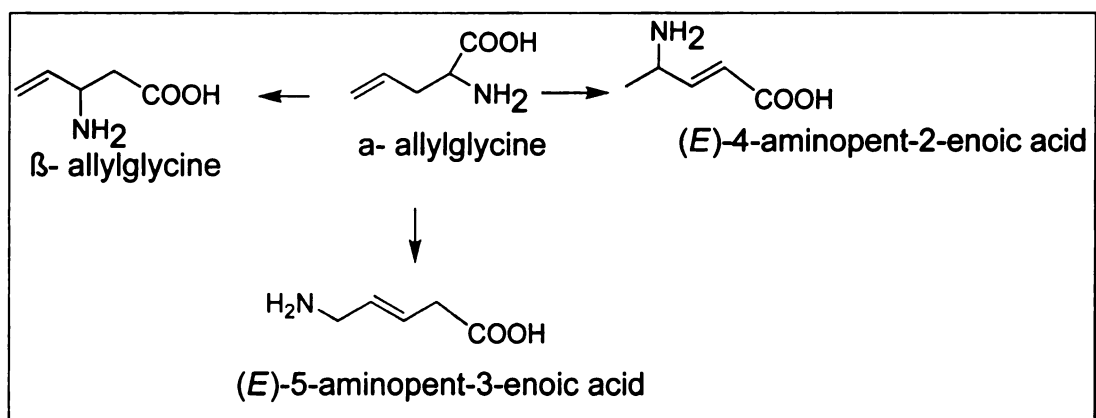
Figure 2.8 Shows the possible products of the α-allylglycine-PAM reaction. The loss of the α-amino group could lead to an extended conjugated system which may result in the addition on the γ and δ positions to form the 4- or 5- amino-*trans*-pent-3-enoic acids. However both compounds were not identifiable by GC/MS/EI analysis.

2.2.3. *In vivo* Screening of Amino acids

Phenylalanine analogues (1 mM) were fed to a 50 mL culture of transformed BL21 (DE3)pLysS over expressing the PAM enzyme. The amino acids were derivatized in both the cell pellets and the supernatant (Figure 2.9).
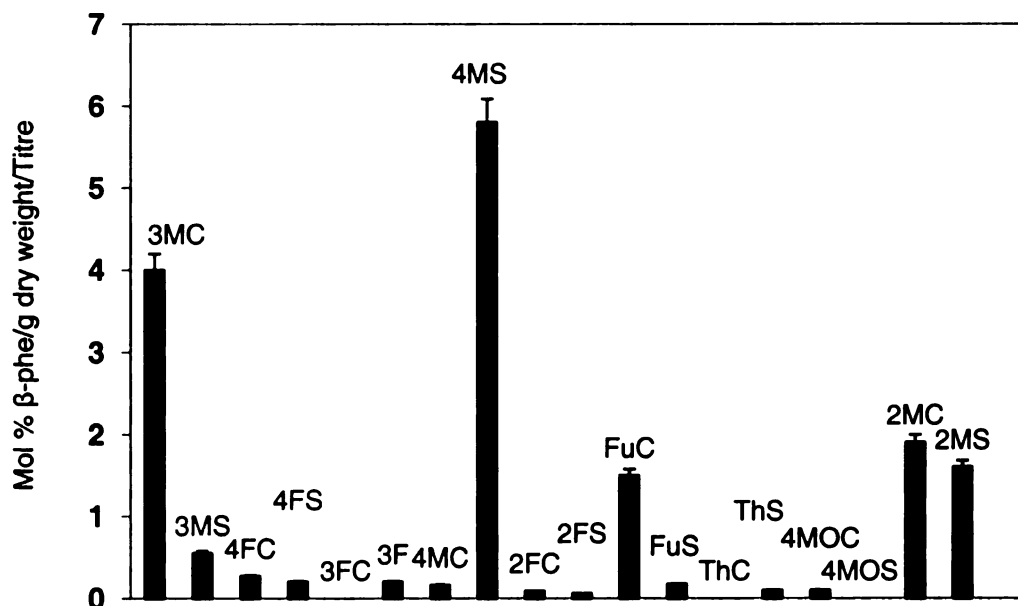
Figure 2.9 A profile of *in vivo* synthesis of a mixture of β- amino acids. The α-amino acids were incubated with *E. coli* transfected with a pam plasmid expressing phenylalanine aminomutase (PAM), at 37 °C 16 h. The PAM expression was induced with IPTG at an $OD_{600} \sim 0.6$. The products were assayed in both (C) cells and supernatant (S). 3M is 3'-methyl-β-phenylalanine; 4M is 4'-methyl-β-phenylalanine; 2M is 2'-methyl-β-phenylalanine; 3F is 3'-flouro-β-phenylalanine; 4F is 4'-flouro-β-phenylalanine; 2F is 2'-flouro-β-phenylalanine; Fu is 2'-furanyl-β-alanine; Th is 2'-thienyl-β-alanine and 4MO is 4'-methoxy-β-phenylalanine.

2.2.2.4 Biocatalysis

The results shown above (Table 2.1) provides a synthetic technique for accessing β-amino acids both *in vivo* and *in vitro* with less toxic waste to the environment compared to the chemical synthesis methods. The general scheme for the biocatalytic synthesis of aryl-β-alanines is shown in figure 1.9.
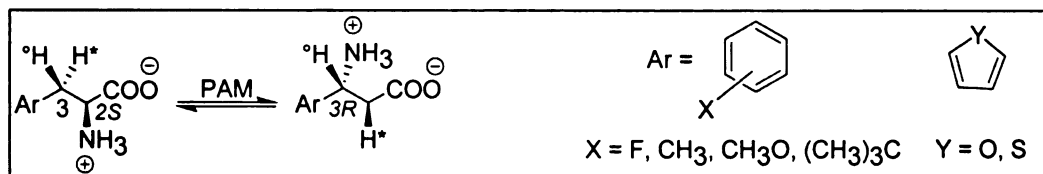
Figure 2.10 General scheme for the synthesis of various stereospecific beta amino acids.

Second generation paclitaxel can be access in a one pot reaction both *in vivo* and *in vitro* by incubating selected recombinant enzymes (acyl transferases, PAM and ligase) expressed in *E. coli* with some metabolites found in the biosynthetic pathway of paclitaxel (Figure 2.11). Most of these enzymes have already been demonstrated to be promiscous just like PAM. The various groups which can be introduced on to the baccatin III core are shown in Figure 2.11.
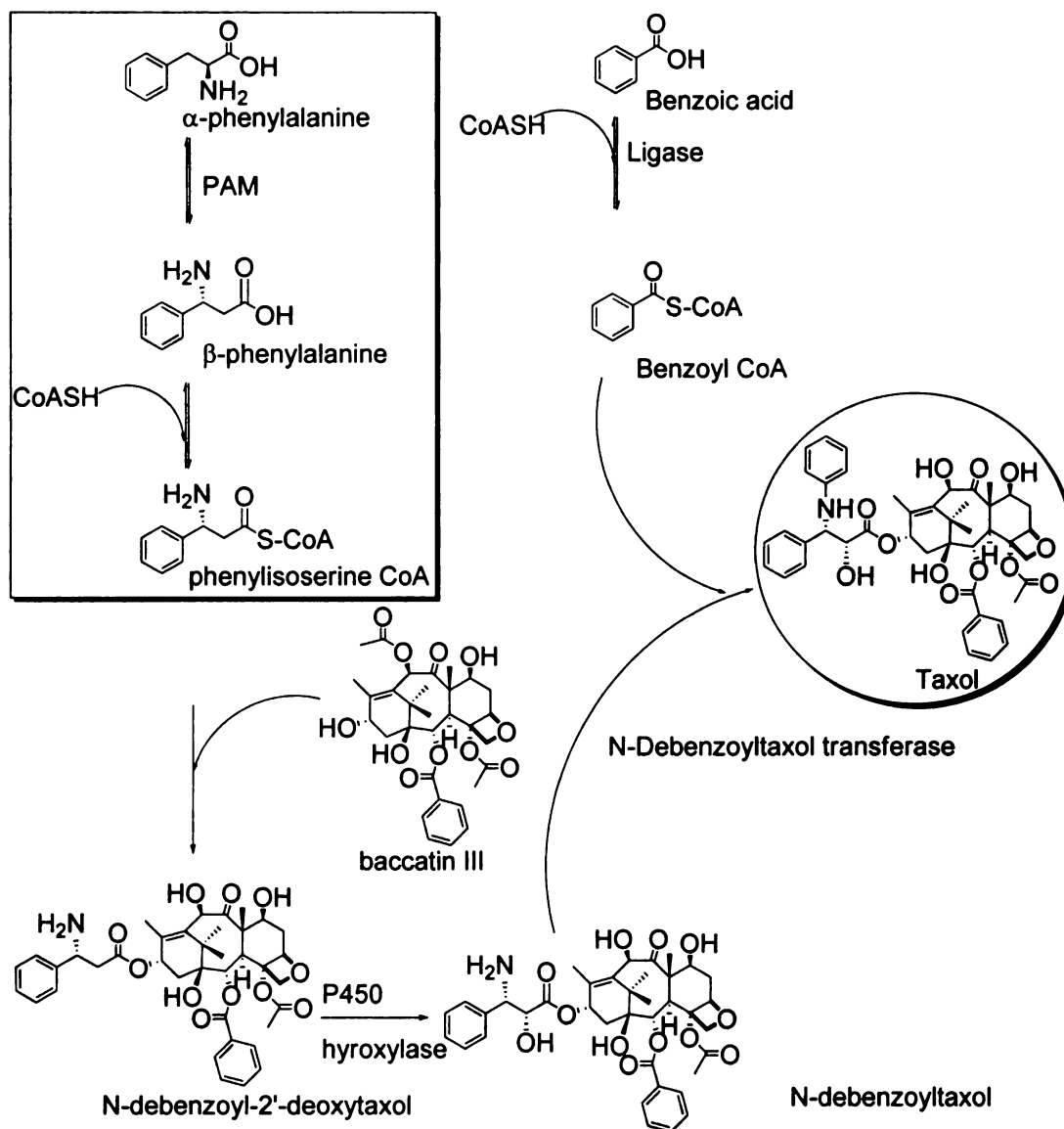
Scheme 2.11 Biosynthesis of taxol from α-phenylalanine which is first converted to β-phenylalanine (boxed) by the enzyme phenylalanine aminomutase(PAM).

73
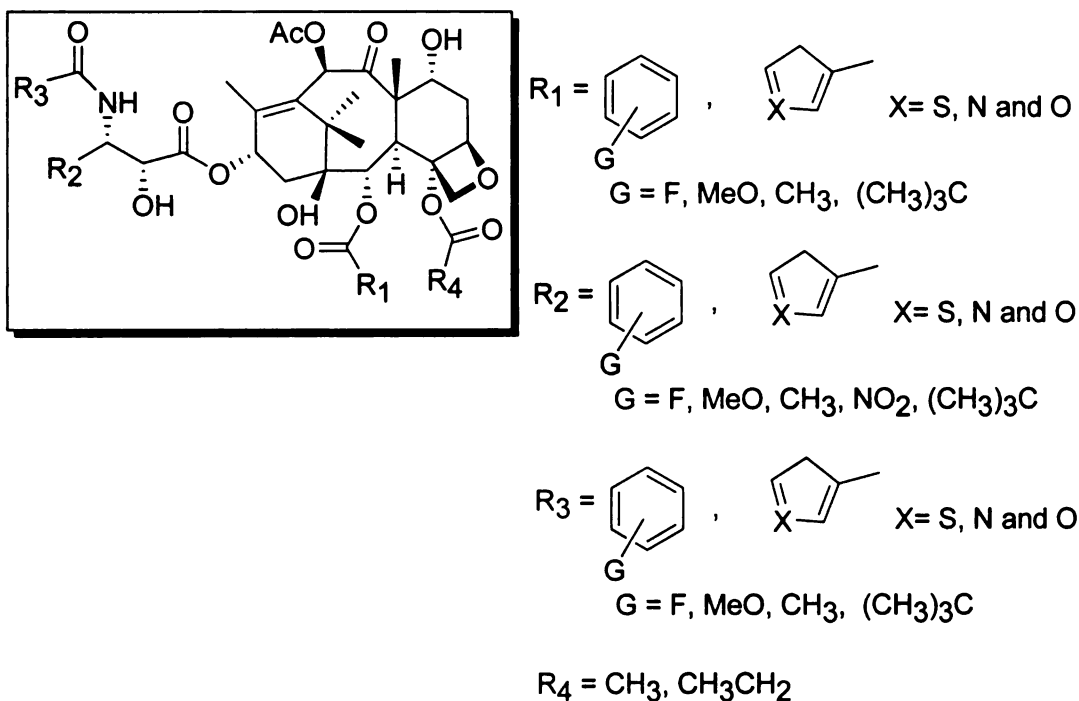
Figure 2.11 The proposed biocatalysis of of Taxol involving various enzymes found in the biosynthetic pathway of taxol.

2.2.2.5 *Mass spectral analysis of biosynthetic products generated by PAM catalysis*

Tandem gas chromatography/mass spectrometry was used to separate the *N*-acetyl (or *N*-benzoyl) methyl ester derivatives of β-amino acids isolated from assays in which corresponding β-amino acids were incubated with PAM. In each pairing, mass spectra of the authentic standards (top panel) and of the corresponding biosynthetic sample (bottom panel) are shown (Figures 2.13.1-12). The retention times of the standards and biosynthetic products on GC were identical. 1, *N*-benzoyl 4'-fluoro-β-phenylalanine methyl ester; 2, *N*--benzoyl-β-(2-thienyl)-β-alanine methyl ester; 3, *N*-benzoyl 4'-methoxy-β-phenylalanine methyl

ester; 4, *N*-benzoyl 2'-fluoro-β-phenylalanine methyl ester; 5, *N*-acetyl 4'-methyl-β-phenylalanine methyl ester; 6, *N*-acetyl β-phenylalanine methyl ester; 7, *N*-acetyl 2'-methyl-β-phenylalanine methyl ester; 8, *N*-benzoyl 3'-fluoro-β-phenylalanine methyl ester; 9, *N*-acetyl 3'-methyl-β-phenylalanine methyl ester; 10, *N*-benzoyl-β-(2-furanyl)-β-alanine methyl ester; 11, *N*-acetyl styryl-β-alanine methyl ester; 12, *N*-acetyl 4'-*t*-butyl-β-phenylalanine methyl ester.
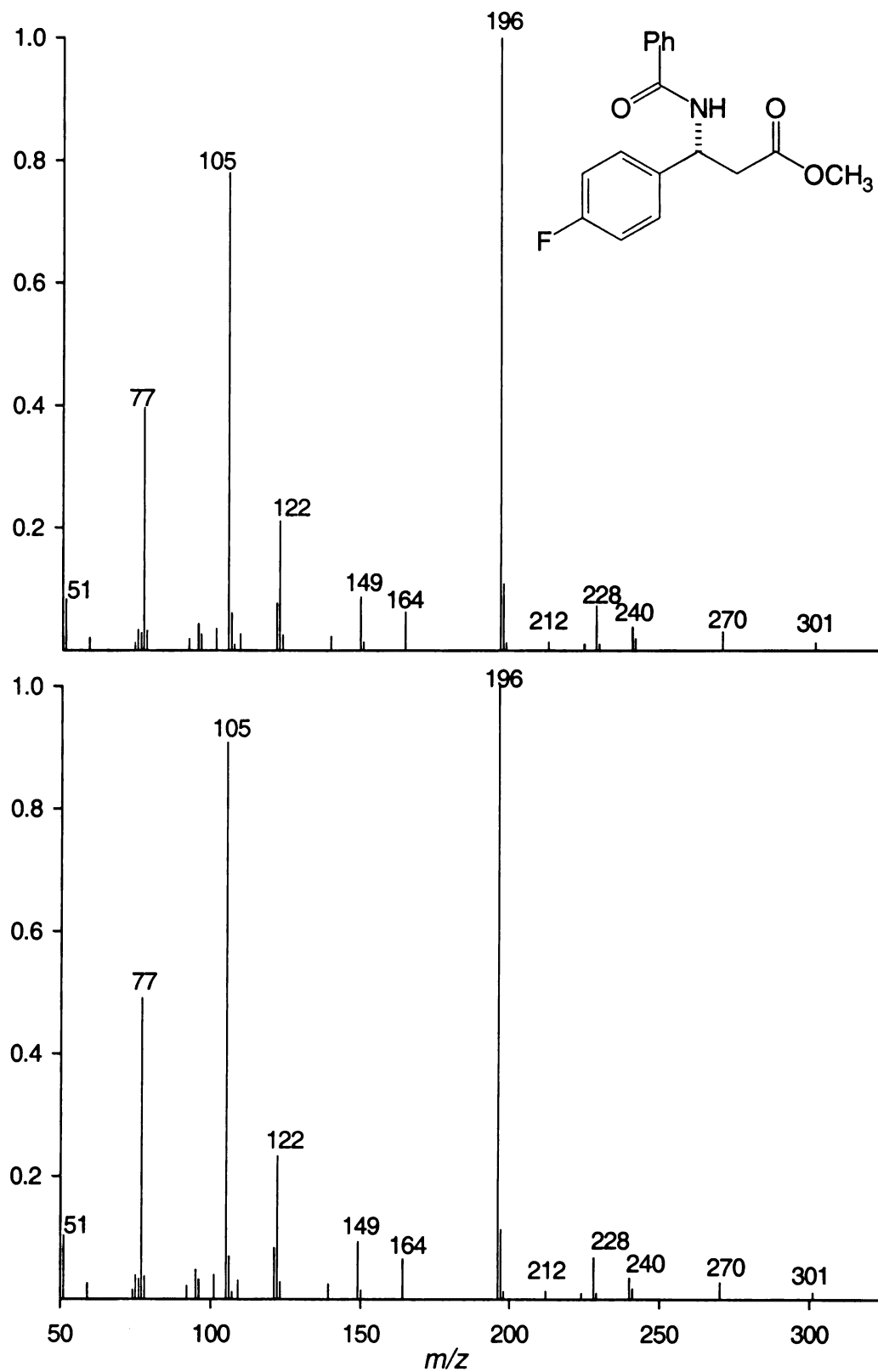
Figure 2.12.1 *N*-benzoyl 4'-fluoro-β-phenylalanine methyl ester

76
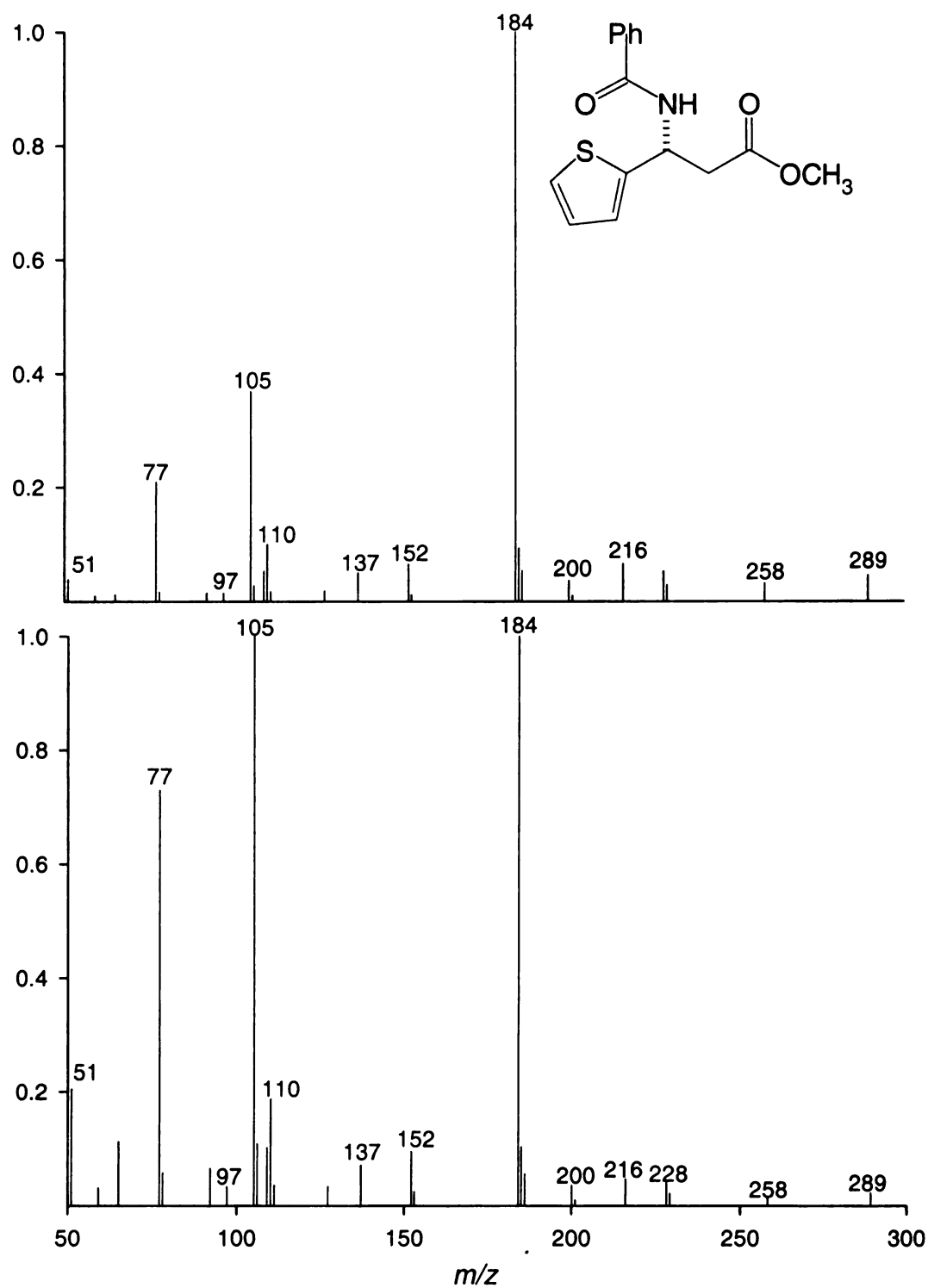
Figure 2.12.2 β-(2'-thienyl)-β-alanine-*N*-benzoyl methyl ester
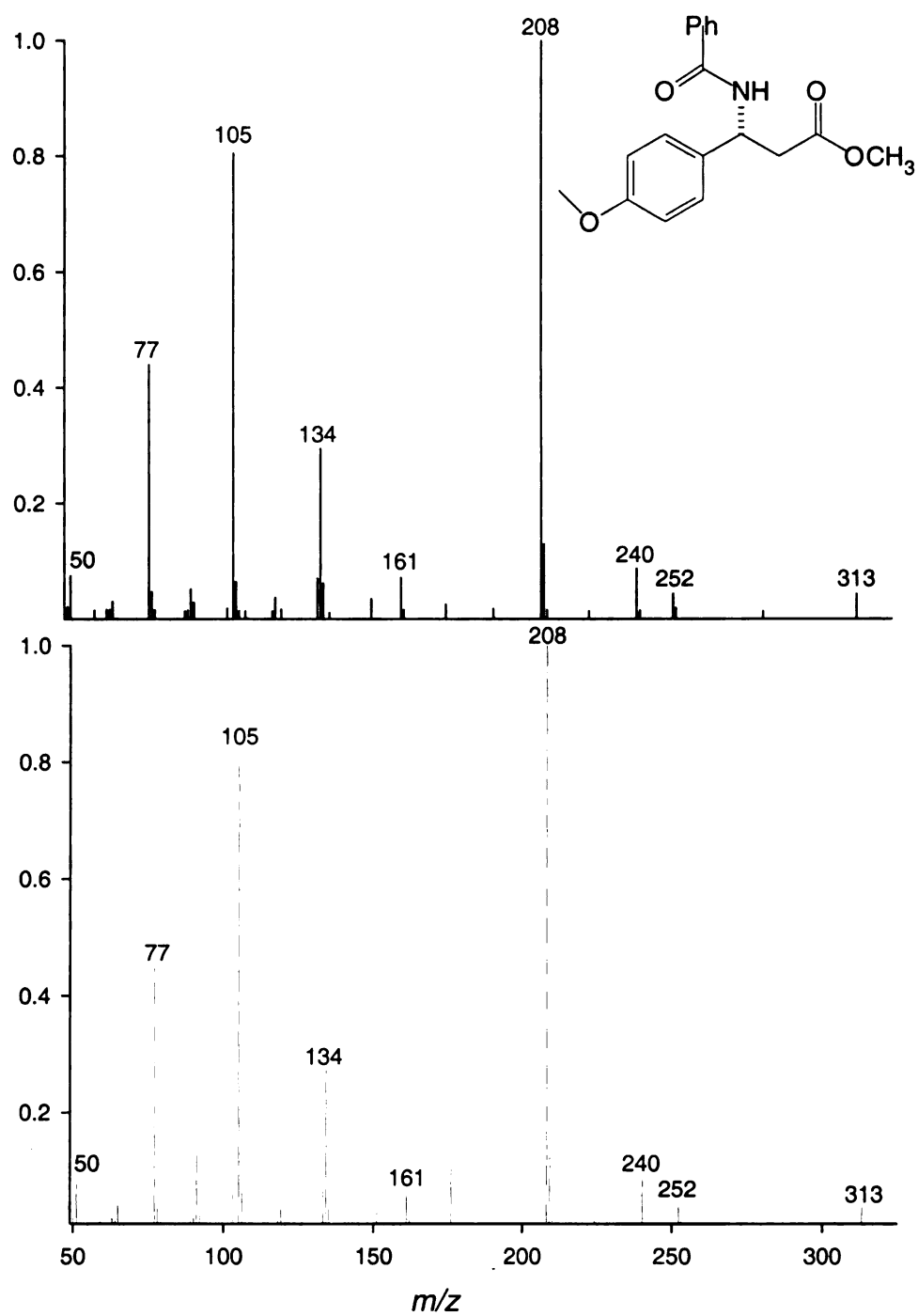
Figure 2.12.3 *N*-benzoyl 4'-methoxy-β-phenylalanine methyl ester
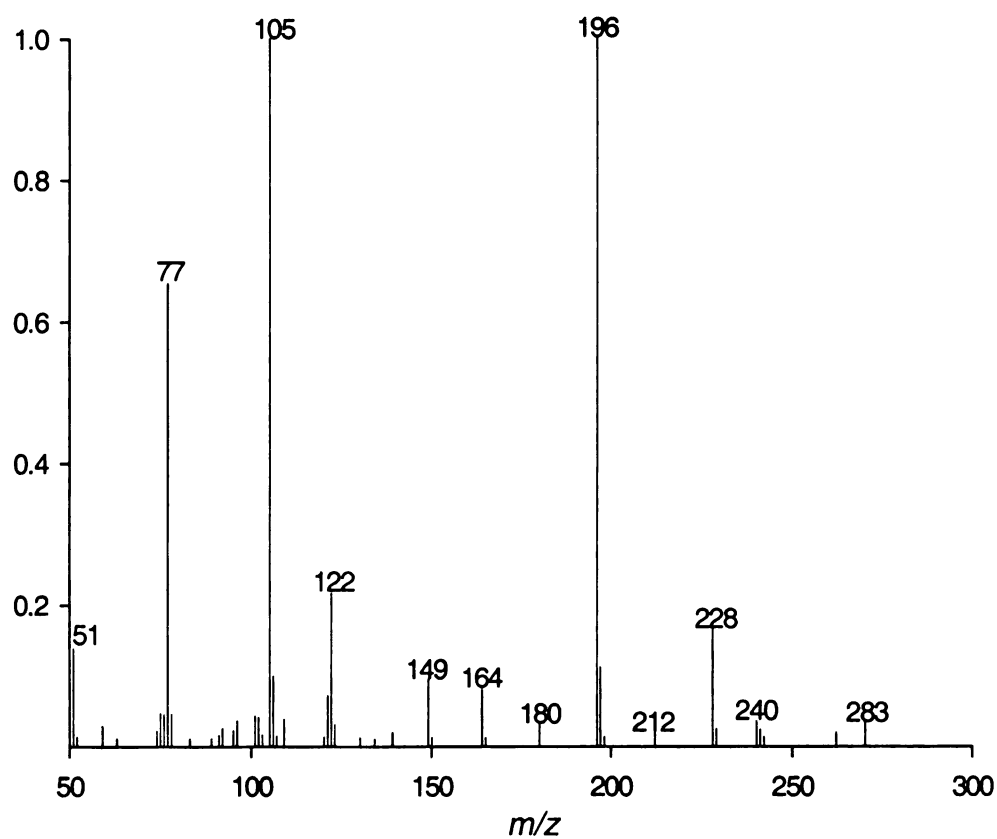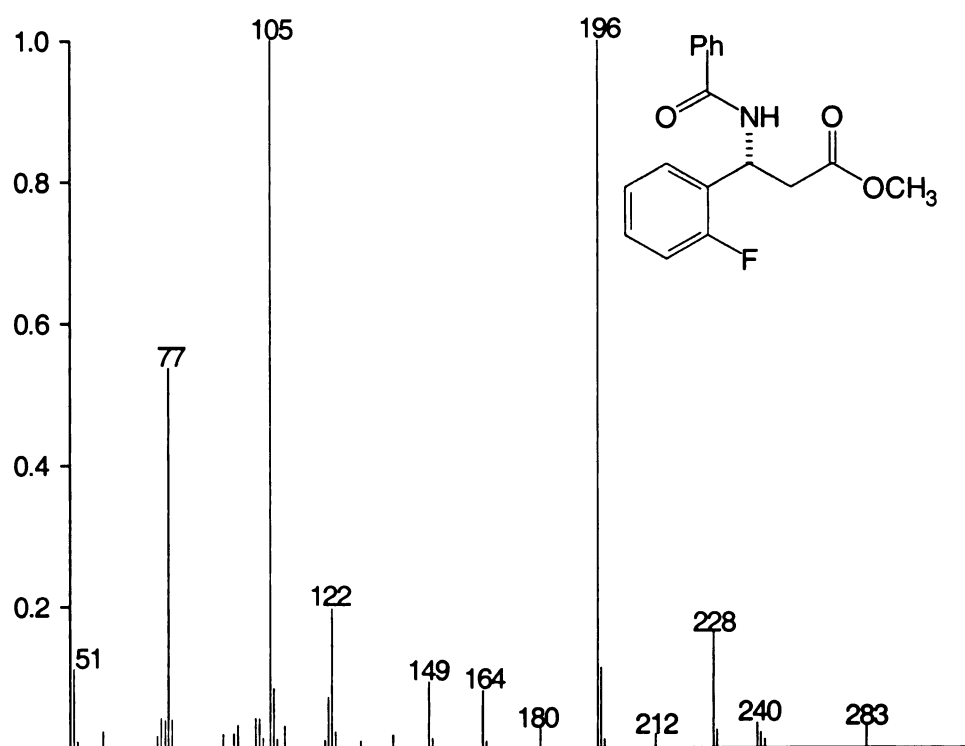
Figure 2.12.4 *N*-benzoyl 2'-fluoro-β-phenylalanine methyl ester

79
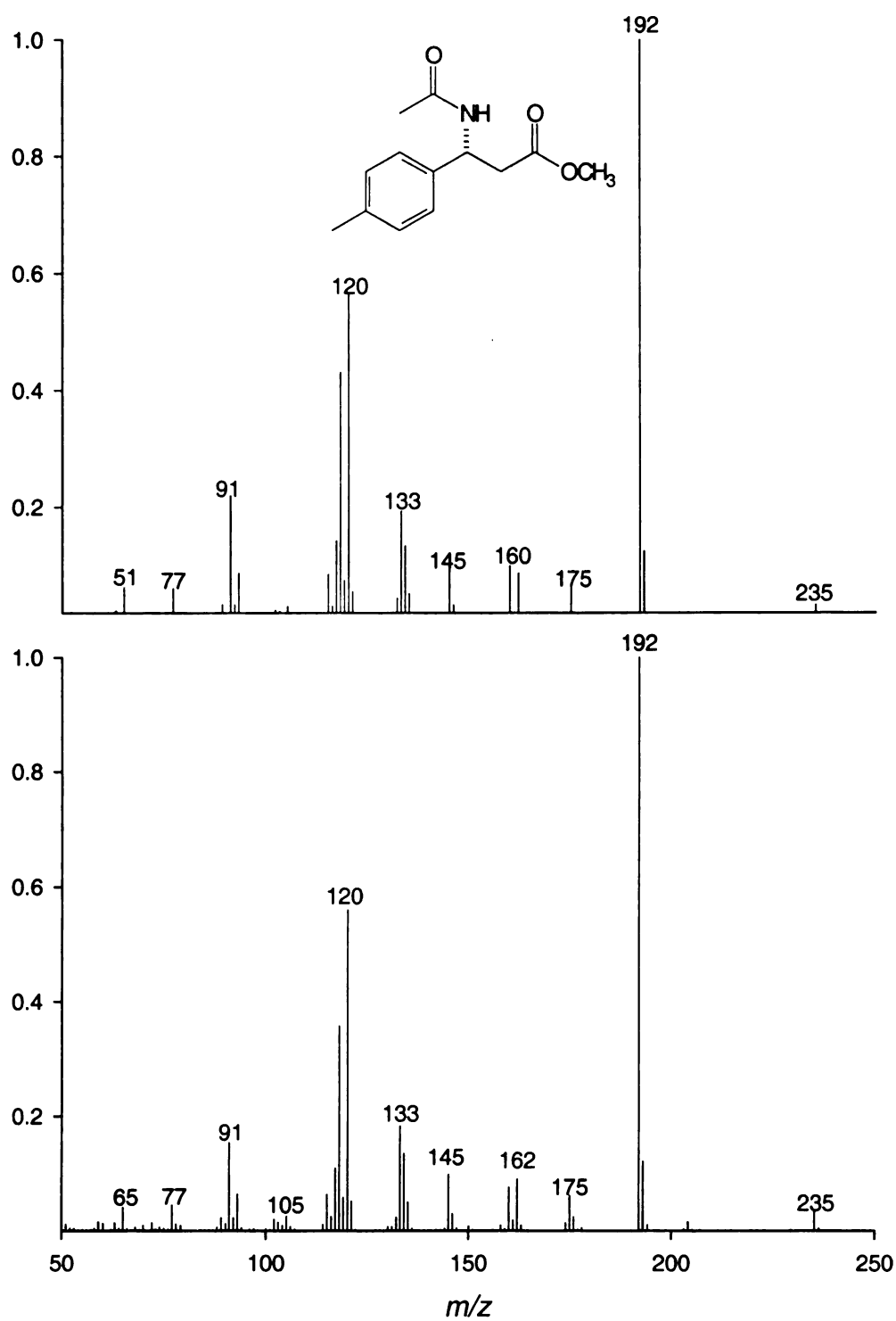
Figure 2.12.5 *N*-acetyl 4'-methyl-β-phenylalanine methyl ester
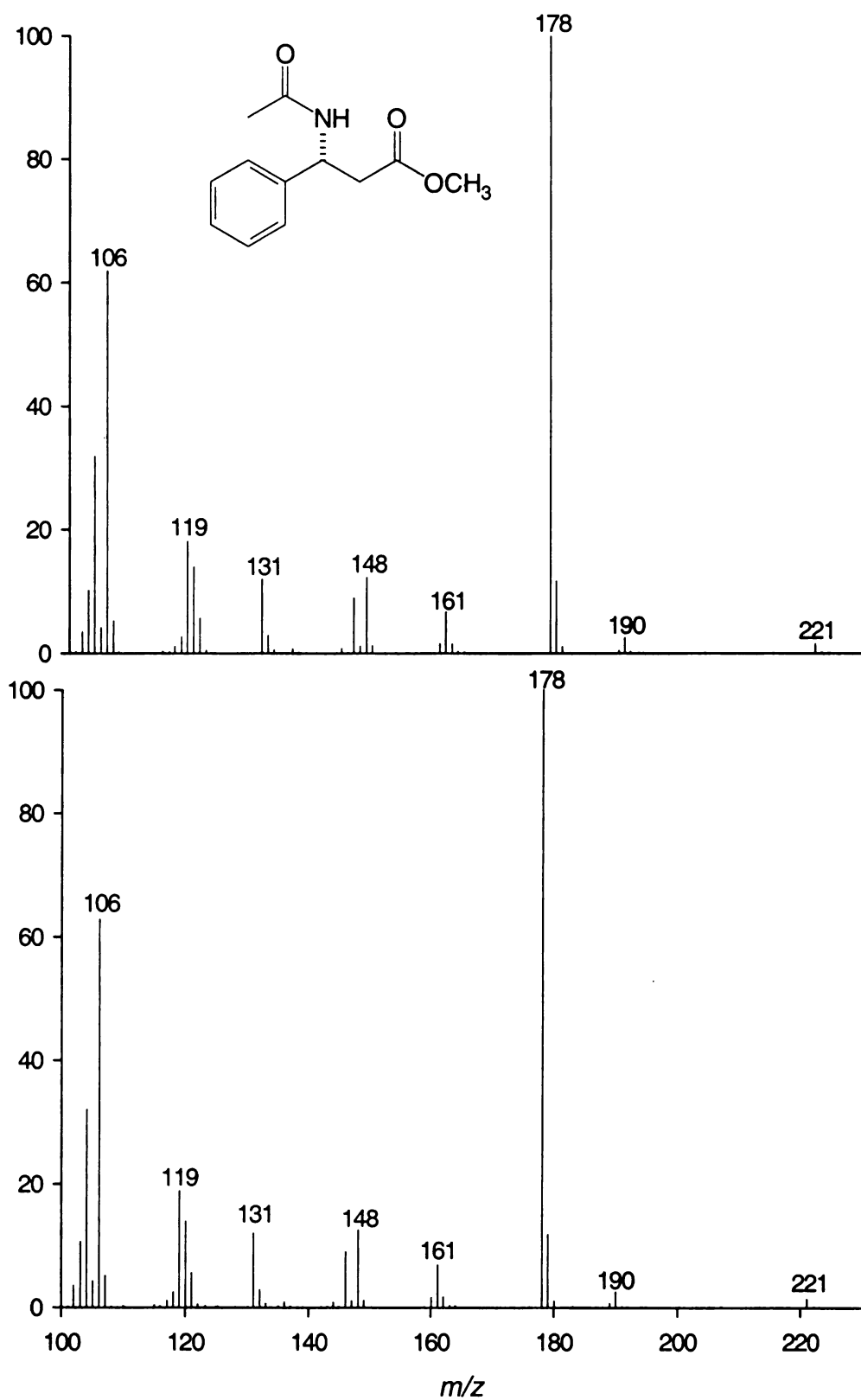
Figure 2.12.6 N-acetyl β-phenylalanine methyl ester
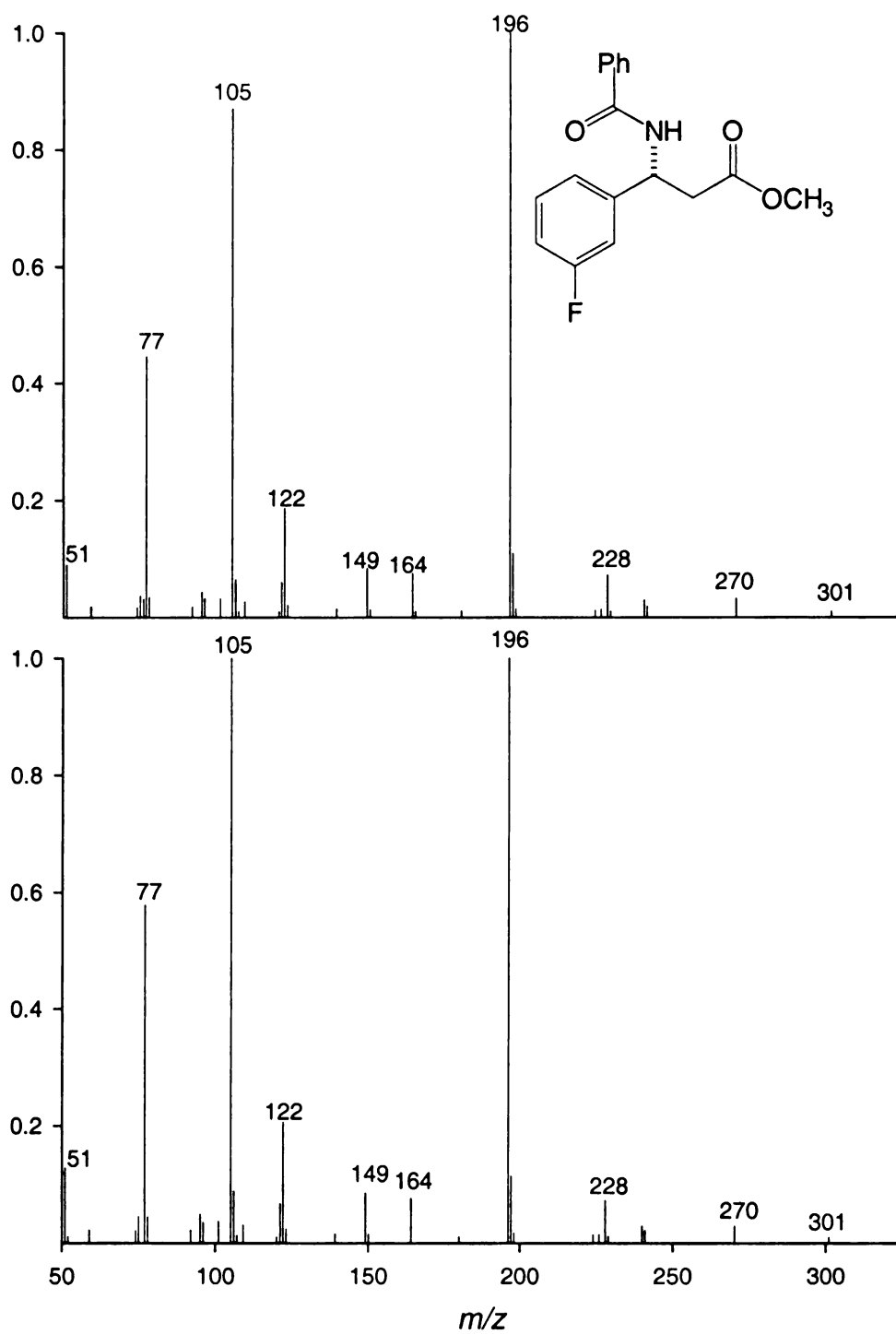
Figure 2.12.7 *N*-benzoyl 3'-fluoro-β-phenylalanine methyl ester

82
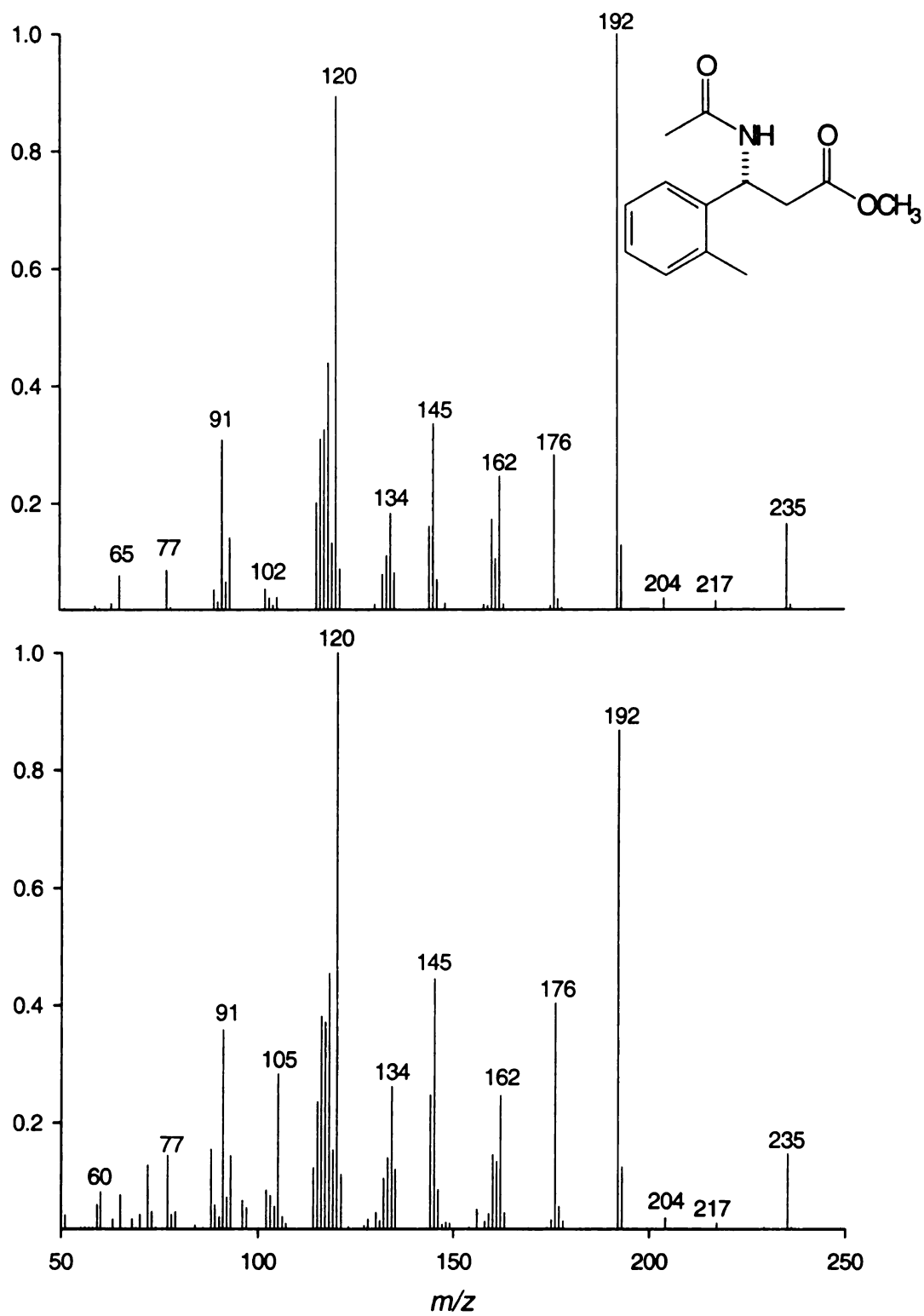
Figure 2.12.8 *N*-acetyl 3'-methyl-β-phenylalanine methyl ester
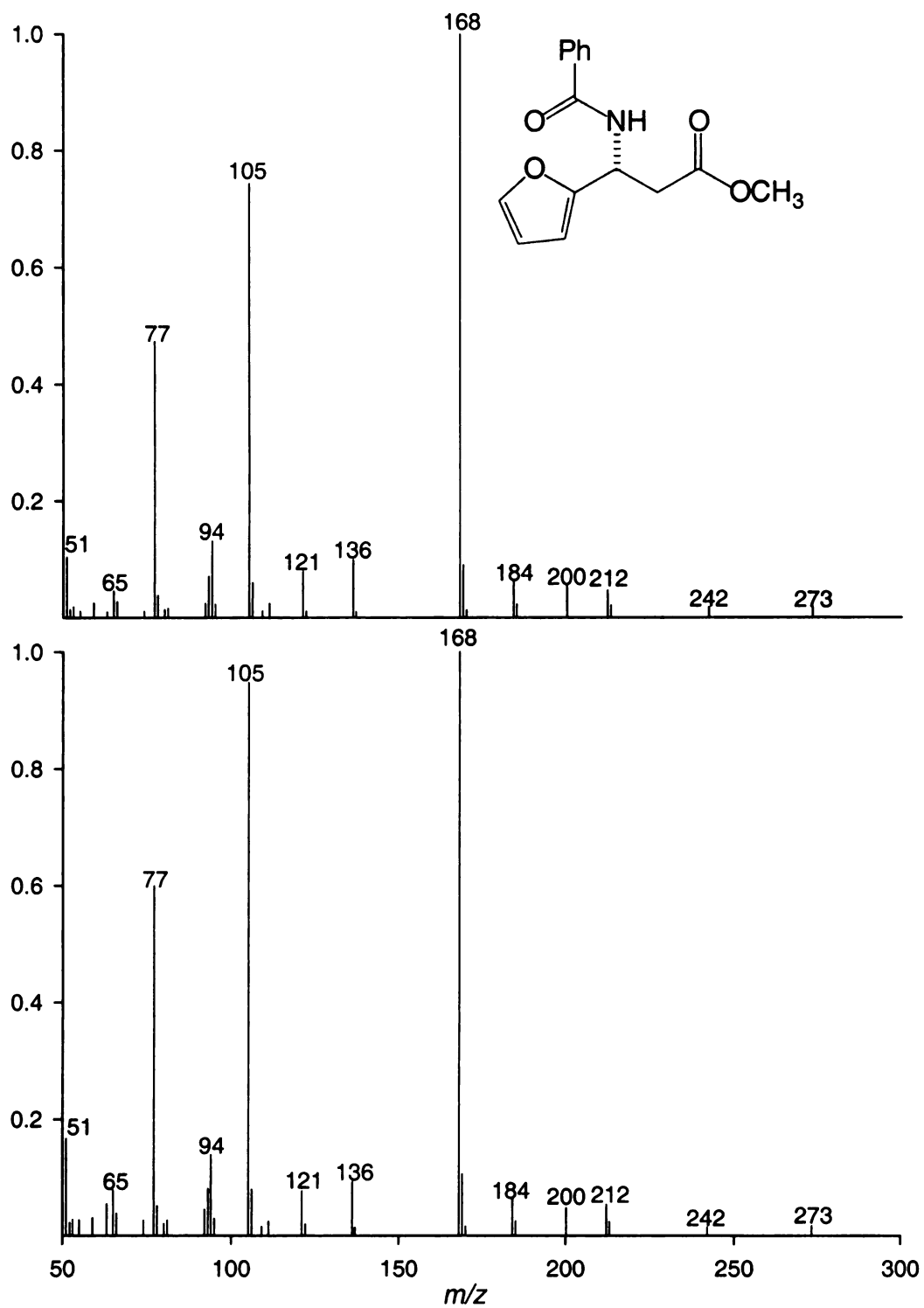
Figure 2.12.9 *N*-benzoyl-β-(2-furanyl)-β-alanine methyl ester

84
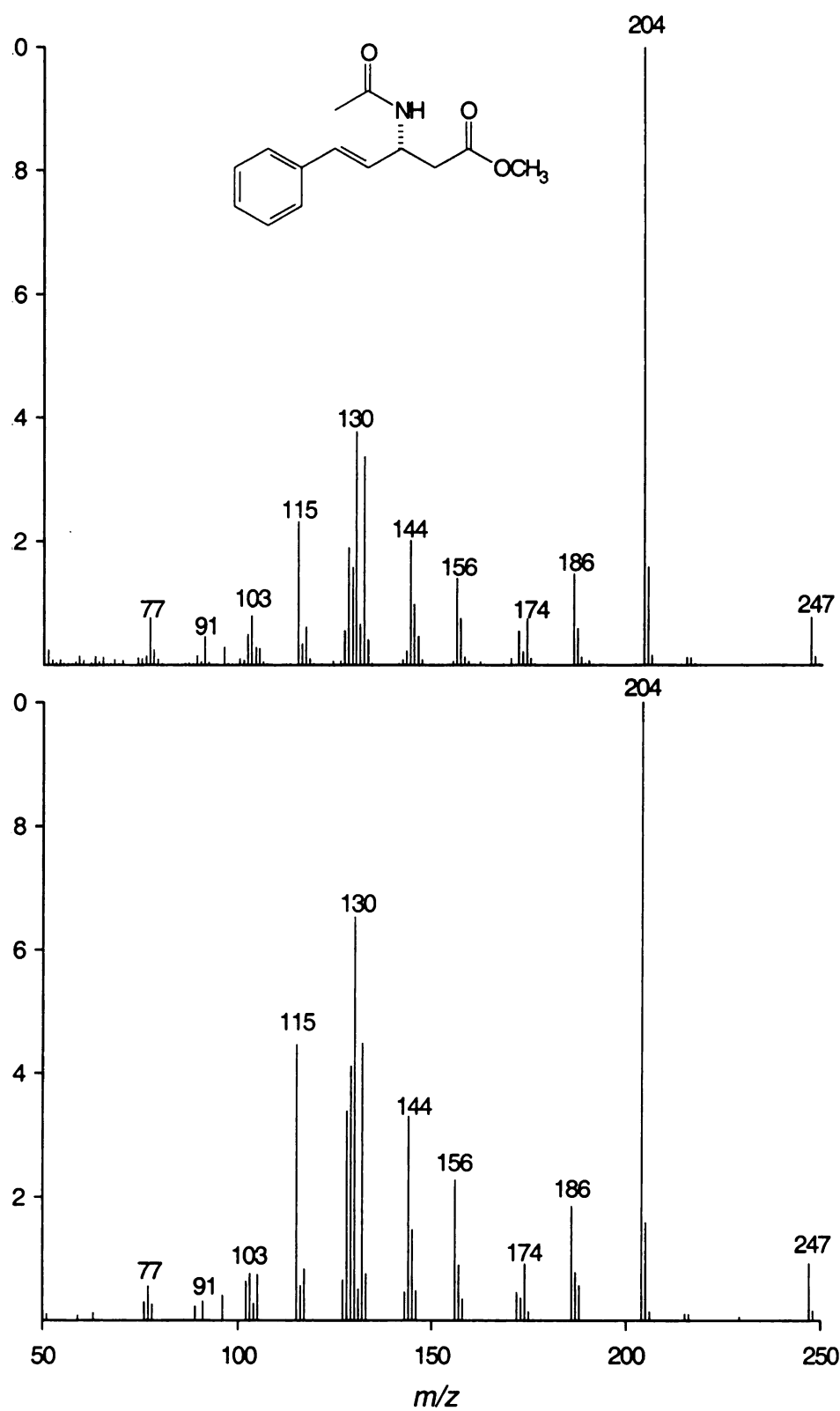
Figure 2.12.10 *N*-acetyl- styryl-β-alanine methyl ester
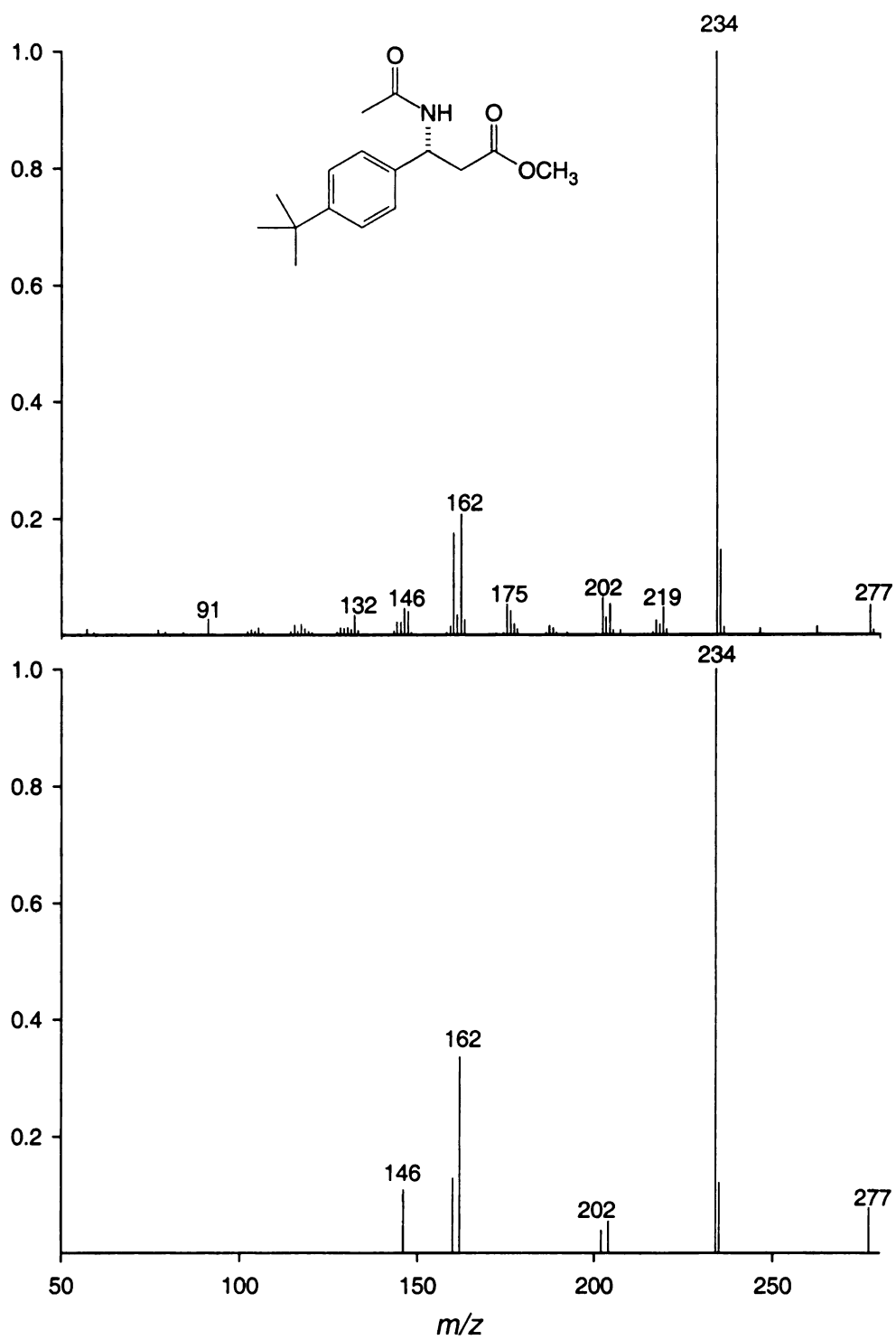
Figure 2.12.11 *N*-acetyl 4'-*t*-butyl-β-phenylalanine methyl ester.

2.3 CONCLUSION

In conclusion, it is evident that the native PAM is able to accept a broad array of arylalanines substrates that possess various substituents on the phenyl rings. However, no definitive trend in the catalytic rate emerged with regards to strong electron-withdrawing or -donating substituents under steady-state kinetics conditions. In this scenario substrate release may be, in part, rate-limiting, and thus may mask other cryptic electron inductive effects associated with the MIO mechanism. The development of single turnover kinetics analysis of PAM is currently being investigated in order to further dissect the mechanism.

As the properties of the phenylalanine aminomutase mechanism are better understood, the strategic integration of amino acid isomerase chemistry into custom asymmetric synthesis becomes practical. Engineering PAM to broaden its substrate specificity for the production of novel nonpeptidic β-amino acids provides building blocks for the design and construction of second-generation compounds such as taxol and januvia. Predictably, genetic engineering approaches to modify this biocatalyst can also be directed toward potentially making PAM more compliant for use in large-scale reactors.

2.4 MATERIALS AND METHODS

2.4.1 *MATERIALS*

Styrylalanine and potential allylglycine products were synthesized as described below. Unless otherwise indicated, *E. coli* strains and the vectors were obtained from Invitrogen. The α-amino acid substrate (*S*)-α-phenylalanine, 2'-fluoro-(*S*)-phenylalanine, 3'-fluoro-(*S*)-phenylalanine, 4'-fluoro-(*S*)-phenylalanine and (*S*)-*nor*-valine were purchased from Sigma-Aldrich-Fluka. 2'-Methyl-(*S*)-α-phenylalanine, 3'-methyl-(*S*)-α-phenylalanine, 4'-*tert*-butyl-(*S*)-α-phenylalanine, (*S*)-2-amino-5-phenylpentanoic, (*S*)-styrylalanine and (*S*)-allylglycine were obtained from Peptech (Burlington, MA), 4'-methyl-(*S*)-α-phenylalanine was purchased from Advanced ChemTech (Louisville, KY), and 3'-methoxy-(*S*)-α-phenylalanine was purchased from Accellant Inc. (Monmouth Junction, NJ). β-Amino acid standards (*R*)-β-phenylalanine ((*R*)-3-amino-3-phenylpropionic acid), (*R*)-3-amino-3-(2-methylphenyl)-propionic acid, (*R*)-3-amino-3-(3-methylphenyl)propionic acid, and (*R*)-3-amino-3-(4-methylphenyl)propionic acid were acquired from Peptech, (*R*)-3-amino-3-(4'-*tert*-butylphenyl)propionic acid was acquired from Accellant Inc., (*R*)-3-aminopentanoic acid and (*R*)-3-amino-5-phenylpentanoic acid were purchased from BioBlocks (San Diego, CA), (*R*)-3-amino-3-(4-fluorophenyl)propionic acid and (*R*)-3-amino-3-(3-fluorophenyl)propionic acid were purchased from Astatech (Bristol, PA), and (*R*)-3-amino-3-(2-fluorophenyl)propionic acid and (*R*)-3-amino-3-(3-methoxyphenyl)propionic acid were purchased from Accellant Inc. (*S*)-2-Amino-5-phenylpentanoic acid was purchased from Chem-Impex International Inc.

(Chicago. IL). These compounds and all other reagents were used without further purification, unless otherwise noted. Tetrahydrofuran (THF) and dichloromethane (DCM) were obtained from a dry-still packed with activated alumina that was pressurized with N_2 gas. Silica gel (230-400 Mesh) and aluminum-backed silica gel 60 TLC plates, embedded with A_{254} chromophores, were purchased from EMD Chemicals Inc. (Gibbstown, NJ.

H-NMR spectra were recorded on a Varian Inova-300 (300.11 MHz), a Varian VXR-500 or a Varian Unity-500-Plus spectrometer (499.74 MHz) and were referenced to residual solvent signals at 7.24 ppm for $CDCl_3$). All apparent coupling constants (*J* values) are measured at the indicated field strengths.

Coupled gas chromatography/mass spectrometry analysis was conducted by loading 1 µL of sample onto an HP 5HS GC column (0.25-mm inner diameter x 30 m, 0.25-µm film thickness) (Agilent, Palo Alto, CA) mounted on a GC (model 6890N, Agilent) coupled to a mass selective detector (model 5973 inert®, Agilent) in ion scan mode from 50 – 300 atomic mass units.

2.4.2. *PROCEDURES*

2.4.2.1 *Heterologous Expression and Purification of PAM*

By a cohesive-end PCR method *pam* cDNA was sub cloned from a previously described expression vector pET1981His into pET14b in order to exchange the poly-His epitope from C- to N-terminal-tagging, respectively. Preliminary purification of small-scale preparations of PAM protein expressed from pET1981His and from pET14b in *E. coli* BL21 *(DE3)* indicated that the N-terminal-tagged protein bound to Ni-affinity column matrix 8-fold better than the C-terminal-tagged protein (<10 % binding). The oligonucleotide primers used for this sub cloning procedure have been described previously, and the new expression vector was designated pET14-1981His. This plasmid was used to transform *E. coli* BL21 (DE3) cells which were then grown for 16 h in 50 mL of minimal growth media (1 L contained 12.8 g $Na_2HPO_4 \cdot 7H_2O$, 3 g KH_2PO_4, 0.5 g NaCl, 1.0 g NH_4Cl, 2 mL 1 M $MgSO_4$, 100 μL 1 M $CaCl_2$, 10 mL 100X BME Vitamin solution, and 20 mL 20% D-glucose solution) at 37 °C with ampicillin selection. These bacteria were used to inoculate 6 L of minimal growth media containing 50 μg/mL ampicillin, and were grown at 37 °C for 5 h to OD_{600} = 0.6.

Expression was induced by addition of 1 mM of isopropyl-β-D-thiogalactopyranoside and the cells were grown for 16 h at 18 °C. The remaining steps were conducted at 4 °C, unless otherwise noted. The cells were harvested by centrifugation at 5,000 × *g* (20 min), diluted in 100 mL of resuspension buffer (50 mM Tris-HCl, pH 8.5), and lysed by brief sonication (five 20-s bursts at 50% power (Misonix sonicator, Farmingdale, NY)) followed by removal of cellular

debris by centrifugation at 15,000 × *g* (30min). Residual light membrane debris was removed by centrifugation at 45,000 × *g* (2 h). The clarified crude supernatant was partially purified by anion exchange and Ni-affinity chromatography as described. The fractions containing soluble PAM were combined, desalted by dialysis, and then used for enzymatic assays. The quantity of PAM (~25 µg/mL) was assessed by SDS-PAGE and Coomassie Blue staining as described elsewhere.

2.4.2.2 Assessing Functional PAM Expression

Natural substrate (*S*)-α-phenylalanine (500 µM) was added to a 1 mL aliquot of the protein extract containing partially pure PAM (at ~250 µg/mL) and incubated for 2 h, and the relative production of (*R*)-β-phenylalanine was evaluated. Enzyme preparations yielding ~7.1 µg of derivatized β-amino acid product per 1 mL assay were used for subsequent kinetic analyses.

2.4.2.3 Screening of productive substrates

Each "unnatural" α-amino acid substrate (Table 2.1), at apparent saturation (1-2 mM), was preliminarily assayed by *in vitro* incubation with ~50 µg PAM overnight. Substrates demonstrating sufficient turnover were then incubated 3 h at 0.01, 0.05, 0.1, 0.25, 0.5, 1, 2 and 3 mM with PAM (~2.50 µg) in duplicate assays. The enzymatically-derived β-amino acids from the single stopped-time incubations were derivatized and quantified as follows: the enzymatically-derived β-amino acids were derivatized to their *N*-acetyl methyl esters and each sample

was quantified by tandem capillary gas chromatography/electron impact-mass spectrometry (GC/EI-MS). Linear regression analysis was used to convert the abundance of the base peak fragment ion produced by the product in each sample by corresponding the abundance of the base peak ion of authentic sample, derivatized similarly, to the concentration of each standard in a dilution series from 0-30 μM, and the data were used to create a concentration dependent curve, v_o vs [S], in order to separately calculate the K_M constants and V_{max} values for each substrate. V_{rel} values are reported as the ratio of V_{max} of the PAM with unnatural substrate to the V_{max} with phenylalanine.

The initial rates (v_o, nmol/h) were plotted against substrate concentration [S] on KALEIDAGRAPH (Synergy Software, Reading, PA) to determine kinetic constants (K_M and V_{max}) of PAM by nonlinear regression analysis (R^2 values were typically > 0.98). The following amino acids were assayed; allylglycine, styrylalanine. 2'-fluoro-(S)-phenylalanine, 3'-fluoro-(S)-phenylalanine, 4'-fluoro-(S)-phenylalanine and (S)-nor-valine 2'-Methyl-(S)-α-phenylalanine, 3'-methyl-(S)-α-phenylalanine, 4'-tert-butyl-(S)-α-phenylalanine, (S)-2-amino-5-phenylpentanoic, (S)-styrylalanine, (S)-allylglycine 4'-methyl-(S)-α-phenylalanine, and 3'-methoxy-(S)-α-phenylalanine. The steric flexibility of the PAM active site was investigated with 2'-, 3'- and 4'-methyl- and 4'-t-butyl-α-phenylalanines.
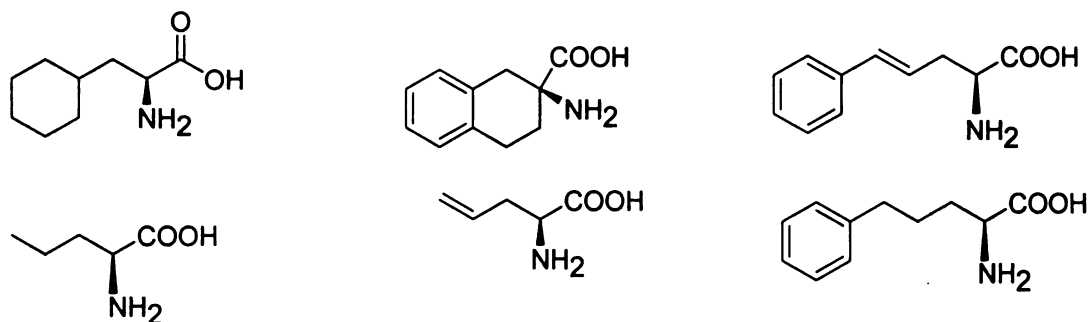
Figure 2.13 Some of the unnatural substrates assayed with PAM.

2.4.2.4 *Quantification of Biosynthetically-derived β-Amino Acids*

Processing of the product mixtures after incubation of PAM with the α-amino acid was analogous to previously described methods. In general the assay buffer was basified (0.1 M NaOH) until pH ≈ 10, treated with acetic anhydride (or benzoyl chloride) (2 × 300 μL for 20 min between each addition), and the reaction was quenched by acidifying to pH 2 with 1 M HCl. The *N*-acetyl amino acids were extracted with ethyl acetate (3 × 1 mL), the organic fractions were combined, and the carboxylic acids were methyl-esterified with diazomethane treatment. The derivatized amino acid mixture was dissolved in 300 μL ethyl acetate, and a 1 μL aliquot of this material was analyzed by tandem gas chromatography/mass spectrometry (Figure 2.7).

2.4.2.5 Determining the Relative Kinetic Constants for Various "Allylglycine" Substrates

After establishing linearity with respect to a fixed protein concentration and time, an incubation time of 3 h at 31 °C was chosen for PAM steady-state kinetics analysis of a homologous series of α-amino acid substrates. Kinetic constants (K_M and V_{max}) were determined initially for the natural α-phenylalanine substrate (at 0.01, 0.05, 0.1, 0.25, 0.5, 1, 2 and 3 mM) in order to later assess the relative kinetics of PAM (~250 ng) for the surrogate α-amino acid substrates.

2.4.2.6 Synthesis of β-allylglycine
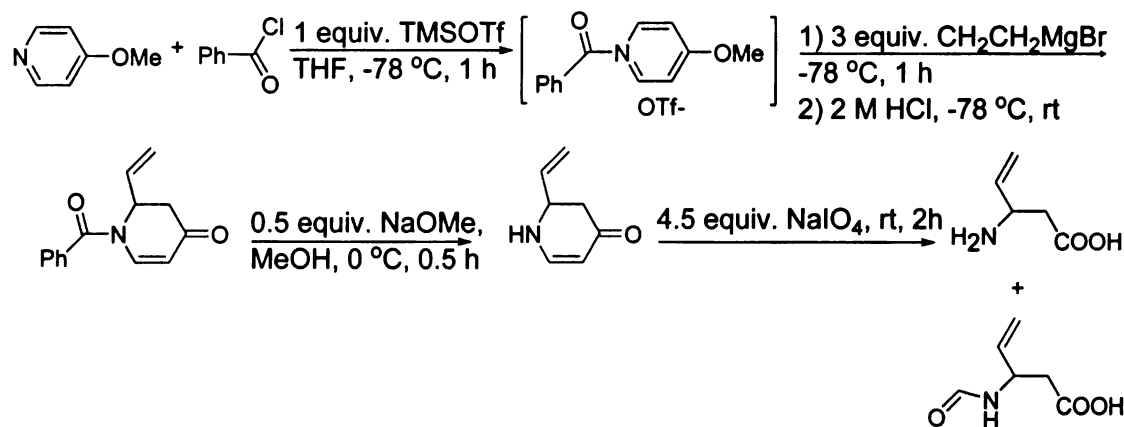
Scheme 2.14 The synthesis of β-allylglycine for use as standard of the PAM α-allylglycine reaction.

2.4.2.6.1 Synthesis of (R, S)-1-benzoyl-2-vinyl-2, 3-dihydro-1H-pyridin-4-one
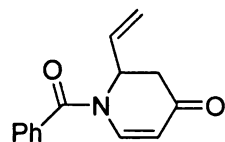
In a 250 mL round bottomed flask was loaded THF (80 mL), stir bar, 4-methoxypyridine (1.64 g, 0.014 mmol), benzoyl chloride (1.72 mL, 0.013 mmol)

and tris(methyl)triflate (2.64 mL, 0.014 mmol). The mixture was stirred at -78 °C in an acetone/dry ice bath for 1 h. Vinyl magnesium bromide (30 mL, 0.043 mmol) was then added and stirring continued for another hour at the same temperature. The reaction was quenched with 2 M HCl and warmed to room temperature. The formation of product was confirmed by both TLC and ^{1}H NMR. The product was extracted with ethyl acetate (3 x 50 mL), washed with brine (2 x 25 mL) and dried with sodium sulfate and concentrated in vacuum. The crude yield was 10.15 g. The product was further purified by flash chromatography by eluting with a PE/EtOAc solvent mixture. The yield of the yellow (*R*, *S*)-1-benzoyl-2-vinyl-2, 3-dihydro-1-*H*-pyridin-4-one product was over 90%.

2.4.2.6.2 *Synthesis of 2-vinyl-2, 3-dihydro-1H-pyridin-4-one*
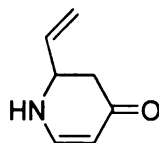
The (*R,S*)-1-benzoyl-2-vinyl-2,3-dihydro-1*H*-pyridin-4-one (681 mg, 3.00 mmol) was added to Na (35 mg, 1.56 mmol) dissolved in 9 mL of methanol at 0 °C for 30 min. The reaction was neutralized with 2 N HCl (7.5 mL), dissolved in EtOAc (25 mL) and extracted with EtOAc (2 x 25 mL). The organic layer was dried with Na$_2$SO$_4$ and concentrated in *vacuo*.

2.4.2.6.3 *Synthesis of β-allylglycine*

$$\text{H}_2\text{N} \quad \text{COOH}$$
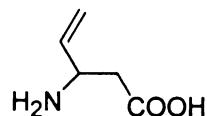
2-vinyl-2, 3-dihydro-1*H*-pyridin-4-one (5 mg, 0.04 mmol) was reacted with

NaIO$_4$ (38.5 mg, 0.18 mmol) for 2 hours at room temperature. The crude product

was mixed with acidic ion exchange resin (Amberlite IR 120), washed with

distilled H$_2$O until neutral pH and eluted with aqueous NH$_3$ (20 %) and

evaporated to dryness.

2.4.2.7 *Synthesis of N-acetyl vinyl-(RS)-β-alanine methyl ester*

$$\underset{\text{H}}{\overset{\text{O}}{\underset{\text{N}}{\bigwedge}}} \quad \text{COOCH}_3$$
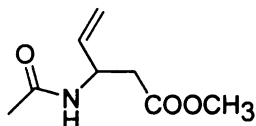
β-allylglycine (10.52 mg, 0.086 mmol) was dissolved in H$_2$O (5 mL) and

0.1 M NaOH added until pH was ~10. Acetic anhydride (8.97 mg, 0.088 mmol)

was added, and the reaction was stirred for 30 min at 25 °C. The solution was

acidified with dilute 0.1 N HCl and extracted twice with 5 mL ether. The ether

fractions were treated with diazomethane until yellow color persisted, and the

solvent was evaporated to dryness to yield *N*-acetyl vinyl-(*RS*)-β-alanine methyl

ester (8.1 mg, 54 % yield, R$_f$ = 0.22 in 90:10 hexane/ethyl acetate, (v/v) on silica

gel TLC).

^{1}H-NMR (300 MHz, CDCl$_3$): δ: 1.69 (s, COCH_3, 3H), 2.43 (dd, CH$_2$CHNH 1H),

2.69 (d, COCH_2CH, 2H), 3.72 (s, OCH_3, 3H), 4.93 (m, CH_2CHCH, 1H), 5.19-

5.23 (m, CH=CH$_2$, 2H), 5.92 (ddd, CH_2=CH, J = 18.5, 11.1, 6.0 Hz, 1H).

GC/EI-MS, diagnostic ions: m/z 171 ([M$^+$], 2%), 156 ([M-CH$_3$]$^+$, 2%), 140 ([M-

OCH$_3$]$^+$, 6%), 129 ([M-CH$_2$CO]$^+$, 38%), 128 ([M-CH$_3$CO]$^+$, 23%), 112 ([M-

CO$_2$CH$_3$], 18%), 98 ([M-CH$_2$CO$_2$CH$_3$]$^+$, 14%), 81 [H$_2$C=CHCH=NH$_2$]$^+$.

2.4.2.8 *Synthesis of (E)-5-aminopent-3-enoic acid*
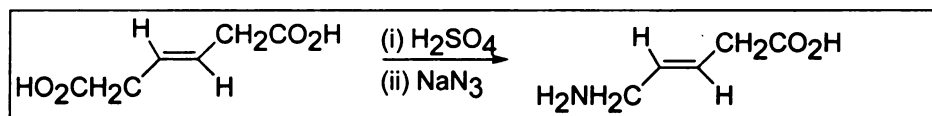
Scheme 2.15 Synthesis of (*E*)-5-aminopent-3-enoic acid.

Trans-β-hyromuconic acid (1.4 g, 0.1 mmol) was suspended in CHCl$_3$ (40

mL) and concentrated H$_2$SO$_4$ (4.0 mL) added. Sodium azide (0.65 g, 0.01 mmol)

was added in small amounts over 30 min while the mixture was stirred rapidly.

After a further 4 h at 40 ºC the CHCl$_3$ layer was decanted from the viscous

residue which was washed again with CHCl$_3$ (30 mL) and the acid layer was

dissolved with water (150 mL) and filtered. The product was derivatized to *N*-

acetylated methyl ester and assayed on GC/MS. The following peaks were

observed on mass spectrometry fragmentation as m/z, 171

([H$_2$NCH$_2$CHCHCH$_2$CO$_2$H = M]$^+$), 156 [M-CH3]$^+$, 128 [M-43]$^+$, 140 [M-31]$^+$, 112

[M-59]$^+$, 113 [M-58]$^+$, 98 [M-73]$^+$, 99 [M-72]$^+$.

2.4.2.9.1 *Synthesis of 4-Bromo-2-pentenoic acid*
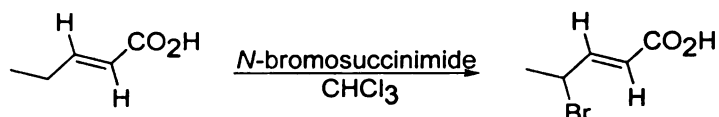
A mixture of *trans*-2-pentenoic acid (2 g, 20 mmol) and recrystallized *N*-bromosuccinimide (3.56 g, 20 mmol) in carbon tetrachloride (40 mL) was magnetically stirred and refluxed until the suspension rose to the surface (24 h). The mixture was then cooled on ice, filtered and evaporated to oil. The product was purified by crystallization from 60-80 °C light petroleum/cyclohexane to give 4-bromo-2-pentenoic acid in 60 % yield (lit). ^{1}H-NMR (300 MHz, CDCl$_3$): δ = 7.24 (dd, C*H*=CH, *J* = 13, 6.5 Hz, 1H), 6.00 (dd, CH=C*H*CH, *J* = 13, 0.7 Hz, 1H), 4.75 (multiplet, CHC*H*CH$_3$, J = 7 Hz, 1H) and 1.86 (d, CHC*H*$_3$, *J* = 5.5, 3H).

2.4.2.9.2 *Synthesis of (E)-4-amino-2-pentenoic acid*
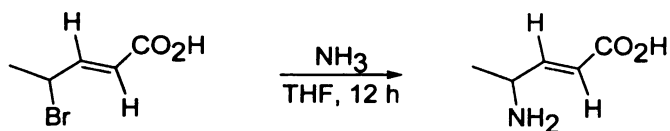
4-bromo-2-pentenoic acid (3.56 g, 20 mmol) was dissolved in Tetrahydrofuran (THF, 15 mL) and added dropwise to liquid ammonia (200 mL)

over 3 min with vigorous stirring for 12 h. The solvent was evaporated and the crude product was dissolved in water (20 mL), acidified with 1 M HCl and extracted with diethyl ether (2 x 20 mL). The aqueous layer was adsorbed on a Dowex 5W (H^+) column (40 mL). The column was eluted with water until neutral and then the amino acid was removed with 1 M ammonium hydroxide. The ammonia wash was evaporated to dryness and the product was purified by crystallization from ethanol to give *trans*-4-amino-2-pentenoic acid in 80 % yield. Mp = 196-7 °C. ^{1}H-NMR (300 MHz, D_2O): δ = 1.42 (d, CH_3CH, J = 16, 3H), 4.10 (CH$_3$CHCH, J = 10, 1H), 6.05 (d, CH=CHCO$_2$H, J = 16, 1H), 6.60 (dd, CHCH=CH, 1H).

2.4.2.10 *Invivo Screening of Amino acids*

Phenylalanine analogues were fed to a 50 mL culture of transformed *BL21 (DE3)* over expressing the PAM enzyme. The culture was initially grown to OD$_{600}$ of 0.7 at 37 °C with ampicillin selection and expression was induced with 1 mM isopropyl-β-D-thiogalactoside (IPTG). Incubation was continued for a further 18 h. The substrate concentrations ranged from 1 – 5 mM. The assay for the formation of the β-product from the *in vivo* biosynthesis was carried out by centrifuging at 5,000 x *g* for 20 min. The supernatant and cell pellet were treated separately.

2.4.2.10.1 *Treatment of the cell pellet.*

The cells were resuspended in 2 mL of phosphate buffer and lysed by sonication (5, 20 s bursts at 50% power [Misonix sonicator, Farmingdale, NY]). The cell debris was pelleted by centrifuging at 5 000 x g for 20 min. The supernatant containing the amino acid residues were basified to pH above 10 with 1 M NaOH, followed by addition of 3 equivalence acetic anhydride. After 30 min the solution was acidified using 1 M HCl and the *N*-acetylated product was extracted with ethyl acetate (3 x 15 mL). The solvent was evaporated to dryness and the solid residue was re-dissolved in a minimum volume of EtOAc, cooled in dry ice and treated with diazomethane to a faint yellow coloration. The derivatized amino acids were analyzed by GC/MS.

2.4.2.10.2 *Treatment of supernatant*

The supernatant was basified with 6 M NaOH and derivatized as described above.

2.4.2.11 *Investigating the racemase in E. coli*

In order to investigate the action of the racemase in *E. coli* a D-[ring, $^2H_5$] phenylalanine was incubated with *E. coli* BL21(DE3) transformed with the *pam* plasmid as described above. Further effect of the D-isomer on the PAM reaction was carried out by incubating various concentration of this amino acid with pure PAM.

2.5 REFERENCES

1. Meier, J. J.; Schmidt, W. E.; Klein, H. H., New concepts in the treatment of type 2 diabetes. *Internist* **2007**, *48*, (7), 698.

2. Smolke, C. D.; Martin, V. J. J.; Keasling, J. D., Tools for metabolic engineering in *Escherichia coli*. *Protein Expression Technologies* **2004**, 149-197.

3. Baloglu, E.; Kingston, D. G. I., The taxane diterpenoids. *J. Nat. Prod.* **1999**, *62*, (10), 1448-1472.

4. Chau, M.; Walker, K.; Long, R.; Croteau, R., Regioselectivity of taxoid-O-acetyltransferases: heterologous expression and characterization of a new taxadien-5a-ol-O-acetyltransferase. *Arch. Biochem. Biophys.* **2004**, *430*, (2), 237-246.

5. Das, B.; Rao, S. P., Review on the chemical constituents of medicinal plants and bioactive natural products. Viii. Naturally occurring oxetane-type taxoids. *Indian J. Chem., Sect. B: Org. Chem. Incl. Med. Chem.* **1996**, 35B, (9), 883-893.

6. Dejong, J. M.; Liu, Y.; Bollon, A. P.; Long, R. M.; Jennewein, S.; Williams, D.; Croteau, R. B., Genetic engineering of taxol biosynthetic genes in Saccharomyces cerevisiae. *Biotechnol. Bioeng.* **2006**, *93*, (2), 212-24.

7. Della Casa de Marcano, D. P.; Halsall, T. G., Structures of some Taxane Diterpenoids, Baccatins-III, -IV, -VI, and -VII and I-Dehydroxybaccatin-IV, Possessing an Oxetan Ring. *J. Chem. Soc., Chem. Commun* **1975**, 365.

8. Hezari, M.; Lewis, N. G.; Croteau, R., Purification and characterization of taxa-4(5),11(12)-diene synthase from Pacific yew (*Taxus brevifolia*) that catalyzes the first committed step of Taxol biosynthesis. *Arch. Biochem. Biophys.* **1995**, *322*, (2), 437-44.

9. Jennewein, S.; Rithner, C. D.; Williams, R. M.; Croteau, R. B., Taxol biosynthesis: Taxane 13-hydroxylase is a cytochrome P450-dependent monooxygenase. *Proc. Nat. Acad. Sci. U. S. A.* **2001**, *98*, (24), 13595-13600.

10. Kingston, D. G. I.; Molinero, A. A.; Rimoldi, J. M., The Taxane Diterpenoids. In *Progress in the Chemistry of Organic Natural Products*, ed.; Herz, W.; Kirby, G. W.; Moore, R. E.; Steglich, W.; Tamm, C., Springer-Verlag: New York, 1993; *61*, 206.

11.   Kobayashi, J. i.; Shigemori, H.; Hosoyama, H.; Ogiwara, A.; Yoshida, N.; Sasaki, T.; Li, Y.; Koiso, Y.; Iwasaki, S.; et al., Taxuspines A-E, new taxoids from Japanese yew, Taxus cuspidata inhibiting drug transport activity of P-glycoprotein on multidrug-resistant cells. *Tennen Yuki Kagobutsu Toronkai Koen Yoshishu* **1995,** 37th, 192-7.

12.   Long, R. M.; Croteau, R., Preliminary assessment of the C13-side chain 2'-hydroxylase involved in Taxol biosynthesis. *Biochem. Biophysical Res. Commun.* **2005,** *338,* (1), 410-417.

13.   Shi, Q.-W.; Oritani, T.; Sugiyama, T.; Kiyota, H., Three Novel Bicyclic 3,8-Secotaxane Diterpenoids from the Needles of the Chinese Yew, *Taxus chinensis var. mairei. J. Nat. Prod.* **1998,** *61,* (11), 1437-1440.

14.   Abdel-Kader, M.; Berger, J. M.; Slebodnick, C.; Hoch, J.; Malone, S.; Wisse, J. H.; Werkhoven, M. C. M.; Mamber, S.; Kingston, D. G. I., Isolation and absolute configuration of ent-halimane diterpenoids from Hymenaea courbaril from the Suriname rain forest. *J. Nat. Prod.* **2002,** *65,* (1), 11-15.

15.   Ahn, H. J.; Kim, Y. S.; Kim, J.-U.; Han, S. M.; Shin, J. W.; Yang, H. O., Mechanism of taxol-induced apoptosis in human SKOV3 ovarian carcinoma cells. *J. Cell. Biochem.* **2004,** *91,* (5), 1043-1052.

16.   Apte, S. M.; Fan, D.; Killion, J. J.; Fidler, I. J., Targeting the platelet-derived growth factor receptor in antivascular therapy for human ovarian carcinoma. *Clin. Cancer Res.* **2004,** *10,* (3), 897-908.

17.   Baloglu, E.; Hoch, J. M.; Chatterjee, S. K.; Ravindra, R.; Bane, S.; Kingston, D. G. I., Synthesis and biological evaluation of C-3'NH/C-10 and C-2/C-10 modified paclitaxel analogues. *Bioorg. Med. Chem.* **2003,** *11,* (7), 1557-1568.

18.   Battaglia, A.; Bernacki, R. J.; Bertucci, C.; Bombardelli, E.; Cimitan, S.; Ferlini, C.; Fontana, G.; Guerrini, A.; Riva, A., Synthesis and Biological Evaluation of 2'-Methyl Taxoids Derived from Baccatin III and 14b-OH-Baccatin III 1,14-Carbonate. *J. Med. Chem.* **2003,** *46,* (23), 4822-4825.

19.   Chaturvedula, V. S. P.; Schilling, J. K.; Miller, J. S.; Andriantsiferana, R.; Rasamison, V. E.; Kingston, D. G. I., New Cytotoxic Bis 5-Alkylresorcinol Derivatives from the Leaves of *Oncostemon bojerianum* from the Madagascar Rainforest. *J. Nat. Prod.* **2002,** *65,* 1222-1224.

20.   Jagtap, P. G.; Baloglu, E.; Barron, D. M.; Bane, S.; Kingston, D. G. I., Design and Synthesis of a Combinatorial Chemistry Library of 7-Acyl, 10-

Acyl, and 7,10-Diacyl Analogues of Paclitaxel (Taxol) Using Solid Phase Synthesis. *J. Nat. Prod.* **2002,** *65,* (8), 1136-1142.

21.   Kingston, D. G. I.; Ganesh, T.; Snyder, J. P.; Lakdawala, A. S.; Bane, S. Preparation of conformationally constrained paclitaxel analogs as anticancer and anti-Alzheimer's agents. PCT WO 2005/070414, January 14, 2005.

22.   Larkin, J. M. G.; Kaye, S. B., Epothilones in the treatment of cancer. *Expert Opin. Investigational Drugs* **2006,** *15,* (6), 691-702.

23.   Liu, C.; Strobl, J. S.; Bane, S.; Schilling, J. K.; McCracken, M.; Chatterjee, S. K.; Rahim-Bata, R.; Kingston, D. G. I., Design, synthesis, and bioactivities of steroid-linked Taxol analogues as potential targeted drugs for prostate and breast cancer. *J. Nat. Prod.* **2004,** *67,* (2), 152-159.

24.   Lu, H.; Li, B.; Kang, Y.; Jiang, W.; Huang, Q.; Chen, Q.; Li, L.; Xu, C., Paclitaxel nanoparticle inhibits growth of ovarian cancer xenografts and enhances lymphatic targeting. *Cancer Chemother. Pharmacol.* **2007,** *59,* (2), 175-181.

25.   McGuire, W. P.; Markman, M., Primary ovarian cancer chemotherapy: current standards of care. *Bri. J. Cancer* **2003,** *89,* (Suppl. 3), S3-S8.

26.   Prakash, C. V. S.; Hoch, J. M.; Kingston, D. G. I., Structure and stereochemistry of new cytotoxic clerodane diterpenoids from the bark of *Casearia lucida* from the Madagascar rainforest. *J. Nat. Prod.* **2002,** *65,* (2), 100-107.

27.   Rowinsky, E. K.; Citardi, M. J.; Noe, D. A.; Donehower, R. C., Sequence-dependent cytotoxic effects due to combinations of cisplatin and the antimicrotubule agents taxol and vincristine. *J. Cancer Res. Clin. Oncol.* **1993,** *119,* (12), 727-33.

28.   Stinchcombe, T. E.; Socinski, M. A.; Walko, C. M.; O'Neil, B. H.; Collichio, F. A.; Ivanova, A.; Mu, H.; Hawkins, M. J.; Goldberg, R. M.; Lindley, C.; Dees, E. C., Phase I and pharmacokinetic trial of carboplatin and albumin-bound paclitaxel, ABI-007 (Abraxane) on three treatment schedules in patients with solid tumors. *Cancer Chemother. Pharmacol.* **2007,** *60,* (5), 759-766.

29.   Tonini, T.; Gabellini, C.; Bagella, L.; D'Andrilli, G.; Masciullo, V.; Romano, G.; Scambia, G.; Zupi, G.; Giordano, A., PRb2/p130 decreases sensitivity to apoptosis induced by camptothecin and doxorubicin but not by taxol. *Clin. Canc. Res.* **2004,** *10,* (23), 8085-8093.

30. Wall, M. E.; Wani, M. C., Camptothecin and taxol: discovery to clinic - thirteenth Bruce F. Cain Memoral Award Lecture. *Cancer Res.* **1995,** *55,* (4), 753-60.

31. Wall, M. E.; Wani, M. C., Camptothecin and taxol: From discovery to clinic. *J. Ethnopharmacol.* **1996,** *51,* (1-3), 239-54.

32. Cheung, M. C.; Pantanowitz, L.; Dezube, B. J., AIDS-related malignancies: emerging challenges in the era of highly active antiretroviral therapy. *Oncologist* **2005,** *10,* (6), 412-426.

33. Fardet, L.; Stoebner, P.-E.; Bachelez, H.; Descamps, V.; Kerob, D.; Meunier, L.; Dandurand, M.; Morel, P.; Lebbe, C., Treatment with taxanes of refractory or life-threatening Kaposi sarcoma not associated with human immunodeficiency virus infection. *Cancer* **2006,** *106,* (8), 1785-1789.

34. Sgadari, C.; Toschi, E.; Palladino, C.; Barillari, G.; Carlei, D.; Cereseto, A.; Ciccolella, C.; Yarchoan, R.; Monini, P.; Sturzl, M.; Ensoli, B., Mechanism of paclitaxel activity in Kaposi's sarcoma. *J. Immunol.* **2000,** *165,* (1), 509-517.

35. Chou, T.-C.; Zhang, X.-G.; Harris, C. R.; Kuduk, S. D.; Balog, A.; Savin, K. A.; Bertino, J. R.; Danishefsky, S. J., Desoxyepothilone B is curative against human tumor xenografts that are refractory to paclitaxel. *Proc. Nat. Acad. Sci. U. S. A.* **1998,** *95,* (26), 15798-15802.

36. Holton, R. A.; Nadizadeh, H.; Biediger, R. J.; Rengan, K.; Suzuki, Y.; Tao, C.; Chai, K.-B.; Idmoumaz, H. Preparation of taxanes having furyl or thienyl substituted side-chain as antileukemia and antitumor agents. PCT WO 9421651, 19940321., 1994.

37. Rowinsky, E. K.; Donehower, R. C.; Jones, R. J.; Tucker, R. W., Microtubule changes and cytotoxicity in leukemic cell lines treated with taxol. *Cancer Res.* **1988,** *48,* (14), 4093-100.

38. Terasawa, H.; Soga, T.; Uoto, K. Preparation of baccatin III derivatives as antitumors. PCT WO 9633998, April 25, 1996, 1996.

39. Woo, D. D. L.; Miao, S. Y. P.; Pelayo, J. C.; Woolf, A. S., Taxol inhibits progression of congenital polycystic kidney disease. *Nature* **1994,** *368,* (6473), 750-753.

40. Parry, T. J.; Brosius, R.; Thyagarajan, R.; Carter, D.; Argentieri, D.; Falotico, R.; Siekierka, J., Drug-eluting stents: Sirolimus and paclitaxel

differentially affect cultured cells and injured arteries. *Eur. J. Pharmacol.* **2005**, *524*, (1-3), 19-29.

41.   Cremers, B.; Biedermann, M.; Mahnkopf, D.; Bohm, M.; Scheller, B., Comparison of two different paclitaxel-coated balloon catheters in the porcine coronary restenosis model. *Clin. Res. Cardiol.* **2009**, *98*, (5), 325-330.

42.   Dangas, G.; Ellis, S. G.; Shlofmitz, R.; Katz, S.; Fish, D.; Martin, S.; Mehran, R.; Russell, M. E.; Stone, G. W., Outcomes of paclitaxel-eluting stent implantation in patients with stenosis of the left anterior descending coronary artery. *J. Am. Coll. Cardiol.* **2005**, *45*, (8), 1186-1192.

43.   Boutte, A. M.; Neely, M. D.; Bird, T. D.; Montine, K. S.; Montine, T. J., Diminished taxol/GTP-stimulated tubulin polymerization in diseased region of brain from patients with late-onset or inherited Alzheimer's disease or frontotemporal dementia with parkinsonism linked to chromosome-17 but not individuals with mild cognitive impairment. *J. Alzheimer's Disease* **2005**, *8*, (1), 1-6.

44.   Butler, D.; Bendiske, J.; Michaelis, M. L.; Karanian, D. A.; Bahr, B. A., Microtubule-stabilizing agent prevents protein accumulation-induced loss of synaptic markers. *Eur. J. Pharmacol.* **2007**, *562*, (1-2), 20-27.

45.   Jakob-Roetne, R.; Jacobsen, H., Alzheimer's Disease: From Pathology to Therapeutic Approaches. *Ang. Chem. Int. Edition* **2009**, *48*, (17), 3030-3059.

46.   Li, G.; Faibushevich, A.; Turunen, B. J.; Yoon, S. O.; Georg, G.; Michaelis, M. L.; Dobrowsky, R. T., Stabilization of the cyclin-dependent kinase 5 activator, p35, by paclitaxel decreases b-amyloid toxicity in cortical neurons. *J. Neurochem.* **2003**, *84*, (2), 347-362.

47.   Michaelis, M. L.; Ranciat, N.; Chen, Y.; Bechtel, M.; Ragan, R.; Hepperle, M.; Liu, Y.; Georg, G., Protection against β-amyloid toxicity in primary neurons by paclitaxel (taxol). *J. Neurochem.* **1998**, *70*, (4), 1623-1627.

48.   Seyb, K. I.; Ansar, S.; Bean, J.; Michaelis, M. L., β-Amyloid and endoplasmic reticulum stress responses in primary neurons: effects of drugs that interact with the cytoskeleton. *J. Mol. Neurosci.* **2006**, 28, (2), 111-124.

49.   Sheffler, D. J.; Roth, B. L., Salvinorin A: the `magic mint' hallucinogen finds a molecular target in the kappa opioid receptor. *Trends in Pharmacol. Sci.* **2003**, *24*, (3), 107-109.

50.   Vongpaseuth, K.; Roberts, S. C., Advancements in the understanding of paclitaxel metabolism in tissue culture. *Curr. Pharm. Biotechnol.* **2007**, *8*, (4), 219-236.

51.   Zhang, Q.; Powers, E. T.; Nieva, J.; Huff, M. E.; Dendle, M. A.; Bieschke, J.; Glabe, C. G.; Eschenmoser, A.; Wentworth, P., Jr.; Lerner, R. A.; Kelly, J. W., Metabolite-initiated protein misfolding may trigger Alzheimer's disease. *Proc. Nat. Acad. Sci. U.S. A.* **2004**, *101*, (14), 4752-4757.

52.   Belyaev, N. A.; Kolesanova, E. F.; Kelesheva, L. F.; Rotanova, T. V.; Panchenko, L. F., Effect of the aminopeptidase inhibitor bestatin on rat brain enkephalin levels. *Bull. Exp. Biol. Med.* **1990**, *110*, (5), 1483-1485.

53.   Sitagliptin (Januvia) for type 2 diabetes. *Med. Let.t Drugs Ther* **2007**, *49*, (1251), 1-3.

54.   Three new drugs for type 2 diabetes. *Drug Ther. Bull.* **2008**, *46*, (7), 49-52.

55.   Davis, J. A.; Singh, S.; Roy, S.; Sundaram, S.; Sethi, S.; Benjamin, B.; Surender, A.; Khanna, V.; Mittra, S.; Pal, C.; Mahajan, D.; Ahmed, S.; Sharma, L.; Rajivkant; Bansal, V. S.; Saini, K. S.; Sattigeri, J.; Palliwal, J.; Ray, A.; Bhatnagar, P. K., Identification of novel orally active dipeptidyl peptidase IV inhibitor 7E8E80B, equipotent and equi-efficaceous to Januvia (TM). *Indian J. Pharm.* **2008**, *40*, 482.

56.   Duh, D.; Vandevijver, A., Sitagliptine (Januvia). *J. Pharm. Belg.* **2008**, *63*, (1), 31-2.

57.   Gallwitz, B., Review of sitagliptin phosphate: a novel treatment for type 2 diabetes. *Vasc Health Risk Manag* **2007**, *3*, (2), 203-10.

58.   Thornberry, N. A.; Weber, A. E., Discovery of JANUVIA[(TM)] (Sitagliptin), a selective dipeptidyl peptidase IV inhibitor for the treatment of type2 diabetes. *Curr. Topic. Med. Chem.* **2007**, 7, (6), 557-568.

59.

60.   Yin, X.; O'Hare, T.; Gould, S. J.; Zabriskie, T. M., Identification and cloning of genes encoding viomycin biosynthesis from *Streptomyces vinaceus* and evidence for involvement of a rare oxygenase. *Gene* **2003**, *312*, 215-224.

61.   Weaver, D. F.; Tan, C. Y. K.; Kim, S. T.; Kong, X.; Wei, L.; Carran, J. R. Antiepileptogenic agents. WO 2002073208, 20020313., 2002.

62. Porter, E. A.; Weisblum, B.; Gellman, S. H., Mimicry of Host-Defense Peptides by Unnatural Oligomers: Antimicrobial b-Peptides. *J. Am. Chem. Soc.* **2002,** *124,* (25), 7324-7330.

63. Baloglu, E.; Kingston, D. G. I., A New Semisynthesis of Paclitaxel from Baccatin III. *J. Nat. Prod.* **1999,** *62,* (7), 1068-1071.

64. Commerçon, A.; Bourzat, J. D.; Didier, E.; Lavelle, F., Practical semisynthesis and antimitotic activity of docetaxel and side-chain analogs. In *Taxane Anticancer Agents: Basic Science and Current Status,* ed.; Georg, G. I.; Chen, T. T.; Ojima, I.; Vyas, D. M., Am. Chem. Soc.: Washington, DC, 1995; 233-246.

65. Gennari, C.; Carcano, M.; Donghi, M.; Mongelli, N.; Vanotti, E.; Vulpetti, A., Taxol Semisynthesis: A Highly Enantio- and Diastereoselective Synthesis of the Side Chain and a New Method for Ester Formation at C-13 Using Thioesters. *J. Org. Chem.* **1997,** *62,* (14), 4746-4755.

66. Georg, G. I.; Cheruvallath, Z. S.; Harriman, G. C. B.; Hepperle, M.; Park, H., an efficient semisynthesis of taxol from (3R,4S)-N-benzoyl-3-[test-butyldimethylsilyl)oxy]-4-phenyl-2-azetidinone and 7-(triethylsilyl)baccatin III. *Bioorg. Med. Chem. Lett.* **1993,** 3, (11), 2467-2470.

67. Holton, R. A.; Biediger, R. J.; Boatman, P. D., Semisynthesis of Taxol and Taxotère. In *Taxol: Science and Applications,* ed.; Suffness, M.,.' CRC Press: Boca Raton, FL, 1995; 97-121.

68. Ojima, I.; Habus, I.; Zhao, M.; Zucco, M.; Park, Y. H.; Sun, C. M.; Brigaud, T., New and efficient approaches to the semisynthesis of taxol and its C-13 side chain analogs by means of .beta.-lactam synthon method. *Tetrahedron* **1992,** *48,* (34), 6985-7012.

69. Wiegerinck, P. H. G.; Fluks, L.; Hammink, J. B.; Mulders, S. J. E.; de Groot, F. M. H.; van Rozendaal, H. L. M.; Scheeren, H. W., Semisynthesis of Some 7-Deoxypaclitaxel Analogs from Taxine B. *J. Org. Chem.* **1996,** *61,* (20), 7092-7100.

70. Baloglu, E.; Miller, M. L.; Cavanagh, E. E.; Marien, T. P.; Roller, E. E.; Chari, R. V. J., A facile one-pot synthesis of 7-triethylsilylbaccatin III. *Synlett* **2005,** (5), 817-818.

71. Brincat, M. C.; Gibson, D. M.; Shuler, M. L., Alterations in Taxol Production in Plant Cell Culture via Manipulation of the Phenylalanine Ammonia Lyase Pathway. *Biotechn. Progr.* **2002,** *18,* (6), 1149-1156.

72.   Dixon, R. A.; Paiva, N. L., Stress-induced phenylpropanoid metabolism. *Plant Cell* **1995**, *7*, (7), 1085-97.

73.   Doernenburg, H.; Knoor, D., Strategies for the improvement of secondary metabolite production in plant cell cultures. *Enzyme Microb. Technol.* **1995**, *17*, (8), 674-84.

74.   Dong, H.-D.; Zhong, J.-J., Enhanced taxane productivity in bioreactor cultivation of Taxus chinensis cells by combining elicitation, sucrose feeding and ethylene incorporation. *Enzyme Microb. Technol.* **2002**, *31*, (1-2), 116-121.

75.   Eichinger, D.; Bacher, A.; Zenk, M. H.; Eisenreich, W., Analysis of metabolic pathways via quantitative prediction of isotope labeling patterns: a retrobiosynthetic 13C NMR study on the monoterpene loganin. *Phytochemistry* **1999**, *51*, (2), 223-236.

76.   Exposito, O.; Bonfill, M.; Moyano, E.; Onrubia, M.; Mirjalili, M. H.; Cusido, R. M.; Palazon, J., Biotechnological Production of Taxol and Related Taxoids: Current State and Prospects. *Anti-Cancer Agents in Med. Chem.* **2009**, *9*, (1), 109-121.

77.   Gibson, D. M.; Ketchum, R. E. B.; Hirasuna, T. J.; Shuler, M. L., Potential of Plant Cell Culture for Taxane Production. In *Taxol: Science and Applications*, ed.; Suffness, M., CRC Press: New York, 1995; 71-95.

78.   Hellwig, S.; Drossard, J.; Twyman, R. M.; Fischer, R., Plant cell cultures for the production of recombinant proteins. *Nature Biotechnol.* **2004**, *22*, (11), 1415-1422.

79.   Ilag, L. L.; Kumar, A. M.; Soll, D., Light regulation of chlorophyll biosynthesis at the level of 5-aminolevulinate formation in Arabidopsis. *Plant Cell* **1994**, *6*, (2), 265-75.

80.   Jung, J. D.; Park, H. W.; Hahn, Y.; Hur, C. G.; In, D. S.; Chung, H. J.; Liu, J. R.; Choi, D. W., Discovery of genes for ginsenoside biosynthesis by analysis of ginseng expressed sequence tags. *Plant Cell Reports* **2003**, *22*, (3), 224-230.

81.   Ketchum, R. E. B.; Gibson, D. M.; Greenspan Gallo, L., Media optimization for maximum biomass production in cell cultures of pacific yew. *Plant Cell, Tissue and Organ Culture* **1995**, *42*, 185-193.

82. Ketchum, R. E. B.; Gibson, D. M., Paclitaxel production in suspension cell cultures of Taxus. *Plant Cell, Tissue and Organ Culture* **1996,** *46,* (1), 9-16.

83. Ketchum, R. E. B.; Croteau, R. B., Recent progress toward an understanding of Taxol biosynthesis in plant cell cultures. *Int. Congr. Ser.* **1998,** 1157, (Towards Natural Medicine Research in the 21st Century), 339-348.

84. Naill, M. C.; Roberts, S. C., Cell cycle analysis of *Taxus* suspension cultures at the single cell level as an indicator of culture heterogeneity. *Biotechnol. Bioeng.* **2005,** *90,* (4), 491-500.

85. Rohmer, M., Mevalonate-independent methylerythritol phosphate pathway for isoprenoid biosynthesis. Elucidation and distribution. *Pure Appl. Chem.* **2003,** *75,* (2-3), 375-387.

86. Croteau, R.; Kutchan, T. M.; Lewis, N. G., Natural products (secondary metabolites). *Biochem. Mol. Biol. Plants* **2000,** 1250-1318.

87. Duvold, T.; Cali, P.; Bravo, J.-M.; Rohmer, M., Incorporation of 2-C-methyl-D-erythritol, a putative isoprenoid precursor in the mevalonate-independent pathway, into ubiquinone and menaquinone of Escherichia coli. *Tetrahedron Lett.* **1997,** *38,* (35), 6181-6184.

88. Lange, B. M.; Wildung, M. R.; McCaskill, D.; Croteau, R., A family of transketolases that directs isoprenoid biosynthesis via a mevalonate-independent pathway. *Proc. Nat. Acad. Sci. U. S. A.* **1998,** *95,* 2100-2104.

89. Lange, B. M.; Croteau, R., Isopentenyl diphosphate biosynthesis *via* a mevalonate-independent pathway: Isopentenyl monophosphate kinase catalyzes the terminal enzymatic step. *Proc. Nat. Acad. Sci. U. S. A.* **1999,** *96,* (24), 13714-13719.

90. Lichtenthaler, H. K., The 1-deoxy-D-xylulose-5-phosphate pathway of isoprenoid biosynthesis in plants. *Ann. Rev. Plant Physiol. Plant Mol. Biol.* **1999,** *50,* 47-65.

91. Rohmer, M.; Knani, M. h.; Simonin, P.; Sutter, B.; Sahm, H., Isoprenoid biosynthesis in bacteria: A novel pathway for the early steps leading to isopentenyl diphosphate. *Biochem. J.* **1993,** *295,* (2), 517-24.

92. Rohmer, M.; Seemann, M.; Horbach, S.; Bringer-Meyer, S.; Sahm, H., Glyceraldehyde 3-phosphate and pyruvate as precursors of isoprenic

units in an alternative non-mevalonate pathway for terpenoid biosynthesis. *J. Am. Chem. Soc.* **1996**, *118*, (11), 2564-6.

93. Arigoni, D.; Eisenreich, W.; Latzel, C.; Sagner, S.; Radykewicz, T.; Zenk, M. H.; Bacher, A., Dimethylallyl pyrophosphate is not the committed precursor of isopentenyl pyrophosphate during terpenoid biosynthesis from 1-deoxyxylulose in higher plants. *Proc. Nat. Acad. Sci. U. S. A.* **1999**, *96*, (4), 1309-1314.

94. Bacher, A.; Rieder, C.; Eichinger, D.; Arigoni, D.; Fuchs, G.; Eisenreich, W., Elucidation of novel biosynthetic pathways and metabolite flux patterns by retrobiosynthetic NMR analysis. *FEMS Microbiol. Rev.* **1998**, *22*, (5), 567-598.

95. Eisenreich, W.; Schwarz, M.; Cartayrade, A.; Arigoni, D.; Zenk, M. H.; Bacher, A., The deoxyxylulose phosphate pathway of terpenoid biosynthesis in plants and microorganisms. *Chem. Biol.* **1998**, *5*, (9), R221-R223.

96. Besumbes, O.; Sauret-Gueeto, S.; Phillips, M. A.; Imperial, S.; Rodriguez-Concepcion, M.; Boronat, A., Metabolic engineering of isoprenoid biosynthesis in Arabidopsis for the production of taxadiene, the first committed precursor of Taxol. *Biotechnol. Bioeng.* **2004**, *88*, (2), 168-175.

97. Barnes, H. J.; Jenkins, C. M.; Waterman, M. R., Baculovirus expression of bovine cytochrome P450c17 in Sf9 cells and comparison with expression yeast, mammalian cells, and *E. coli*. *Arch. Biochem. Biophys.* **1994**, *315*, (2), 489-94.

98. Barnes, H. J., Maximizing expression of eukaryotic cytochrome P450s in Escherichia coli. *Methods Enzymol.* **1996**, 272, (Cytochrome P450, Part B), 3-14.

99. Bertea, C.; Schalk, M.; Karp, F.; Maffei, M.; Croteau, R., Demonstration that menthofuran synthase of mint (*Mentha*) is a cytochrome P450 monooxygenase: Cloning, functional expression, and characterization of the responsible gene. *Arch. Biochem. Biophys.* **2001**, *390*, (2), 279-286.

100. Bolwell, G. P.; Bozak, K.; Zimmerlin, A., Review article number 96: Plant cytochrome P450. *Phytochemistry* **1994**, *37*, (6), 1491-506.

101. Chau, M.; Jennewein, S.; Walker, K.; Croteau, R., Taxol biosynthesis: Molecular cloning and characterization of a cytochrome P450 taxoid 7b-hydroxylase. *Chem. Biol.* **2004**, *11*, (5), 663-672.

102. Dixon, R. A., Plant natural products: the molecular genetic basis of biosynthetic diversity. *Curr. Opin. Biotechnol.* **1999**, *10*, (2), 192-197.

103. Hasler, J. A.; Harlow, G. R.; Szklarz, G. D.; John, G. H.; Kedzie, K. M.; Burnett, V. L.; He, Y. A.; Kaminsky, L. S.; Halpert, J. R., Site-directed mutagenesis of putative substrate recognition sites in cytochrome P450 2B11: importance of amino acid residues 114, 290, and 363 for substrate specificity. *Mol. Pharm.* **1994**, *46*, (2), 338-345.

104. Haudenschild, C.; Schalk, M.; Karp, F.; Croteau, R., Functional expression of regiospecific cytochrome P450 limonene hydroxylases from mint (*Mentha* spp.) in *Escherichia coli* and *Saccharomyces cerevisiae. Arch. Biochem. Biophys.* **2000**, *379*, (1), 127-136.

105. He, Y.; Luo, Z.; Klekotka, P. A.; Burnett, V. L.; Halpert, J. R., Structural determinants of cytochrome P450 2B1 specificity: evidence for five substrate recognition sites. *Biochemistry* **1994**, *33*, (14), 4419-24.

106. Hefner, J.; Rubenstein, S. M.; Ketchum, R. E. B.; Gibson, D. M.; Williams, R. M.; Croteau, R., Cytochrome P450-catalyzed hydroxylation of taxa-4(5),11(12)-diene to taxa-4(20),11(12)-dien-5?-ol: the first oxygenation step in taxol biosynthesis. *Chem. Biol.* **1996**, *3*, (6), 479-489.

107. Helliwell, C. A.; Chandler, P. M.; Poole, A.; Dennis, E. S.; Peacock, W. J., The CYP88A cytochrome P450, ent-kaurenoic acid oxidase, catalyzes three steps of the gibberellin biosynthesis pathway. *Proc. Nat. Acad. Sci. U.S.A.* **2001**, *98*, (4), 2065-2070.

108. Hiroya, K.; Murakami, Y.; Shimizu, T.; Hatano, M.; de Montellano, P. R. O., Differential roles of Glu318 and Thr319 in cytochrome P450 1A2 catalysis supported by NADPH-cytochrome P450 reductase and tert-butyl hydroperoxide. *Arch. Biochem. Biophys.* **1994**, *310*, (2), 397-401.

109. Hoffmann, L.; Maury, S.; Martz, F.; Geoffroy, P.; Legrand, M., Purification, Cloning, and Properties of an Acyltransferase Controlling Shikimate and Quinate Ester Intermediates in Phenylpropanoid Metabolism. *J. Biol. Chem.* **2003**, *278*, (1), 95-103.

110. Jennewein, S.; Wildung, M. R.; Chau, M.; Walker, K.; Croteau, R., Random sequencing of an induced *Taxus* cell cDNA library for identification of clones involved in Taxol biosynthesis. *Proc. Nat. Acad. Sci. U.S. A.* **2004**, *101*, (24), 9149-9154.

111. Lupien, S.; Karp, F.; Ponnamperuma, K.; Wildung, M.; Croteau, R., Cytochrome P450 Limonene Hydroxylases of *Mentha* Species. *Drug Metab. Drug Interact.* **1995**, *12*, 245-260.

112. Lupien, S.; Karp, F.; Wildung, M.; Croteau, R., Regiospecific cytochrome P450 limonene hydroxylases from mint (*Mentha*) species: cDNA isolation, characterization, and functional expression of (-)-4*S*-limonene-3-hydroxylase and (-)-4S-limonene-6-hydroxylase. *Arch. Biochem. Biophys.* **1999**, *368*, (1), 181-192.

113. Morant, M.; Bak, S.; Moller, B. L.; Werck-Reichhart, D., Plant cytochromes P450: Tools for pharmacology, plant protection and phytoremediation. *Current Opin. Biotechnol.* **2003,** *14*, (2), 151-162.

114. Oritz de Montellano, P. R.; Shirane, N.; Sui, Z.; Fruetel, J.; Peterson, J. A.; De Voss, J. J. In *Cytochrome P450: Topology and catalysis*, 1994; Lechner, M. C., Libbey, Montrouge, Fr.: 1994; Meeting Date 1993, 409-16.

115. Otey, C. R.; Landwehr, M.; Endelman, J. B.; Hiraga, K.; Bloom, J. D.; Arnold, F. H., Structure-guided recombination creates an artificial family of cytochromes P450. *PLoS Biology* **2006,** *4*, (5), 789-798.

116. Oudin, A.; Hamdi, S.; Ouelhazi, L.; Chenieux, J.-C.; Rideau, M.; Clastre, M., Induction of a novel cytochrome P450 (CYP96 family) in periwinkle (Catharanthus roseus) cells induced for terpenoid indole alkaloid production. *Plant Science (Shannon, Ireland)* **1999,** *149*, (2), 105-113.

117. Schalk, M.; Croteau, R., A single amino acid substitution (F363I) converts the regiochemistry of the spearmint (-)-limonene hydroxylase from a C6- to a C3-hydroxylase. *Proc. Nat. Acad. Sci. U.S. A.* **2000,** *97*, (22), 11948-11953.

118. Schlichting, I.; Berendzen, J.; Chu, K.; Stock, A. M.; Maves, S. A.; Benson, D. E.; Sweet, R. M.; Ringe, D.; Petsko, G. A.; Sligar, S. G., The catalytic pathway of cytochrome P450cam at atomic resolution. *Science* **2000,** *287*, (5458), 1615-1622.

119. Schoendorf, A.; Rithner, C.; Williams, R.; Croteau, R., Molecular cloning of a cytochrome 450 taxane 10b-hydroxylase cDNA from *Taxus* and functional expression in yeast. *Proc. Nat. Acad. of Sci. U.S. A.* **2001,** *98*, (4), 1501-1506.

120. Wang, E.; Gan, S.; Wagner, G. J., Isolation and characterization of the CYP71D16 trichome-specific promoter from Nicotiana tabacum L. *J. Exp. Botany* **2002,** *53*, (376), 1891-1897.

121. Wang, E.; Wagner, G. J., Elucidation of the functions of genes central to diterpene metabolism in tobacco trichomes using posttranscriptional gene silencing. *Planta* **2003,** *216,* (4), 686-691.

122. Wheeler, A. L.; Long, R. M.; Ketchum, R. E. B.; Rithner, C. D.; Williams, R. M.; Croteau, R., Taxol Biosynthesis: Differential Transformations of Taxadien-5α-ol and Its Acetate Ester by Cytochrome P450 Hydroxylases from Taxus Suspension Cells. *Arch. Biochem. Biophys.* **2001,** *390,* (2), 265-278.

123. Allina, S. M.; Pri-Hadash, A.; Theilmann, D. A.; Ellis, B. E.; Douglas, C. J., 4-Coumarate:coenzyme A ligase in hybrid poplar. Properties of native enzymes, cDNA cloning, and analysis of recombinant enzymes. *Plant Physiol.* **1998,** *116,* (2), 743-754.

124. Beuerle, T.; Pichersky, E., Enzymatic Synthesis and Purification of Aromatic Coenzyme A Esters. *Anal. Biochem.* **2002,** *302,* (2), 305-312.

125. Beuerle, T.; Pichersky, E., Purification and characterization of benzoate:coenzyme A ligase from Clarkia breweri. *Arch. Biochem. Biophys.* **2002,** *400,* (2), 258-264.

126. Cukovic, D.; Ehlting, J.; VanZiffle, J. A.; Douglas, C. J., Structure and evolution of 4-coumarate:coenzyme A ligase (4CL) gene families. *Biol. Chem.* **2001,** *382,* (4), 645-654.

127. Egland, P. G.; Gibson, J.; Harwood, C. S., Benzoate-coenzyme A ligase, encoded by badA, is one of three ligases able to catalyze benzoyl-coenzyme A formation during anaerobic growth of Rhodopseudomonas palustris on benzoate. *J. Bacteriol.* **1995,** *177,* (22), 6545-51.

128. Preston, G. G.; Wall, J. D.; Emerich, D. W., Purification and properties of acetyl-CoA synthetase from Bradyrhizobium japonicum bacteroids. *Biochem. J.* **1990,** *267,* (1), 179-83.

129. Walker, K.; Croteau, R., Molecular cloning of a 10-deacetylbaccatin III-10-*O*-acetyl transferase cDNA from *Taxus* and functional expression in *Escherichia coli. Proc. Nat. Acad. Sci. U.S. A.* **2000,** *97,* (2), 583-587.

130. D'Auria, J. C.; Chen, F.; Pichersky, E., Characterization of an Acyltransferase Capable of Synthesizing Benzylbenzoate and Other Volatile Esters in Flowers and Damaged Leaves of *Clarkia breweri. Plant Physiol.* **2002,** *130,* (1), 466-476.

131. D'Auria, J. C., Acyltransferases in plants: a good time to be BAHD. *C. Opin. Plant Biol.* **2006,** *9,* (3), 331-340.

132. Maurer, K.; Knoevenagel, K., The effect of amino acids on α-Keto hexone acid ester. *Berichte Der Deutschen Chemischen Gesellschaft* **1941,** *74,* 1003-1006.

133. Node, M.; Hashimoto, D.; Katoh, T.; Ochi, S.; Ozeki, M.; Watanabe, T.; Kajimoto, T., Asymmetric Michael addition of a recyclable chiral amine: Inversion of stereoselectivity caused by the difference of ethereal solvents. *Org. Lett.* **2008,** *10,* (13), 2653-2656.

134. Della Rosa, C.; Gil, S.; Rodriguez, P.; Parra, M., A new approach to the synthesis of β-amino acids. *Synthesis-Stuttgart* **2006,** (18), 3092-3098.

135. Christenson, S. D.; Liu, W.; Toney, M. D.; Shen, B., A novel 4-methylideneimidazole-5-one-containing tyrosine aminomutase in enediyne antitumor antibiotic C-1027 biosynthesis. *J. Am. Chem. Soc.* **2003,** *125,* (20), 6062-6063.

136. Montavon, T. J.; Christianson, C. V.; Festin, G. M.; Shen, B.; Bruner, S. D., Design and characterization of mechanism-based inhibitors for the tyrosine aminomutase SgTAM. *Bioorg. Med. Chem. Lett.* **2008,** *18,* (10), 3099-102.

137. Liu, W. G., Asymmetric synthesis of unnatural amino acids using phenylalanine ammonia lyase. *Abstract. Paper. Am. Chem. Soc.* **1999,** *217,* 162-BIOT.

CHAPTER 3

Characterization of Phenylalanine Aminomutase (PAM): Confirming the Presence and Role of 3, 5-Dihydro-5-Methylidene-4-*H*-Imidazol-4-one (MIO).

3.1 INTRODUCTION

The 3,5-dihydro-5-methylidene-4*H*-imidazol-4-one(MIO) prosthetic motif present in Phenylalanine ammonia lyase (PAL) and histidine ammonia lyase (HAL) acts as a Lewis acid or electron sink during catalysis.[1-18] The MIO is auto catalytically formed from the triad sequence of alanine, serine and glycine (ASG) which is also present in enzymes like PAL, tyrosine aminomutase (TAM) and HAL.[19-28] Earlier studies had proposed a dehydroalanine formed serine dehydration as the electrophile.[29-31] X-ray analysis of the HAL from *Pseudomonas putida* showed the true electrophile to be the MIO.[31-37] The phenyl ring or the amine group of the substrate is proposed to act as the nucleophile. The long known mechanism of PALs suggested the amino group of the α-amino acid is the nucleophile. However some modeling calculations and broad substrate specificity studies (see Chapter 2 for more details) by Rétey and co-workers[38-44] point to the aromatic ring of the substrate acting as the electron donor (discussed in detail in Chapter 5).
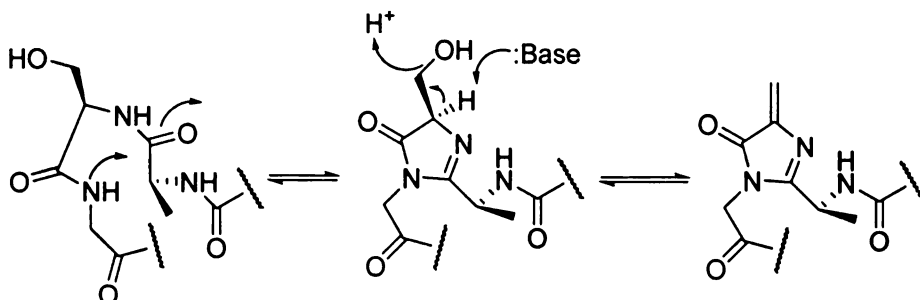
Scheme 3.1 Shows the formation 3, 5-dihydro-methylidene-4H-imidazol-4-one prosthetic group (far right) which occurs in the active site of HAL from P. putida. The alanine-serine-glycine triad undergoes cyclization and dehydration to form the MIO motif.

Christenson and Calabrese working on different enzymes (TAM and HAL, respectively) were able to confirm that the MIO binds to the amine group.[2,14]

Amid all the controversy what is universally acceptable is that the MIO promote the elimination of NH_3 and H^+ from arylalanines substrate by lowering the pKa of the β-hydrogens of the amino acid. The pKa of the β-hydrogens drop by 30 units upon MIO binding, 26 of those units are attributed to the six positive helices pointing towards the active site and the other 4 units are due to the contribution of the MIO. That observation minimizes the role of the MIO[6,31] because it implies that in its absence the reaction still goes on to completion. However studies in which L-5'-nitrohistidine is used as a substrate for HAL from *Pseudomonas putida* react with MIO-less mutants (in which the serine of the ASG triad has been replaced with glycine or threonine) and with wild-type HAL to the same extent.[45] Similar observations have been made with PAL from *R. tolouride* in which serine-202 was mutated to alanine, glycine and threonine by site directed mutagenesis. These results may not favor the mechanism by which the amine is

the nucleophile and prefers the one involving a transient Friedel-Crafts-like alkylation via aromatic ring. The nitro- group is believed to act in place of the MIO by its electron withdrawing effects which makes the β- protons acidic enough to be de-protonated by a general base (histidine, cysteine or tyrosine) to set an E1cb elimination of ammonia (Figure 3.5). The electron withdrawing nature of the nitro group would still result in acidic β hydrogen even if the amine was the nucleophile as opposed to the phenyl ring.
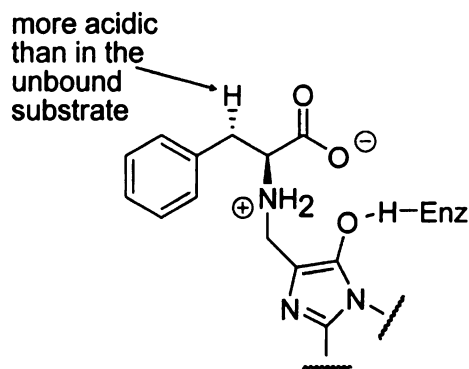
Figure 3.2 shows the amine group of L-α-phenylalanine bound to the MIO prosthetic group. The pH of the β-hydrogen drops by nearly 40 pKa units.

In this work the role of the MIO on the PAM reaction is investigated by mutating serine-176 to alanine, threonine, glycine and cysteine, comparative kinetic assays between wild-type and mutant enzyme, with various α-amino acids will be employed.

Characterization and optimization of overexpression of PAM

The full-length *pam* cDNA has open reading frame of 2094 bp, which encodes 698 amino acid residues. It has a calculated molecular mass of 76,530 kDa and an experimental mass of 80 kDa by SDS-PAGE analysis.[18] The turnover k_{cat} has been reported as 0.015 s^{-1} with K_M value of 45 μM measured with the natural substrates. Inhibition studies conducted mainly on phenylalanine ammonia lyase (PAL), histidine ammonia lyase (HAL) and tyrosine ammonia lyase (TAM) have demonstrated the presence of the catalytic moiety (methylidene imidazolone).[46-48] The functionality of the exocyclic double bond of the MIO makes it reactive with nucleophiles. The requirement for a electrophile in ammonia lyases was first reported in 1967 when these enzymes were inhibited by several nucleophilic reagents, such as hydroxylamine, hydrazine, bromocyanide, sodium borohydride and cysteine.[49-51] The inhibition of both PAL and HAL with cysteine was determined at a pH of 10.5 in a Na_2CO_3/HCO_3 buffer. The reaction is reversible under anaerobic conditions and irreversible in presence of oxygen. The cysteine-MIO complex (Scheme 3.1) absorbs maximally at a wavelength of 340 nm and which has become a qualitative test for the presence of the MIO.
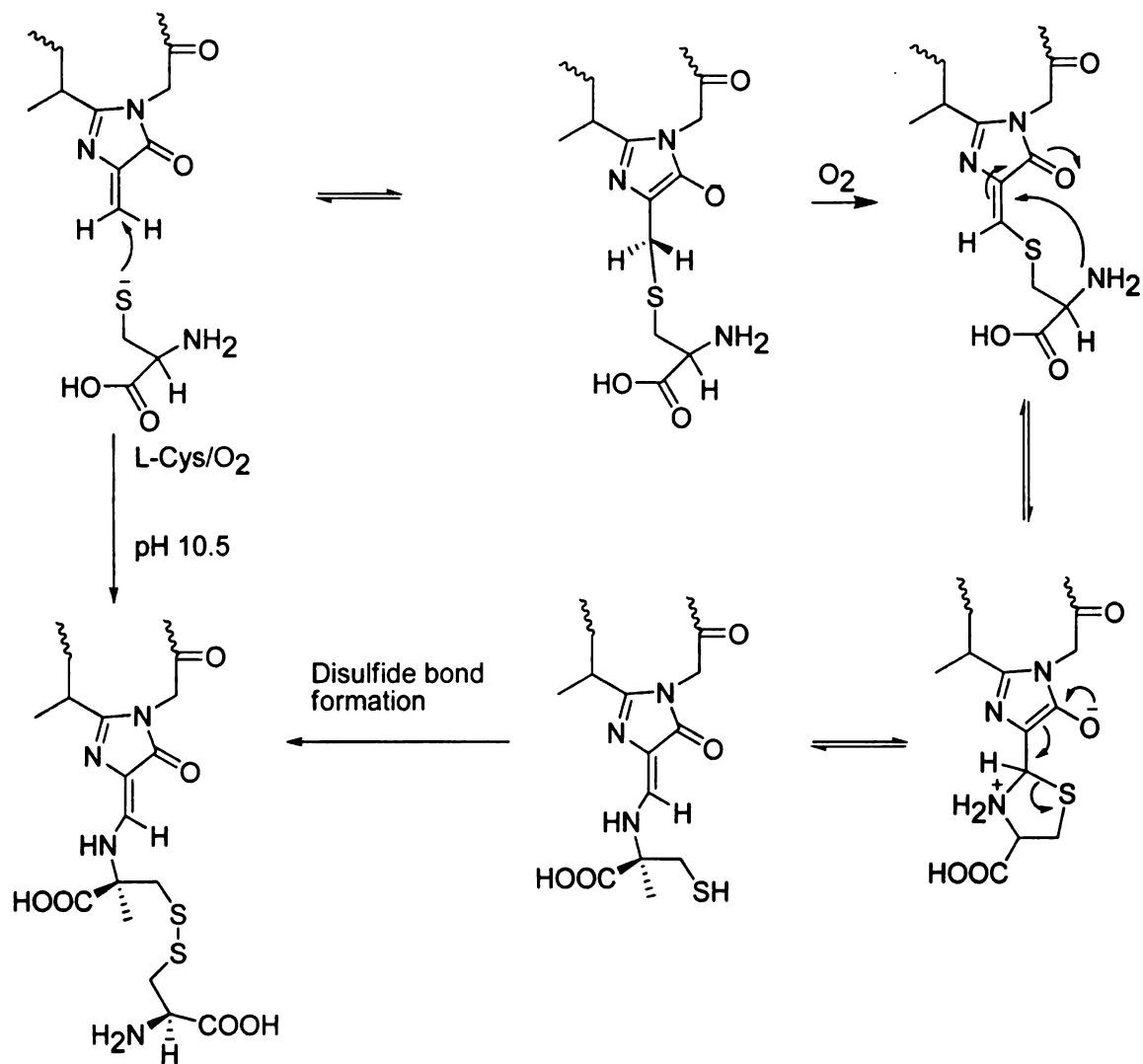
Scheme 3.3   The reaction of cysteine with the MIO moiety of PAL or HAL at pH 10.5. The reaction is irreversible in the absence of oxygen and is stable under aerobic conditions [49].

Walker and coworkers have demonstrated that PAM from *Taxus canadensis* is inhibited by both cyanide and sodium borohydride,[18] but no studies have been reported on whether cysteine has an effect. Further investigations will be conducted to confirm the presence of the MIO in PAM by utilizing cysteine as an inhibitor and measuring the formation of the cys-MIO complex by UV/visible spectroscopy.

The active site of PAL from *R. toruloides*[52, 53] show that phenylalanine is anchored in the active site by arginine and lysine on the carboxylate end of the molecule, the phenyl ring forms hydrophobic interactions with leucine and isoleucine residues, the amine group interacts with a tyrosine and histidine. The amine group of the substrate must be neutral for the conversion to occur, suggesting slightly basic conditions in the active site. The amine is striped of a proton by a basic residue of the enzyme prior to entry into the active site. Both suggested mechanisms (amine or phenyl ring as nucleophile) for PALs and HALs point to a requirement of a base which de-protonate the β hydrogen to set an E1cb mechanism which results in the elimination of ammonia.

Previous studies on PAM have proved that although the primary reaction is the conversion of 2-(*S*)-α-phenylalanine to 3-(*R*)-β-phenylalanine the reverse reaction in which 3-(*R*) and 3-(*S*) act as substrates produce only 2-(*S*)-phenylalanine.[18] We intend to carry out an investigation to confirm the reversibility of the PAM reaction in order to determine the equilibrium constant and chirality of the reaction products.

Although PAM *T. canadensis* has a 99 % amino acid sequence identity with the functionality similar PAM *T. chinensis* the later has a relatively high K_M value of nearly 1 mM.[54] This large discrepancy could be due to the different assay conditions and detection parameters used to analyze the properties of PAM in the separate studies. The studies on PAM *T. chinensis* were carried at concentration of 5 mM to 35 mM using HPLC and LCMS techniques. Walker and coworkers used concentration in the micromolar range but utilized GCMS which

is a more sensitive detection method. The GCMS method sensitivity is due to its low detection limits being in the nanomolar range, and is useful in identifying analytes based on the *m/z* fragmentation patterns. However, the technique requires that analytes be relatively volatile, therefore amino acids are derivatized to the *N*-acetylated methyl ester forms using acetic anhydride diazomethane (as shown in scheme 3.3). The multiple steps involved could potentially introduce both systematic and random errors in the results. Beside derivatizing analytes for GCMS analysis; another complimentary technique is to use a chiral column on HPLC. No expensive sample preparation is required and sensitivity and selectivity can be enhanced by derivatizing with *O*-phethaldehyde (OPA).[55-68] The HPLC method which excludes the derivatization steps will be a faster and less costly technique than GCMS providing a better linear dynamic range of up to 35 mM.
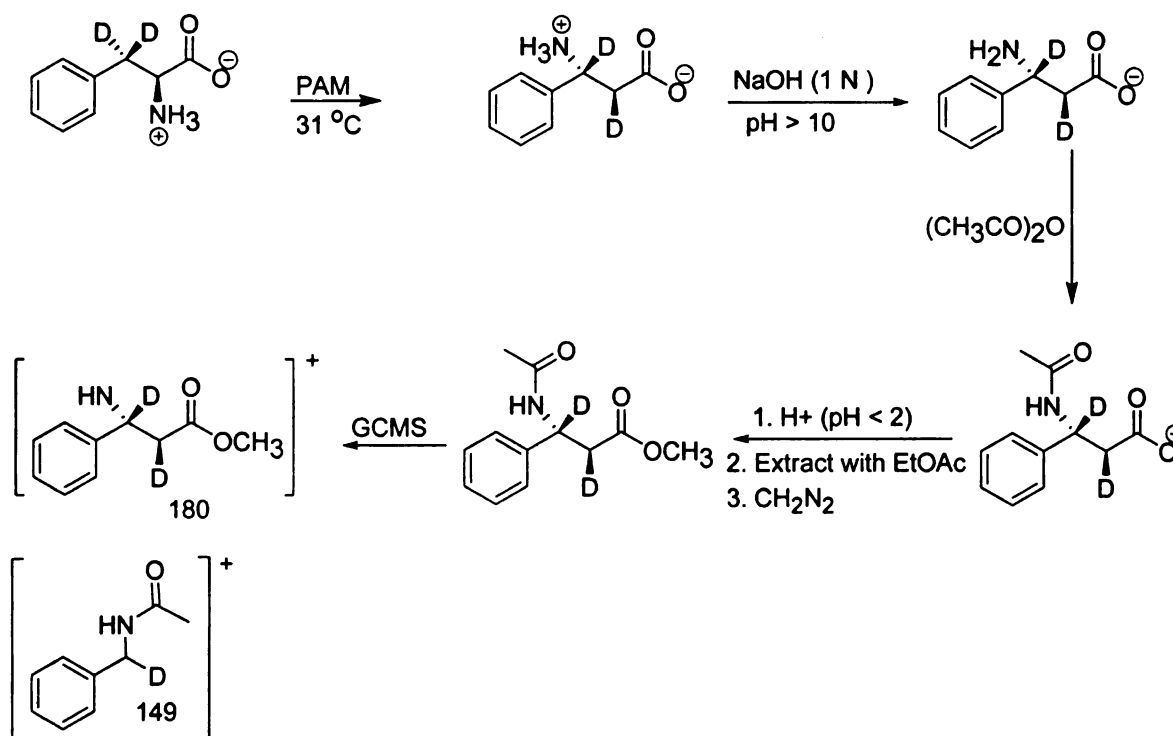
Scheme 3.4 The PAM reaction is assayed by incubating the enzyme with the substrate at 31 °C. The reaction is quenched with 1 N NaOH before adding acetic anhydride followed by diazomethane after extraction with ethylacetate at pH 2.

The acquisition of pure enzyme is a determinant factor in enzymology, especially for structural and kinetics studies. The enzyme is overexpressed in *E. coli* as host and requires purification to over 95% homogeneity. There are essentially four factors that determine the extent of protein expression: the host in most cases *E. coli* or yeast; the temperature of induction; the carbon source; and the induction procedure. The expression of PAM at 18 °C or higher in *E. coli* cell line BL21 (DE3) *LysS* has previously resulted in low yield of PAM (less than 10% of the whole cell protein content). Here we report how the effect of the combination of low temperature and cell line with a built in rare codon (arginine,

proline, isoleucine and lysine) optimization mechanism increased PAM expression.

Investigating the BASIC residue required during phenylalanine aminomutase catalysis

The major role of the prosthetic group methylidene imidazolone (MIO) is believed to be reduction of the pKa of the β-hydrogens of the substrate, for easy abstraction by a general base.[36] Enzymes which exhibit similar behavior are phenylalanine, histidine and tyrosine ammonia lyases (PAL, HAL and TAL).[69-75] Tyr363 in PAL *R. toruloides,*[53] Tyr300 in TAL from *R. sphaeroides* [2, 12, 76] equivalent to Try322 in PAM *Taxus. Canadensis* [77] based on sequence alignment (Figure 1.4). Mutations of the Y280, 300 and 363 to phenylalanine showed no or reduced activity[19]. In PAL the tyrosine promotes the breakdown of the MIO-NH$_2$ complex by donating a proton to the -NH$_2$- group (Figure 3.6). Try363 is near a positive helix which increases its acidity and its role as a general acid. Its resting state is in the neutral form with a pKa~ 10. The phenolate form of tyr363 is stabilized by the nearby guanidinium group of Arg366 which also interacts with one of the positive helices. Dissociation of the MIO-NH$_2$ complex and release of NH$_3$ and cinnamic acid to the bulk solvent put the enzyme in its resting state. The general base will be most essential if the amine is the nucleophile. If the phenyl ring was the nucleophile there won't be any need for a base because the stabilization of the ipso positive charge will not necessarily

require the loss of the β proton through abstraction by an enzymatic base. Any water in the active site will be able to act as a general base, to remove the highly acidic proton.
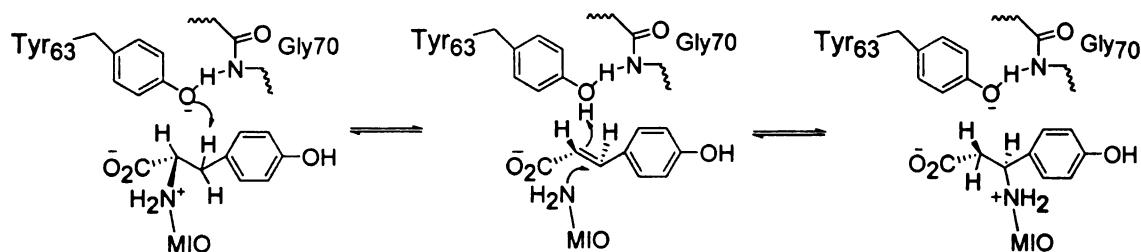
Figure 3.5 The mechanism of SgTAM based on established crystal structure. The tyrosine substrate is shown bound to the MIO via the amine group. Tyrosine 63 acts as a general base to de-protonate the pro-(R)-β-hydrogen stereospecifically. A coumarate is formed as an intermediate. The MIO shuttles the amine group to the β position, the subsequent breakdown of the MIO-amine complex results in release of the β-amino acid as a product.
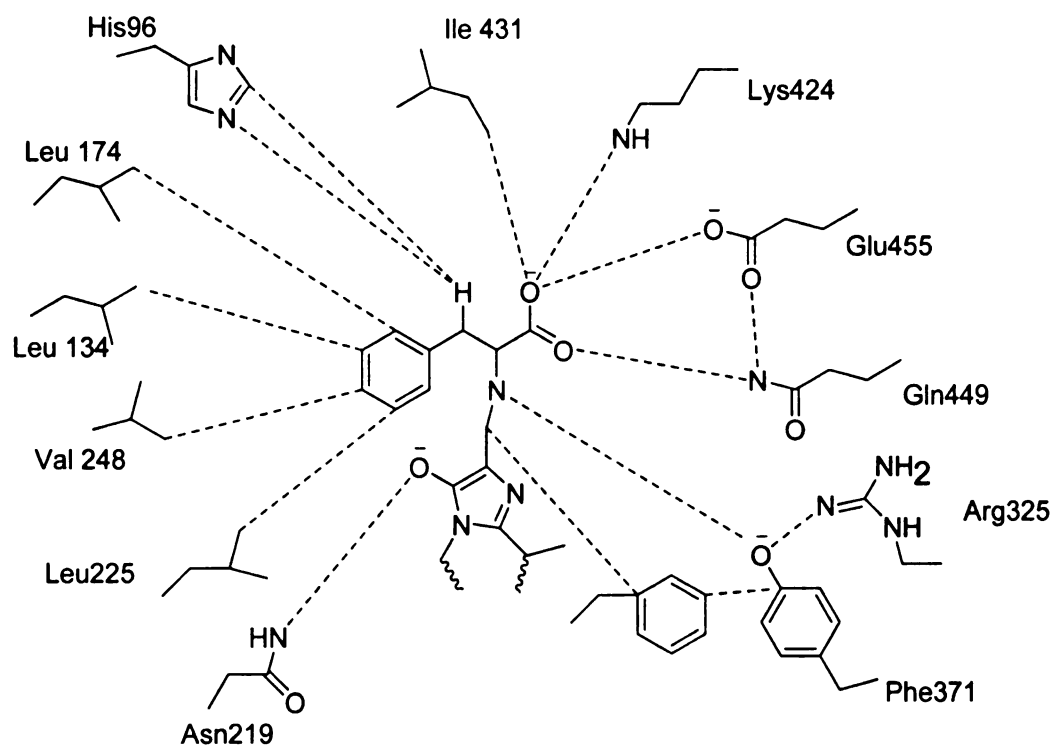
Figure 3.6 The active sites of PAL *R. tolouride* at the top showing the binding of the substrate at the active site.

In this work, we intend to demonstrate that tyrosine 322 from PAM act as a general base in the mechanism, by studying the activity of various mutants of PAM; Y322H, Y322F and Y322A. The last 2 mutants are expected to be inactive towards the natural substrate if tyrosine 322 of PAM is essential during the catalysis. If there is no difference in activity, it may suggest that the tyrosine 322 is not very essential and the mechanism could be involving a short lived carbocationic transition state, which is neutralized by the spontaneous loss of the β-protons. Although histidine may be a better base than tyrosine, the shorter bond length may not allow for the shuttling of the proton which is perceived to take place during the course of the reaction. The contribution of the cysteine 107 in PAM will also be studied. Two mutants will be constructed for that purpose,

125

C107A and C107H. Mutant C107A is expected to show decreased activity and

C107H showed have higher if the cysteine is considered to be acting as a base.

3.2 RESULTS

3.2.1 *Optimization of the over expression of phenylalanine aminomutase.*

The recombinant plasmid of the pam gene and pET 14b was used to transform *E.coli* cells line BL21-CodonPlus-RIPL competent with rare codon optimization for arginine, isoleucine, proline and lysine. The expression of PAM in either BL21(DE3) or BL21-CodonPlus-RIPL cells at 18 °C resulted in low yields (Figure 3.7). The expression temperature was reduced to 16 °C with IPTG induction (Figure 3.8). The recombinant protein was purified using a Ni-NTA column. The elutions collected from the column were analyzed by SDS-PAGE and Coomassie blue staining (Figure 3.9).

75 kDa →

1 2   3 4   5 6   7 8   9

Figure 3.7; SDS-PAGE of proteins expressed in BL21-CodonPlus-RIPL cells transformed with a pam plasmid at 18 °C or 37 °C. The PAM protein with a size of 76 kDa is barely distinct from the rest of the cellular proteins pointing to weak expression. Lane 1 the Lonza protein marker with the 75 kDa bark shown on the left. Lanes 2-9 are whole cells from different flasks and treated by spinning the cell cultures at 13 000 rpm, boiling the pellet in βME for 20 min.
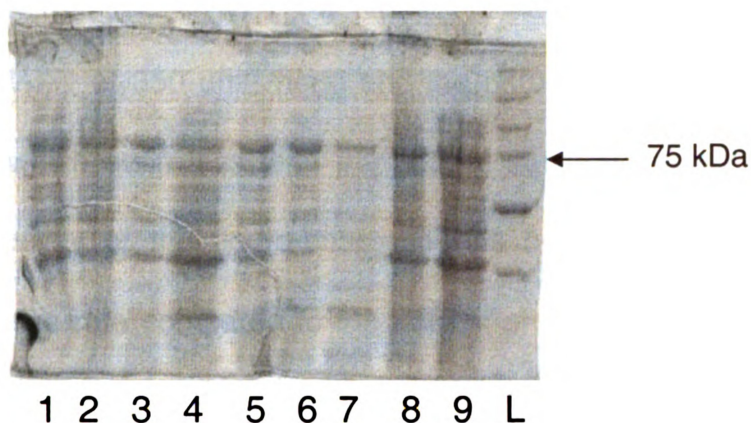
Figure 3.8; SDS-PAGE of proteins expressed in BL21-CodonPlus-RIPL cells transformed with a pam plasmid at 16 °C. The PAM protein with a size of 76 kDa (lanes 1,3,4,5 and 6) was over 60% of the cellular proteins suggesting a successful over expression. Lane 8 is the protein ladder (Lonza) and the 75 kDa marker is indicated on the right.
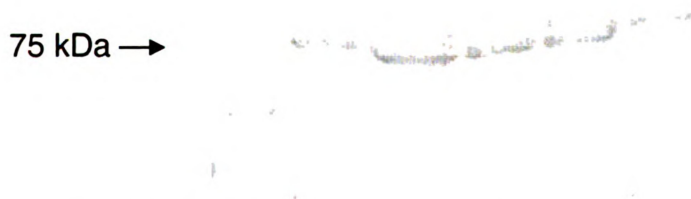
Figure 3.9 The SDS-PAGE gel of elutions of PAM from the Ni-NTA column. The PAM has a measured mass of about 75 ± 5 kDa based on the protein ladder in lane 1. The protein was over expressed in BL21-CodonPlus-RIPL at 16 °C and induced with 1 mM IPTG.

3.2.2 *Enzymatic Assay Techniques*

PAM was confirmed as activity if 10 µg of the enzyme converted 1 mM of the natural or unnatural amino acids such as 4'-NO$_2$, 4'-F, and 4'-MeO, -phenylalanine as substrates to 52% of product overnight. The activity of wild-type PAM with electron-withdrawing and donating substrates was assayed by incubating 50 µg of enzyme with 1 mM of substrate at 31 °C for 3 h. All the

128

substrates tested were reactive as expected, the flouro-substrate was the most reactive with a V_{MAX} of 350 units/h/mg and the nitro- was the least reactive at 150 units/h/mg which even less than the natural substrate at about 200 units. The higher reactivity of the flouro-substrate has been reported previously,[78] although its relative rate compared to the natural product was much higher (95 times faster) than what we report here (2 times faster).
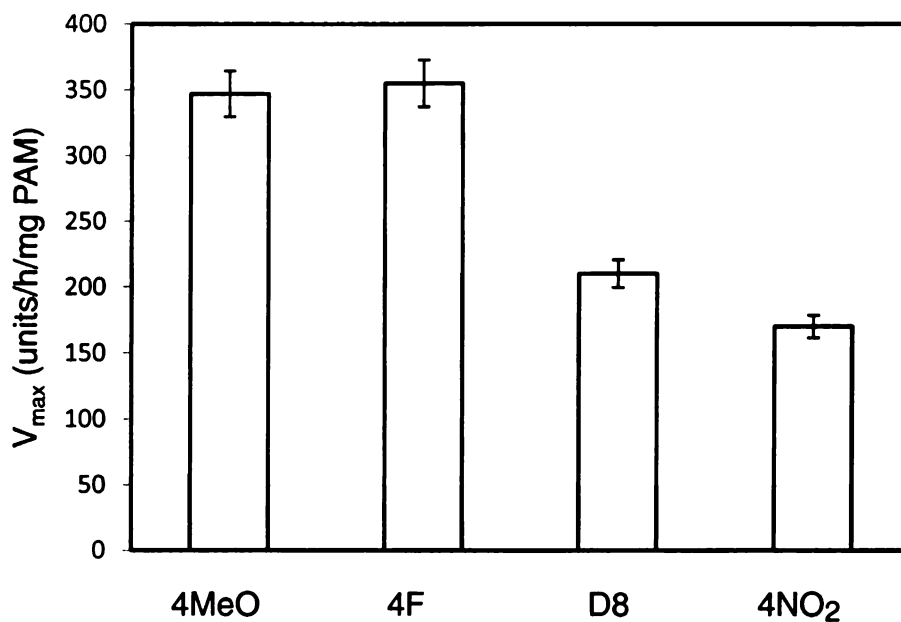
Figure 3.10 An activity assay PAM (50 µg) incubated for 3 hours. The 4'-methoxyphenylalanine and 4'-Flourophenylalanine is converted to over 50%, the universally deuterated phenylalanine and the 4'-nitrophenylalanine are at 30% conversion.

3.2.3 The PAM pH dependence

The pH dependence of PAM was determined by measuring the activity at different pH values. The pH of PAM was adjusted from 8.5 to 11 and the substrate added and incubated at 30 °C for 1 h. The samples were derivatized as

before and injected into the GCMS. The pH profile (Figure 3.11) shows a rapid decrease in PAM activity as pH decreases and a more tolerance of PAM to more alkaline conditions. PAM activity peaks at a pH of 8.5.
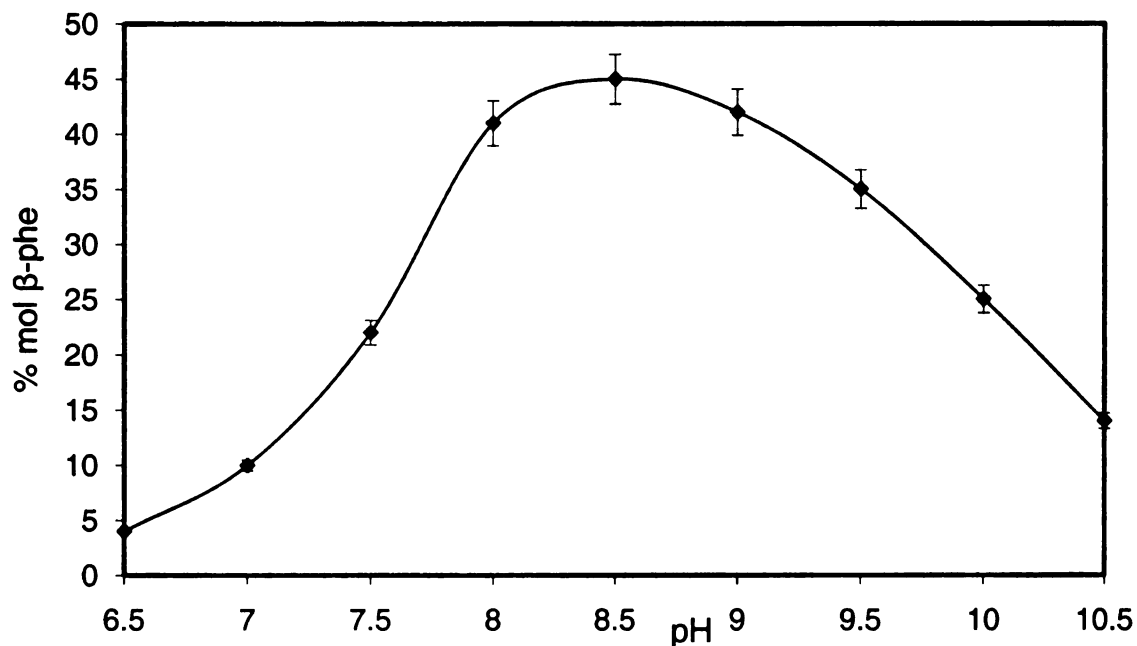
Figure 3.11 The pH dependence of the PAM reaction. The activity increases rapidly form pH 6.5 and peaks at pH 8.5 before it gradually decreases at higher pH.

3.2.4 Cysteine Inhibition studies

The reaction of cysteine with PAM was monitored spectroscopically and by activity assay, measuring the amount of β-product formed during the reaction. Samples were collected every 10 min and derivatized as described elsewhere and analyzed by GCMS.

3.2.4.1 *Spectral evaluation*

The reaction was monitored by scanning from a wavelength of 300 nm to 400 nm at a rate of 1200 nm/mn. The spectrum show a peak at about 340 nm (Figure 2.12) which is typical of most enzymes carrying the autocatalytically synthesized methylidene imidazole cofactor.
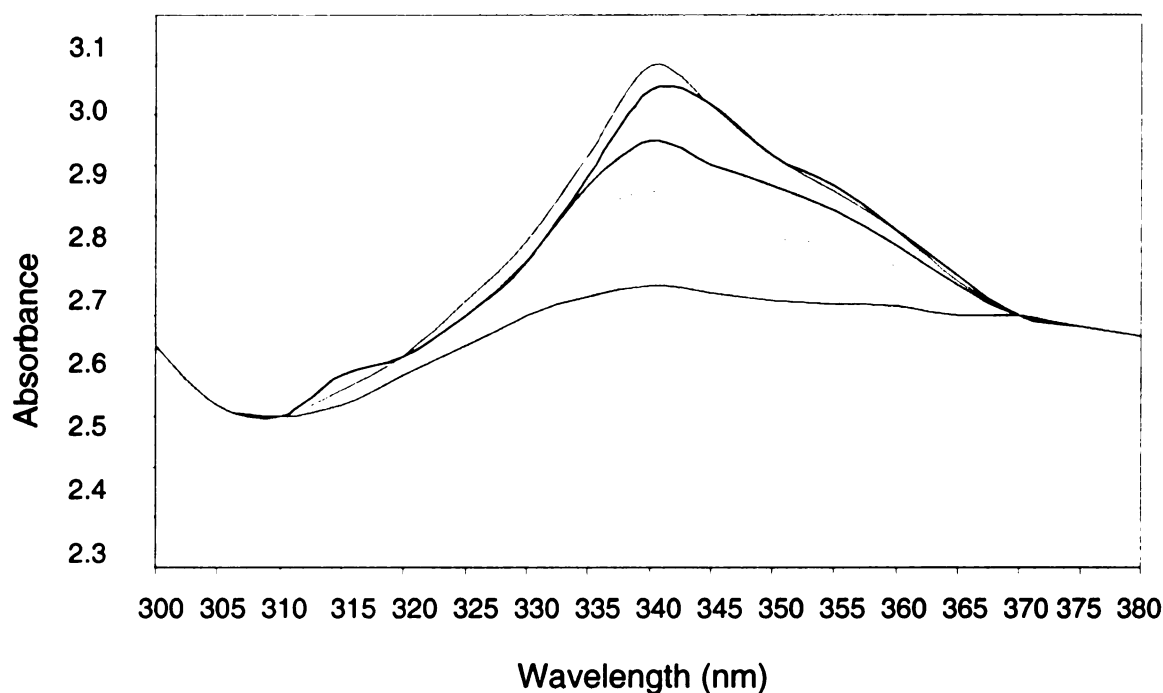
Figure 3.12 Spectra of the formation of the MIO-cysteine complex monitored over a period of 60 min. The spectra were at 10 min intervals after incubating with 10 mM L-cysteine and show increase of absorbance at 340 nm with time.

3.2.4.2 *Activity Assay with cysteine inhibition*

The activity of the cysteine inhibited PAM was monitored for 60 min with samples at 10 minutes intervals. A sharp decrease in activity is observed falling to less than 5% (black line in figure 3.13). The activity was restored to 100% after dialysis, to remove cysteine.

131
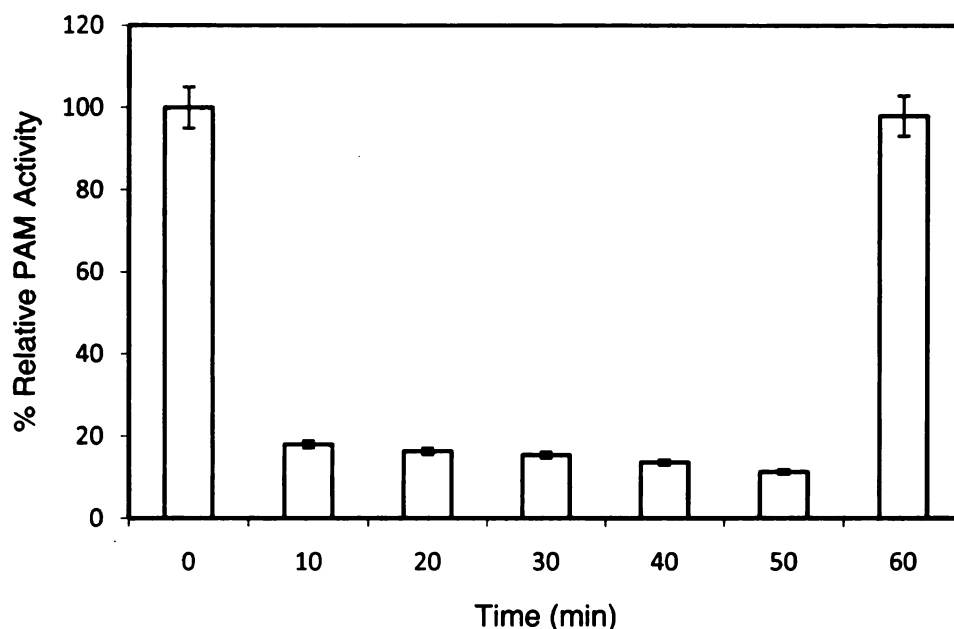
Figure 3.13 The effect of cysteine inhibition on PAM activity. PAM was reacted with 10 mM cysteine at 30 °C for 50 min. After 50 min the cysteine was removed by filtering through a 30 kDa cut of Amicon filter and the activity of PAM was fully restored as measured by the relative activity of the free versus the uninhibited enzyme.

3.2.5.1 *Expression and Purification of Recombinant Wild-type PAM and Mutants S176A, S176C, S176G and S176T.*

The mutants S176A/C/G and T were over expressed in BL21(DE3)CodonPlus-RIPL cells and purified using Ni-NTA technique to over 95% homogeneity. The elutions from the NTA column were denatured by heating at 95 °C for 15 min in 50% SDS-βME solution. About 0.1-01 μg of protein was loaded on polyacrylamide gel (20 μL well) prepared by mixing; water (3.4 mL), 1.5 mM Tris-HCl (2.5 mL), 20% SDS buffer (50 μL), 30%/0.8% bis/tris-acrylamide (4 mL), 10 % ammonium sulfate (10 μL) and TEMED (5 μL). The

electrophoresis was run in SDS buffer at 180 V for 2 hours; the gel was stained

in Coomassie for 1 h and de-stained in water/methanol/acetic acid (Figure 3.15).

75 kDa

1 2   3   4   5   6   7   8   9   10 11
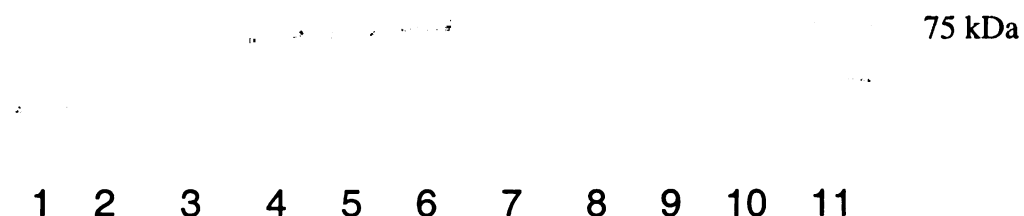
Figure 3.14 The SDS/PAGE gel with Coomassie staining showing over expressed wild-type PAM (lanes 2 and 3), S176A (lanes 4 and 7), S176G (lanes 5 and 8), S176T (lanes 6 and 9), showing that the 4 proteins are of the same size (75 ± 5 kDa).

3.2.5.2 *Difference Spectra between wild-type PAM and MIO-less mutants*

The difference spectra in which the mutant S176A, G and T were used as

blank to measure the UV-visible spectrum of wild-type PAM is shown in figure

3.15 with a absorption maxima at about 308 nm which is characteristic of

phenylalanine ammonia lyase enzymes which have an MIO moiety. The

absorption at 308 nm increases with increase in concentration of the wild-type

PAM.
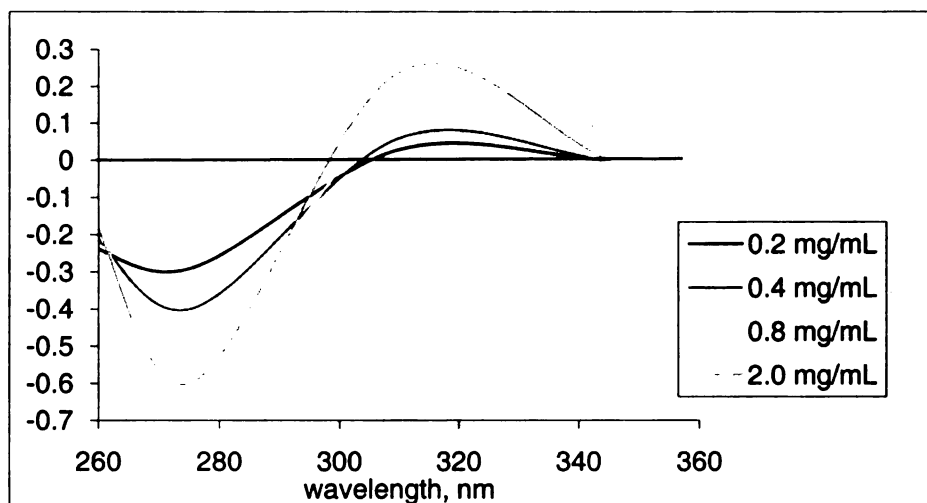
Figure 3.15 The difference spectra between the mutants S176A/G/T versus wild-type PAM exhibiting a λmax at 310 nm which increase in strength with increase in the wild-type enzyme concentration.

3.2.5.3 Activity Assay for the mutant S176C

The mutant S176C (50 μg) was incubated with 1 mM mixture of L-phenylalanine, 4'-MeO-, 4'-NO$_2$-, 4'-F-phenylalanines for 3 h. The assay mixture was derivatized as described above and the rates were measured as mol % conversion of the substrate to the product.
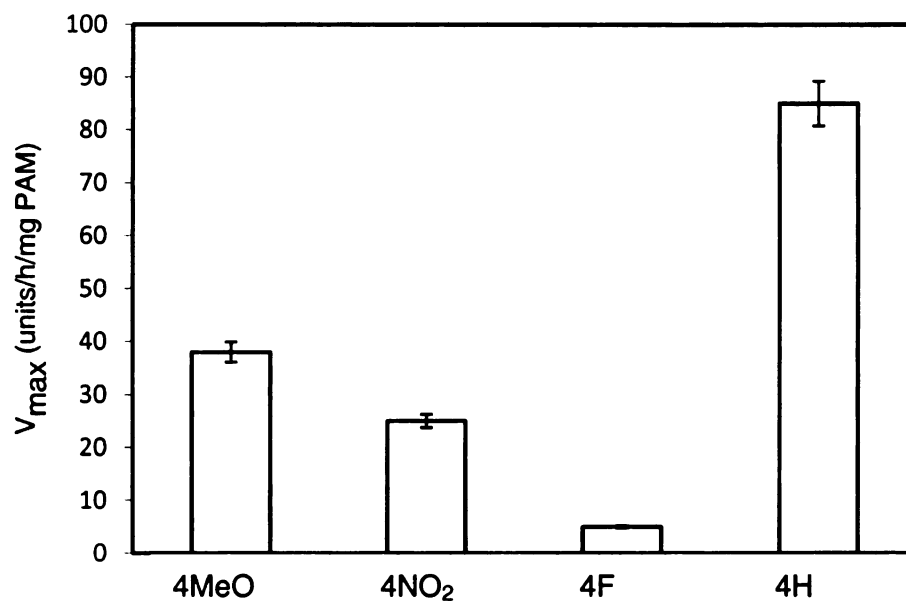
Figure 3.16 The activity of the mutant S176C was assayed by incubating with various amino acids for a period of 3 hr. The natural substrate showed more reactivity than the 4'-F-Phe which exhibit higher with wild type PAM.

3.2.5.4 *The Linewevear-Burk plot for wild-type PAM vs 4'-nitrophenylalanine*

In order to calculate the accurate values for the V_{max} and K_M for the PAM-4'-nitrophenylalanine reaction, a Lineweaver-Burk was plotted (1/V vs 1/[S]) and the values were 0.4 unit/h/mg and 286 μM respectively (Figure 3.17).
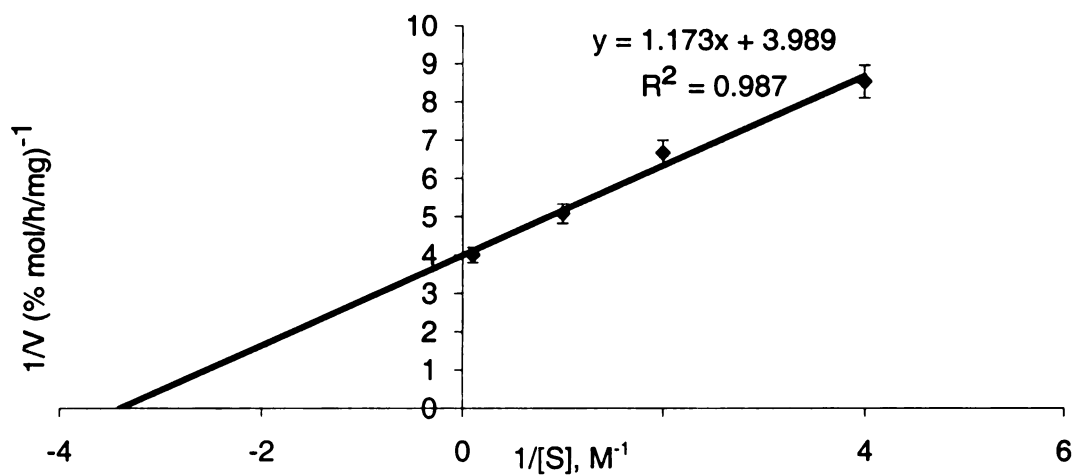
Figure 3.17 The Lineweaver-Burk plot for wild-type PAM vs 4'-nitrophenylalanine. The calculated K_M value is 0.3 mM.

Table 3.1 Kinetics parameters of wild-type PAM with substrates L-phenylalanine, 4'-NO₂-L-phenylalanine, 4'-F-L-phenylalanine and 4'- MeO-L-phenylalanine.

Substrate	V_{max}, units/mg	K_M, mM
Phenylalanine	200 ± 18	0.097±0.008
4'-NO₂-L-phenylalanine	166 ± 18	0.286 ± 0.058
4'-F-L-phenylalanine	360 ± 30	0.075 ± 0.007
4'-MeO-L-phenylalanine	346 ± 24	0.41 ± 0.008

3.2.5.5 Kinetics for mutant S176A with 4'-NO₂-L-Phe as substrate

To assess the reaction between the mutant S176A with the α-nitrophenylalanine as substrate, 50 µg of the enzyme was incubated with varying concentrations of substrate (ranging from 100 µM to 25 mM) for 2 hours (based

on time course assay). The Lineweaver-Burk plot for the mutant S176A versus the 4'-nitrophenylalanine is shown in figure 3.19. The calculated K_M value was 1 mM.
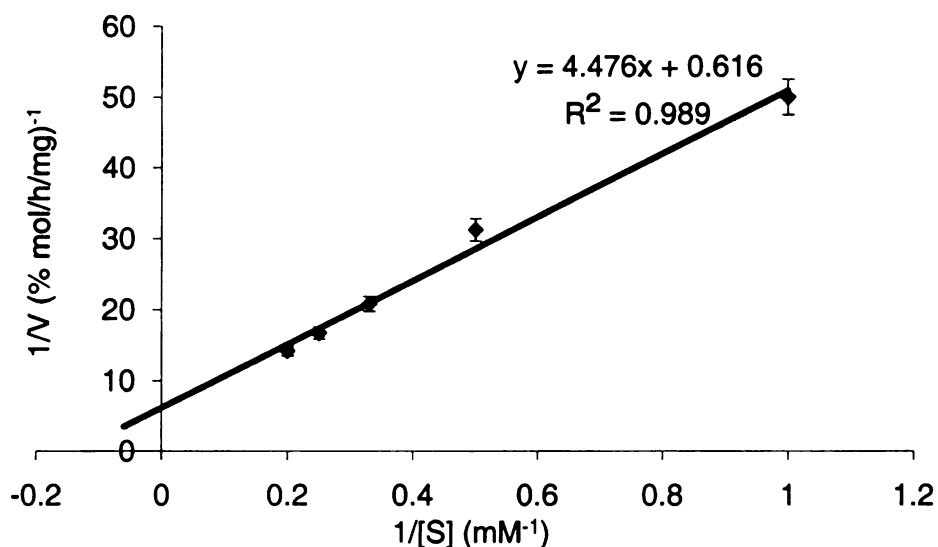
Figure 3.18 Plot of 1/Vmax versus 1/[S] for the reaction between the mutant S176A and α-4'-nitrophenylalanine as substrate. The K_M is 1 mM.

3.2.5.6 *Activity Assay of mutant S176G*

The mutant S176G was reactive with electron-withdrawing substrate such as 4'-nitro- and 4'-flouro-phenylalanine but was not reactive with neutral or electron donating substrate such as phenylalanine and 4'-methoxy-phenylalanine. The nitro substrate was relatively 5 times more reactive than the flouro substrate suggesting an increased electron-withdrawing with the former compound (Figure 3.19).
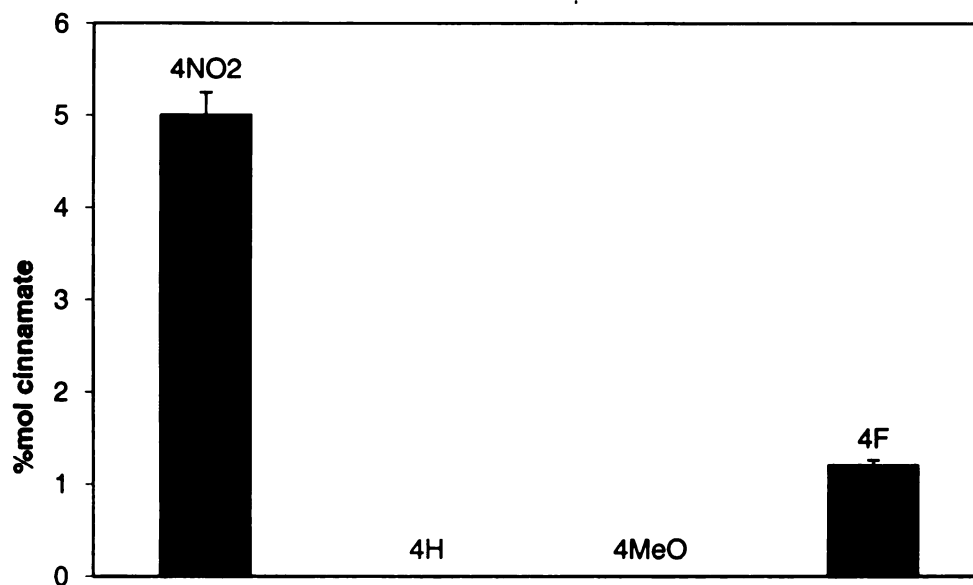
Figure 3.19 Activity of mutant S176G as measured by the amount mol% of cinnamate formed from the α-amino acids (4'-nitrophenylalanine and 4'-flourophenylalanine). The β-product was below the detection limit. The results suggest the influence of the electron withdrawing groups on the phenyl ring of the substrate.

3.2.5.7 *The Michael-Menten plot for mutant S176C with the 4'-nitrophenylalanine substrate.*

The V_{max} and K_M for the mutPAM S176C with the 4'-nitrophenylalanine

substrate were determined using the Michael-Menten plot of $1/V$ versus $1/[S]$

(Figure 3.21). The V_{max} values was calculated as 12.5 units/h/mg of the mutant

and the K_M was 0.91 mM.

138
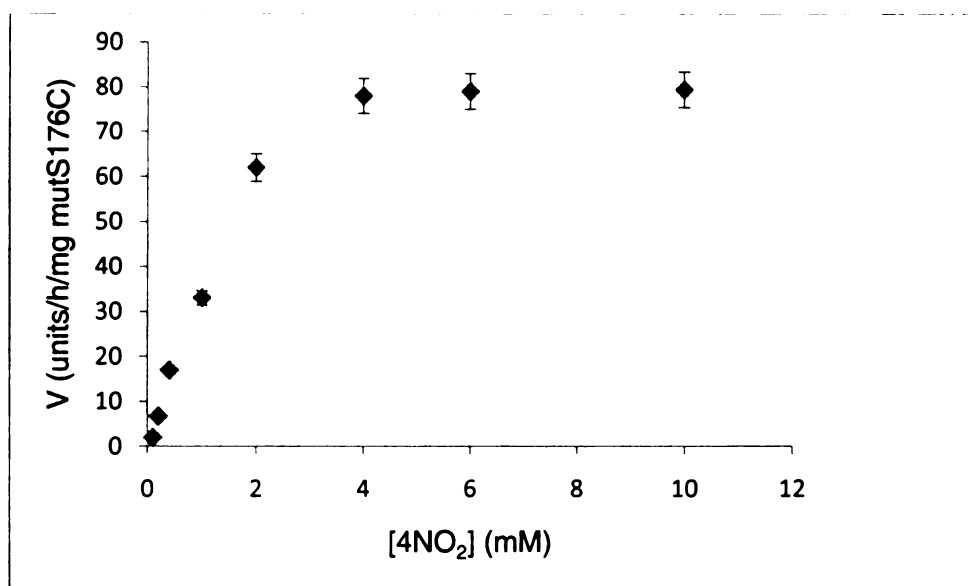
Figure 3.20 The Michael-Menten plot for mutant S176C with the 4'-nitrophenylalanine substrate.

3.2.5.8 *Comparison of the kinetic parameters of wild-type PAM against the mutants S176A/C/G and T with both the natural and 4'-nitrophenylalanine substrates.*

Except for the S176T mutant all other mutants were reactive with 4'-nitrophenylalanine as substrate Table 3.2).

Table 3.2 Comparison of kinetic parameters from wild-type PAM, the mutants S176G, S176A, S176T and S176C with 4'-nitrophenylalanine as substrate.

Enzyme	K_M 4-NO$_2$-L-Phe, (mM)	V_{max} Phe, unit/h/mg	V_{max} 4-NO$_2$-Phe, units/h/mg)	$V_{MAXwtPAM}$/ V_{maxPhe}
wt PAM	0.91±0.085	32.5±2.5	27±2.2	0.83±0.072
S176A	1.0±0.09	-	0.135±0.013	-
S176C	1.1±0.01	4.22±0.04	0.51±0.045	0.12±0.01

139

3.2.5.9 *Investigating the base involved in PAM catalysis*

The assay to check the activity of the of the five mutants Y322A, F, H and C107A, H was carried out by incubating the enzymes with 1 mM of the natural substrate. Only mutants C107 A and C107F showed activity (Figure 3.22), suggesting that Y322 is essential during PAM catalysis. He Y322F could potentially be used to study the mechanism of PAM.
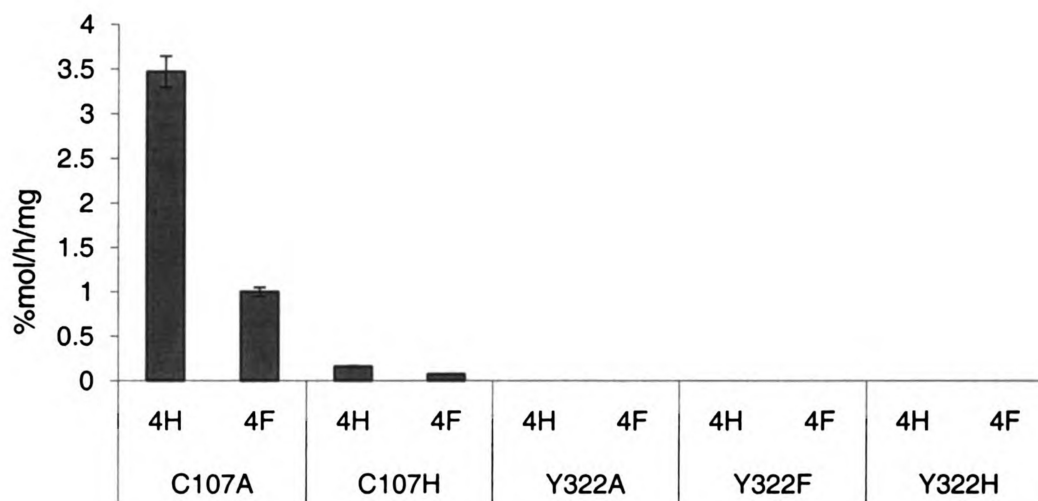
Figure 3.21 The assay to check the activity of the of the five mutants Y322A, F, H and C107A, H was carried out by incubating the enzymes with 1 mM of the natural substrate (4H) and 4'-flouro-α-phenylalanine (4F). Only mutants C107 A and C107F showed activity.

3.3 DISCUSION

The over expression of phenylalanine aminomutase (PAM) a plant enzyme as a recombinant protein in *E. coli* presents a special challenge because of some codons which are unique to plants but rare are in bacterial cells. The codons for arginine, isoleucine, proline and leucine are conspicuously absent in *E.coli* and results in low expression of heterologous proteins. There are two approaches in overcoming the codon utilization dilemma that is; 1) rare codon optimization through targeted mutation of the gene by substituting the plant codons with E. *coli* compatible codons, 2) utilize *E. coli* cells with a plasmid carrying the plant codons. The two approaches have been applied in our lab with a measure of success. However the disadvantage of the gene optimization technique is the cost. The expression of PAM in BL21-CodonPlus-RIPL cells resulted in the six fold increase in the ratio of the recombinant protein to the non-recombinant cellular proteins (Figures 3.8 versus 3.9). A low expression of the recombinant protein makes the purification steps very difficult and time consuming and may present interferences to the assay reaction. This is particular noticeable for the PAM reaction because the use of impure enzyme results in the epimerization of the substrate because of the presence of a phenylalanine racemase from *E. coli*. When crude PAM enzyme is fed with an octa deuterated substrate both the unreacted α phenylalanine and the corresponding β product show loss of a ^{2}H which is not observed when the same reaction is carried out with the pure enzyme. With pure enzyme the diagnostic peak for the β product is 186 *m/z*) but with impure enzyme a 185 or 184 peak is observed.

The mechanism of phenylalanine racemase[79-86] involves the loss of an α-hydrogen of the L-phenylalanine to form D-phenylalanine (Scheme 3.22)
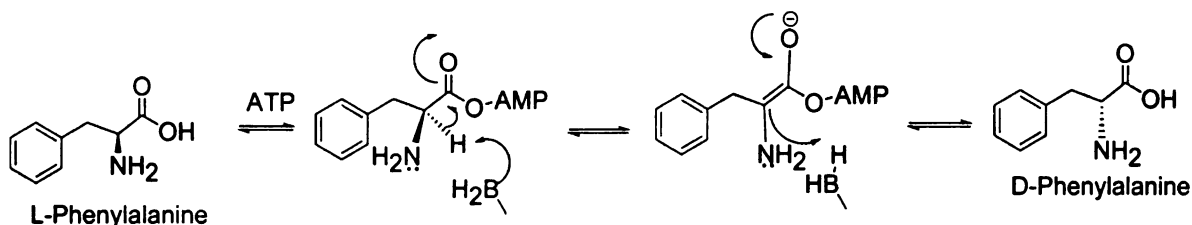
Scheme 3.22; A summary of the epimerization reaction catalyzed by the phenylalanine racemase, the imine intermediate attacks a proton from both faces to form a racemic mixture of L and D phenylalanine.

The combination of low temperature and use of "CodonPlus-RIPL" cells provides the best conditions for PAM overexpression. The optimum temperature for PAM expression is 16 °C. The low temperature slows down the metabolic pathways of *E. coli* allowing only the heterologously protein to be expressed preferentially since it is encoded by a different plasmid from the bacterial chromosome. Lowering the temperature below 15 °C up to 10 °C may still produce better results but is likely to be counterproductive because it lengthens the incubation time and making the whole process of protein purification unnecessarily long.

The equilibrium of the PAM reaction is 1.1 at 31 °C in favor of product based on assays with the natural substrate. The Jansen group reported an equilibrium of 51/49[87] which is the same as what we reported. Chen and coworkers reported an equilibrium value of nearly 50% for the tyrosine aminomutase reaction which is mechanistically similar o PAM.[54] The relatively low conversion of L-α-amino acids to corresponding β-product in plants and

142

bacterial may be a natural selection process to prevent a competing reaction in which the formation of *trans*-cinnamic acid a precursor of many structural and metabolites of both plants and animals will not be compromised.[88-99] However the equilibrium mixture produced presents challenges in the separation and purification of the amino acids at the end of the reaction given the close physical and chemical properties of α and β aromatic amino acids. However the separation can easily be accomplished using HPLC (Figure 3.24). D and L phenylalanine racemic mixtures can be separated with a high resolution by utilizing the chiral column. The β- and α- are less chemically equivalent and should be separable even with a higher resolution than the D and L isomers. With the capability of high injection volumes and high concentrations of the amino acids HPLC technique can be use in preparative methodologies to give 99% enantiomeric excess.
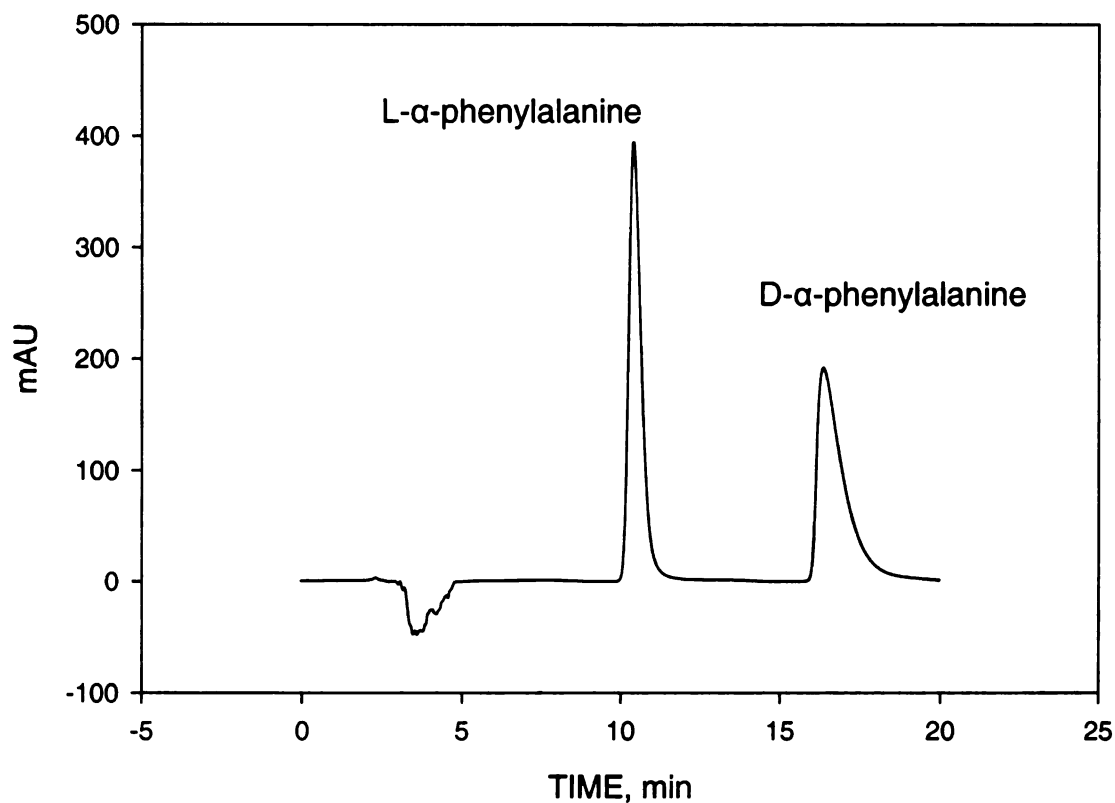
Figure 3.23 The HPLC spectrum of a mixture of D and L phenylalanine. The amino acids were separated with 100% methanol isocratic gradient and no derivatization was necessary.

The identification and confirmation of the presence of the MIO in PAM is central in determining its mechanistic pathway. PAM shares a peptide sequence homology with PAL and HAL which have been demonstrated to utilize the MIO mechanistically. The simplest and most direct way of verifying the presence of the MIO is the reaction with nucleophiles such as the cysteine inhibition reaction. As shown in Figure 3.13 PAM forms a complex with cysteine which absorbs at 338 nm typical of MIO carrying enzymes. Similar inhibition studies carried out with sodium borotetrahydride or bromocyanide confirms the complete inhibition of

144

PAM.[100] The fairly high pH conditions required for this reaction suggest the need for a free thio group which nucleophilically attacks the MIO in the enzyme active site. Independent pH studies of PAM shows a tolerance of basic conditions which could point to the requirement of a free amine of the substrate as the nucleophile. The activity of PAM drops sharply at low pH which could be due to; formation of an ammonium form of the substrate making it difficult to bind into the activity site; inhibition of the de-protonation of the β-hydrogens due to the acidification of the responsible basic residue and the failure of the amine to rebound to the C3 position a required step to complete the synthesis of the β-product. The optimum pH of 8.5 allows the substrate to be de-protonated off the ammonium proton before it enters the active site, the free amine so generated and the carboxylate provides the binding sites of the substrate to compliment the hydrophobic interactions between the phenyl of phenylalanine and the leucine and isoleucine residues (Figure 3.2). The argument in support of the aromatic ring as nucleophile will be favored by low pH to ensure the ammonium form of the substrate which will be prevalent to give way to the lost of ammonia to form the cinnamic intermediate. The ammonium form however will be difficult to maintain under more basic conditions.

Site directed mutagenesis

The purified PAM mutants S176C, S176A and S176G were productive with 4'-nitrophenylalanine, and 4'-flourophenylalanine which has electron withdrawing groups (Figure 3.16 and 3.19). The S176C mutant was also active

towards substrate with the natural substrate (Figure 3.16). The active of the MIO-less mutants with substrates carrying electron-withdrawing substituents is especially an interesting phenomenon and it explains the possible function of the MIO during PAM catalysis. The nitro- or flouro- groups are believed to withdraw electrons from the phenyl rind rendering the β-hydrogen acidic enough to be de-protonated by a general base as shown in figure 3.24 below.
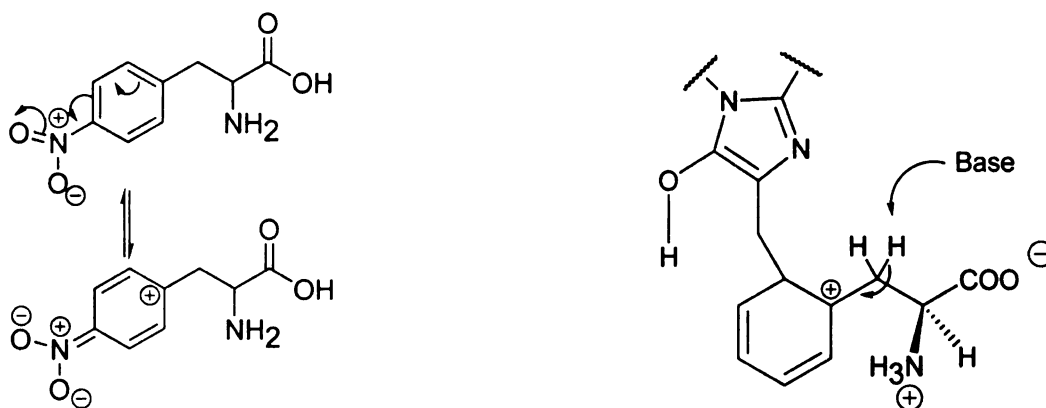
Figure 3.24 The nitro group withdraws electrons from the phenyl ring causing the β hydrogen to be acidic enough to be de-protonated by a general base. The same electron withdrawal is proposed to apply with fluorinated substrates.

Both activity assays and differential spectroscopy evidence points to the formation of the MIO in the S176C mutant. The thio group could be hydrolyzed the same as the serine of the ASG triad is in wild PAM. However the MIO yield in the S176C might be less that in the wild type PAM (Figure 3.25). This aspect will need to be investigated further.
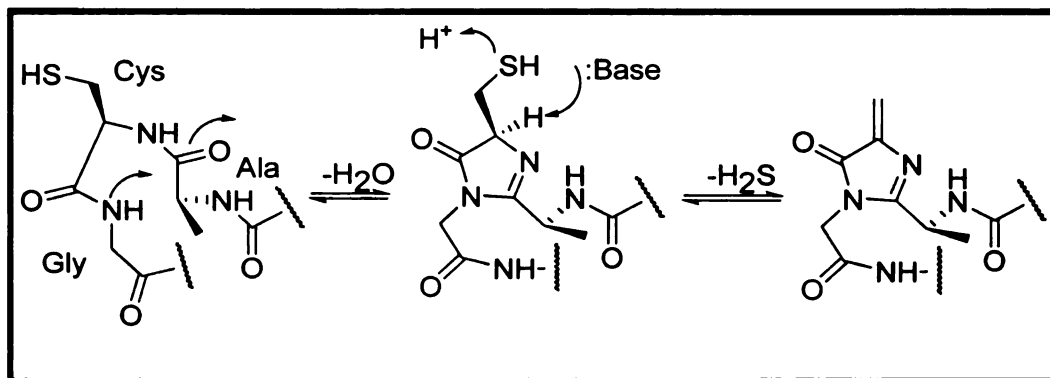
Scheme 3.25 The proposed formation of the MIO from the cyclization and condensation of the ala-cys-gly triad. The reaction results in the loose of one water molecule and one hydrogen sulfide molecules.

The use of crude S176G did not result in the formation of any β- product even with electron withdrawing substrates. Instead the corresponding D amino acid is formed from the L isomer which is used as substrate. However the reaction results in the formation of 4'-nitrocinnamic acid as determined by UV/visible spectroscopy. It is not clear why the crude mutant will not from the β-4'-nitrophenylalanine, it is most likely that the mutation reaction is in competition with the phenylalanine racemase enzyme present in crude extracts from *E. coli* or the β-product is formed below the detection limit. In the absence of the MIO in mutant PAM and the presence of a racemase in the crude extract the reaction may not favor the mutase activity but the racemase activity in which ammonia does not rebound to the C3 position because it is not held in position by a covalent bond which is the case in wild-type PAM (Figure 3.26).
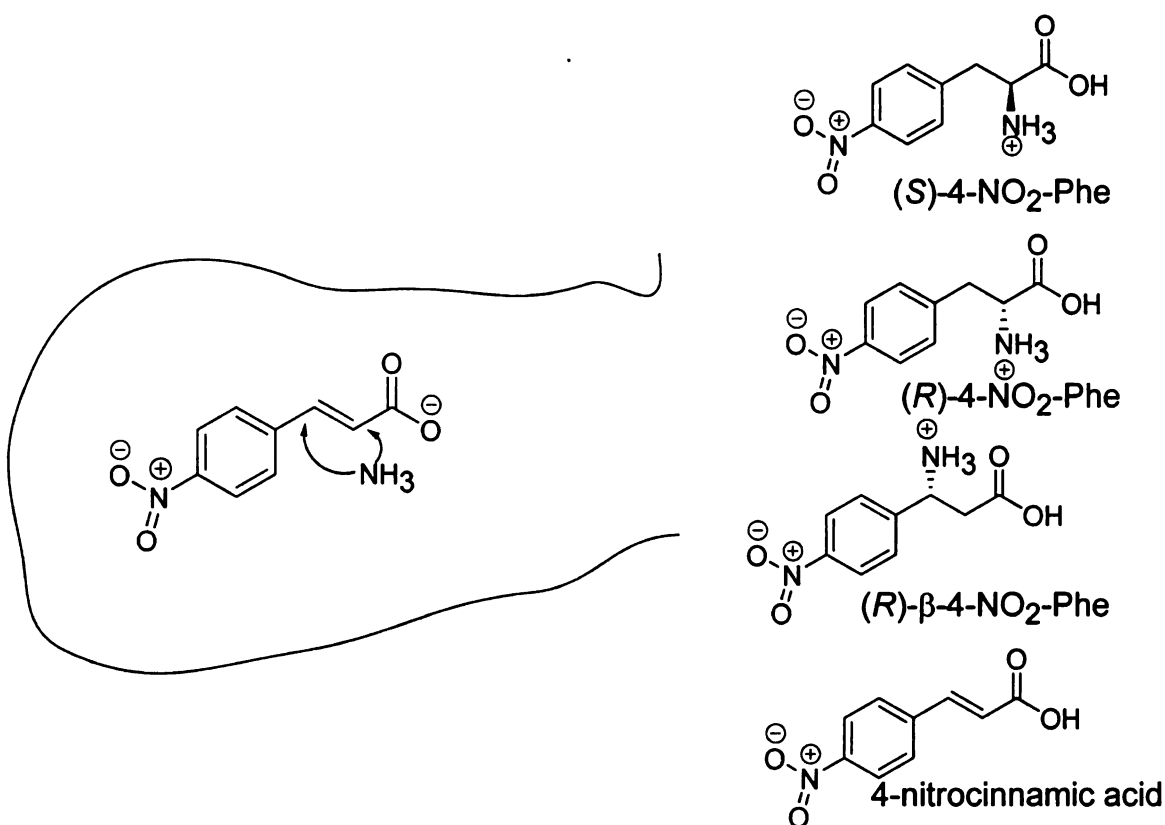
Figure 3.26 The possible products formed from the reaction between crude wild-type PAM with 4'-nitrophenylalanine. The reaction is complicated by the presence of phenylalanine racemase form E. coli which isomerizes D phenylalanine to the L isomer.

In wild-type PAM the MIO is involved in the elimination of ammonia from the α-position and delivering it to the β-position as the *trans*-cinnamate intermediate shifts or slowly moves out of the active site as is the case with PALs in which the release of the cinnamate from the site is the rate determining factor.[101] However the suggestion by Rétey concluded that in MIO-less HAL and PAL mutants the ammonia may be held by coulombic forces may not be very plausible without defining the origin of these forces and how specific they will be. The fact that the HAL reaction is barely reversal may not be in support of such a mechanism. The

148

K_M value of 4-NO$_2$-L- α-phenylalanine and PAM reaction is ~1mM which is significantly different from the natural substrate L- α-phenylalanine (45 μM). Our K_M is however similar to the one obtained by the Janssen group (1.8 mM). The electron withdrawing of the nitro group might be acting syngestically with the six positive helices which point towards the aromatic ring of the substrate as suggested by Calabrese basing on the crystal structure of PAL from *Rhodosporidium toruloides.*[6, 52, 53]
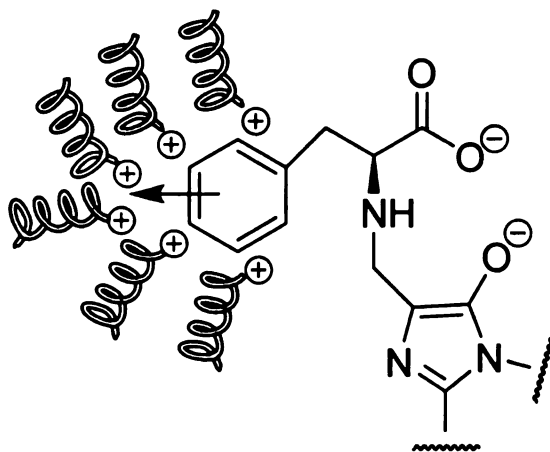
Figure 3.27 Seven α helices associated with the active sites of PAL and HAL. Shown are the six positive poles and one negative pole of the seven α helices, directed towards active-site residues, with cofactor shown for reference.

Investigating the basic residue which deprotonates the β-hydrogen

The general base which de-protonate the β hydrogen is essential for the PAM catalysis. In the absence of the base the reaction is greatly compromised and decreases by more than 100 fold. The base not only does it act in removing the proton, but it is believed to assist in shuttling to the free amine generated

149

when the first NH$_2$-MIO complex breaks down. The created ammonium-MIO complex donates a proton to the α-carbon of cinnamate intermediate to create a carbocation of the β carbon of the alkene which is quenched by reacting with the MIO-NH$_3$ complex through 1, 4 Michael addition. The new intermediate generated, C3-NH$_2$-MIO complex is formed and the subsequent cleavage of the NH$_2$-MIO bond forms the β-acid and the free MIO to complete the catalysis. The proton exchange between the tyrosine base and the amine explains why Mutatu and co-workers reported a 30% transfer of deuterium from the C3 of the substrate to the C2 position. It is envisaged that once the ammonium ion (MIO-NH$_3$) is formed there are equal chances (30%) of each of the three protons adding to the C2 carbon of the cinnamate.

3.4 CONCLUSIONS

Phenylalanine aminomutase (PAM) from *Taxus Canadensis* carries a catalytic moiety the 3,5-dihyro-methylidene-4*H*-imidazol-4-one (MIO based on the cysteine inhibition results). In the absence of a crystal structure this evidence places PAM in a family cofactor-less enzymes like ammonia lyases and other aminomutases such as TAM from Streptomyces globisporous.[15] PAM performs best at pH 8.5 but tolerates more basic conditions than acidic conditions, which supports the proposed mechanism in which a general base is involved in shuttling protons during the reaction. PAM is over expressed best in *E. coli* cells with rare codon optimization at temperatures lower than room temperature. The

lack of reactivity of Y322F is further evidence that NH_2 is the nucleophile because the general base has dual role in both de-protonating the β hydrogen and setting up the elimination of the MIO-amine complex to form the cinnamate intermediate, this warrant further investigation.

3.5 MATERIALS AND METHODS

3.5.1 *MATERIALS*

Complete, EDTA-free protease inhibitor cocktail tablets were purchased from Roche Applied Science(Germany). Luria Bertani (LB) broth from Acumedia and isopropyl-β-D-thiogalactopyranoside (IPTG) was purchased from Gold BioTechnology (St. Louis, Missouri). All other chemicals were purchased from Sigma-Aldrich.

3.5.2 *PROCEDURES*

3.5.2.1 *PAM Expression Optimization and Purification*

The pam plasmid (pam + pET14b) was purified from *E.coli* BL21(DE3) (Stragene) cell cultures and was used to transform *E. coli* BL21(DE3) CodonPlus-RIPL (Strategene). In brief, a bacteria colony was used to inoculate 5 mL of LB media with ampicillin (100 µg/µL) and chloramphenicol (50 µg/µL) selection. The cultures were incubated at 37 °C for 16 hours and used to inoculate 1 L of LB and incubation continued until optical density (OD_{600}) reached 0.6. Then IPTG (1 mM) was added and incubation continued at 16 °C for 16 hours.

The Culture was centrifuged at 5,000 x g for 20 min at 4 °C and the supernatant was discarded. The pellet was resuspended in lysis buffer (50 mM NaH_2PO_4, 300 mM NaCl, 10 mM imidazole, pH 8.0, 2 tablets Complete protease inhibitor per 20 mL of lysis buffer and 10 mg lysozyme), incubated on ice for 30 min and then sonicated on ice at 1 minute pulses for 5 minutes with 1 min interval in between pulses. The lysate was centrifuged at 15,000 x g for 20 min at

4 °C and the pellet discarded. The semi-clear supernatant was centrifuged at 45,000 x g for 2 h at 4 °C, the pellet was discarded.

The cleared lysate was loaded to a pre-equilibrated nickel-nitriloacetic acid (Ni-NTA) column (10 mL of 50% gel suspension) and mixed gently at 4 °C for 5 min and left to settle. The flow through was drained out and the resin washed using 10 times column volume (150 mL) of wash buffer consisting of 50 mM NaH_2PO_4, 300 mM NaCl, 20 mM imidazole, pH 8.0). The PAM was eluted with elution buffer (50 mM, NaH_2PO_4, 300 mM NaCl, 250 mM imidazole, pH 8.0). The elutions were assayed for PAM by SDS-PAGE with Coomassie staining.

3.5.2.2 Enzymatic Assay Techniques

The general enzymatic assay involved incubating the substrate (1 mM) with PAM (10 µg – 5 mg) at pH of 8.5 in either 50 mM Tris-HCl or 50 mM Phosphate buffer. The mixture was incubated in 31 °C water bath for time periods ranging from 30 min to 24 hours. The reaction was quenched with 0.1 N NaOH, to a pH of 11 before adding 5 equivalence of acetic anhydride or ethylchoroformate, and reacted for 30 min at room temperature. The pH of the solution was lowered to 2 with 1 N HCl and the acetylated amino acids extracted with ethylacetate (3 x 2 mL). The organic layer was dried in a rotor vapor resusupended in 100 µL methanol and titrated with tris (methyl)siylyldiazomethane to a pale yellow permanent coloration.

3.5.2.3 *Equilibrium Constant Measurements*

To assess the equilibrium between product and substrate in the PAM reaction, α-phenylalanine at 100 μM was added to 10 ml of PAM (at ∼ 250 μg/mL) in 50 mM phosphate buffer (pH 8.0) and incubated at 30 °C. Aliquots (1 mL) were withdrawn from the reaction at various time points between 15 min-50 h and quenched by careful addition of 0.1 M sodium hydroxide, then the amino acids were derivatized and analyzed by GC/EI-MS (Agilent Technologies, California, USA). The relative amounts of product and reactant at equilibrium were determined by linear regression analysis of the area of the base peak fragment ion of the derivatized α- or β-phenylalanines (*m/z* 162 and 178, respectively). Peak area was converted to concentration-of-product (or - substrate) by solving the corresponding linear equation, which was derived by plotting the area of the signature base peak ion, produced by the corresponding authentic N-acetyl-amino acid methyl ester standard, against the concentration of each standard in a dilution series ranging from 0 – 30 μM, (5 μM intervals).

3.5.2.4 *The pH dependence of the PAM reaction*

PAM was incubated with L-phenylalanine (1 mM) at pH values ranging from 6.5. to 10.5 at a temperature of 31 °C for 3 hours (before reaching equilibrium). The reactions were quenched and derivatized as described above. In order to adjust for the buffering capacities at different pH two buffer systems: pH 6.5 to 9.5, 50 mM Phosphate and pH 9.5 and above values a 50 mM sodium carbonate buffer system was employed.

154

3.5.2.5 *Cysteine Inhibition studies*

The wild-type PAM and mutants were incubated with L-cysteine (10 mM) and stirred for 1 h under aerobic conditions and absorbance measured at λ_{max} 338 nm every 10 minutes or as described by Röther et al[42,43] except dithiothreitol (1 mM) was added to keep the cysteine in reduced form.

3.5.2.6 *Reversibility of the reaction*

The reverse reaction by PAM was tested by incubating the enzyme (25 μg) with 1 mM of β-phenylalanine at 31 °C for an hour. The product was derivatized as described before. The *N*-acetylated methyl ester was injected into the GC-MS equipped with a chiral column (Varian, CP-Chirasil-Val, 25 m x 5 μm in diameter).

3.5.2.7 *Kinetic isotope effect*

In order to determine the rate determining step of the reaction a labeled substrate ([3,3-^{2}H]-phenylalanine and 100 μg of PAM in 1 mL of 50 mM Phosphate buffer, pH 8.5) were incubated. The rate of reaction of the labeled substrate was compared with the same concentration of unlabeled natural substrate and an equivalent amount of enzyme.

155

3.5.2.8 *Site-Directed mutagenesis.*

The mutants (S176 to Ala, Cys, Gly and Thr) were constructed using Strategene Quick-change XL Site-Directed Mutagenesis kit. The following primers were synthesized by the MSU Genomics Technology Support Facility (GTSF) for the following mutants;

Table 3.4 The primers used to construct mutants S176A, G, C and T, the mutated codons are in bold underlined.

Mutant	Primers
S176G	Reverse; 5'-AG GTC TCC **TCC** AGC GCT CAC AGA TC-3'
	Forward; 5'-TG AGC GCT **GGA** GAC CTC ATC CCG CT-3'
S176A	Reverse; 5'- AG GTC TCC **AGC** AGC GCT CAC AGA TC- 3'
	Forward; 5'-TG AGC GCT **GCT** GAC CTC ATC CCG CT-3'
S176C	Reverse; 5'- AG GTC TCC **GCA** AGC GCT CAC AGA TC- 3'
	Forward; 5'-TG AGC GCT **TGC** GAC C TC ATC CCG CT-3'
S176T	Reverse; 5'- AG GTC TCC **CGT** AGC GCT CAC AGA TC- 3'.
	Forward; 5'-TG AGC GCT **ACG** GAC CTC ATC CCG CT-3'

The following mixture was put together for PCR;

10X reaction buffer (5 μL), *pam* plasmid template (10 ng, 0.3 μL), primers (125 ng each, 0.5 μL), dNTP mix (10 mM, 1 μL), Quick Solution (3 μL), ddH$_2$O (39 μL) and *PfuTurbo* DNA polymerase (2.5 U/μL, 1 μL).

156

The thermo cycle was set up as follows: segment 1, 1 cycle, 95 °C for 1 minute denaturing, 18 cycles at 95 °C for 50 s each, anneal at 60 °C for 50 s, extend at 68 °C for 7 min, and further extension at 68 °C for 7 min. The PCR product was digested with *Dpnl* for 1 hr, to digest all the methylated DNA template plasmids.

3.5.2.9 *Transformation of XL10-Gold Ultra competent E. coli Cells.*

The XL10-Gold® ultra competent *E. coli* cells (Strategene, USA) were gently thawed on ice and a 45 µl aliquot was transferred to a pre-chilled 14-mL BD Falcon polypropylene round-bottom tube. β-mercaptoethanol (βME, 2 µL) was added to the cells and swirled gently, incubated on ice for 10 minutes and swirled gently every 2 minutes. The *Dpnl* treated DNA (2 µL) was added to aliquot of the ultra competent cells, swirled gently to mix and incubated on ice for 30 minutes. The tubes were pulse-heated in a 42 °C water bath for 30 s, incubated for 2 minutes and pre-heated LB (0.5 mL) added to each tube, then incubated the tubes at 37 °C for 1 hour with shaking. The cells (250 µL) were spread on ampicillin (100 µg/L) plates and incubated at 37 °C for > 16 hours.

3.5.2.10 *Making Agar plates*

To Luria Bertini (LB) (25 g) was added 20 g of agar and MQ H_2O to a final volume of 1 liter. The mixture was autoclaved for 30 min and cooled to 55 °C before adding 1 mL of 50 mg/mL chloromphenicol and 1 mL of 100 mg/mL

ampicillin. The agar was poured (30 mL) into each plate and gently swirled to make even. The solidify plates were wrapped and stored at 4 °C.

3.5.2.11 *Purification and sequencing of Plasmid*

Colonies (BL21-CodonPlus) from transformations were transferred to 5 mL LB media treated with ampicillin (100 µg/mL) and grown overnight at 37 °C. The cells were centrifuged at 5,000 x *g* for 12 min. The supernatant was discarded and the plasmid purified from the cells following the Qiagen Protocol. The plasmids were quantified using the UV method by measuring the absorbance at 260 nm and comparing with absorbance at 280 nm. Sequencing was done at the MSU Genomics Facility and using forward primers and reverse primers (Table 3.5).

Table 3.5 Primers used to sequence the *pam* gene

Forward primers	Reverse primers
T7 promoter; 5'-TAA TAC GAC TCA	T7terminator; 5'-GCT AGT TAT TGC
500 bp; 5'-TGC CTC TCC GAG GAT	500 bp; 5'-CAG GCA CCG CTT TGG
1000 bp; 5'-TGG TGC AGA CAA TCA	1000 bp; 5'-GGA GAG CCC TGT
1500 bp; 5'-GAA GCC CTA GTA AAA	1500 bp; 5'-GCC TAT GCG AGC
2000 bp; 5'-GCC TCT GCT GCA CTG	2000 bp; 5'-GGT CGT ACC GTC TAC

3.5.2.13 *Culture Conditions.*

E. coli BL21CodonPlus -RIPL cells were used to over express both wild type and mutant PAMs. Cells were grown in 1 liter Miller LB medium supplemented with ampicillin (100 µg/µL) and chloromphenicol (50 µg/µL) initially at 37 °C. At an OD_{600} of 0.6, 1 mM of isopropyl β-D-thiogalactoside was added, the temperature reduced to 16 °C and incubation continued for 16 hours.

3.5.2.14 *Comparison of Kinetic Characteristics of Wild-Type PAM, the mutants S176A, S176G, S176T and S176C with 4'-nitro-L-Phenylalanine and 4'-F-phenylalanine as substrates.*

The kinetic measurements were determined by GC-MS analysis, HPLC and uv-visible spectrophotometer. The substrate concentrations were 0.25, 0.5, 1, 2, 3, 4, 6, 8 and 10 mM. The concentrations of product were plotted on Excel (Microsoft 2007) by fitting all initial rate data to the Michaelis-Menten equation using nonlinear regression (R^2= 0.99). The assays were carried out as described above.

3.5.2.15 *Spectroscopic studies of PAMs*

The difference absorption spectra of the PAM mutants were measured by scanning from 240 to 360 nm. The mutants S176G, S176A, S176C and S176T were used as blanks, against the wild-type.

3.5.2.16 *Construction of the mutants to investigating the basic residues*

The mutants Y322A, H, and Y and C107A and H were constructed following the Strategene Quick-change XL Site-Directed mutagenesis kit. The following primers were synthesized by the MSU Genomics Technology Support Facility (GTSF) as shown in table 3.6;

Table 3.6 The primers used to construct mutants Y322A,H and F, and C107A and H; the mutated codons are in bold underlined.

Mutant	Primers
Y322A	Reverse; 5'-CT CAG AGC **ATA** GCG ATC CTG TTT CG-3'
	Forward; 5'-AG GAT CGC **TAT** GCT CTG GGT CGA GC-3'
Y322H	Reverse; 5'-CT CAG AGC **ATG** GCG ATC CTG TTT CG-3'
	Forward; 5'-AG GAT CGC **CAT** GCT CTG GGT CGA GC-3'
Y322F	Reverse; 5'-CT CAG AGC **GAA** GCG ATC CTG TTT CG-3'
	Forward; 5'-AG GAT CGC **TTC** GCT CTG GGT CGA GC-3'
C107A	Reverse; 5'-CG GAG CAG **TGC** GCG TAT AAG CGA CT- 3'
	Forward; 5'-TT ATA CGC **GCA** CTG CTC GCG GGG GT-3'
C107H	Reverse; 5'-CG GAG CAG **ATG** GCG TAT AAG CGA CT- 3'
	Forward; 5'-TT ATA CGC **CAT** CTG CTC GCG GGG GT-3'

PCR protocol: The following mixture was put together; 10X reaction buffer (5 µL), *pam* plasmid template (10 ng, 0.3 µL), primers (125 ng each, 0.5 µL), dNTP mix (10 mM, 1 µL), Quick Solution (3 µL), ddH2O (39 µL) and *PfuTurbo* DNA polymerase (2.5 U/µL, 1 µL).

The thermo cycle was set up as follows; segment 1, 1 cycle at 95 °C for 1 minute denaturing, 18 cycles (at 95 °C for 50 s each, anneal at 60 °C for 50 s, extend at 68 °C for 7 min) and further extension at 68 °C for 7 min. The PCR product was digested with DpnI for 1 h, to digest all the methylated plasmids including the DNA template.

3.5.2.18 Growth and harvest of mutant enzymes

The mutants Y322 and C107 were grown and harvested as described above for wild type PAM.

3.5.2.19 Activity Assay

The activities of the mutants were performed as described for the wild-type above.

3.6 REFERENCES

1. Christenson, S. D.; Wu, W. M.; Spies, M. A.; Shen, B.; Toney, M. D., Kinetic analysis of the 4-methylideneimidazole-5-one-containing tyrosine aminomutase in enediyne antitumor antibiotic C-1027 biosynthesis. *Biochemistry* **2003**, *42*, (43), 12708-12718.

2. Christianson, C. V.; Montavon, T. J.; Van Lanen, S. G.; Shen, B.; Bruner, S. D., The structure of L-tyrosine 2,3-aminomutase from the C-1027 enediyne antitumor antibiotic biosynthetic pathway. *Biochemistry* **2007**, *46*, (24), 7205-7214.

3. Asano, Y.; Kato, Y.; Levy, C.; Baker, P.; Rice, D., Structure and function of amino acid ammonia-lyases. *Biocatal. Biotransform.* **2004**, *22*, (2), 133-138.

4. Baedeker, M.; Schulz, G. E., Autocatalytic peptide cyclization during chain folding of histidine ammonia-lyase. *Structure* **2002**, *10*, (1), 61-67.

5. Baedeker, M.; Schulz, G. E., Structures of two histidine ammonia-lyase modifications and implications for the catalytic mechanism. *Eur. J. Biochemistry* **2002**, *269*, (6), 1790-1797.

6. Calabrese, J. C.; Jordan, D. B.; Boodhoo, A.; Sariaslani, S.; Vannelli, T., Crystal structure of phenylalanine ammonia lyase: Multiple helix dipoles implicated in catalysis. *Biochemistry* **2004**, *43*, (36), 11403-11416.

7. Langer, B.; Langer, M.; Retey, J., Methylidene-imidazolone (MIO) from histidine and phenylalanine ammonia-lyase. *Advances in Protein Chemistry, 58* **2001**, *58*, 175-214.

8. Montavon, T. J.; Christianson, C. V.; Festin, G. M.; Shen, B.; Bruner, S. D., Design and characterization of mechanism-based inhibitors for the tyrosine aminomutase *Sg*TAM. *Bioorg. Medic. Chem. Lett.* **2008**, *18*, (10), 3099-3102.

9. Poppe, L., Methylidene-imidazolone: a novel electrophile for substrate activation. *Curr. Opin. Chem. Biol.* **2001**, *5*, (5), 512-524.

10. Rettig, M.; Sigrist, A.; Retey, J., Mimicking the reaction of phenylalanine ammonia lyase by a synthetic model. *Helv. Chim. Acta* **2000**, *83*, (9), 2246-2265.

11. Rother, R.; Poppe, L.; Viergutz, S.; Langer, B.; Retey, J., Characterization of the active site of histidine ammonia-lyase from *Pseudomonas putida*. *Eur. J. Biochem.* **2001**, *268*, (23), 6011-6019.

12. Schroeder, A. C.; Kumaran, S.; Hicks, L. M.; Cahoon, R. E.; Halls, C.; Yu, O.; Jez, J. M., Contributions of conserved serine and tyrosine residues to catalysis, ligand binding, and cofactor processing in the active site of tyrosine ammonia lyase. *Phytochemistry* **2008**, *69* (7), 1496-1506.

13. Viergutz, S.; Retey, J., Kinetic analysis of the reactions catalyzed by histidine and phenylalanine ammonia lyases. *Chem. Biodivers.* **2004**, *1*, (2), 296-302.

14. Christenson, S. D.; Liu, W.; Toney, M. D.; Shen, B., A novel 4-methylideneimidazole-5-one-containing tyrosine aminomutase in enediyne antitumor antibiotic C-1027 biosynthesis. *J. Am. Chem.Soc.* **2003**, *125*, (20), 6062-6063.

15. Christenson, S. D.; Wu, W.; Spies, M. A.; Shen, B.; Toney, M. D., Kinetic analysis of the 4-methylideneimidazole-5-one-containing tyrosine aminomutase in enediyne antitumor antibiotic C-1027 biosynthesis. *Biochemistry* **2003**, *42*, (43), 12708-12718.

16. Merkel, D.; Retey, J., Further insight into the mechanism of the irreversible inhibition of histidine ammonia-lyase by L-cysteine and dioxygen. *Helv. Chim. Acta* **2000**, *83*, (6), 1151-1160.

17. Montavon, T. J.; Christianson, C. V.; Festin, G. M.; Shen, B.; Bruner, S. D., Design and characterization of mechanism-based inhibitors for the tyrosine aminomutase SgTAM. *Bioorg. Medic. Chem. lett.* **2008**, *18*, (10), 3099-102.

18. Walker, K. D.; Klettke, K.; Akiyama, T.; Croteau, R., Cloning, heterologous expression, and characterization of a phenylalanine aminomutase involved in Taxol biosynthesis. *J. Biol. Chem.* **2004**, *279*, (52), 53947-53954.

19. Alunni, S.; Cipiciani, A.; Fioroni, G.; Ottavi, L., Mechanisms of inhibition of phenylalanine ammonia-lyase by phenol inhibitors and phenol/glycine synergistic inhibitors. *Arch. Biochem. Biophys.* **2003**, *412*, (2), 170-175.

20. Brincat, M. C.; Gibson, D. M.; Shuler, M. L., Alterations in Taxol Production in Plant Cell Culture via Manipulation of the Phenylalanine Ammonia Lyase Pathway. *Biotechn. Progr.* **2002**, *18*, (6), 1149-1156.

21. Cai, Z.-N.; Yu, Y.-N.; Chen, X.-X.; Yuan, L.-F., High-level expression of phenylalanine ammonia lyase with enzyme activity in *E. coli* by BL21DE3pET28C-rPAL-1-cDNA. *Zhongguo Yaolixue Yu Dulixue Zazhi* **2000**, *14*, (3), 211-215.

22. Charan, R. D.; McKee, T. C.; Boyd, M. R., Thorectandrols A and B, new cytotoxic sesterterpenes from the marine sponge Thorectandra species. *J. Nat. Prod.* **2001**, *64*, (5), 661-663.

23. Cochrane, F. C.; Davin, L. B.; Lewis, N. G., The *Arabidopsis* phenylalanine ammonia lyase gene family: kinetic characterization of the four PAL isoforms. *Phytochemistry* **2004**, *65*, (11), 1557-1564.

24. Croteau, R.; Kutchan, T. M.; Lewis, N. G., Natural products (secondary metabolites). *Biochem. Mol. Biol. Plants* **2000**, 1250-1318.

25. Gloge, A.; Zon, J.; Kovari, A.; Poppe, L.; Retey, J., Phenylalanine ammonia-lyase: The use of its broad substrate specificity for mechanistic investigations and biocatalysis - Synthesis of L-arylalanines. *Chemistry-a Eur. J.* **2000**, *6*, (18), 3386-3390.

26. Hashimoto, M.; Hatanaka, Y.; Nabeta, K., Novel photoreactive cinnamic acid analogues to elucidate phenylalanine ammonia-lyase. *Bioorganic & Medicinal Chem. Lett.* **2000**, *10*, (21), 2481-2483.

27. Kim, W., Development of Modified Phenylalanine Ammonia-lyase for the Treatment of Phenylketonuria. *Biomol. Therap.* **2009**, *17*, (1), 104-110.

28. Kluczyk, A.; Szefczyk, B.; Amrhein, N.; Zon, J., (*E*)-cinnamic acid analogues as inhibitors of phenylalanine ammonia-lyase and of anthocyanin biosynthesis. *Polish J. Chemistry* **2005**, *79*, (3), 583-592.

29. Almstead, J.-I. K.; Demuth, T. P.; Ledoussal, B., An investigation into the total synthesis of clerocidin: Stereoselective synthesis of a clerodane intermediate. *Book of Abstracts, 216th ACS National Meeting, Boston, August 23-27* **1998**, ORGN-364.

30. Rettig, M.; Sigrist, A.; Rétey, J., Mimicking the reaction of phenylalanine ammonia lyase by a synthetic model. *Helv. Chim. Acta,* **2000**, *83*, (9), 2246-2265.

31. Schwede, T. F.; Retey, J.; Schulz, G. E., Crystal structure of histidine ammonia-lyase revealing a novel polypeptide modification as the catalytic electrophile. *Biochemistry* **1999**, *38*, (17), 5355-5361.

32. Consevage, M. W.; Phillips, A. T., Sequence-Analysis of the Huth-Gene Encoding Histidine Ammonia-Lyase in *Pseudomonas-Putida*. *J. Bacteriology* **1990**, *172*, (5), 2224-2229.

33. Hernandez, D.; Phillips, A. T., Purification and Characterization of Pseudomonas-Putida Histidine Ammonia-Lyase Expressed in Escherichia-Coli. *Protein Expression and Purification* **1993**, *4*, (5), 473-478.

34. Langer, M.; Lieber, A.; Retey, J., Histidine Ammonia-Lyase Mutant-S143c Is Posttranslationally Converted into Fully Active Wild-Type Enzyme - Evidence for Serine-143 to Be the Precursor of Active-Site Dehydroalanine. *Biochemistry* **1994**, *33*, (47), 14034-14038.

35. Langer, M.; Reck, G.; Reed, J.; Retey, J., Identification of Serine-143 as the Most Likely Precursor of Dehydroalanine in the Active-Site of Histidine Ammonia-Lyase - a Study of the Overexpressed Enzyme by Site-Directed Mutagenesis. *Biochemistry* **1994**, *33*, (21), 6462-6467.

36. Röther, D.; Poppe, L.; Viergutz, S.; Langer, B.; Rétey, J., Characterization of the active site of histidine ammonia-lyase from *Pseudomonas putida*. *European J. Biochemistry* **2001**, *268*, (23), 6011-6019.

37. Wu, P. C.; Kroening, T. A.; White, P. J.; Kendrick, K. E., Histidine Ammonia-Lyase from *Streptomyces-Griseus*. *Gene* **1992**, *115*, (1-2), 19-25.

38. Gloge, A.; Langer, B.; Poppe, L.; Rétey, J., The behavior of substrate analogs and secondary deuterium isotope effects in the phenylalanine ammonia-lyase reaction. *Arch. Biochem. and Biophys.* **1998**, *359*, (1), 1-7.

39. Katona, A.; Tosa, M. I.; Paizs, C.; Retey, J., Inhibition of histidine ammonia lyase by heteroaryl-alanines and acrylates. *Chem. Biodivers.* **2006**, *3*, (5), 502-508.

40. Langer, M.; Pauling, A.; Retey, J., The Role of Dehydroalanine in Catalysis by Histidine Ammonia-Lyase. *Angewandte Chemie-International Edition in English* **1995**, *34*, (13-14), 1464-1465.

41. Langer, B.; Starck, J.; Langer, M.; Retey, J., Formation of the Michaelis complex without involvement of the prosthetic group dehydroalanine of histidine ammonialyase. *Bioorg. Med. Chem. Lett.* **1997**, *7*, (8), 1077-1082.

42. Rother, D.; Poppe, L.; Viergutz, S.; Langer, B.; Retey, J., Characterization of the active site of histidine ammonia-lyase from *Pseudomonas putida*. *Eur. J. Biochem.* **2001**, *268*, (23), 6011-9.

43. Rother, D.; Poppe, L.; Morlock, G.; Viergutz, S.; Retey, J., An active site homology model of phenylalanine ammonia-lyase from *Petroselinum crispum*. *Eur. J. Biochem.* **2002**, *269*, (12), 3065-3075.

165

44. Weber, K.; Retey, J., On the nature of the irreversible inhibition of histidine ammonia lyase by cysteine and dioxygen. *Bioorg. Med. Chem.* **1996**, *4*, (7), 1001-1006.

45. Schuster, B.; Rétey, J., The mechanism of action of phenylalanine ammonia-lyase: the role of prosthetic dehydroalanine. *Proc. Nat. Acad. Sci. the USA* **1995**, *92*, (18), 8433-8437.

46. Cheung, M. C.; Pantanowitz, L.; Dezube, B. J., AIDS-related malignancies: emerging challenges in the era of highly active antiretroviral therapy. *Oncologist* **2005**, *10*, (6), 412-426.

47. Skolaut, A.; Rétey, J. In *3-(2,5-Cyclohexadienyl)-L-alanine (1,4-dihydro-L-phenylalanine). Its synthesis and behavior in the phenylalanine ammonia-lyase reaction*, 2000; Pombo-Villar, E., Molecular Diversity Preservation International, Basel, Switz.: 2000; Meeting Date 1999-2000, 836-846.

48. Toyooka, Y.; Wada, C.; Ohnuki, Y.; Takada, F.; Ohtani, H., Molecular diagnosis of a kindred with novel mutation of methylmalonyl - CoA mutase gene using non-RI SSCP. *Rinsho Byori* **1995**, *43*, (6), 625-9.

49. Galpin, J. D.; Ellis, B. E.; Tanner, M. E., The inactivation of histidine ammonia-lyase by L-cysteine and oxygen: Modification of the electrophilic center. *J. Amer. Chem. Soc.* **1999**, *121*, (46), 10840-10841.

50. Klee, C. B.; Gladner, J. A., Isolation of a Cysteine-Peptide at Active-Site of Histidine Ammonia-Lyase. *J. Biol. Chem.* **1972**, *247*, (24), 8051-8057.

51. Klee, C. B., Stereospecific Irreversible Inhibition of Histidine Ammonia-Lyase by L-Cysteine. *Biochemistry* **1974**, *13*, (22), 4501-4507.

52. Chen, Y. F.; Raney, K. D., Cloning and overexpression of phenylalanine ammonia lyase from R. toruloides in *E.Coli* BL21(DE3). *Faseb J.* **2002**, *16*, (5), A905-A905.

53. Shi Ru, J.; Jian Dong, C.; Yan, L.; Ai You, S., Production of L-phenylalanine from trans-cinnamic acids by high-level expression of phenylalanine ammonia lyase gene from Rhodosporidium toruloides in Escherichia coli. *Biochemical Engineer. J.* **2008**, *42*, (3), 42 (3) 193-197.

54. Steele, C. L.; Chen, Y.; Dougherty, B. A.; Li, W.; Hofstead, S.; Lam, K. S.; Xing, Z.; Chiang, S.-J., Purification, cloning, and functional expression of phenylalanine aminomutase: the first committed step in Taxol side-chain biosynthesis. *Arch. Biochem. Biophys.* **2005**, *438*, (1), 1-10.

55. Abbenante, G.; Hughes, R.; Prager, R. H., Potential GABAB receptor antagonists. IX. The synthesis of 3-amino-3-(4-chlorophenyl)propanoic acid, 2-amino-2-(4-chlorophenyl)ethylphosphonic acid and 2-amino-2-(4-chlorophenyl)ethanesulfonic acid. *Australian J. Chem.* **1997,** *50,* (6), 523-527.

56. Aberhart, D. J.; Cotting, J. A., Mechanistic studies on lysine 2,3-aminomutase: Carbon-13-deuterium crossover experiments. *J. Chem Soc., Perkin Transactions 1* **1988,** (8), 2119-2122.

57. Berkecz, R.; Sztojkov-Ivanov, A.; Ilisz, I.; Forro, E.; Fueloep, F.; Hyun, M. H.; Peter, A., High-performance liquid chromatographic enantioseparation of b-amino acid stereoisomers on a (+)-(18-crown-6)-2,3,11,12-tetracarboxylic acid-based chiral stationary phase. *J. Chromatogr., A* **2006,** *1125,* (1), 138-143.

58. Bjorklund, J. A.; Leete, E., Biosynthesis of the benzoyl moiety of cocaine from cinnamic acid via *R*-(+)-3-hydroxy-3-phenylpropanoic acid. *Phytochemistry* **1992,** *31,* 3883-3887.

59. Coolong, A.; Kuntz, R. E., Understanding the drug-eluting stent trials. *Amer. J. Cardiol.* **2007,** 100, (5A), 17K-24K.

60. Croteau, R. B.; Walker, K. D.; Schoendorf, A.; Wildung, M. R. Cloning of transacylases of the paclitaxel biosynthetic pathway in Taxus. US 2003108891, 20020918., 2003.

61. Cukovic, D.; Ehlting, J.; VanZiffle, J. A.; Douglas, C. J., Structure and evolution of 4-coumarate:coenzyme A ligase (4CL) gene families. *Biol.Chem.* **2001,** *382,* (4), 645-654.

62. D'Auria, J. C.; Chen, F.; Pichersky, E., Characterization of an Acyltransferase Capable of Synthesizing Benzylbenzoate and Other Volatile Esters in Flowers and Damaged Leaves of *Clarkia breweri*. *Plant Physiol.* **2002,** *130,* (1), 466-476.

63. Fleming, P. E.; Floss, H. G.; Haertel, M.; Knaggs, A. R.; Lansing, A.; Mocek, U.; Walker, K. D., Biosynthetic studies on taxol. *Pure Appl. Chem.* **1994,** *66,* (10/11), 2045-8.

64. Hahlbrock, K.; Scheel, D., Physiology and molecular biology of phenylpropanoid metabolism. *Annual Review of Plant Physiology and Plant Molecular Biology* **1989,** *40,* 347-69.

65. Hamamoto, H.; Mamedov, V. A.; Kitamoto, M.; Hayashi, N.; Tsuboi, S., Chemoenzymatic synthesis of the C-13 side chain of paclitaxel (Taxol) and docetaxel (Taxotere). *Tetrahedron: Asymmetry* **2000**, *11*, (22), 4485-4497.

66. Hashimoto, M.; Hatanaka, Y.; Nabeta, K., Novel photoreactive cinnamic acid analogues to elucidate phenylalanine ammonia-lyase. *Bioorg. Medic.l Chem. Lett.* **2000**, *10*, (21), 2481-2483.

67. Jaffe, E. K.; Markham, G. D.; Rajagopalan, J. S., ^{15}N and ^{13}C NMR studies of ligands bound to the 280,000-dalton protein porphobilinogen synthase elucidate the structures of enzyme-bound product and a Schiff base intermediate. *Biochemistry* **1990**, *29*, (36), 8345-8350.

68. Johannsen, M.; Sachs, M.; Roigas, J.; Hinke, A.; Staack, A.; Loening, S. A.; Schnorr, D.; Wille, A. H., Phase II trial of weekly paclitaxel and carboplatin chemotherapy in patients with advanced transitional cell cancer. *Eur. Urol.* **2005**, *48*, (2), 246-251.

69. Gloge, A.; Zon, J.; Kövári, Á.; Poppe, L.; Rétey, J., Phenylalanine ammonia-lyase: The use of its broad substrate specificity for mechanistic investigations and biocatalysis - synthesis of L-arylalanines. *Chemistry - A Eur. J.* **2000**, *6*, (18), 3386-3390.

70. MacDonald, M. J.; D'Cunha, G. B., A modern view of phenylalanine ammonia lyase. *Biochemistry and Cell Biology-Biochimie Et Biologie Cellulaire* **2007**, *85*, (3), 273-282.

71. Okada, T.; Mikage, M.; Sekita, S., Molecular Characterization of the Phenylalanine Ammonia-Lyase from Ephedra sinica. *Biol. Pharm. Bull.***2008**, *31*, (12), 2194-2199.

72. Röther, D.; Poppe, L.; Morlock, G.; Viergutz, S.; Rétey, J., An active site homology model of phenylalanine ammonia-lyase from *Petroselinum crispum*. *Eur. J. biochem.* **2002**, *269*, (12), 3065-75.

73. Sarkissian, C. N.; Gamez, A., Phenylalanine ammonia lyase, enzyme substitution therapy for phenylketonuria, where are we now? *Molecular Genetics and Metabolism* **2005**, *86*, S22-S26.

74. Singh, K.; Kumar, S.; Rani, A.; Gulati, A.; Ahuja, P., Phenylalanine ammonia-lyase (PAL) and cinnamate 4-hydroxylase (C4H) and catechins (flavan-3-ols) accumulation in tea. *Functional & Integrative Genomics* **2009**, *9*, (1), 125-134.

75. Wanner, L. A.; Li, G.; Ware, D.; Somssich, I. E.; Davis, K. R., The phenylalanine ammonia-lyase gene family in *Arabidopsis thaliana*. *Plant Mol. Biol.* **1995**, *27*, (2), 327-38.

76. Louie, G. V.; Bowman, M. E.; Moffitt, M. C.; Baiga, T. J.; Moore, B. S.; Noel, J. P., Structural Determinants and Modulation of Substrate Specificity in Phenylalanine-Tyrosine Ammonia-Lyases. *Chem. Biol.* **2006**, *13*, (12), 1327-1338.

77. Steele, C. L.; Chen, Y.; Dougherty, B. A.; Hofstead, S.; Lam, K. S.; Li, W.; Xing, Z. *Taxus* Phenylalanine Aminomutase and Methods to Improve Taxol Production. Patent: WO 03/066871 A2, February 10, 2003.

78. Klettke, K. L.; Sanyal, S.; Mutatu, W.; Walker, K. D., beta-styryl- and beta-aryl-beta-alanine products of phenylalanine aminomutase catalysis. *J. Am. Chem. Soc.* **2007**, *129*, (22), 6988-.

79. Bae, H. S.; Hong, S. P.; Lee, S. G.; Kwak, M. S.; Esaki, N.; Sung, M. H., Application of a thermostable glutamate racemase from Bacillus sp SK-1 for the production of D-phenylalanine in a multi-enzyme system. *J. Mol. Catalysis B-Enzymatic* **2002**, *17*, (6), 223-233.

80. Stein, T.; Kluge, B.; Vater, J.; Franke, P.; Otto, A.; Wittmannliebold, B., Gramicidin-S Synthetase-1 (Phenylalanine Racemase), a Prototype of Amino-Acid Racemases Containing the Cofactor 4'-Phosphopantetheine. *Biochemistry* **1995**, *34*, (14), 4633-4642.

81. Kanda, M.; Hori, K.; Kurotsu, T.; Miura, S.; Saito, Y., Reaction-Mechanism of Gramicidin-S Synthetase-1, Phenylalanine Racemase, of Bacillus-Brevis. *J. Biochemistry* **1989**, *105*, (4), 653-659.

82. Asano, Y.; Endo, K., Amino-Acid Racemase with Broad Substrate-Specificity, Its Properties and Use in Phenylalanine Racemization. *Appl. Microbio. Biotechn.* **1988**, *29*, (6), 523-527.

83. Vater, J.; Kleinkauf, H., Gramicidin S-Synthetase - Further Characterization of Phenylalanine Racemase, Light Enzyme of Gramicidin S-Synthetase. *Biochimica Et Biophysica Acta* **1976**, *429*, (3), 1062-1072.

84. Takahash.H, Racemization of Phenylalanine by Adenosine Triphosphate-Dependent Phenylalanine Racemase of *Bacillus-Brevis Nagano*. *J. Biochem.* **1971**, 69, (5), 973.

85. Yamada, M.; Kurahash.K, Further Purification and Properties of Adenosine Triphosphate-Dependent Phenylalanine Racemase of Bacillus Brevis Nagano. *Biochemistry* **1969**, *66*, (4), 529-&.

86. Yamada, M.; Kurahash.K, Adenosine Triphosphate and Pyrophosphate Dependent Phenylalanine Racemase of Bacillus Brevis Nagano. *J. Biochem.* **1968**, *63*, (1), 59.

87. Wu, B.; Szymanski, W.; Wietzes, P.; de Wildeman, S.; Poelarends, G. J.; Feringa, B. L.; Janssen, D. B., Enzymatic Synthesis of Enantiopure alpha- and beta-Amino Acids by Phenylalanine Aminomutase-Catalysed Amination of Cinnamic Acid Derivatives. *Chembiochem* **2009**, *10*, (2), 338-344.

88. Chen, F.; Duran, A. L.; Blount, J. W.; Sumner, L. W.; Dixon, R. A., Profiling phenolic metabolites in transgenic alfalfa modified in lignin biosynthesis. *Phytochemistry (Elsevier)* **2003**, *64*, (5), 1013-1021.

89. Chen, M. J.; Vijaykumar, V.; Lu, B. W.; Xia, B.; Li, N., Cis- and trans-cinnamic acids have different effects on the catalytic properties of Arabidopsis phenylalanine ammonia lyases PAL1, PAL2, and PAL4. *J. Integrative Plant Biology* **2005**, *47*, (1), 67-75.

90. Conkerton, E. J.; Chapital, D. C., High-Performance Liquid-Chromatography Separation of the Cis-Trans Isomers of Cinnamic Acid-Derivatives - Ultraviolet and Electrochemical Detection. *J. Chromatography* **1983**, *281*, 326-329.

91. Davin, L. B.; Lewis, N. G., An historical perspective on lignan biosynthesis: monolignol, allylphenol and hydroxycinnamic acid coupling and downstream metabolism. *Phytochemistry Reviews* **2004**, *2*, (3), 257-288.

92. De Jong, A. W. K., The germs of cis-cinnamic acid. *Recueil Des Travaux Chimiques Des Pays-Bas* **1932**, *51*, 397-400.

93. Easton, C. J.; Fryer, N. L.; Kelly, J. B.; Kociuba, K., Stereocontrolled synthesis of deuterated phenylalanine derivatives through manipulation of an N-phthaloyl protecting group for the recall of stereochemistry. Application in the study of phenylalanine ammonia lyase. *ARKIVOC [online computer file]* **2001**, *2*, (5).

94. Fokin, V. V.; Sharpless, K. B., A practical and highly efficient aminohydroxylation of unsaturated carboxylic acids. *Ang. Chemie, Int. Edition* **2001**, *40*, (18), 3455-3457.

95. Graf, E.; Boeddeker, H., The taxus alkaloids. III. The optical activity and configuration of the α-aminohydrocinnamic acids and their N-methyl derivatives. *Ann.* **1958**, *613*, 111-20.

96. Havinga, E.; Nivard, R. J. F., Ultraviolet Absorption Spectra and Stereochemical Structure of Plant Growth Substances of the Cis Cinnamic Acid Type and of Stilboestrol. *Recueil Des Travaux Chimiques Des Pays-Bas-J. Royal Netherlands Chem. Soc.* **1948**, *67*, (11), 846-854.

97. Hedvati, L.; Nudelman, A.; Falb, E.; Kraiz, B.; Zhuk, R.; Sprecher, M., Cinnamic acid derived oxazolinium ions as novel cytotoxic agents. *Eur. J. Medic. Chem.* **2002**, *37*, (7), 607-616.

98. Hocking, M. B., Photochemical and thermal isomerizations of *cis*- and *trans*-cinnamic acids, and their photostationary state. *Can. J. Chem.* **1969**, *47*, (24), 4567-76.

99. Moore, B. S.; Hertweck, C.; Hopke, J. N.; Izumikawa, M.; Kalaitzis, J. A.; Nilsen, G.; O'Hare, T.; Piel, J.; Shipley, P. R.; Xiang, L.; Austin, M. B.; Noel, J. P., Plant-like Biosynthetic Pathways in Bacteria: From Benzoic Acid to Chalcone. *J. Nat. Prod.* **2002**.

100. Langer, M.; Pauling, A.; Rétey, J., The role of dehydroalanine in catalysis by histidine ammonia lyase. *Angewandte Chemie, Int. Edition in English* **1995**, *34*, (13), 1464-5.

101. Butler, D.; Bendiske, J.; Michaelis, M. L.; Karanian, D. A.; Bahr, B. A., Microtubule-stabilizing agent prevents protein accumulation-induced loss of synaptic markers. *Eur. J. Pharm.* **2007**, *562*, (1-2), 20-27.

CHAPTER 4

Recombinantly Expressed Phenylalanine Aminomutase (PAM) Shows Increased Activity in *E. Coli* Grown Under Light Illumination

4. 1 INTRODUCTION

Light illumination has been implicated in shifting the redox state of bacterial, yeast and mammalian cells and activating the synthesis of ATP and DNA,[1,2] hence stimulating the synthesis of both recombinant and non-recombinant proteins. This photobiological reaction involves the absorption of a specific wavelength of light by photoreceptors which are not normally involved in light responses such as in photosynthetic organisms (e.g. chlorophyll). The photoreceptor must be a key structure that can regulate a metabolic pathway in the organism. Examples of such receptors are redox chains such as cytochromes and flavoproteins. Evidence has shown that mitochondria are sensitive to irradiation with monochromatic visible and near-infrared light.[3] The light response has been observed in both bacterial (*E. coli*) and mammalian cells in which there is increased ATP synthesis and O_2 consumption.[3-5] Light irradiation, increases the mitochondrial membrane potential, proton gradient, optical properties, rate of ADP/ATP exchange and a shift in the NADH/NAD, NADP/NADPH, and GSH/GSSG ratios.[6] The respiratory chain of mitochondria as represented by cytochrome c oxidase presents a fulcrum into the link between the light activation and the change of the redox potential. The enzyme contains metal ion centers which are prone to photoredox reactions and has influence on

the bioenergetics of the cell. Different wavelengths of light will give different and sometimes antagonistic responses on the cellular metabolism, for example red light at 650 nm has been reported to increase oxidative phosphorylation, but far-red at 725 nm inhibited it,[5] which point to the absorption of different chromophores which are in different redox states and are involved in different metabolic pathways. In brief the terminal respiratory chain oxidases in eukaryotic cells (cytochrome c oxidase) and in prokaryotic cells (cytochrome bd and bo complexes) are believed to be photoacceptors molecules for red-to-near-IR radiation and the flavoproteins (NADH dehydrogenase) are response to the violet-to-blue light.[1] The irradiation of cytochromes with light shifts to more reduced form thus promoting electron transport which may also trigger folding of the proteins. Apart from the electronic effects of the chromophores and photosensitive proteins, there is a possibility that irradiation may increase temperature of the biomolecules which may cause structural (conformational) changes and trigger biochemical activity (secondary dark reactions) such as activation or inhibition of enzymes. The increased electron flow in the respiratory chain, increases the superoxide anion $(O_2^{\cdot -})$ production, which provides a source of electrons for the oxidative phosphorylation of ADP under physiological conditions.[7] The related increase in H_2O_2, results in multiple responses such as increase in; $[Ca^{2+}]$, pH, activation of Na^+/H^+ antiport (involved in the photosignal transduction and amplification chain), Ca^{2+} ATPase, Na^+, K^+ ATPase (which control cAMP levels in the cell) and alteration of Na^+-Ca^{2+} exchange.[8,9] Catalase

173

the enzyme involved in the conversion of O_2^{-} to H_2O_2 has been observed to increase in activity in yeast cells.[10] The absorption of light (visible) by certain porphyrins and flavoproteins generate singlet oxygen which act as a mediator in achieving the biological effects of radiation.[11-23] Trushin demonstrated that light can increase the expression of a recombinant protein barstar in *E. coli*.[19-23]

The most extensive studies on the effect of light on living cells is provided by the plant systems. Plants have been reported to respond to environmental factors such as heat, light and predators.[24-72] The response of plants to such external stimuli may change the metabolic pathway by regulating expression of enzymes or synthesis of special metabolites which may act to protect the plant. The studies on plant systems has been focused on the phenylpropanoid pathway, which is initiated by phenylalanine ammonia lyase (PAL) and/or tyrosine ammonia lyase (TAL). PAL and TAL are involved in the non-oxidatively de-amination of phenylalanine and tyrosine to *trans*-cinnamic and *p*-coumaric acid respectively.[73-100] Hahlbrock and co-workers observed that plant cell cultures of *Petroselinum hortense* had a marked increase in phenylalanine ammonia lyase (PAL) activity when grown under light illumination versus dark conditions.[101-105] Their results suggest that light increases both the de novo synthesis of PAL and its activity. Speculations about the effect of light on the enzymes has been implicated on the influence of light, especially UV on *trans*-cinnamic acid which is photochemically transformed to *cis*-cinnamic acid. The depletion of *trans*-cinnamic to *cis*-cinnamic acid will probably cause a negative

efflux of *trans*-cinnamic acid and hence increase the activity of the phenylpropanoid pathway enzymes.[106] Similar studies on histidine ammonia lyase (HAL) which catalyzes the conversion of L-histidine to urocanate have indicated a positive response to light. PAL and TAL are structurally and mechanistic similar to phenylalanine aminomutase (PAM) which converts α-phenylalanine to β-phenylalanine. Not only do these enzymes share a 56% homology, the possess 12 conserved residues and have a catalytic moiety 3,5-dihydro-5-methylidene imidazolone-4-one (MIO) which is implicated in the mechanism of catalysis.[107-129] The cofactor is auto catalytically and post transitionally synthesized by the cyclization and dehydration of the alanine-serine-glycine (ASG) triad. Yu and coworkers[130] demonstrated using mass spectrometry that a high proportion (90%) of the TAL protein is in the MIO-less hence inactive form. The light illumination could be increasing the MIO per protein ratio thereby increasing the active form of the enzyme relative to the total enzyme. The light regulation could still be attributed to the phenomena described above related to the shift in the redox potential of the cell, which has effect of phosphorylation of enzymes.

The study of the phenylpropanoid provides a direct link between increase in protein expression and activity. Interestingly the bacterial and plant metabolic pathways are linked by the phenylpropanoid pathway (Figure 4.1). Specifically the ubiquitous plant enzymes phenylalanine ammonia-lyase (PAL) and chalcone synthase (CHS) are key biosynthetic catalysts in phenylpropanoid and flavonoid assembly, respectively. Bacteria such as *Streptomyces maritimus*

and *E. coli* produce benzoyl-CoA in a plant-like manner from phenylalanine involving a PAL-mediated reaction through cinnamic acid during the biosynthesis of the polyketides. The recent discovery that bacteria harbor homodimeric PKSs belonging to the plant CHS superfamily of condensing enzymes has further linked the biosynthetic capabilities of plants and bacteria suggesting a similar mechanistic response to light irradiation. If the light activation is specific to the phenylpropanoid enzymes, which is arguable since some mammalian enzymes have been reported to be responsive to light, then it may point to the fact that all enzymes are activated by light, whether they are recombinant or not. It follows then that an enzyme like PAM which is heterologously expressed in *E. coli* should be activated by light through any of the mechanisms described above.

In this study we focus on measuring both the expression and activity of PAM. The activity of PAM will be measured by the rate of β-phenylalanine formation *in vivo* and the results compared with a control samples kept under non-illuminating conditions. An attempt will be made to assess whether the observed increase in β-phenylalanine formation under light illumination is attributed to the post-transcriptional modification of PAM or the stimulation of the biosynthetic pathways of *E. coli* through the mechanisms explained above. The variation of PAM activity over time in response to light illumination and the effect of light on the growth and cell viability as measured by cell density (optical density at 600 nm) of transformed bacteria is also reported. The effect of light on the thermal activation via increase in temperature of the medium was addressed by monitoring the temperature over time. The type of radiation responsible for

PAM activation was determined by irradiating the cell cultures with white light filtered from red and/or IR radiation. The effect of sonication on the activity of PAM was investigated and also the effect of visible light and ultra-violet light on the activity of pure PAM was studied. If indeed light increases activity of PAM and other enzymes it will provide an easy and inexpensive way of producing more efficient enzymes per gram of cell pellet without increasing the amount of cell cultures.
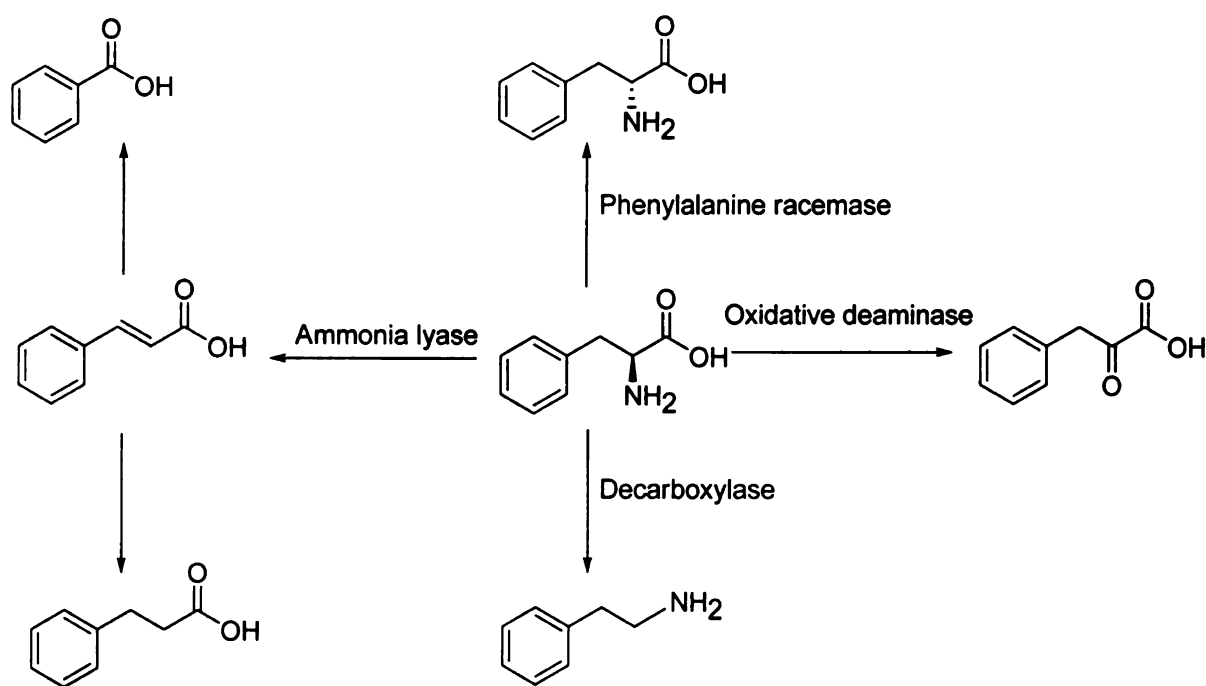
Figure 4.1. A scheme showing the fate of L-phenylalanine in *E. coli*. The presence of PAM in E. coli will increase the flux of *trans*-cinnamic acid thereby upsetting the cellular metabolism which may contribute to different response to light conditions.

4.2 RESULTS AND DISCUSSION

4.2.1 Results

4.2.1.1 *Assaying for PAM activity*

The activity of recombinant PAM in cells exposed to total white light was of 3.8 ± 0.5 % at 16 °C (Figure 4.2) and 18 ± 3% at 25 °C as measured by the amount of endogenous α -phenylalanine converted to β-phenylalanine. The cells kept in the dark had an activity of 1 ± 0.5% (Figure 4.2) and 10 ± 2% at 16 °C and 25 °C respectively. The activity was measured as the mole fraction of (*R*)-β-phenylalanine relative to the total phenylalanines in the culture. The cells were lysed chemically and the amino acids derivatized to their N-acetylated and methyl ester form and analyzed using GC-MS. PAM is usually harvested after IPTG induction at 16 °C, 18 °C or 25 °C and incubation for 18 h. The optimum temperature is 16 °C as reported and discussed in Chapter 2. The optimum temperature for PAM activity is 28 °C.[131]
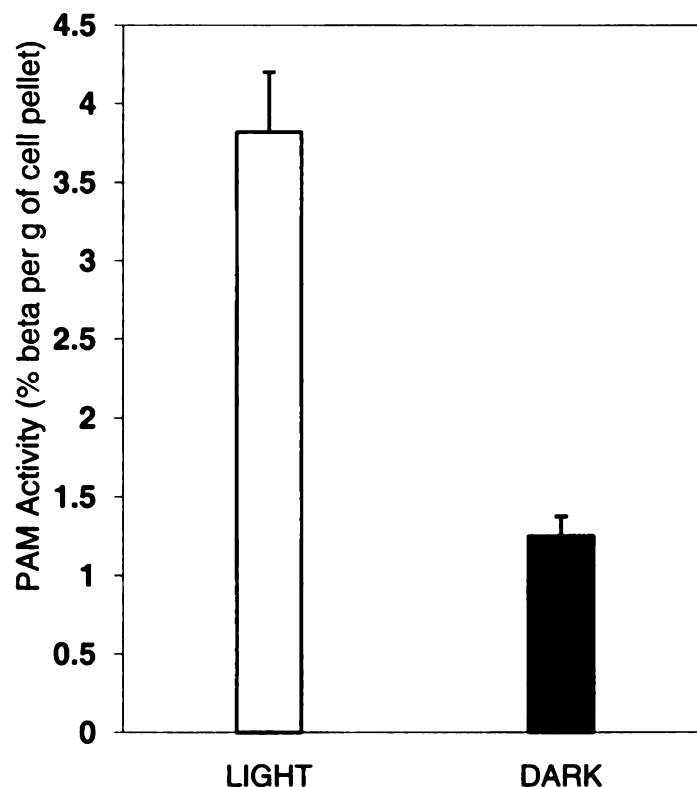
Figure 4.2 Effect of total white light illumination on phenylalanine aminomutase activity in *E. coli* at 16 °C. The amino acids were derivatized as described above and assayed by GC/MS. The light illuminated had an average activity of 3.8% per gram of cell pellet and the non-illuminated had about 1% (black).

4.2.1.2 *Effect of lysis technique on PAM activity measurement under light illumination conditions*

The cells from the illuminated and covered control experiments were lysed by either sonication or by chemical lysis using a series of buffers. The sonicated set of samples (Figure 4.3), DSL (covered and lysed by sonication) and LSL (illuminated and lysed by sonication) there was no significant difference between light illuminated and non-illuminated conditions whereas for the chemically lysed set of samples showed a 6 fold difference.
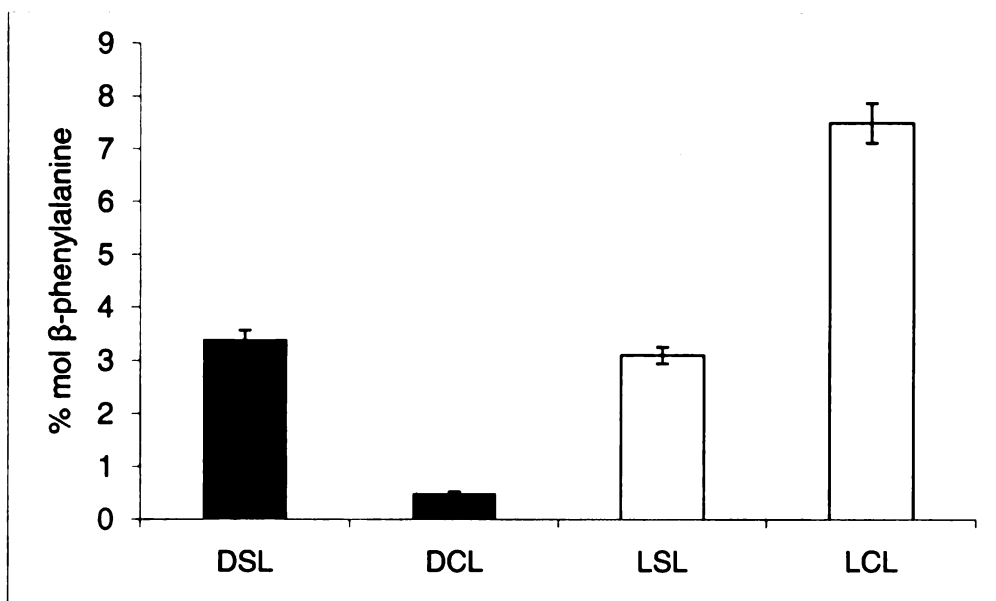
Figure 4.3 Effect of method of lysis on PAM activity measurement -Cells illuminated by total white light or grown under non-illumination conditions were either lysed by sonication (DSL and LSL) or chemically (DCL and LCL).
DSL- sample covered (dark) and lysed by sonication
DCL- sample covered (dark) and lysed chemically
LSL- illuminated by light and lysed by sonication
LCL-illuminated by light and lysed chemically

4.2.1.3 *Investigation of the effect of UV light on the activity of pure PAM.*

To investigate whether the increase in PAM activity when exposed to light was due to activation of the expressed enzyme, pure PAM was incubated with substrate and exposed to UV-B (254 nm) at room temperature for 1 hour, alongside a control covered in aluminum foil. The UV exposed reaction light showed a less that one percentage point increase in activity compared to the control (Figure 4.4). UV radiation has a small contribution to the activity of pure PAM. The small increase could perhaps be due the activation of the exocyclic

double bond of the methylidene imidazolone (MIO). The slight increase in β-phenylalanine formation could also be attributed to thermal effects which could cause an increase in the local temperature.
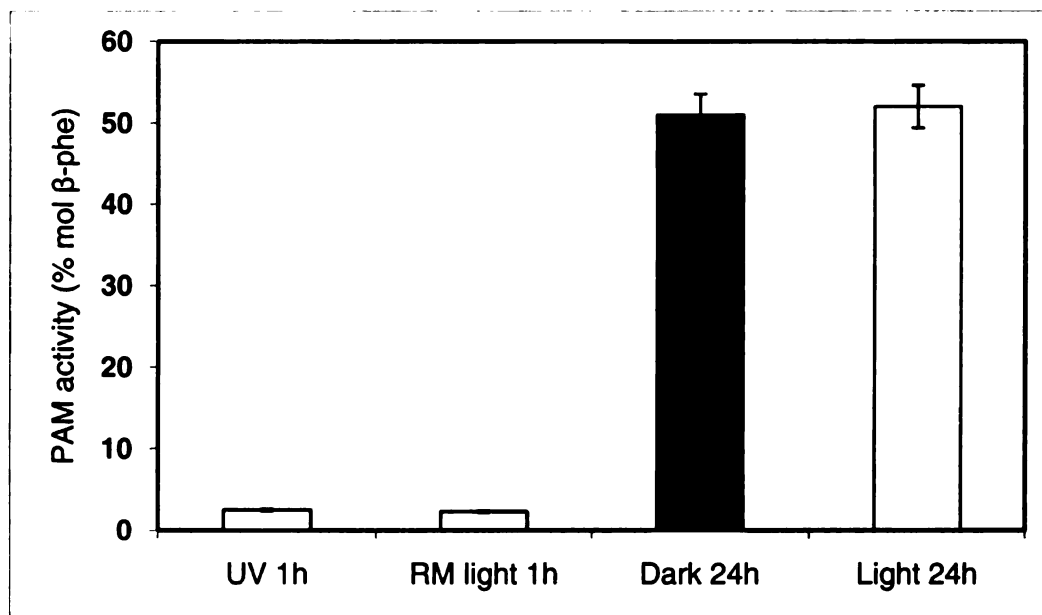
Figure 4.4 The effect of UV radiation (254 nm) on the activity of pure PAM, incubated with 1 mM of α-phenylalanine at room temperature for 1 h and 24 h respectively. There is a slight increase (0.1%) in activity under UV light illumination (A) than room temperature light (B). The samples exposed to light (120, 65 W light bulb) but covered in aluminum foil (C) and an uncovered (D) and incubated overnight showed no significant difference.

4.2.1.4 *Effect of sonication and light illumination on pure PAM*

The effect of sonication was investigated by running 4 parallel reactions one in which a purified PAM-substrate mixture was sonicated for 5 min (1 min pulse, 1 min intervals) in ice; the second sample was incubated at room temperature under total white light illumination; the third sample was covered in aluminum foil and incubated at room temperature and the fourth sample was

incubated in ice for 10 min. The control sample kept in ice for 10 min had no activity. The sonicated sample had 4 % activity and the two samples kept at room temperature under dark and light illumination conditions respectively had 30 % activity (Figure 4.5).
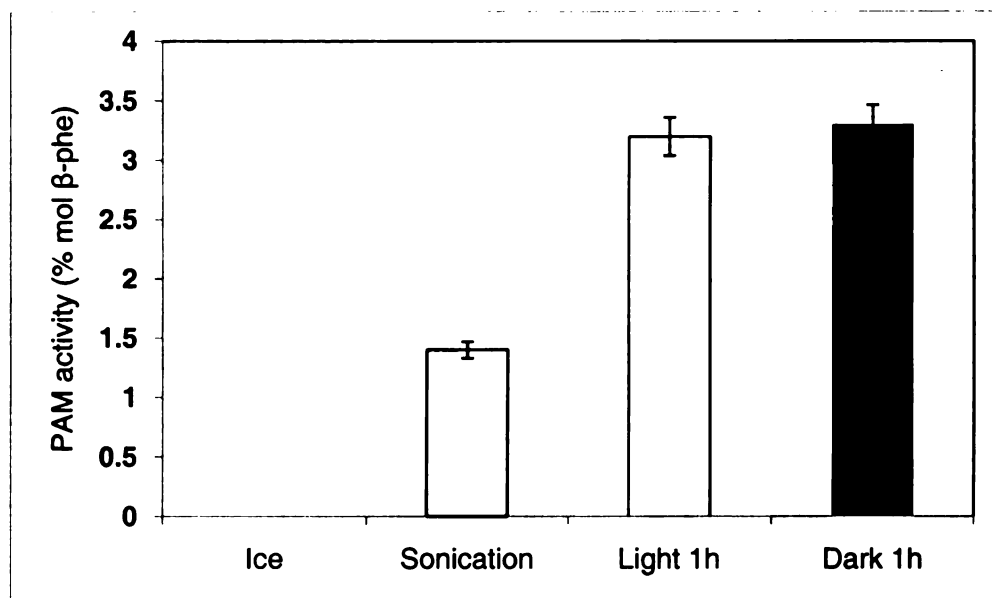
Figure 4.5 The effect of sonication on the activity of pure PAM. Samples kept in ice (ICE) showed no activity. Samples sonicated for a total of 5 minutes had 1.4 % mol conversion. Control samples incubated for 1 hour at 31 °C under light illumination and dark/covered had about 3.2 % mol conversion.

4.2.1.4 *Effect of pre-sonication on the activity of pure PAM*

The cell pellets lysed by sonication did not show any difference in activity between light illuminated and dark/covered samples (Figure 4.6). Sonication seems to allow the covered samples to 'catch up' with that exposed to light. Its either the sonication increases the rate of reaction by improved intermolecular collisions or there is an increase in temperature which accelerate the reaction.

Sonication could also be allowing the refolding of the protein and maybe able to form the more active form of the enzyme possibly via additional MIO formation. In order to verify this phenomenon pure PAM was sonicated first before incubating with substrate. If sonication increases amount of active enzyme then an unsonicated sample will have less activity. The results in Figure 4.6, shows a slight increase in PAM activity in the sonicated sample.
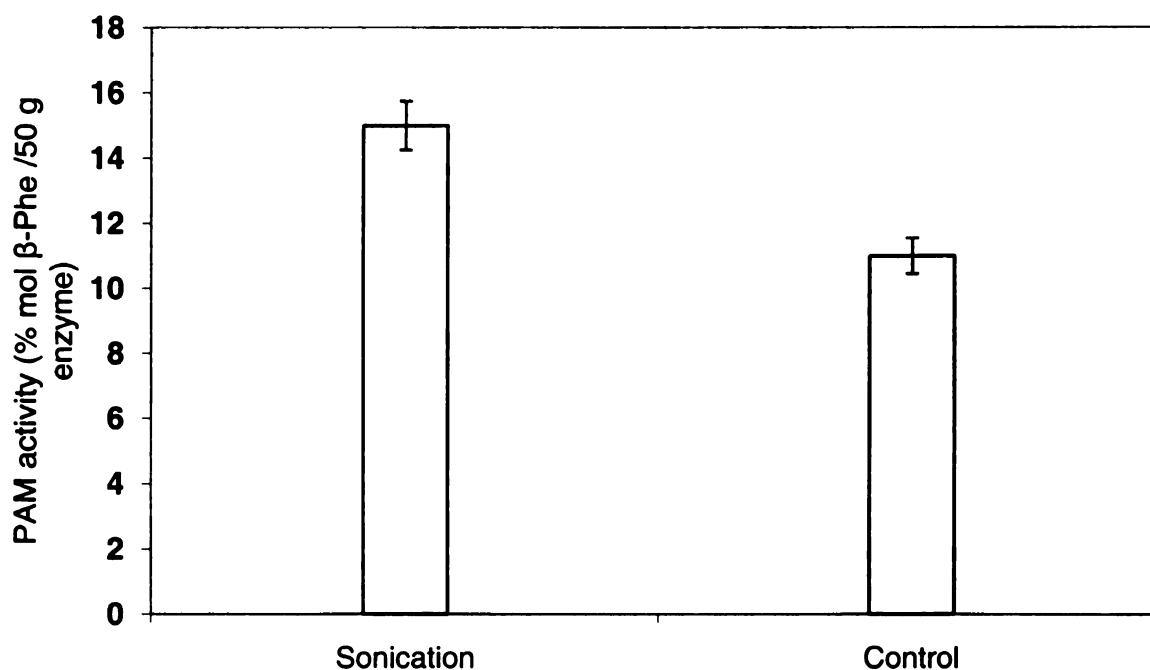
Figure 4.6: Shows the effects of sonication on PAM activity. PAM was first sonicated for 5 min before addition of substrate and incubation for 1 hour. The control was incubated for the same time and temperature and time without sonication.

4.2.1.6 Time course assay

Time course assay shows a time dependent variation of PAM activity which peaks between 6 to 8 hours after IPTG induction at 25 °C (Figure 4.7).
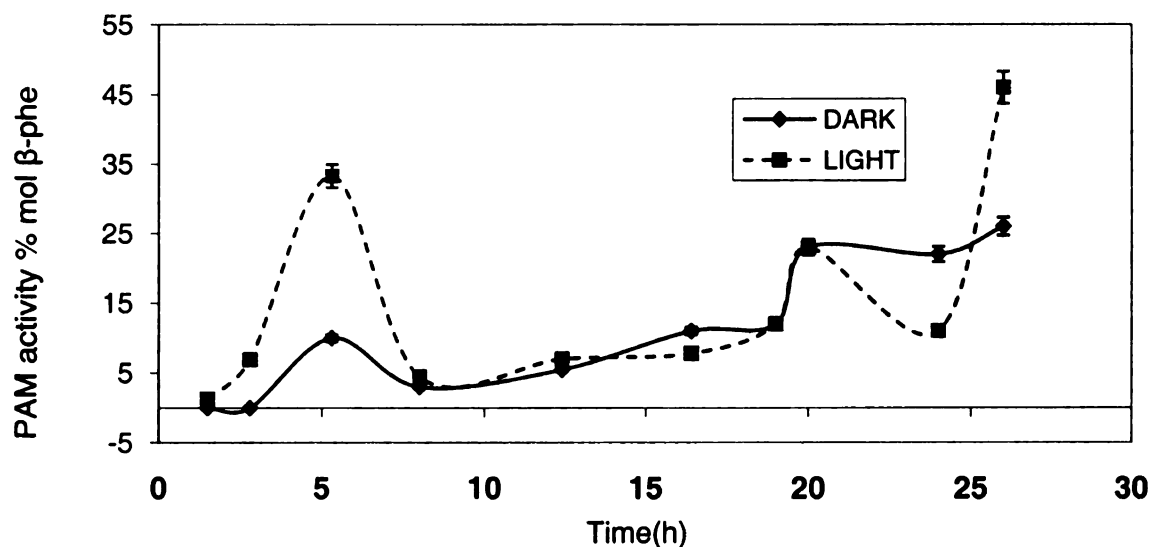
Figure 4.7 Shows the averaged time course assay trend of the variation of PAM activity under light illumination (square) and non-illumination (rhombic).

4.2.1.7 Monitoring of E. coli growth illuminated with light filtered from red and/or IR radiation

The growth of *E.coli* was monitored over an 18 hour period by measuring the cell density at a wavelength of 600 nm. The uncovered sample exposed to total white light appeared to reach the saturation phase earlier than the covered cultures or where a portion of the spectrum was cut off (Figure 4.8).
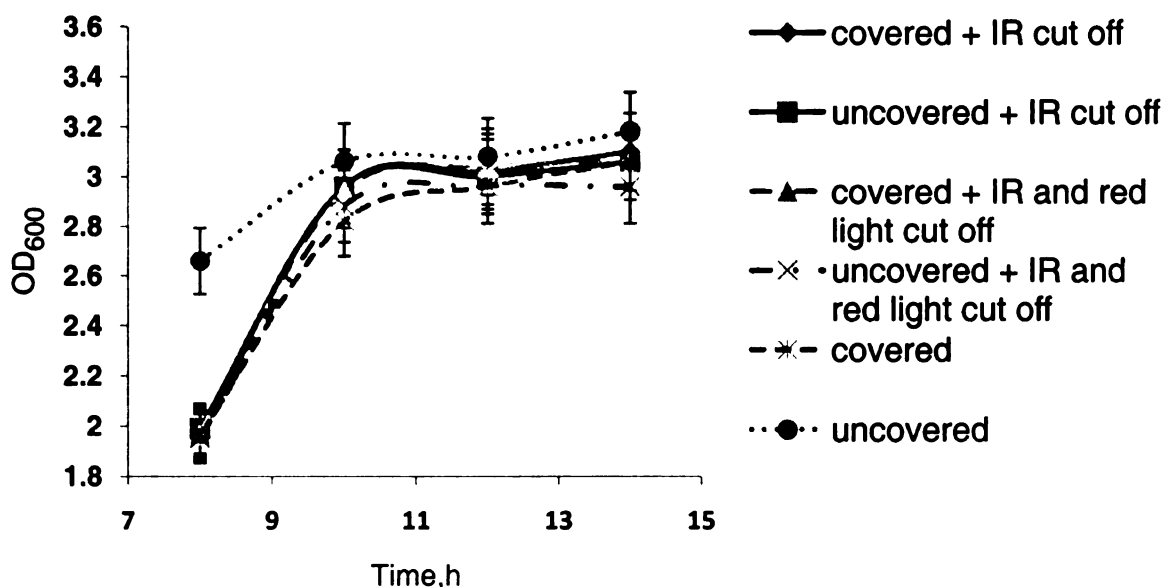
Figure 4.8 Monitoring the growth of *E.coli* cells transformed with the pam gene under various light conditions. The cultures illuminated with total white light without any filters had higher OD_{600} (•) before the saturation phase. The covered cultures and those exposed to light in which the red and/or IR radiation had been cut off showed reduced growth during the log phase.

4.2.1.7.2 *Effect of Different Types of Radiation on the Activity of Recombinant PAM Grown in E. Coli.*

A comparative study of the effects of red, infrared and visible light on the activity of PAM in *E. coli* was conducted by having; 1) a set-up in which red and infrared radiation had been eliminated, 2) only the infrared radiation was used to illuminate the *E.coli*, and 3) total white light (+ IR) was used to illuminate the samples. Each set-up was run parallel to *E. coli* cultures which were covered in aluminum.
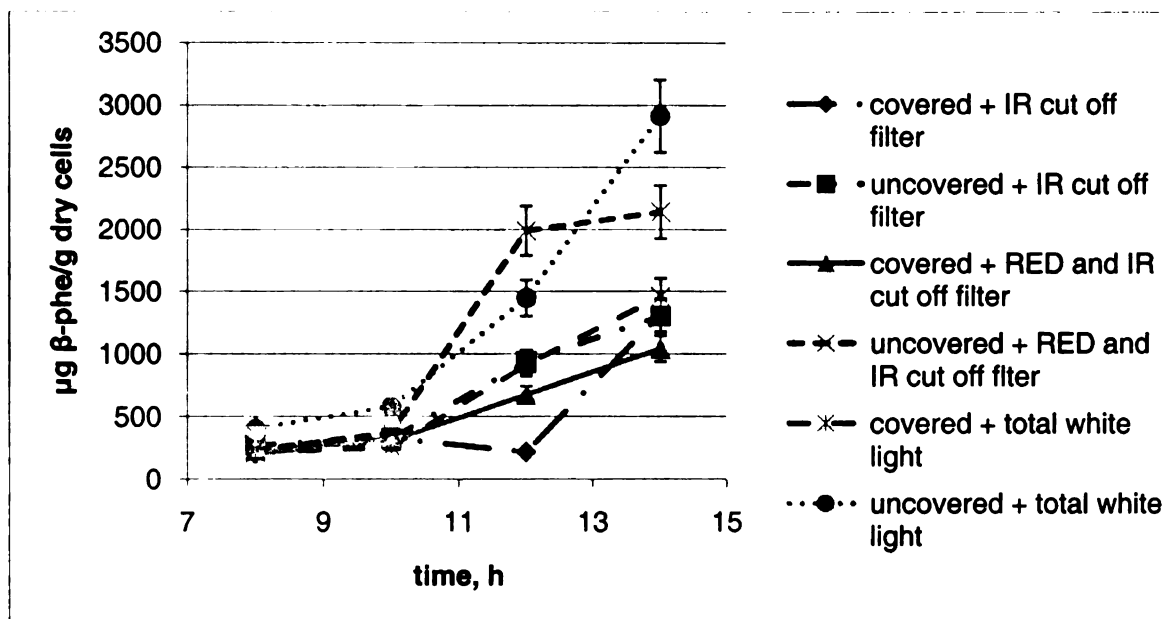
Figure 4.9 Comparative assays to study the effects of red light, infrared and visible radiation on the activity of PAM expressed in *E. coli*. All the uncovered samples had higher activity than the covered ones, with the uncovered and unfiltered giving the highest values.

4.2.1.8 *Identifying phosphorylation sites in PAM*

Peptide sequencing showed less than 12% probability of phosphorylation. Phosphorylation sites are usually on serine residues. The trypsin digested PAM was assayed by LC/MS/MS and the peaks searched against all bacterial and green plant protein sequences and confirmed the presence of phenylalanine aminomutase from *T. Canadensis*. The Mascott output analyzed by protein computer algorithm at 95% probability did not show any phosphorylation. Only two sites were identified but the probability was below 12% for both of them.

4.2.2 DISCUSSION

The exposure of *E. coli* transformed with the *pam* gene plasmid to continuous light produced the mutase with more than 3 fold increase in activity compared to the dark (Figure 4.2). The exposure of light to purified PAM does not increase activity significantly compared to samples kept in the dark (Figure 4.4). The observed increase in activity of PAM expressed in *E. coli* could be due to several possible phenomenon ranging from the perturbation of the bacterial metabolism to the production of more active enzyme possibly influenced by oxidative phosphorylation and/or increased MIO formation. *E. coli* metabolic rate has been observed to be increased by light illumination particularly visible, IR and red light through the increased production of DNA and ATP resulting from the retrograde process in which the mitochondria are bio-stimulated. The photo-stimulation causes increase in cell proliferation and upregulation of genes and hence heightens the synthesis of both non-recombinant and recombinant proteins. Although we could not quantitatively measure the amount of proteins produced under different light conditions the cell density offers an approximation of the cellular composition and indication of increased metabolic rate. The cell density measurements shows that light illumination seem to accelerate the rate at which *E. coli* reaches the saturation phase (Figure 4.8]. The observed difference in cell density between illuminated and non-illuminated cells does not correspond to the difference in the reactivity of the enzyme (PAM), which suggests that the mechanism of the increased activity under light could not be related to cell growth and may be specific to PAM as an enzyme observed with

187

homologous enzymes such as phenylalanine and histidine ammonia lyases which have been demonstrated to be activated by light in plants.[132-173] These enzymes have a characteristic MIO cofactor which also is also present in phenylalanine aminomutase (PAM). It appears like the increase in PAM activity could be *de novo* and reaches a maximum limit before it levels off or decreasing (Figure 4.7), similar to observations made on PAL. The regulation of PAM by light likely occurs *in vivo* suggesting the involvement of cellular transformation either through phosphorylation, synthesis of higher amounts of the MIO and possibly the decrease in the *trans*-cinnamic acid flux attributed to its photochemical conversion to its *cis*-isomer. The lack of response of pure PAM suggests the regulatory factors which increase its activity are *de novo*. The expression of PAM based on SDS-PAGE with Commassie blue staining did not show any significant difference between light and dark samples.

Effect of phosphorylation

Phosphorylation and de-phosphorylation have been implicated in stimulating PAL expression and activity in tomato seedlings and Parsley cell cultures. Similar mechanism could be happening to PAM, regulated through the mitochondrial photoactivation and the effect on the respiratory chain. However no phosphorylation could be confirmed in our study following trypsin digestion and LC/MS/MS analysis. The involvement of kinases in PAL activation has not been conclusive due to the different iso-forms of PAL (PAL I, II and III). If phosphorylation decreases PAL activity, then de-phosphorylation of pure PAM

should reverse the loss of activity. There is a likely would that the formation of the MIO could be related to phosphorylation since phosphorylation requires serine or threonine and a serine is involved in the formation of the MIO. Once the protein is phosphorylated no MIO could be formed, since phosphorylation will block MIO formation. De-phosphorylation will free up the serine for MIO formation hence increased activity. However LC/MS/MS results have shown no phosphorylation on the serine making up the ASG triad which makes the MIO. The evidence of PALII phosphorylation could not be proved by immuno-assay techniques. Further studies need to be done to confirm phosphorylation in PAM, by both immunoassay and mass spectrometry.

MIO formation

The mechanism by which the MIO is auto-catalytically formed in PAL or PAM is not yet understood, but similar synthetic process has been observed in the green fluorescent protein (GFP) found in *Aequorea victoria* bacteria in which serine, tyrosine and glycine cyclize followed with an oxidative process. Further investigation need to be carried out to verify whether there is an increased, in MIO formation under light conditions versus dark conditions. Mass spectrometry experiments with TAL have shown that, not all enzyme molecules carry the MIO motif. In fact as much as over 90% of TAL could be in the unmodified form. Our LC/MS/MS results did not confirm the presence of the MIO moiety in PAM probably due to its low concentration, yet the ASG triad was abundant. There is

need to quantitatively compare the amount of MIO synthesized under light illumination and non-illumination conditions.

The trans-cinnamic Feedback mechanism

Another perspective to the increase in activity under light illumination conditions is the perceived feedback mechanism in which trans-cinnamic acid is isomerized to cis-cinnamic acid (Figure 4.10), a reaction that is accelerated by light.[174] More trans-cinnamic would have to be made thus up regulating the phenylpropanoid pathway. Alternatively the trans-cinnamic acid formed from the heterologously expressed PAM reaction may be pertubing the bacterial metabolism by increasing the activity of the enzymes downstream of the cinnamic acid pathway (Figure 4.2).
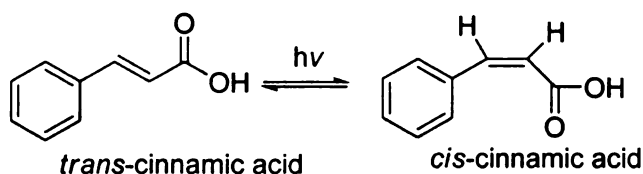
Figure 4.10 The conversion of trans-cinnamic acid to cis-cinnamic acid under ultraviolet light.

PAM expression could be regulated by trans-CA conversion to cis-CA and hence change the ratio of α to β-phenylalanine in the cell. Trans-cinnamic acid has been observed to inhibit PAL at pH ranging from 8.3 to 9.3 which falls within the optimal pH for PAM (Chapter 2). NMR kinetic studies have shown that the conversion of β-phenylalanine to trans-cinnamic acid is much faster than α-phenylalanine to the same product (Chapter 5). The depletion of t-CA would off-

190

set the equilibrium between α-phenylalanine, *trans*-cinnamic and β-phenylalanine is shown below (Figure 4.11), resulting in less β-product being synthesized which is contrary to our findings, thus ruling out the t-CA flux theory.
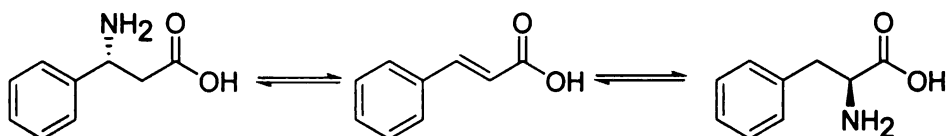
Figure 4.11 The equilibrium between β-phenylalanine, trans-cinnamic and α-phenylalanine

Effect of sonication and heat on PAM activity

Sonication increases the activity of PAM both *in vivo* and *in vitro* (Figure 4.5 and 4.6). The mechanism may not be clear but its most likely through thermal activation and increased vibrational motions. However an interesting phenomenon is the increased activity of pre-sonicated PAM (Figure 4.6). Perhaps sonication causes the re-folding of the enzyme into an active form or speculatively may form more of the catalytic moiety (MIO).

4.4 CONCLUSION

The presence of light during *de novo* synthesis of PAM regulates its expression and activity in a fluctuative manner in which activity increases during the initial growth phase and decreases at later stages. It's not clear how the regulation happens but it's likely that light affects the synthesis of the catalytic moiety MIO which is directly linked to the mechanism of PAM and similar enzymes. The perceived light illumination regulation will open up an opportunity to attenuate MIO based enzymes expression and activity. Increasing the activity of enzymes will overcome solubility challenges encountered during protein expression and purification. There is still remaining a possibilty that light could be influencing the protein expression in *E. coli* by tweaking the redox potential of the cell resulting in increased metabolic activity.

Further investigation need to be carried to confirm the relative amounts of MIO formed under light illumination and non-illumination conditions.

4.5 MATERIALS AND METHODS

4.5.1 *Instruments and Reagents*

All reagents were purchased Sigma Aldrich - unless otherwise noted and used without further purification, except for 3'-methylphenylalanine which was purchased from Peptech (Burlington, USA), 4'-nitrocinnamic acid from Fluka (Steinheim, Germany), Buffers P1, P2 and N3 were sourced from the QIAprep® Spin Miniprep Kit-250 (Qiagen, Maryland, USA). IR and red light Cut-off filters (50 mm x 50 mm x 3 mm) were purchased from CV Melles Griot (Rochester, USA). The light emission wavelength spectrum was measured on an Ocean Optics instrument; model USB 2000+ (Dunedin, Florida). Radiant power was measured with a Nova II instrument from Ophir (Jerusalem, Israel).

4.5.2 EXPERIMENTAL PROCEDURES

4.5.2.1 *General assay of amino acids in cell cultures*

At each sampling time point, the cell cultures were harvested and centrifuged at 4,500 g for 20 min at 4 °C. The supernatant was basified to pH 10 (3 M NaOH), acetic anhydride (500 μL) was added to each sample, and the reaction mixed for 10 min at room temperature (25 °C). The pH was decreased to 2 (3 M HCl) and the N-acetylated amino acid was extracted with ethyl acetate (2 x 3 mL). The ethyl acetate was evaporated, and the residue was resuspended in 100 μL methanol and trimethylsilyl diazomethane solution in diethyl ether was added until the yellow color of diazomethane persisted. The solvent was evaporated, and the residue re-dissolved in ethyl acetate (250 μL) and analyzed by gas chromatography (model 6890N, Agilent, Palo Alto, CA) coupled to a mass

193

selective detector (model 5973 *inert*[®], Agilent) equipped with a 5HS GC column (0.25-mm inner diameter × 30 m, 0.25-µm film thickness) mounted in the GC oven. The MS conditions were set with an ion scan mode from 100 – 300 atomic mass units and the ionization voltage was set to 70 eV. The GC conditions were as follows: column temperature was programmed from 70 °C (3 min hold) to 320 °C at 10 °C /min and then a 3-min hold at 320 °C, splitless injection was selected, and helium was used as the carrier gas at a flow rate of 1.2 mL/min.

4.5.2.2 *Over Expressing PAM under continuous white light illumination conditions*

E. *coli* BL21CodonPlus (DE3-RIPL) colonies transformed with the *pam* gene sub-cloned into pET14b vector were used to inoculate 5 ml of Luria Bertani (LB) media containing 100 µg/µL of ampicillin and 50 µg/µL of chloromphenicol antibiotics. The tubes were wrapped in aluminum foil to block light and incubated at 37 °C overnight. The 5 mL cultures were transferred to a 2.8 L flask containing 1 L LB media and covered with aluminum foil and incubated at 37 °C until OD_{600} was about 0.6. The 1L culture was induced with 1 mM isopropyl-D-thiogalactopyranoside and divided into two, one of the flasks covered in aluminum foil, and incubated at 16 °C or 25 °C with light illumination from a 65 W, 120V bulb (Maximum overall length, 770 lumens, 100 CRI, Spot-Gro Sylvania, light intensity of 0.14 W/cm^2) for 18 h. The cell cultures were divided into 50 mL portions and centrifuged at 4,500 × g for 30 min. The supernatant was discarded and the cell pellet treated as above.

194

4.5.2.3 Monitoring of trans-cinnamic acid

The cell cultures were centrifuged as above except that the pH was reduced to 2 before extracting with EtOAc. The organic layer was dried and the residue dissolved in methanol before adding diazomethane solution and reacted for 30 min. The solvent was evaporated in a speed *vacuo* and the residue resuspended in EtOAc and analyzed by GC/MS.

4.5.2.4 Purification of PAM

E.coli BL21 Codon plus (DE3-RIPL) cells were grown in 1 liter Miller LB medium supplemented with ampicillin (100 µg/µL) and chloromphenicol (50 µg/µL) at 37 °C until OD_{600} of about 0.6 and induced with 1 mM IPTG. The temperature was reduced to 16 °C or 25 °C and incubation continued for 16 hours or longer. The culture was centrifuged at 7,500 x g for 20 min at 4 °C and supernatant discarded. The pellet was resuspended in lysis buffer (50 mM NaH_2PO_4 pH 8.0, 300 mM NaCl, 10 mM imidazole, 2 tablets (*Complete*, Roche, German), protease inhibitor and 10 mg lysozyme, incubated on ice for 30 min and then sonicated on ice at 1 minute pulses for 5 minutes. The lysate was centrifuged at 15,000 rpm for 20 min at 4 °C and the pellet discarded, the semi-clear supernatant was further clarified at 45,000 rpm for 2 h, the pellet was discarded and the supernatant processed as below. The cleared lysate was loaded onto a pre-equilibrated (50 mM NaH_2PO_4 pH 8.0, 300 mM NaCl, 20 mM imidazole) Ni-NTA column and mixed gently at 4 °C for 5 min and left to settle. The flow-through was drained out and the column washed with 10 times column

volume of wash buffer consisting of 50 mM NaH_2PO_4, 300 mM NaCl, 20 mM imidazole, pH 8.0. The PAM was eluted with elution buffer (50 mM, NaH_2PO_4, 300 mM NaCl, 250 mM imidazole, pH 8.0) and the fractions were assayed for PAM using SDS-PAGE with Coommassie Blue staining as described elsewhere. The fractions containing pure PAM were pooled together and concentrated by ultra filtration through an Amicon 50 kDa membrane (Centriprep® Centrifugal Filter Units 50,000 MWCO, Millipore, Billerica, MA) at 4 000 x g to 1mL final volume. The PAM content was analyzed using the Bradford method (9) using BSA as the standard. The enzyme with a purity of over 95 % was kept at -80 °C (after adding 5% glycerol) until required.

4.5.2.5 *Investigation of the effect of light on the activity of pure PAM*

In order to investigate whether the activity of PAM was light dependent, purified PAM (50 µg) was incubated with 1 mM of α-phenylalanine under light illumination and non-illumination conditions, for a period of 1 hour or overnight. Another pair of samples were set up with one exposed to UV light (254 nm) and the other covered with aluminum or exposed to normal light. The amino acids were derivatized after the incubation period and analyzed as described above.

4.5.2.6 *Effect of sonication and light illumination on pure PAM*

The effect of sonication was investigated by running 4 parallel reactions; one in which a purified PAM-substrate mixture was sonicated for 5 min (1 min pulse, 1 min intervals) on ice and another was incubated at room temperature

196

under total white light illumination, another was covered in aluminum foil and incubated at room temperature and a control sample was incubated in ice for 10 min. The control sample kept on ice had no activity. The sonicated sample had 4% activity and the two samples kept at room temperature under dark and light conditions respectively had 30 % activity.

4.5.2.7 Effect of type of radiation on PAM activity in E. coli.

E. coli BL21CodonPlus (DE3) RIPL colonies transformed with the pam gene that was sub-cloned into vector pET14b[97] were used to inoculate four 5 ml of Luria Bertani broth (LB, 25 g/L) media containing 100 µg/µL of ampicillin and 50 µg/µL of chloromphenicol antibiotics. E. coli grown under non-illumination were inoculated in tubes wrapped in aluminum foil to block light and incubated at 37 °C overnight. The 5 mL cultures were mixed, and 5 mL aliquots were transferred into four 250 mL conical glass (Pyrex™) flasks containing 100 mL LB media; two of the flasks were completely covered with aluminum foil and the other two were left uncovered. The cultures were incubated at 37 °C until OD_{600} ~ 0.6. The incubation temperature was reduced to 18 °C and the cultures were induced with 1 mM isopropyl-β-D-thiogalactopyranoside (IPTG) to induce expression of the pam gene. Each flask was exposed to similar light source, at an intensity of 14 mW/cm^2 from a separate Spot-Gro Sylvania light bulb (maximum 770 lumens, 100 Color Rendering Index, 120 volts and 120 watts). The lights were positioned outside of the shaker (50 cm) cabinet with a double-walled glass door with 5 cm gap between panes. The distance between the lights

and the flasks was 137 cm. Two of the flasks (one covered with aluminum foil; the other uncovered) were shielded with IR IF cut-off filters placed 2 cm in front of the flasks and 135 cm away from the light bulbs. Under these conditions only visible light between 295 to 850 nm with the maximum intensity at 546 nm is irradiated. The intensity of light reaching the interior of the flasks was 27 mW/cm^2 with a power of 0.97 mW, and the wavelength ranged from 300 to 750 nm with the maximum intensity at 500 nm. The wavelengths range of light illuminating the flasks was scanned and the intensities at the measured wavelengths were compared to those provided by the manufacturer. Aliquots of cell cultures were collected in duplicates (2 x 10 mL) from each flask at 6, 10, 12, 14, 16 and 18 h after IPTG induction. To test the effects of blue light on the turnover of the PAM *in vivo*, the above experiment was repeated except cut-off filter that reflects IR and red light was used instead of only a filter that reflects IR.

4.5.2.7 *Identifying phosphorylation in PAM using* LC/MS/MS

Gel bands were subjected to in-gel tryptic digestion. The extracted peptides were then automatically injected by a Waters nano Acquity Sample Manager and loaded for 5 minutes onto a Waters Symmetry C18 peptide trap (5µm, 180µm x 20mm) at 4 µL/min in 5% Acetonitrile/0.1% Formic Acid. The bound peptides were then eluted onto a MICHROM Bioresources 0.1 x 150mm column packed with 3µ, 200A Magic C18AQ material over 35 minutes with a gradient of 2% B to 35% B in 21 min, 90% B from 21-24 min and back to constant 5% B at 24.1 min using a Waters nano Acquity UPLC (Buffer A = 99.9%

Water/0.1% Formic Acid, Buffer B = 99.9% Acetonitrile/0.1% Formic Acid) using an initial flow rate of 800 nL/min, ramping to 1200 nL/min at 24 min and back to 800 nL/min at 35 min. Eluted peptides were sprayed into a Thermo Fisher LTQ Linear Ion trap mass spectrometer outfitted with a MICHROM Bioresources ADVANCE nano spray source. The top five ions in each survey scan were then subjected to data-dependant zoom scans followed by low energy collision-induced dissociation (CID) and the resulting MS/MS spectra were converted to peak lists using BioWorks Browser v 3.3.1 (Thermo Fisher) using the default LTQ instrument parameters. Peak lists were searched against all bacterial and green plant protein sequences available in the NCBInr database, downloaded on 11-16-2008 from NCBI, using the Mascot searching algorithm, v2.2. The Mascot output was then analyzed using Scaffold to probabilistically validate protein identifications using the ProteinProphet computer algorithm. Assignments validated above the Scaffold 95% confidence filter were considered true. Mascot parameters for all databases were as follows: - allow up to 2 missed tryptic sites; fixed modification of Carbamidomethyl Cysteine; - variable modification of Oxidation of Methionine, Phosphorylation of Serine and Threonine; - peptide tolerance of +/- 200ppm, - MS/MS tolerance of 0.8 Da; - peptide charge state limited to +2/+3.

4.6 REFERENCES

1. Karu, T., Primary and secondary mechanisms of action of visible to near-IR radiation on cells. *J. Photochem. Photobiol. B-Biology* **1999**, *49*, (1), 1-17.

2. Kanazawa, A.; Kramer, D. M., In vivo modulation of nonphotochemical exciton quenching (NPQ) by regulation of the chloroplast ATP synthase. *Proc. Nat. Acad. Sci. USA* **2002**, *99*, (20), 12789-12794.

3. Kato, M.; Shinzawa, K.; Yoshikawa, S., Cytochrome-Oxidase Is a Possible Photoreceptor in Mitochondria. *Photobiochem. Photobiophys.* **1981**, *2*, (4-5), 263-269.

4. Passarella, S.; Casamassima, E.; Molinari, S.; Pastore, D.; Quagliariello, E.; Catalano, I. M.; Cingolani, A., Increase of Proton Electrochemical Potential and Atp Synthesis in Rat-Liver Mitochondria Irradiated Invitro by Helium-Neon Laser. *Febs Lett.* **1984**, *175*, (1), 95-99.

5. Gordon, S. A.; Surrey, K., Red and Far-Red Action on Oxidative Phosphorylation. *Radiation Res.* **1960**, *12*, (4), 325-339.

6. Passarella, S.; Perlino, E.; Quagliariello, E.; Baldassarre, L.; Catalano, I. M.; Cingolani, A., Evidence of Changes, Induced by Hene Laser Irradiation, in the Optical and Biochemical-Properties of Rat-Liver Mitochondria. *Bioelectrochem. Bioenerget.* **1983**, *10*, (2-3), 185-198.

7. Mailer, K., Superoxide Radical as Electron-Donor for Oxidative-Phosphorylation of Adp. *Biochemical and Biophys. Res. Commun.* **1990**, *170*, (1), 59-64.

8. Murphy, J. G.; Smith, T. W.; Marsh, J. D., Mechanisms of Reoxygenation-Induced Calcium Overload in Cultured Chick-Embryo Heart-Cells. *American J. Physiol.* **1988**, *254*, (6), H1133-H1141.

9. Shibanuma, M.; Kuroki, T.; Nose, K., Superoxide as a Signal for Increase in Intracellular Ph. *J. Cellular Physiol.* **1988**, *136*, (2), 379-383.

10. Karu, T. I.; Pyatibrat, L. V.; Moskvin, S. V.; Andreev, S.; Letokhov, V. S., Elementary processes in cells after light absorption do not depend on the degree of polarization: Implications for the mechanisms of laser phototherapy. *Photomed. Laser Surg.* **2008**, *26*, (2), 77-82.

11. Karu, T. I.; Pyatibrat, L. V.; Kolyakov, S. F.; Afanasyeva, N. I., Absorption measurements of a cell monolayer relevant to phototherapy: Reduction of

cytochrome c oxidase under near IR radiation. *J. Photochem. Photobiol. B-Biology* **2005**, *81*, (2), 98-106.

12. Karu, T. I.; Pyatibrat, L. V.; Afanasyeva, N. I., Cellular effects of low power laser therapy can be mediated by nitric oxide. *Lasers in Surg. Med.* **2005**, *36*, (4), 307-314.

13. Karu, T. I.; Pyatibrat, L. V.; Kalendo, G. S., Photobiological modulation of cell attachment via cytochrome c oxidase. *Photochemical & Photobiol. Sci.* **2004**, *3*, (2), 211-216.

14. Karu, T. I.; Pyatibrat, L. V.; Afanasyeva, N. I., A novel mitochondrial signaling pathway activated by visible-to-near infrared radiation. *Photochemistry and Photobiology* **2004**, *80*, (2), 366-372.

15. Karu, T. I.; Pyatibrat, L. V.; Ryabykh, T. P., Melatonin modulates the action of near infrared radiation on cell adhesion. *J. Pineal Res.* **2003**, *34*, (3), 167-172.

16. Karu, T. I.; Pyatibrat, L. V.; Kalendo, G. S., Donors of NO and pulsed radiation at lambda=820 nm exert effects on cell attachment to extracellular matrices. *Toxicology Lett.* **2001**, *121*, (1), 57-61.

17. Karu, T. I.; Pyatibrat, L. V.; Kalendo, G. S., Thiol reactive agents eliminate stimulation of cell attachment to extracellular matrices induced by irradiation at lambda=820 nm: Possible involvement of cellular redox status into low power laser effects. *Laser Therapy* **1999**, *11*, (4), 177-187.

18. Karu, T.; Tiphlova, O.; Esenaliev, R.; Letokhov, V., 2 Different Mechanisms of Low-Intensity Laser Photobiological Effects on Escherichia-Coli. *J. Photochem. Photobiol. B-Biology* **1994**, *24*, (3), 155-161.

19. Trushin, M. V., Light-mediated "conversation" among microorganisms. *Microbiol. Res.* **2004**, *159*, (1), 1-10.

20. Trushin, M. V., Culture-to-culture physical interactions causes the alteration in red and infrared light stimulation of Escherichia coli growth rate. *J. Microbiol. Immun. Infect.* **2003**, *36*, (2), 149-152.

21. Trushin, M. V., Studies on distant regulation of bacterial growth and light emission. *Microbiology-Sgm* **2003**, *149*, 363-368.

22. Trushin, M. V., The effect of red and infrared light on the growth of Escherichia coli and the production of the recombinant protein barstar. *Microbio.* **2002**, *71*, (4), 383-385.

23. Trushin, M. V.; Yagodina, L. O.; Chernov, V. M., The modification of biostimulating effect of IR laser radiation by genetic transformation. *Laser Physics* **2002**, 12, (4), 656-658.

24. Arigoni, D.; Eisenreich, W.; Latzel, C.; Sagner, S.; Radykewicz, T.; Zenk, M. H.; Bacher, A., Dimethylallyl pyrophosphate is not the committed precursor of isopentenyl pyrophosphate during terpenoid biosynthesis from 1-deoxyxylulose in higher plants. *Proc. Nat. Acad. Sci. the USA* **1999**, *96*, (4), 1309-1314.

25. Ascensao, L.; Figueiredo, A. C.; Barroso, J. G.; Pedro, L. G.; Schripsema, J.; Deans, S. G.; Scheffer, J. J. C., *Plectranthus madagascariensis*: morphology of the glandular trichomes, essential oil composition, and its biological activity. *Int. J. Plant Sc.* **1998**, *159*, (1), 31-38.

26. Aubourg, S.; Lecharny, A.; Bohlmann, J., Genomic analysis of the terpenoid synthase (AtTPS) gene family of *Arabidopsis thaliana*. *Mol. Genetics Genom.* **2002**, *267*, (6), 730-745.

27. Betz, B.; Schafer, E.; Hahlbrock, K., Rates of Synthesis and Degradation of Light-Induced Phenylalanine Ammonia-Lyase in Cell-Suspension Cultures of Parsley. *Hoppe-Seylers Zeitschrift Fur Physiologische Chemie* **1977**, *358*, (10), 1179-1179.

28. Betz, B.; Schafer, E.; Hahlbrock, K., Light-Induced Phenylalanine Ammonia-Lyase in Cell-Suspension Cultures of Petroselinum-Hortense - Quantitative Comparison of Rates of Synthesis and Degradation. *Arch. Biochem. Biophys.* **1978**, *190*, (1), 126-135.

29. Bolwell, G. P.; Bozak, K.; Zimmerlin, A., Review article number 96: Plant cytochrome P450. *Phytochemistry* **1994**, *37*, (6), 1491-506.

30. Braun, W. E., Autosomal dominant polycystic kidney disease: Emerging concepts of pathogenesis and new treatments. *Cleveland Clinic J. Med.* **2009**, *76*, (2), 97-104.

31. Brincat, M. C.; Gibson, D. M.; Shuler, M. L., Alterations in Taxol Production in Plant Cell Culture via Manipulation of the Phenylalanine Ammonia Lyase Pathway. *Biotechnol. Progr.* **2002**, *18*, (6), 1149-1156.

32. Broun, P., Transcription factors as tools for metabolic engineering in plants. *Curr. Opin. Plant Biol.* **2004**, *7*, (2), 202-9.

33. Bruns, B.; Hahlbrock, K.; Schafer, E., Fluence Dependence of the Ultraviolet-Light-Induced Accumulation of Chalcone Synthase Messenger-

Rna and Effects of Blue and Far-Red Light in Cultured Parsley Cells. *Planta* **1986**, *169*, (3), 393-398.

34. Calixto, J. B.; Otuki, M. F.; Santos, A. R. S., Anti-inflammatory compounds of plant origin. Part I. Action on arachidonic acid pathway, nitric oxide and nuclear factor kB (NF-kB). *Planta Medica* **2003**, *69*, (11), 973-983.

35. Cane, D. E.; Watt, R. M., Expression and mechanistic analysis of a germacradienol synthase from streptomyces coelicolor implicated in geosmin biosynthesis. *Proc. Nat. Acad. Sci. U.S. A.* **2003**, *100*, (4), 1547-1551.

36. Cleland, G. H.; Niemann, C., Some observations on the Dakin-West reaction. *J. Am. Chem. Soc* **1949**, *71*, 841-3.

37. Cochrane, F. C.; Davin, L. B.; Lewis, N. G., The Arabidopsis phenylalanine ammonia lyase gene family: kinetic characterization of the four PAL isoforms. *Phytochemistry* **2004**, *65*, (11), 1557-1564.

38. Croteau, R., The Discovery of Terpenes. In *Discoveries in Plant Biology*, ed.; Kung, S.-D.; Yang, S.-F., World Scientific Publ.: Hong Kong, **1998**; *1*, 329-343.

39. Dangl, J. L.; Hauffe, K. D.; Lipphardt, S.; Hahlbrock, K.; Scheel, D., Parsley Protoplasts Retain Differential Responsiveness to Uv-Light and Fungal Elicitor. *Embo J.* **1987**, *6*, (9), 2551-2556.

40. Ebermann, R.; Alth, G.; Kreitner, M.; Kubin, A., Natural products derived from plants as potential drugs for the photodynamic destruction of tumor cells. *J. Photochem. Photobiol., B: Biol.* **1996**, *36*, (2), 95-97.

41. Fernandez, J.; Gharahdaghi, F.; Mische, S. M., Routine identification of proteins from sodium dodecyl sulfate-polyacrylamide gel electrophoresis (SDS-PAGE) gels or polyvinyl difluoride membranes using matrix assisted laser desorption/ionization- time of flight-mass spectrometry (MALDI-TOF-MS). *Electrophoresis* **1998**, *19*, (6), 1036-1045.

42. Fernie, A. R., Metabolome characterization in plant system analysis. *Functional Plant Biol.* **2003**, *30*, (1), 111-120.

43. Fisher, A. J.; Baker, B. M.; Greenberg, J. P.; Fall, R., Enzymatic Synthesis of Methylbutenol from Dimethylallyl Diphosphate in Needles of *Pinus sabiniana*. *Arch. Biochem. Biophys.* **2000**, *383*, (1), 128-134.

44. Fradin, M. S.; Day, J. F., Comparative efficacy of insect repellents against mosquito bites. *New England J. Med.* **2002**, *347*, (1), 13-18.

45. Frohnmeyer, H.; Hahlbrock, K.; Schafer, E., A Light-Responsive in-Vitro Transcription System from Evacuolated Parsley Protoplasts. *Plant J.* **1994**, *5*, (3), 437-449.

46. Geissler, J. F.; Harwood, C. S.; Gibson, J., Purification and properties of benzoate-coenzyme A ligase, a Rhodopseudomonas palustris enzyme involved in the anaerobic degradation of benzoate. *J. Bacteriol.* **1988**, *170*, (4), 1709-1714.

47. Goldring, W. P. D.; Pattenden, G., The Phomactins. A novel group of terpenoid platelet activating factor antagonists related biogenetically to the taxanes. *Acc. Chem. Res.* **2006**, *39*, (5), 354-361.

48. Gomis, J. M.; Santolini, J.; Cavelier, F.; Verducci, J.; Pinet, E.; Andre, F.; Noel, J. P., Synthesis of a [14C]-labeled photoactivatable cyclic tetrapeptide: [carbonyl-14C]-4-benzoylbenzoyl MeSer1-tentoxin. *J. Labelled Compounds & Radiopharmaceuticals* **2000**, *43*, (4), 323-330.

49. Graf, E.; Boeddeker, H., The taxus alkaloids. III. The optical activity and configuration of the α-aminohydrocinnamic acids and their N-methyl derivatives. *Ann* **1958**, *613*, 111-20.

50. Grassmann, J.; Hippeli, S.; Elstner, E. F., Plant defense and its benefits for animals and medicine: Role of phenolics and terpenoids in avoiding oxygen stress. *Plant Physiol. Biochem. (Paris, France)* **2002**, *40*, (6-8), 471-478.

51. Guengerich, F. P.; Hosea, N. A.; Parikh, A.; Bell-Parikh, L. C.; Johnson, W. W.; Gillam, E. M. J.; Shimada, T., Twenty years of biochemistry of human P450S purification, expression, mechanism, and relevance to drugs. *Drug Metab. Dispos.* **1998**, *26*, (12), 1175-1178.

52. Hahlbroc.K; Wellmann, E., Light-Induced Flavone Biosynthesis and Activity of Phenylalanine Ammonia-Lyase and Udp-Apiose Synthetase in Cell Suspension Cultures of *Petroselinum-Hortense*. *Planta* **1970**, *94*, (3), 236-&.

53. Hahlbroc.K; Wellmann, E., Light-Independent Induction of Enzymes Related to Phenylpropanoid Metabolism in Cell Suspension Cultures from *Parsley*. *Biochimica Et Biophysica Acta* **1973**, *304*, (3), 702-706.

54. Hahlbrock, K.; Ragg, H., Light-Induced Changes of Enzyme-Activities in Parsley Cell-Suspension Cultures - Effects of Inhibitors of RNA and Protein-Synthesis. *Arch. Biochem. Biophys.* **1975,** *166,* (1), 41-46.

55. Hahlbrock, K.; Knobloch, K. H.; Kreuzaler, F.; Potts, J. R. M.; Wellmann, E., Coordinated Induction and Subsequent Activity Changes of 2 Groups of Metabolically Interrelated Enzymes - Light-Induced Synthesis of Flavonoid Glycosides in Cell-Suspension Cultures of *Petroselinum-Hortense. Eur. J. Biochem.* **1976,** *61,* (1), 199-206.

56. Hare, J. D., Seasonal variation in the leaf resin components of *Mimulus aurantiacus. Biochemical Systematics and Ecology* **2002,** *30,* (8), 709-720.

57. Hesketh, A. R.; Chandra, G.; Shaw, A. D.; Rowland, J. J.; Kell, D. B.; Bibb, M. J.; Chater, K. F., Primary and secondary metabolism, and post-translational protein modifications, as portrayed by proteomic analysis of *Streptomyces coelicolor. Mol. Microbio.* **2002,** *46,* (4), 917-932.

58. Ilag, L. L.; Kumar, A. M.; Soll, D., Light regulation of chlorophyll biosynthesis at the level of 5-aminolevulinate formation in *Arabidopsis. Plant Cell* **1994,** *6,* (2), 265-75.

59. Jordan, P. M., Highlights in haem biosynthesis. *Curr. Opin. Struct. Biol.* **1994,** *4,* (6), 902-11.

60. Keene, C. K.; Wagner, G. J., Direct demonstration of duvatrienediol biosynthesis in glandular heads of tobacco trichomes. *Plant Physiol.* **1985,** *79,* (4), 1026-32.

61. Kieffer, B. L.; Gaveriaux-Ruff, C., Exploring the opioid system by gene knockout. *Progress in Neurobiol.* **2002,** *66,* (5), 285-306.

62. Kim, J.; DellaPenna, D., Defining the primary route for lutein synthesis in plants: the role of Arabidopsis carotenoid β-ring hydroxylase CYP97A3. *Proc. Nat. Acad. Sci. USA* **2006,** *103,* (9), 3474-3479.

63. Laflamme, P.; St-Pierre, B.; De Luca, V., Molecular and Biochemical Analysis of a Madagascar Periwinkle Root-Specific Minovincinine-19-Hydroxy-O-Acetyltransferase. *Plant Physiol.* **2001,** *125,* (1), 189-198.

64. Lamparter, T.; Michael, N.; Mittmann, F.; Esteban, B., Phytochrome from *Agrobacterium tumefaciens* has unusual spectral properties and reveals an N-terminal chromophore attachment site. *Proc. Nat. Acad. Sc. USA* **2002,** *99,* (18), 11628-11633.

65. Leigh, W. J.; Srinivasan, R., Organic photochemistry with 6.7-eV photons. The divergent photobehavior of exo- and endo-7-methyl-2-norcarene. *J. Org. Chem.* **1983,** *48,* (22), 3970-9.

66. Liu, C.; Strobl, J. S.; Bane, S.; Schilling, J. K.; McCracken, M.; Chatterjee, S. K.; Rahim-Bata, R.; Kingston, D. G. I., Design, synthesis, and bioactivities of steroid-linked Taxol analogues as potential targeted drugs for prostate and breast cancer. *J. Nat. Prod.* **2004,** *67,* (2), 152-159.

67. Logemann, E.; Wu, S. C.; Schroder, J.; Schmelzer, E.; Somssich, I. E.; Hahlbrock, K., Gene activation by UV light, fungal elicitor or fungal infection in *Petroselinum crispum* is correlated with repression of cell cycle-related genes. *Plant Journal* **1995,** *8,* (6), 865-876.

68. Logemann, E.; Tavernaro, A.; Schulz, W. G.; Somssich, I. E.; Hahlbrock, K., UV light selectively coinduces supply pathways from primary metabolism and flavonoid secondary product formation in *parsley. Proc. Nat. Acad. Sci. USA* **2000,** *97,* (4), 1903-1907.

69. Lois, R.; Dietrich, A.; Hahlbrock, K.; Schulz, W., A phenylalanine ammonia-lyase gene from parsley: structure, regulation and identification of elicitor and light responsive cis-acting elements. *EMBO J.* **1989,** *8,* (6), 1641-1648.

70. Loschke, D. C.; Hadwiger, L. A.; Schroder, J.; Hahlbrock, K., Effects of Light and of Fusarium-Solani on Synthesis and Activity of Phenylalanine Ammonia-Lyase in Peas. *Plant Physiol.* **1981,** *68,* (3), 680-685.

71. Lozoya, E.; Hahlbrock, K.; Scheel, D., Biosynthesis of Flavonoids and Furanocoumarins in Parsley Cell Cultures after Simultaneous Treatment with Fungal Elicitor and Uv Light. *Planta Medica* **1990,** *56,* (6), 497.

72. Ma, Y.-Z.; Holt, N. E.; Li, X.-P.; Niyogi, K. K.; Fleming, G. R., Evidence for direct carotenoid involvement in the regulation of photosynthetic light harvesting. *Proc. Nat. Acad. Sc. U.S. A.* **2003,** *100,* (8), 4377-4382.

73. Allina, S. M.; Pri-Hadash, A.; Theilmann, D. A.; Ellis, B. E.; Douglas, C. J., 4-Coumarate:coenzyme A ligase in hybrid poplar. Properties of native enzymes, cDNA cloning, and analysis of recombinant enzymes. *Plant Physiol.* **1998,** *116,* (2), 743-754.

74. Berner, M.; Krug, D.; Bihlmaier, C.; Vente, A.; Mueller, R.; Bechthold, A., Genes and enzymes involved in caffeic acid biosynthesis in the actinomycete *Saccharothrix espanaensis. J. Bacteriol.* **2006,** *188,* (7), 2666-2673.

75. Croteau, R.; Kutchan, T. M.; Lewis, N. G., Natural products (secondary metabolites). *Biochem. Mol. Biol. Plants* **2000**, 1250-1318.

76. Croteau, R. B.; Walker, K. D.; Schoendorf, A.; Wildung, M. R. Cloning of transacylases of the paclitaxel biosynthetic pathway in *Taxus*. US 2003108891, 20020918., **2003**.

77. Cukovic, D.; Ehlting, J.; VanZiffle, J. A.; Douglas, C. J., Structure and evolution of 4-coumarate:coenzyme A ligase (4CL) gene families. *Biolog.Chem.* **2001,** *382*, (4), 645-654.

78. Dixon, R. A.; Paiva, N. L., Stress-induced phenylpropanoid metabolism. *Plant Cell* **1995,** *7*, (7), 1085-97.

79. Ehlting, J.; Shin, J. J. K.; Douglas, C. J., Identification of 4-coumarate:coenzyme A ligase (4CL) substrate recognition domains. *Plant Journal* **2001,** *27*, (5), 455-465.

80. Fleming, P. E.; Floss, H. G.; Haertel, M.; Knaggs, A. R.; Lansing, A.; Mocek, U.; Walker, K. D., Biosynthetic studies on taxol. *Pure Appl. Chem.* **1994,** 66, (10/11), 2045-8.

81. Galis, I.; Simek, P.; Narisawa, T.; Sasaki, M.; Horiguchi, T.; Fukuda, H.; Matsuoka, K., A novel R2R3 MYB transcription factor NtMYBJS1 is a methyl jasmonate-dependent regulator of phenylpropanoid-conjugate biosynthesis in tobacco. *Plant J.* **2006,** *46*, (4), 573-592.

82. Hahlbrock, K.; Scheel, D., Physiology and molecular biology of phenylpropanoid metabolism. *Ann. Rev. Plant Physiol. Plant Mol. Biol.* **1989,** *40*, 347-69.

83. Hanson, K. R.; Havir, E. A., An introduction to the enzymology of phenylpropanoid biosynthesis. *Biochemistry of plant phenolics.* **1979**, 91-137.

84. Hashimoto, M.; Hatanaka, Y.; Nabeta, K., Novel photoreactive cinnamic acid analogues to elucidate phenylalanine ammonia-lyase. *Bioorg. And Med. Chem. Lett.* **2000,** *10*, (21), 2481-2483.

85. Hashimoto, M.; Hatanaka, Y.; Nabeta, K., Novel photoreactive cinnamic acid analogues to elucidate phenylalanine ammonia-lyase. *Bioorg. Med. Chem. Lett.* **2000,** *10*, (21), 2481-2483.

86. Hoffmann, L.; Maury, S.; Martz, F.; Geoffroy, P.; Legrand, M., Purification, Cloning, and Properties of an Acyltransferase Controlling Shikimate and

Quinate Ester Intermediates in Phenylpropanoid Metabolism. *J. Biol. Chem.* **2003**, *278*, (1), 95-103.

87. Lee, S.; Suh, M.; S, K.; Kwon, J.; Kim, M.; Paek, K.; Choi, D.; Kim, B., Molecular cloning of a novel pathogen-inducible cDNA encoding a putative acyl-CoA synthetase from *Capsicum annuum* L. *Plant Mol. Biol.* **2001**, *46*, (6), 661-671.

88. Lehfeldt, C.; Shirley, A. M.; Meyer, K.; Ruegger, M. O.; Cusumano, J. C.; Viitanen, P. V.; Strack, D.; Chapple, C., Cloning of the SNG1 gene of *Arabidopsis* reveals a role for a serine carboxypeptidase-like protein as an acyltransferase in secondary metabolism. *Plant Cell* **2000**, *12*, (8), 1295-1306.

89. Moore, B. S.; Hertweck, C.; Hopke, J. N.; Izumikawa, M.; Kalaitzis, J. A.; Nilsen, G.; O'Hare, T.; Piel, J.; Shipley, P. R.; Xiang, L.; Austin, M. B.; Noel, J. P., Plant-like Biosynthetic Pathways in Bacteria: From Benzoic Acid to Chalcone. *J. Nat. Prod.* **2002**, ACS ASAP.

90. Ritter, H.; Schulz, G. E., Structural basis for the entrance into the phenylpropanoid metabolism catalyzed by phenylalanine ammonia-lyase. *Plant Cell* **2004**, *16*, (12), 3426-3436.

91. Shelton, D.; Leach, D.; Baverstock, P.; Henry, R., Isolation of genes involved in secondary metabolism from *Melaleuca alternifolia* (Cheel) using expressed sequence tags. *Plant Science (Shannon, Ireland)* **2002**, *162*, (1), 9-15.

92. Singh, K.; Kumar, S.; Rani, A.; Gulati, A.; Ahuja, P., Phenylalanine ammonia-lyase (PAL) and cinnamate 4-hydroxylase (C4H) and catechins (flavan-3-ols) accumulation in tea. *Functional & Integrative Genomics* **2009**, *9*, (1), 125-134.

93. Stoyanova, M.; Ivanov, P.; Stoyanov, I., Investigation of Certain Enzymes of Phenylpropanoid Biosynthesis with Different Brown Rust Resistance 2. Tyrosine Ammonia Lyase. *Fiziologiya na Rasteniyata (Sofia)* **1984**, 10, (3), 13-18.

94. Vom Endt, D.; Kijne, J. W.; Memelink, J., Transcription factors controlling plant secondary metabolism: What regulates the regulators? *Phytochemistry* **2002**, *61*, (2), 107-114.

95. Walker, K. The use of stereospecifically-labeled phenylpropanoid compounds to determine the steric course of key reaction steps in the biosynthesis of Taxol, hyoscyamine, and cycloheptyl fatty acids. Ph.D. Thesis, University of Washington, Seattle, WA, 1997.

96. Walker, K.; Fujisaki, S.; Long, R.; Croteau, R., Molecular cloning and heterologous expression of the C-13 phenylpropanoid side chain-CoA acyltransferase that functions in Taxol biosynthesis. *Proc. of the Nat. Acad. Sci. USA* **2002**, *99*, (20), 12715-12720.

97. Walker, K. D.; Klettke, K.; Akiyama, T.; Croteau, R., Cloning, heterologous expression, and characterization of a phenylalanine aminomutase involved in Taxol biosynthesis. *J. Bio. Chem.* **2004**, *279*, (52), 53947-53954.

98. Wanner, L. A.; Li, G.; Ware, D.; Somssich, I. E.; Davis, K. R., The phenylalanine ammonia-lyase gene family in *Arabidopsis thaliana*. *Plant Mol. Biol.* **1995**, *27*, (2), 327-38.

99. Wen, P. F.; Chen, J. Y.; Wan, S. B.; Kong, W. F.; Zhang, P.; Wang, W.; Zhan, J. C.; Pan, Q. H.; Huang, W. D., Salicylic acid activates phenylalanine ammonia-lyase in grape berry in response to high temperature stress. *Plant Growth Regulation* **2008**, *55*, (1), 1-10.

100. Ye, Z. H.; Zhong, R.; Morrison, W. H., III; Himmelsbach, D. S., Caffeoyl coenzyme A *O*-methyltransferase and lignin biosynthesis. *Phytochemistry* **2001**, *57*, (7), 1177-1185.

101. Merkle, T.; Frohnmeyer, H.; Schulze-Lefert, P.; Dangl, J. L.; Hahlbrock, K.; Schafer, E., Analysis of the Parsley Chalcone-Synthase Promoter in Response to Different Light Qualities. *Planta* **1994**, *193*, (2), 275-282.

102. Ohl, S.; Hahlbrock, K.; Schaefer, E., A Stable Blue-Light-Derived Signal Modulates Uv-Light-Induced Activation of the Chalcone-Synthase Gene in Cultured *Parsley* Cells. *Planta (Heidelberg)* **1989**, *95*, (3), 228-236.

103. Schroder, J.; Kreuzaler, F.; Hahlbrock, K., Regulation on Messenger-Rna Level of Light-Induced Enzyme-Activities in a Plant-Tissue. *Hoppe-Seylers Zeitschrift Fur Physiologische Chemie* **1977**, *358*, (10), 1278-1278.

104. Weisshaar, B.; Armstrong, G. A.; Block, A.; Silva, O. D. E.; Hahlbrock, K., Light-Inducible and Constitutively Expressed DNA-Binding Proteins Recognizing a Plant Promoter Element with Functional Relevance in Light Responsiveness. *Embo. J.* **1991**, *10*, (7), 1777-1786.

105. Zimmermann, A.; Hahlbrock, K., Light-Induced Changes of Enzyme-Activities in Parsley Cell-Suspension Cultures - Purification and Some Properties of Phenylalanine Ammonia-Lyase (Ec 4315). *Arch. Biochem. Biophys.* **1975**, *166*, (1), 54-62.

106. Textor, S.; Wendisch, V. F.; De Graaf, A. A.; Muller, U.; Linder, M. I.; Linder, D.; Buckel, W., Propionate oxidation in Escherichia coli: evidence for operation of a methylcitrate cycle in bacteria. *Arch. Microbiol.* **1997**, *168*, (5), 428-436.

107. Asano, Y.; Kato, Y.; Levy, C.; Baker, P.; Rice, D., Structure and function of amino acid ammonia-lyases. *Biocatal. Biotransformation* **2004**, *22*, (2), 133-138.

108. Baedeker, M.; Schulz, G. E., Autocatalytic peptide cyclization during chain folding of histidine ammonia-lyase. *Structure* **2002**, *10*, (1), 61-67.

109. Baedeker, M.; Schulz, G. E., Structures of two histidine ammonia-lyase modifications and implications for the catalytic mechanism. *Eur. J. of Biochem.* **2002**, *269*, (6), 1790-1797.

110. Calabrese, J. C.; Jordan, D. B.; Boodhoo, A.; Sariaslani, S.; Vannelli, T., Crystal structure of phenylalanine ammonia lyase: Multiple helix dipoles implicated in catalysis. *Biochemistry* **2004**, *43*, (36), 11403-11416.

111. Cheung, M. C.; Pantanowitz, L.; Dezube, B. J., AIDS-related malignancies: emerging challenges in the era of highly active antiretroviral therapy. *Oncologist* **2005**, *10*, (6), 412-426.

112. Christenson, S. D.; Liu, W.; Toney, M. D.; Shen, B., A novel 4-methylideneimidazole-5-one-containing tyrosine aminomutase in enediyne antitumor antibiotic C-1027 biosynthesis. *J. American Chemical Society* **2003**, *125*, (20), 6062-6063.

113. Christenson, S. D.; Wu, W.; Spies, M. A.; Shen, B.; Toney, M. D., Kinetic analysis of the 4-methylideneimidazole-5-one-containing tyrosine aminomutase in enediyne antitumor antibiotic C-1027 biosynthesis. *Biochemistry* **2003**, *42*, (43), 12708-12718.

114. Christianson, C. V.; Montavon, T. J.; Van Lanen, S. G.; Shen, B.; Bruner, S. D., The structure of L-tyrosine 2,3-aminomutase from the C-1027 enediyne antitumor antibiotic biosynthetic pathway. *Biochemistry* **2007**, *46*, (24), 7205-7214.

115. Langer, B.; Langer, M.; Retey, J., Methylidene-imidazolone (MIO) from histidine and phenylalanine ammonia-lyase. *Advances in Protein Chem.*, *58* **2001**, 58, 175-214.

116. Merkel, D.; Retey, J., Further insight into the mechanism of the irreversible inhibition of histidine ammonia-lyase by L-cysteine and dioxygen. *Helv. Chim. Acta* **2000**, *83*, (6), 1151-1160.

117. Montavon, T. J.; Christianson, C. V.; Festin, G. M.; Shen, B.; Bruner, S. D., Design and characterization of mechanism-based inhibitors for the tyrosine aminomutase SgTAM. *Bioorg. Med. Chem. Lett.* **2008**, *18*, (10), 3099-102.

118. Montavon, T. J.; Christianson, C. V.; Festin, G. M.; Shen, B.; Bruner, S. D., Design and characterization of mechanism-based inhibitors for the tyrosine aminomutase *Sg*TAM. *Bioorg. Medic. Chem. Lett.* **2008**, *18*, (10), 3099-3102.

119. Poppe, L., Methylidene-imidazolone: a novel electrophile for substrate activation. *Curr. Opin. Chem. Biol.* **2001**, *5*, (5), 512-524.

120. Rettig, M.; Sigrist, A.; Rétey, J., Mimicking the reaction of phenylalanine ammonia lyase by a synthetic model. *Helv. Chim. Acta* **2000**, *83*, (9), 2246-2265.

121. Rother, R.; Poppe, L.; Viergutz, S.; Langer, B.; Retey, J., Characterization of the active site of histidine ammonia-lyase from Pseudomonas putida. *Eur. J. Biochemistry* **2001**, *268*, (23), 6011-6019.

122. Rother, D.; Poppe, L.; Viergutz, S.; Langer, B.; Retey, J., Characterization of the active site of histidine ammonia-lyase from *Pseudomonas putida*. *Eur. J. Biochem.* **2001**, *268*, (23), 6011-9.

123. Schroeder, A. C.; Kumaran, S.; Hicks, L. M.; Cahoon, R. E.; Halls, C.; Yu, O.; Jez, J. M., Contributions of conserved serine and tyrosine residues to catalysis, ligand binding, and cofactor processing in the active site of tyrosine ammonia lyase. *Phytochemistry* **2008**, *69*, (7), 1496-1506.

124. Skolaut, A.; Rétey, J. In *3-(2,5-Cyclohexadienyl)-L-alanine (1,4-dihydro-L-phenylalanine). Its synthesis and behavior in the phenylalanine ammonia-lyase reaction*, 2000; Pombo-Villar, E., Molecular Diversity Preservation International, Basel, Switz.: 2000; Meeting Date 1999-2000, 836-846.

125. Toyooka, Y.; Wada, C.; Ohnuki, Y.; Takada, F.; Ohtani, H., Molecular diagnosis of a kindred with novel mutation of methylmalonyl - CoA mutase gene using non-RI SSCP. *Rinsho Byori* **1995**, *43*, (6), 625-9.

126. Viergutz, S.; Retey, J., Kinetic analysis of the reactions catalyzed by histidine and phenylalanine ammonia lyases. *Chem. Biodiversity* **2004**, *1*, (2), 296-302.

127. Yu, M.; Facchini, P. J., Purification, characterization, and immunolocalization of hydroxycinnamoyl-CoA: tyramine *N*-

(hydroxycinnamoyl)transferase from opium poppy. *Planta* **1999**, *209*, (1), 33-44.

128. Walker, K. D.; Floss, H. G., Detection of a phenylalanine aminomutase in cell-free extracts of *Taxus brevifolia* and preliminary characterization of its reaction. *J. Am. Chem. Soc.* **1998**, *120*, (21), 5333-5334.

129. Adam, K.-P.; Croteau, R., Monoterpene Biosynthesis in the Liverwort *Conocephalum conicum*: Demonstration of Sabinene Synthase and Bornyl Diphosphate Synthase. *Phytochemistry* **1998**, *49*, 475-480.

130. Adler, J. H.; Grebenok, R. J., Biosynthesis and distribution of insect-molting hormones in plants - a review. *Lipids* **1995**, *30*, (3), 257-62.

131. Allwood, E. G.; Davies, D. R.; Gerrish, C.; Ellis, B. E.; Bolwell, G. P., Phosphorylation of phenylalanine ammonia-lyase: evidence for a novel protein kinase and identification of the phosphorylated residue. *Febs Lett.* **1999**, *457*, (1), 47-52.

132. Alonso, W. R.; Rajaonarivony, J. I. M.; Gershenzon, J.; Croteau, R., Purification of 4S-limonene synthase, a monoterpene cyclase from the glandular trichomes of peppermint (*Mentha X piperita*) and spearmint (*Mentha spicata*). *J. Biol. Chem.* **1992**, *267*, (11), 7582-7.

133. Atta Ur, R.; Choudhary, M. I., Recent studies on bioactive natural products. *Pure Appl. Chem.* **1999**, *71*, (6), 1079-1081.

134. Bartley, G. E.; Scolnik, P. A.; Giuliano, G., Molecular biology of carotenoid biosynthesis in plants. *Annu. Rev. Plant Physiol. Plant Mol. Biol.* **1994**, *45*, 287-301.

135. Beekwilder, J.; Alvarez-Huerta, M.; Neef, E.; Verstappen, F. W. A.; Bouwmeester, H. J.; Aharoni, A., Functional Characterization of Enzymes Forming Volatile Esters from Strawberry and Banana. *Plant Physiol.* **2004**, *135*, (4), 1865-1878.

136. Besumbes, O.; Sauret-Gueeto, S.; Phillips, M. A.; Imperial, S.; Rodriguez-Concepcion, M.; Boronat, A., Metabolic engineering of isoprenoid biosynthesis in *Arabidopsis* for the production of taxadiene, the first committed precursor of Taxol. *Biotechn. and Bioengin.* **2004**, *88*, (2), 168-175.

137. Bjorklund, J. A.; Leete, E., Biosynthesis of the tropane alkaloids and related compounds. Part 49. Biosynthesis of the benzoyl moiety of cocaine from cinnamic acid via (R)-(+)-3-hydroxy-3-phenylpropanoic acid. *Phytochemistry* **1992**, *31*, (11), 3883-7.

138. Bogdanova, N.; Hell, R., Cysteine synthesis in plants: protein-protein interactions of serine acetyltransferase from Arabidopsis thaliana. *Plant J.* **1997**, *11*, (2), 251-262.

139. Bohlmann, J.; Martin, D.; Oldham, N. J.; Gershenzon, J., Terpenoid Secondary Metabolism in *Arabidopsis thaliana*: cDNA Cloning, Characterization, and Functional Expression of a Myrcene/(E)-.beta.-Ocimene Synthase. *Arch. Biochemistry and Biophysics* **2000**, *375*, (2), 261-269.

140. Bouwmeester, H. J.; Wallaart, T. E.; Janssen, M. H.; van Loo, B.; Jansen, B. J.; Posthumus, M. A.; Schmidt, C. O.; De Kraker, J. W.; Konig, W. A.; Franssen, M. C., Amorpha-4,11-diene synthase catalyses the first probable step in artemisinin biosynthesis. *Phytochemistry* **1999**, *52*, (5), 843-54.

141. Braun, E. L.; Dias, A. P.; Matulnik, T. J.; Grotewold, E., Transcription factors and metabolic engineering: Novel applications for ancient tools. *Recent Advances in Phytochemistry* **2001**, 35, (Regulation of Phytochemicals by Molecular Techniques), 79-109.

142. Broun, P.; Somerville, C., Progress in plant metabolic engineering. *Proc. Nat. Acad. Sci. U.S.A.* **2001**, *98*, (16), 8925-8927.

143. Campbell, M. M.; Sederoff, R. R., Variation in lignin content and composition: mechanisms of control and implications for the genetic improvement of plants. *Plant Physiol.* **1996**, *110*, (1), 3-13.

144. Carlson, T. J. S., Medical ethnobotanical research as a method to identify bioactive plants to treat infectious diseases. *Adv Phytomed* **2002**, 1, (Ethnomedicine and Drug Discovery), 45-53.

145. Caspi, R.; Foerster, H.; Fulcher, C. A.; Hopkinson, R.; Ingraham, J.; Kaipa, P.; Krummenacker, M.; Paley, S.; Pick, J.; Rhee, S. Y.; Tissier, C.; Zhang, P.; Karp, P. D., MetaCyc: a multiorganism database of metabolic pathways and enzymes. *Nucl. Acids Res.* **2006**, *34*, (suppl_1), D511-516.

146. Chang, Y.-J.; Song, S.-H.; Park, S.-H.; Kim, S.-U., Amorpha-4,11-diene synthase of *Artemisia annua*: cDNA isolation and bacterial expression of a terpene synthase involved in artemisinin biosynthesis. *Archives of Biochem. Biophys.* **2000**, *383*, (2), 178-184.

147. Chappell, J., Biochemistry and molecular biology of the isoprenoid biosynthetic pathway in plants. *Ann. Review of Plant Physiol. Plant Mol. Biol.* **1995**, *46*, 521-47.

148. Chen, H.; Tan, R.-X.; Liu, Z.-L.; Zhang, Y.; Yang, L., Antibacterial neoclerodane diterpenoids from *Ajuga lupulina*. *Journal of Natural Products* **1996**, *59*, (7), 668-670.

149. Chen, F.; Duran, A. L.; Blount, J. W.; Sumner, L. W.; Dixon, R. A., Profiling phenolic metabolites in transgenic alfalfa modified in lignin biosynthesis. *Phytochemistry (Elsevier)* **2003**, *64*, (5), 1013-1021.

150. Chesters, N. C. J. E.; O'Hagan, D.; Robins, R. J., The biosynthesis of tropic acid in plants: evidence for the direct rearrangement of 3-phenyllactate to tropate. *J. Chem. Soc., Perkin Trans. 1* **1994**, (9), 1159-62.

151. Chitwood, D. J., Phytochemical based strategies for nematode control. *Annual Review of Phytopathology* **2002**, *40*, 221-249.

152. Contestabile, R.; Jenn, T.; Akhtar, M.; Gani, D.; John, R. A., Reactions of Glutamate 1-Semialdehyde Aminomutase with R- and S-Enantiomers of a Novel, Mechanism-Based Inhibitor, 2,3-Diaminopropyl Sulfate. *Biochemistry* **2000**, *39*, (11), 3091-3096.

153. Cunningham, F. X., Jr., Regulation of carotenoid synthesis and accumulation in plants. *Pure and Appl. Chem.* **2002**, *74*, (8), 1409-1417.

154. D'Auria, J. C., Acyltransferases in plants: a good time to be BAHD. *Curr. Opin. Plant Biol.* **2006**, *9*, (3), 331-340.

155. Darwish Rula, M.; Aburjai, T.; Al-Khalil, S.; Mahafzah, A., Screening of antibiotic resistant inhibitors from local plant materials against two different strains of Staphylococcus aureus. *J. Ethnopharmacol.* **2002**, *79*, (3), 359-364.

156. Das, B.; Rao, S. P., Review on the chemical constituents of medicinal plants and bioactive natural products. Viii. Naturally occurring oxetane-type taxoids. *Indian J. Chem., Sect. B: Org. Chem. Incl. Med. Chem.* **1996**, 35B, (9), 883-893.

157. Delano, J. P.; Dombrowski, J. E.; Ryan, C. A., The Expression of Tomato Prosystemin in Escherichia coli: A Structural Challenge. *Protein Expression Purif.* **1999**, *17*, (1), 74-82.

158. Dixon, R. A.; Steele, C. L., Flavonoids and isoflavonoids - a gold mine for metabolic engineering. *Trends in Plant Sci.* **1999**, *4*, (10), 394-400.

159. Dixon, R. A., Natural products and plant disease resistance. *Nature* **2001**, *411*, (6839), 843-847.

160. Doernenburg, H.; Knoor, D., Strategies for the improvement of secondary metabolite production in plant cell cultures. *Enzyme and Microbial Techn.* **1995,** *17,* (8), 674-84.

161. Dong, X.; Braun, E. L.; Grotewold, E., Functional conservation of plant secondary metabolic enzymes revealed by complementation of *Arabidopsis* flavonoid mutants with maize genes. *Plant Physiol.* **2001,** *127,* (1), 46-57.

162. Durbin, M. L.; McCaig, B.; Clegg, M. T., Molecular evolution of the chalcone synthase multigene family in the morning glory genome. *Plant Mol. Bio.* **2000,** *42,* (1), 79-92.

163. Eichinger, D.; Bacher, A.; Zenk, M. H.; Eisenreich, W., Analysis of metabolic pathways via quantitative prediction of isotope labeling patterns: a retrobiosynthetic 13C NMR study on the monoterpene loganin. *Phytochemistry* **1999,** *51,* (2), 223-236.

164. Eisenreich, W.; Schwarz, M.; Cartayrade, A.; Arigoni, D.; Zenk, M. H.; Bacher, A., The deoxyxylulose phosphate pathway of terpenoid biosynthesis in plants and microorganisms. *Chem. Biol.* **1998,** *5,* (9), R221-R223.

165. Ellis, D. D.; Zeldin, E. L.; Brodhagen, M.; Russin, W. A.; McCown, B. H., Taxol production in nodule cultures of *Taxus. J. Nat. Prod.* **1996,** 59, (3), 246-250.

166. Faldt, J.; Arimura, G.-i.; Gershenzon, J.; Takabayashi, J.; Bohlmann, J., Functional identification of AtTPS03 as (E)-beta-ocimene synthase: a monoterpene synthase catalyzing jasmonate- and wound-induced volatile formation in *Arabidopsis thaliana. Planta* **2003,** *216,* (5), 745-51.

167. Fischbach, R. J.; Zimmer, W.; Schnitzler, J.-P., Isolation and functional analysis of a cDNA encoding a myrcene synthase from holm oak (Quercus ilex L.). *Eur. J. Biochemistry* **2001,** *268,* (21), 5633-5638.

168. Fischer, F. J.; Miller, J. W.; Andrews, M. O. Implantable medical device with anti-neoplastic drug. US 2006030826, Cont -in-part of U S Ser No 410,587, February 09, 2006.

169. Fuchs, S.; Sewenig, S.; Mosandl, A., Monoterpene biosynthesis in *Agathosma crenulata* (Buchu). *Flavour and Fragrance J.* **2001,** *16,* (2), 123-135.

215

170. Gaikwad, N. W.; Madyastha, K. M., Biosynthesis of b-Substituted Furan Skeleton in the Lower Furanoterpenoids: A Model Study. *Biochemical and Biophysical Research Commun.* **2002,** *290,* (1), 589-594.

171. Kluczyk, A.; Szefczyk, B.; Amrhein, N.; Zon, J., (*E*)-cinnamic acid analogues as inhibitors of phenylalanine ammonia-lyase and of anthocyanin biosynthesis. *Polish J. Chem.* **2005,** *79,* (3), 583-592.

CHAPTER 5

An Attempt to Decipher the Mechanism of Phenylalanine Aminomutase (PAM) using ^{15}N and ^{13}C NMR

5.1 INTRODUCTION

The mechanism of the cofactor-less ammonia lyases and aminomutases is believed to involve the nucleophilic attack of the substrate on the 3,5-dihydro-5-methylidene-4H-imidazol-4-one (MIO) of the enzyme.[1-4] Two conflicting theories have been postulated as to whether the phenyl ring or the amine group of the substrate (α-phenylalanine) is the nucleophile and this has been debatable for the past 45 years (Figure 5.1). The most recent contribution to this mechanistic debate is based on the crystal structure of tyrosine aminomutase from *Streptomyces globisporus* (*Sg*TAM)[5,6] published by Christenson and co-workers in which they show 2′, 2′-difluorotyrosine as a pseudo-substrate bound to the enzyme via the amine group of the substrate (Figure 5.2). The evidence in support of the phenyl group of the substrate as the nucleophile is spearheaded by Rétey and co-workers,[7-20] based on theoretical calculations and broad substrate specificities of phenylalanine ammonia lyase (PAL) and histidine ammonia lyase (HAL). The trend of reactivity of the ring substituted phenylalanine analogues appear to depend on the nucleophilicity of the phenyl ring of the substrate.

217
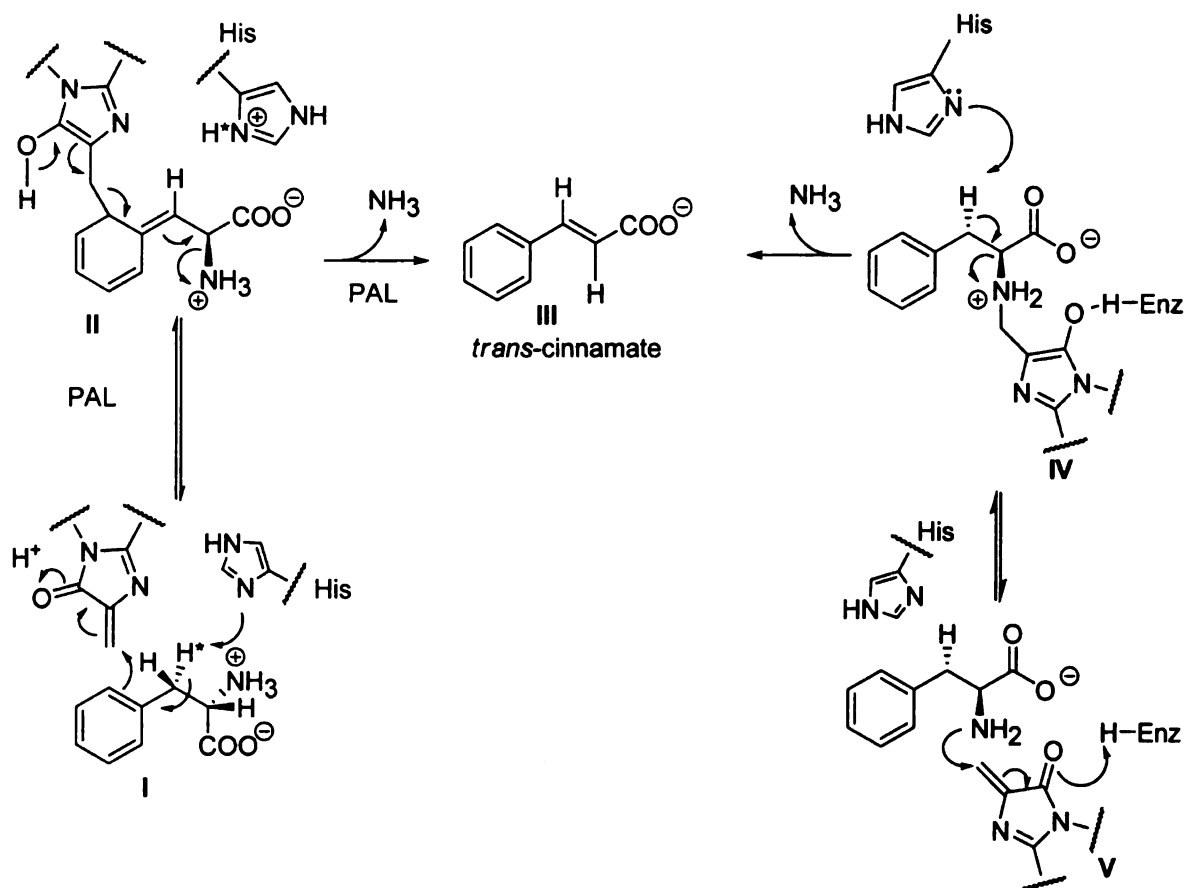
Figure 5.1 The two proposed mechanisms of PALs. On the left shows the aromatic ring of the substrate attacking the MIO and on the right shows the amine group of the substrate attacking the MIO.
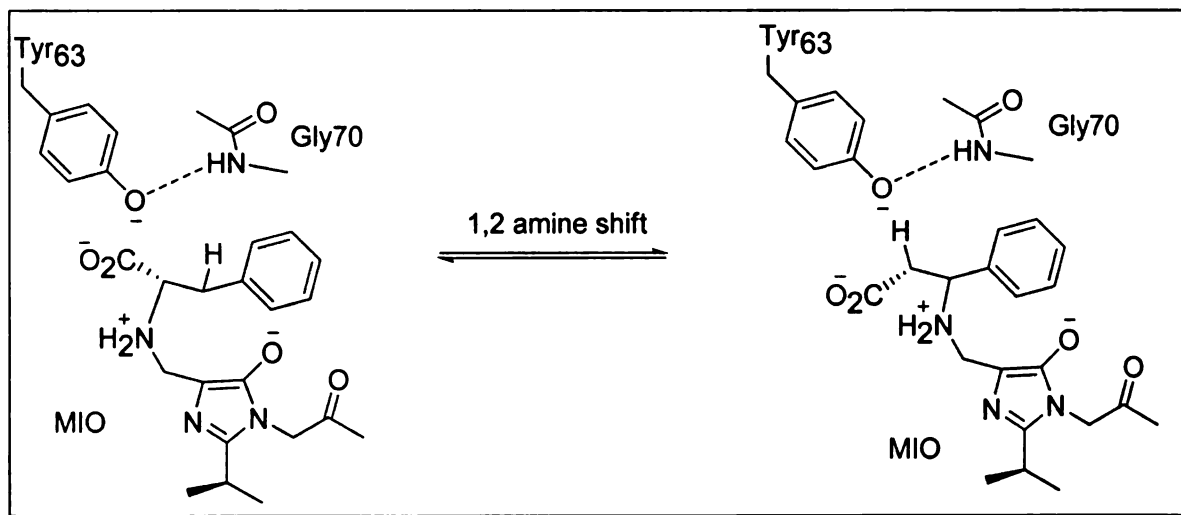
Scheme 5.2 The 1, 2 shift of the amine group is initiated by the binding of the amine of the substrate to the catalytic MIO cofactor. The mechanism is based on the crystal structure of *Sg*TAM.

The theoretical calculations by Rêtey and coworkers are based on the stability of the sigma complex formed between the phenyl ring of the substrate and the MIO (Figure 5.1.II). However, no comparison was made between the energies of this transient state with that of the corresponding complex formed if the amine was the nucleophile, which renders their data inconclusive. In support of their conclusions and why the sigma complex would not collapse through a re-aromatization through the loss of the 2'-proton, Rêtey and coworkers present that the aromatic ring is sandwiched between the MIO and phenylalanine399 (PAL *R. toluroides*) which protects the proton by pi-pi interaction. The proton is positioned perpendicular to the aromatic ring of and is hence 'protected' from de-protonation. The same phenyl399 is believed to stabilize the highly unstable carbocation generated on the *ipso* carbon. However no experiments have been conducted to confirm these theoretical predictions. In this research we intend to

contribute to this unresolved mechanistic question, especially in consideration of the mechanistic and functional differences between PALs and the target enzyme phenylalanine aminomutase (PAM). Whereas the PALs just de-aminates, (Figure 5.3), PAM allows a partial rebounding of the amino group to the β position. The aminomutases allows for the re-bounding of the NH_3, possibly by restricting the loss of the cinnamate intermediates from the active site, due to a narrow channel from the active site.[21-30] Although PAM is functionally similar to SgTAM, it only forms one isomer of the β acid whereas SgTAM has been observed to form both the R and S β isomers at equilibrium, suggesting a slight mechanistic difference.
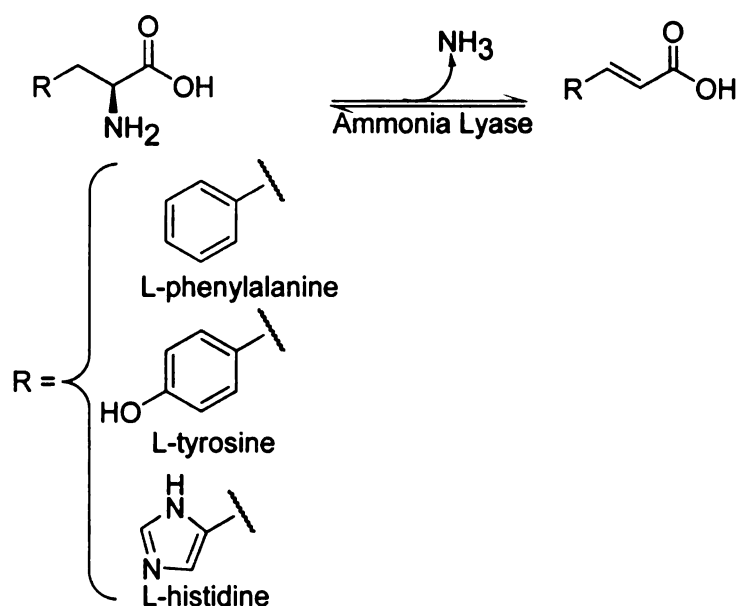
Scheme 5.3 General reaction of ammonia lyases. The aromatic amino acids are non-oxidatively de-aminated to their corresponding α, β-unsaturated acids.

5.1.2 *Structural evidence for the amino group as nucleophile based on PAL*

The first three-dimensional structure of phenylalanine ammonia lyase (PAL) has been determined at 2.1 Å resolution for PAL from *Rhodosporidium toruloides*.[31,32] The enzyme is structurally similar to the mechanistically related histidine ammonia lyase (HAL), with PAL having an additional 160 residues extending from the common fold.[31] The catalysis of PAL is proposed to be governed by the dipole moments of seven α helices oriented towards the active site.[31] The MIO cofactor resides atop the positive poles of three helices, to putatively increase its electrophilicity.[31] The helix dipoles appear to be fully compatible with a model of phenylalanine docked in the active site of PAL in which the amino group of substrate is bound to methylidene group of MIO as a cationic ammonium. There are 12 highly conserved residues near the *N*- termini of helices whose functions are; substrate recognition, MIO activation, product release,[18] proton donation, and/or polarizing the electrons in the phenyl ring of substrate for increasing the acidity of the protons at C3. The dipole near the C-terminus of one helix is proposed to increase the basicity of a histidine residue in the active site.[33-35] The imidazolone is positioned to act as a general base that abstracts the pro-*S* hydrogen from C3 of the substrate. A similar mechanism and structure is proposed for HAL.[31] Thus, the presence of the helix dipoles appears incompatible with a proposed mechanism that proceeds through a carbocation intermediate.

5.1.3 *Use of NMR in mechanistic Investigation*

Nuclear Magnet Resonance (NMR) can be used to qualitatively and quantitatively identify compounds. The major challenge is its relatively low sensitivity which may be improved by use of large amounts of substrates and/or enzyme. In enzymatic assays further complications may arise from the low solubility of some proteins. Even more challenging is the study of the mechanism based on analyzing the intermediates which usually have a short lived half-life. One strategy is to trap the intermediate by using a mutant of the enzyme which will not allow the reaction to go to completion. For sufficiently slow reactions if the enzyme can be sufficiently concentrated then the transition states can be detected using NMR spectroscopy. Sensitivity can be further increased by either isotopically labeling the amino acid residue which binds or react with the substrate or by utilizing a labeled substrate. In this experiment we make use of universally labeled α-phenylalanine ($^{13}C_9$ and ^{15}N-α-phenylalanine), to enhance the signal-to-noise ratio. The change in the chemical shift of the ^{13}C and ^{15}N will be monitored over time and will be used to establish the nucleophile. If the amine is the nucleophile it will covalently bond to the MIO and cause a relatively high ^{15}N chemical shift. The chemical shift of the ^{15}N of the amine is expected to shift up field since the MIO is electron withdrawing. The aromatic carbons which are three bonds away from the N there are not expected to shift significantly, although the C1, C2 and C3 may change considerably. The binding of the amine to the MIO will result in an E1cb elimination of the pro-(*S*)-hydrogen and the amine as an NH_2-MIO-Enz complex (Figure 5.4.III). An NH_3-MIO-Enz complex is

then formed by protonation of the amine (Figure 5.4.IV) by an acidic tyrosine. A 1, 4 Michael addition would result in the NH_2-MIO-Enz complex (V) binding to the C3 position of α, β-unsaturated acid. The NH_2-MIO bond then expected to break to form the β acid and reconstituting the enzyme (Figure 5.4.VI). Intermediate IV is the cinnamic acid which is expected to have a much longer half life and can be isolated.
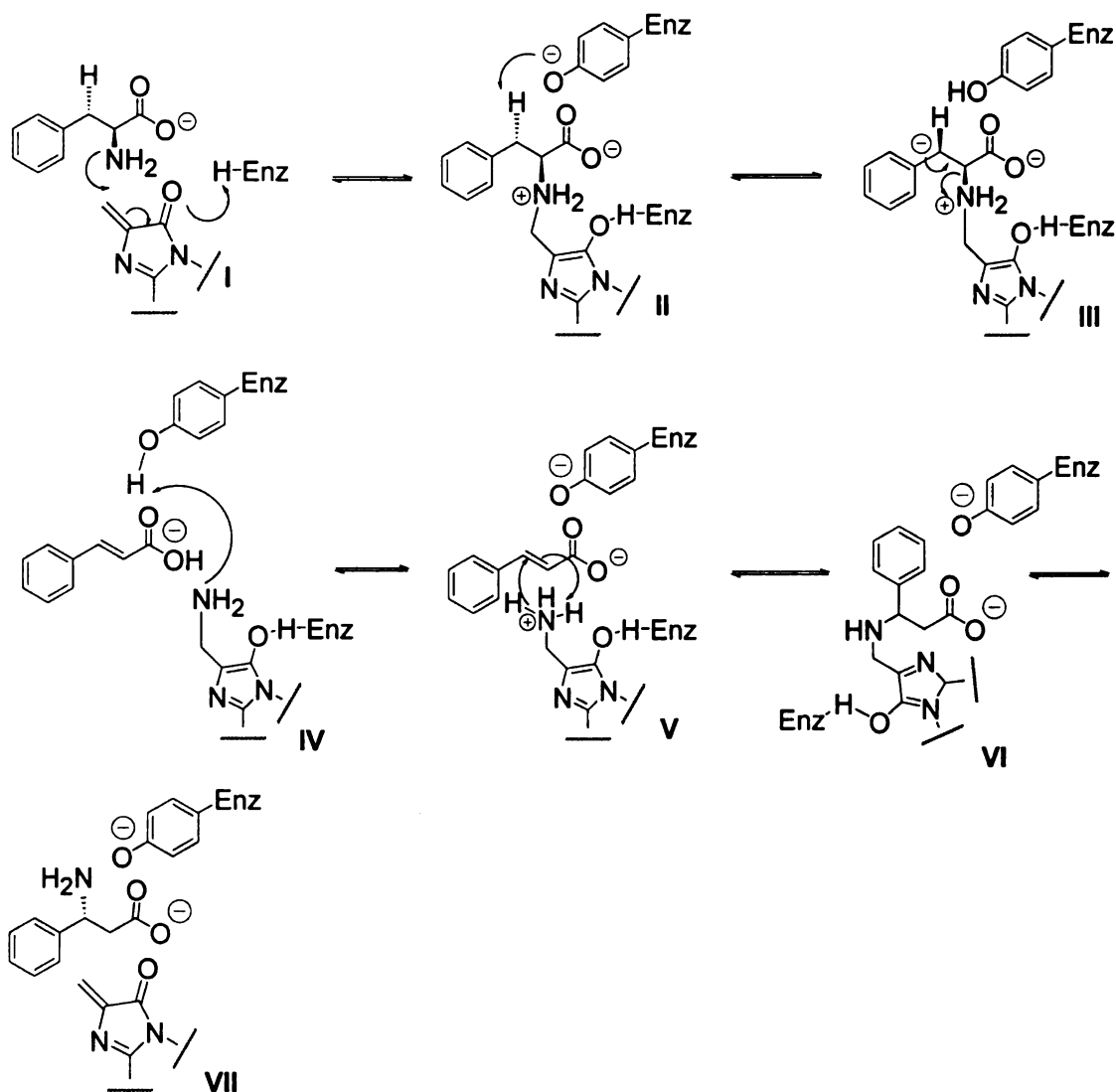
Figure 5.4 The expected intermediates of the substrate during the course of the reaction based on the assumption that the amine of the substrate is the nucleophile. The reaction is expected to go through three intermediates II, III, IV, V and VI before the product VII is formed.

The change in the chemical shift if the phenyl group of the substrate is a nucleophile will be a general downward shift of the aromatic carbons. The *ipso* carbon (figure 5.4.II) will be a signature transient carbocation with an expected chemical shift above 200 pm, however it is expected to be too short lived to be detected on the NMR time scale.
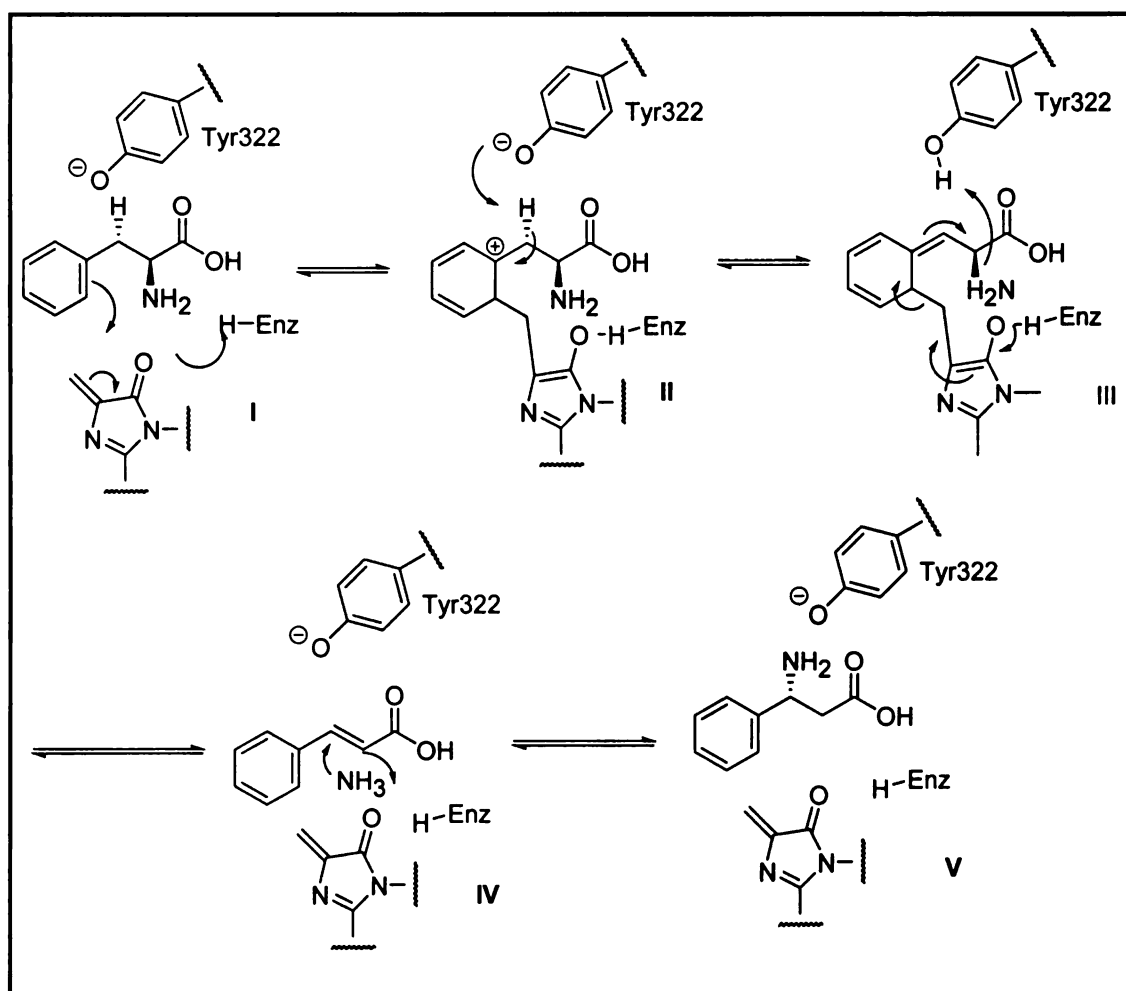
Scheme 5.5 The schematic reaction mechanism proposed if the aromatic ring of the substrate is the nucleophile. The *ipso* carbocation (II) is expected to be very short lived, although its detection will provide valuable information. The phenyl ring attacks the MIO to form the complex II. The tyrosine residue de-protonates the β-H to form intermediate III. The free amine picks up the proton from the tyrosine to form IV which is followed by the re-aromatization of the substrate and the elimination of free NH₃, which re-bounds to the C3 position to form the product.

225

5.2 RESULTS AND DISCUSSION

5.2.1 RESULTS

5.2.1.1 ^{13}C NMR spectrum of the substrate

In order to examine whether the aromatic ring or amine is the nucleophile, the steady state turnover of $[^{13}C_9, {}^{15}N]$-α-phenylalanine by PAM was analyzed. The ^{13}C NMR of the substrate was collected prior to the addition of a catalytic amount of PAM (Figure 5.6A). The only feature of the spectrum is that of $C_9H_{11}NO_2$, with resonance at 41 ppm (m, PhCH$_2$C(NH$_2$)COOH), 57 ppm (dd, PhCH$_2$$C$H(NH$_2$)COOH), 126 ppm (m, aromatic), 183 ppm (d, C(NH$_2$)COOH), 138 ppm (m, aromatic) (Figures 5.6B, C and D respectively).

.
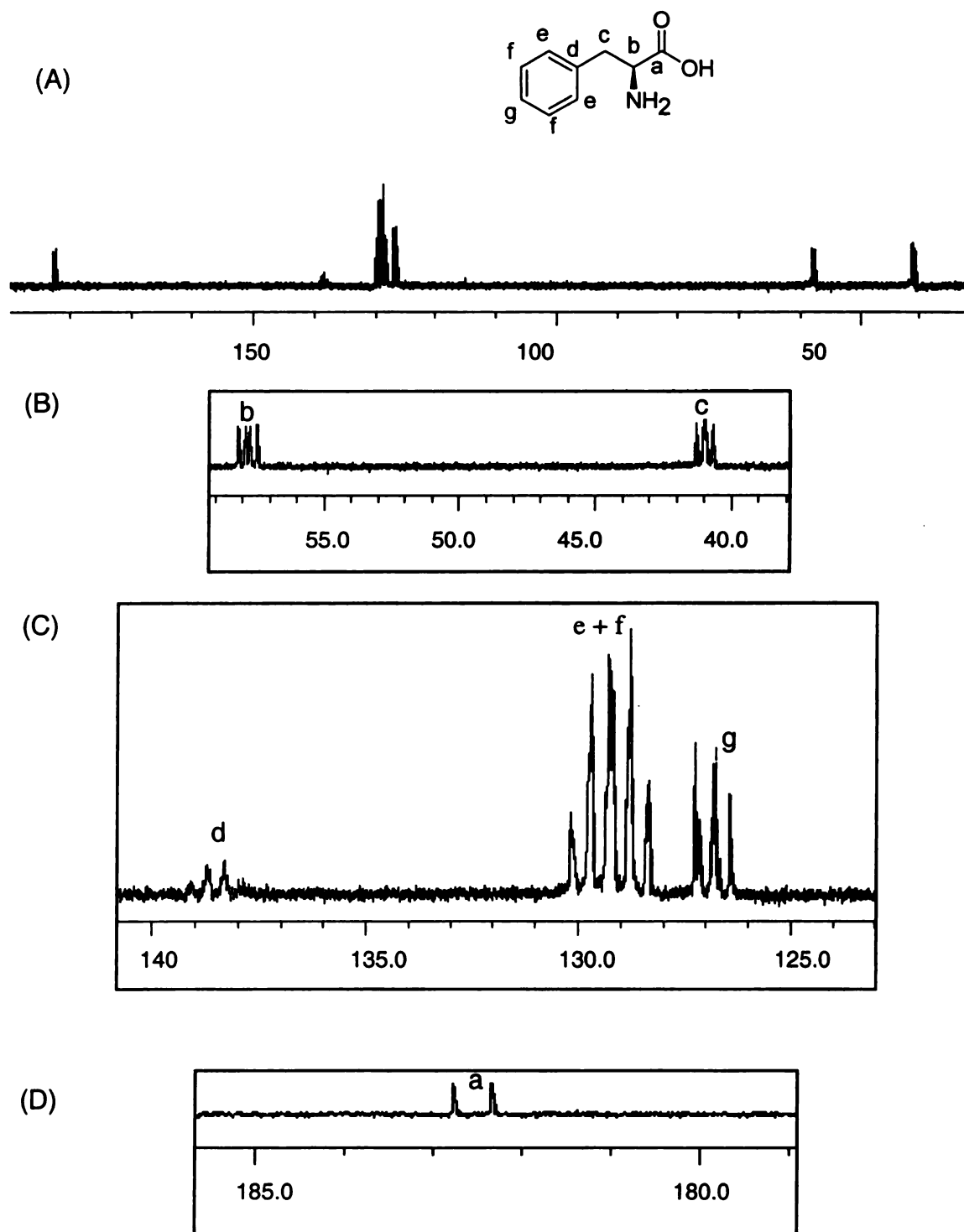
Figure 5.6 ^{13}C-NMR of the uniformly ^{13}C labeled substrate (A), expanded aliphatic region (B), expanded aromatic region (C) and the carbonyl region (D), showing the C-C and/or C-N coupling.

227

5.2.1.2 *Kinetic array of the PAM reaction monitored by NMR*

The reaction was monitored by ^{13}C NMR for a total period of 17 hrs with spectrum acquisition every 30 min. The total acquisition was 6 min and a delay time of 24 min. Altogether 33 spectra were collected. Selected spectra are shown in figure 5.7 for the aliphatic region. The product started showing after 30 min of incubation and is persistent throughout the time of the reaction. New peaks appear at 41, 51 (aliphatic region), 135, 142 (aromatic region) and 178 for the carbonyl. The aromatic peaks do not integrate with the aliphatic region suggesting the presence of three compounds; α and β phenylalanine and cinnamic acid which were confirmed by comparing with authentic standards.
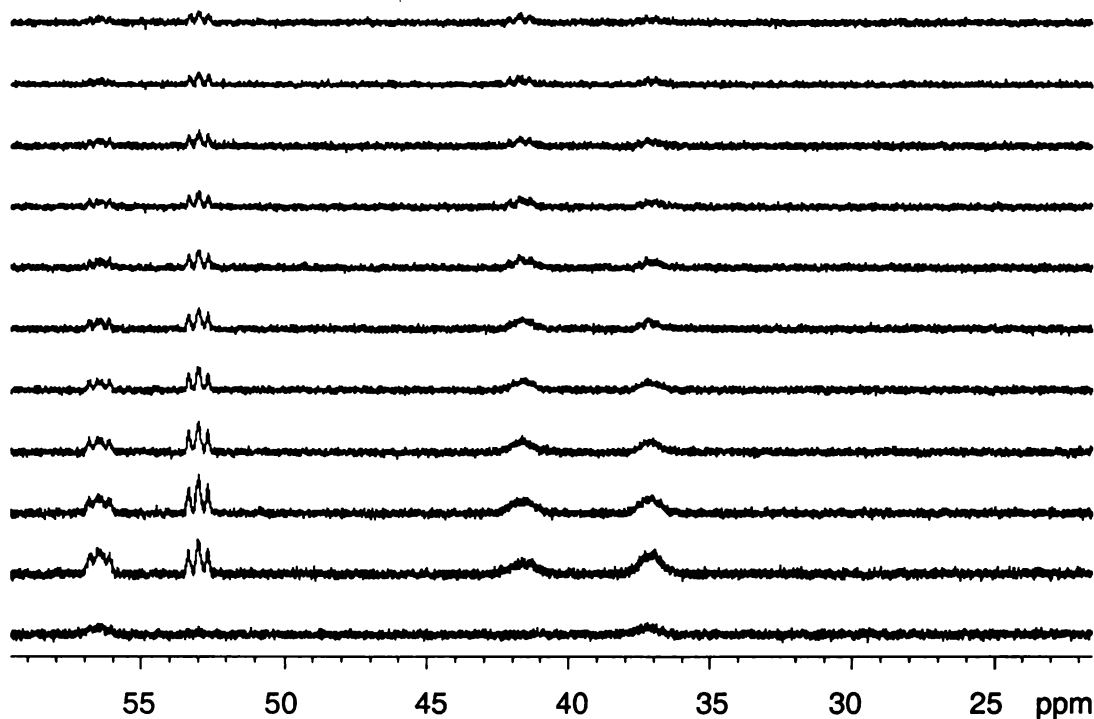
Figure 5.7 Array of ^{13}C NMR spectra for the PAM reaction with isotopically enriched L-α-phenylalanine. The lowest spectrum was acquired before adding the enzyme. One of every 3 scans is shown out of a total of 33 scans.

5.2.1.3 *Identification of the products of the PAM reaction by* ^{13}*C NMR*

PAM (5 mg, 0.13 mM) was added to the solution of universally labeled α-phenylalanine. After the first 30 min new signals were observed at chemical shifts of 43 ppm (triplet, PhCH₂(NH₂)*C*H₂COOH), 51 ppm (Ph*C*H₂(NH₂), 122 ppm (triplet, alkenic), 128-130 (m, aromatic), 135 ppm (q, aromatic), 137 ppm (aromatic), 140 ppm (multiplet, aromatic) 142 ppm (aromatic), 178 (d, C=O), 181 ppm (d, C=O), and 182 (d, C=O) (Figure 5.8B). Peaks at 41, 57, 126 and 182 are due to the unreacted α-phenylalanine (Figure 5.6). The appearance of new signals is due to the formation of products and/or intermediates. One of the

products was confirmed as β-phenylalanine based on the NMR spectrum of an aunthetic standard (Figure 5.9B) which has matching resonances with the biosynthetic product (Figure 5.9A) at 43 and 51.
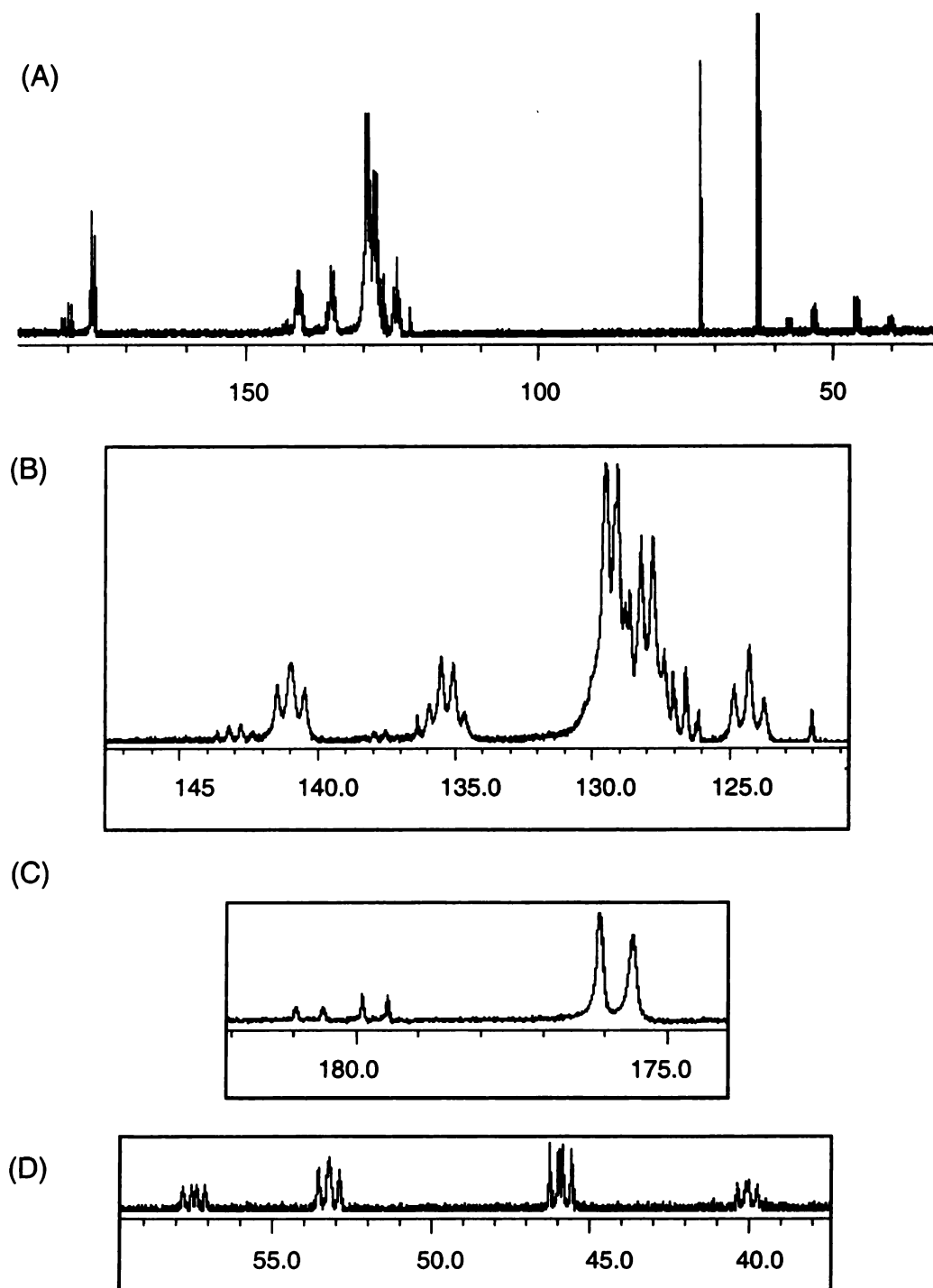
Figure 5.8 ^{13}C NMR Spectra of the product after 16 h incubation with PAM. (A) full spectrum, (B) an expanded aromatic region, (C) and expanded carbonyl region and (D) an expanded aliphatic region.

(A)

150   100   50

(B)

150.0   100.0   50.0
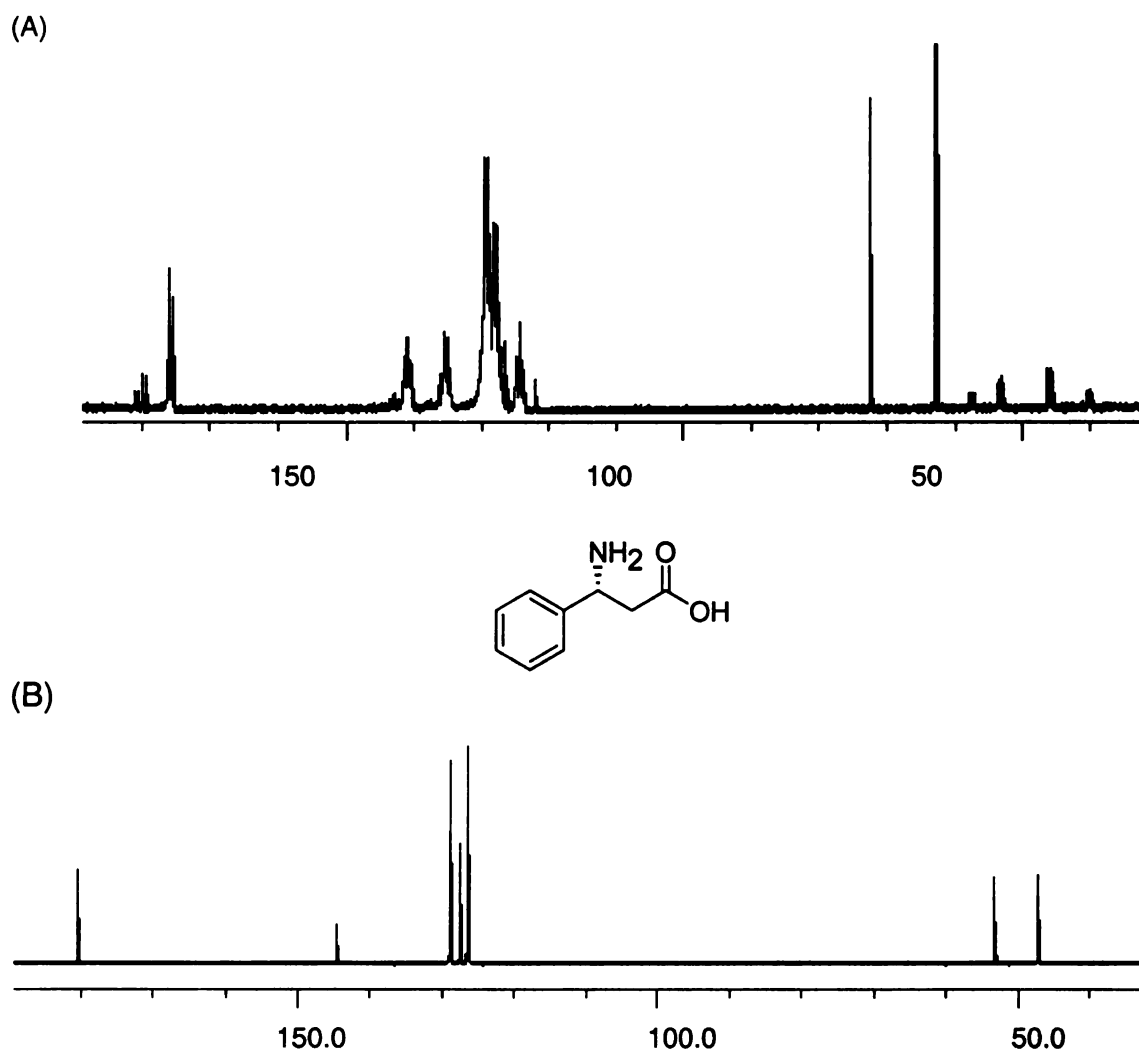
Figure 5.9 Comparison of the ^{13}C NMR spectrum of the biosynthetically made product (A) versus the authentic β-phenylalanine (B).

5.2.1.4 Identification of intermediates

The PAM reaction (overnight) product was treated with 1 N HCl to precipitate the protein and separate enzyme bound and free products and intermediates. The residue was filtered through a cotton pad. The pH was re-adjusted to 8.0 and the solution assayed with ^{13}C NMR spectroscopy in 10%

D$_2$O (Figure 5.10). The work-up product (Figure 5.10B) had no evidence of the α

and β-phenylalanine (Figure 5.10A).
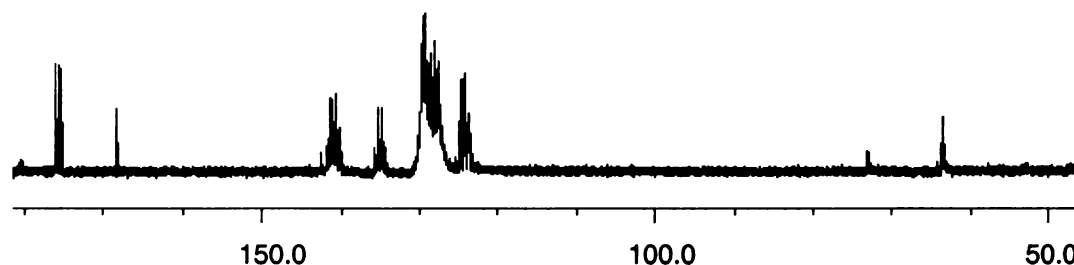
Figure 5.10 ^{13}C NMR of the PAM reaction product after work-up by precipitating the enzyme. No α- and β-phenylalanine peaks are exhibited (c.f Figure 5.9A).

The work-up product was identified as *trans*-cinnamic acid and not the *cis*-isomer as shown below (Figure 5.11) as confirmed by the spectra of authentic *trans*-cinnamic acid (Figure 5.11C).
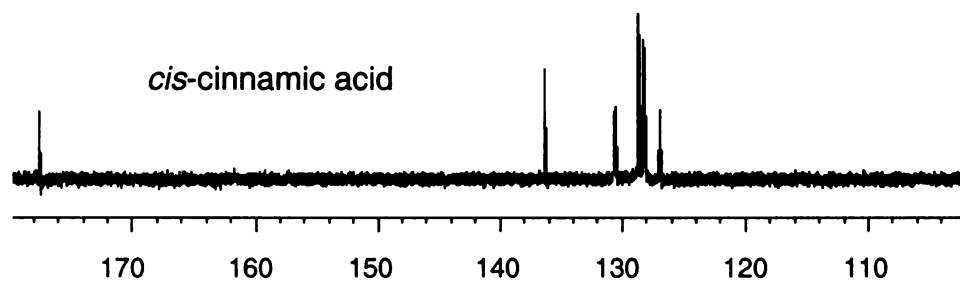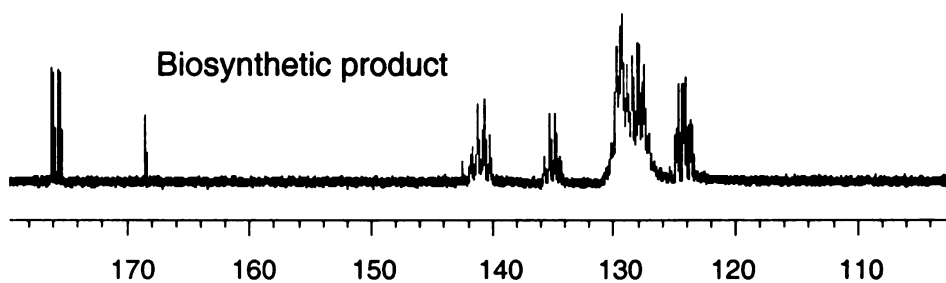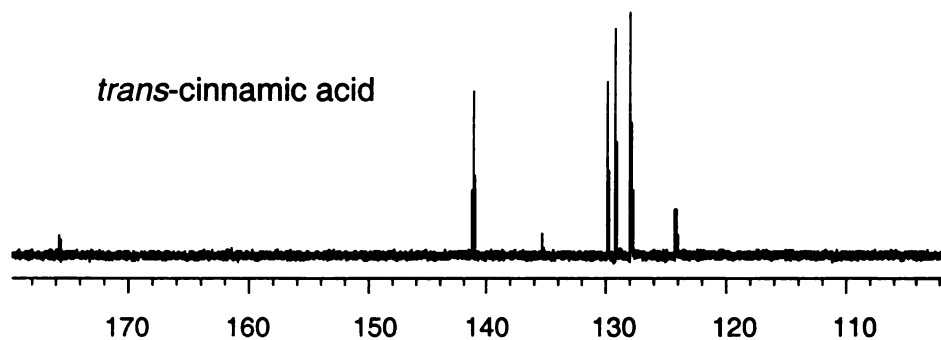
Figure 5.11 ^{13}C NMR for *cis*-cinnamic acid (A), biosynthetically synthesized product (B) and *trans*-cinnamic acid (C). The chemical shifts of the biosynthesis product corresponds to the authentic *trans*-cinnamic acid.

5.2.1.6 ^{15}N MNR SPECTRA

The ^{15}N NMR spectrum for the pure substrate without enzyme has a single resonance at 34 ppm (Figure 5.12A). Within 15 minutes of adding enzyme (0.13 mM) to substrate four new peaks appeared (Figure 5.12B), at -10, 11, 36 and 80 ppm. After an hour only three peaks (11, 36 and 42 ppm) persist and two of them are visible throughout the 16 hour incubation period (Figure 5.13). The peak 80 ppm is characteristic of a nitrogen bound to an electron withdrawing group such as an aromatic system (an N in aniline resonate at 60-70 ppm). Although the intensity of the peak at 42 ppm remains constant throughout the course of the reaction, there is an observed 'negative NOE' like feature on the 36 ppm peak which seems to decrease as the 11 ppm peak increases. The 'NOE' like behavior could be caused by the long longitudinal and transverse relaxation times of the ^{15}N nuclear (between 60 and 120 s) in small molecules. The relaxation delay was set at 1.2 s in order to analyze enzyme-substrate complex which have a short relaxation time. The frequent pulsing required for the kinetic experiment may also have caused pulsing by greater than 90º thus not allowing the ^{15}N in the substrate to sufficiently relax.

A

B
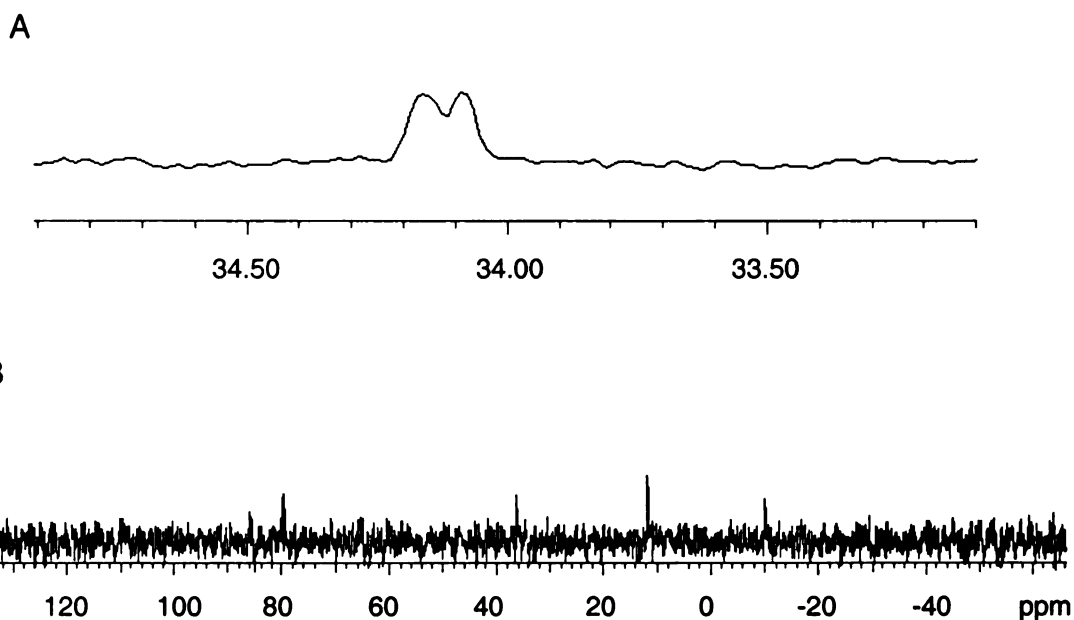
Figure 5.12 ^{15}N NMR for [^{13}C9, ^{15}N]-phenylalanine with PAM. NMR spectrum taken (A) before adding PAM and (B) 15 min after initiating the reaction by mixing enzyme with the substrate in an NMR tube.
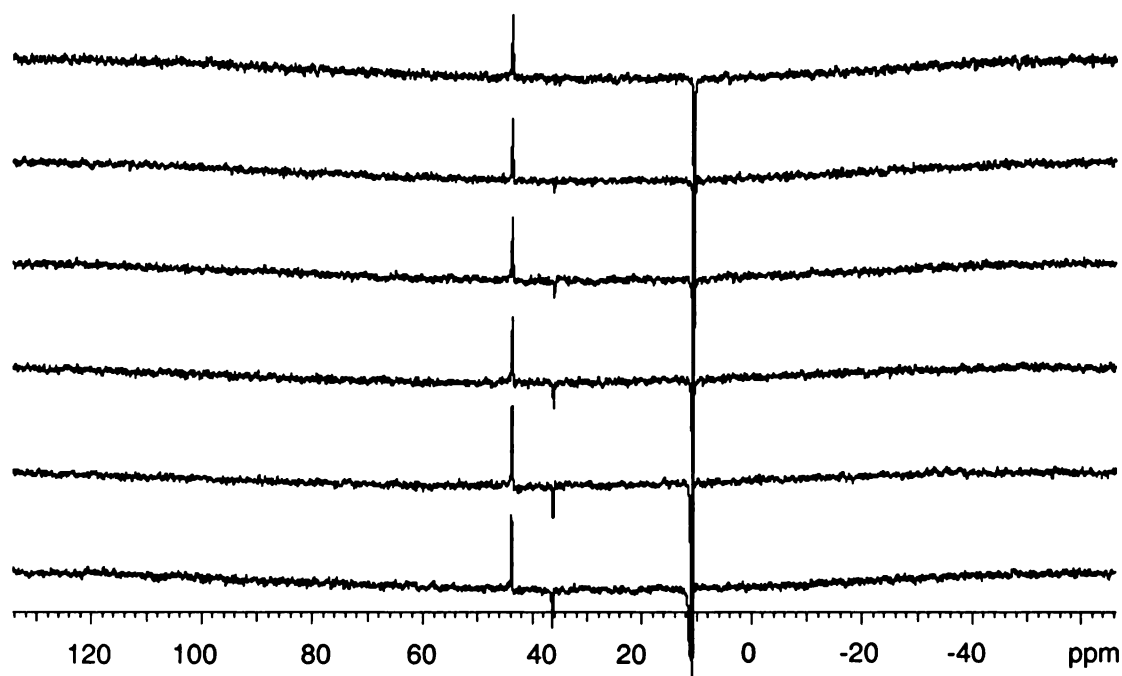
Figure 5.13 The ^{15}N NMR spectrum of isotopically enriched substrate incubated with wild type PAM over 16 hours. Initially 3 peaks are distinguishable at 11 ppm, 36 ppm and 44 ppm.

236

5.2.1.6 *Relative kinetic rates of the substrate, trans-cinnamic acid and β-phenylalanine reaction as measured by* ^{13}C *NMR*

The relative rates of formation of the products were measured by comparing the integration of the peak areas of α and β phenylalanine and *trans-*cinnamic acid over a 17 h period. The ratios of the concentrations are shown in figure 5.14. The α-phenylalanine substrate decreases exponentially, whilst the β-phenylalanine initially increases rapidly before it starts to exponentially decay as it is converted to trans-cinnamic acid. The *trans-*cinnamic profile increases constantly to an equilibrium and is most dominant product.
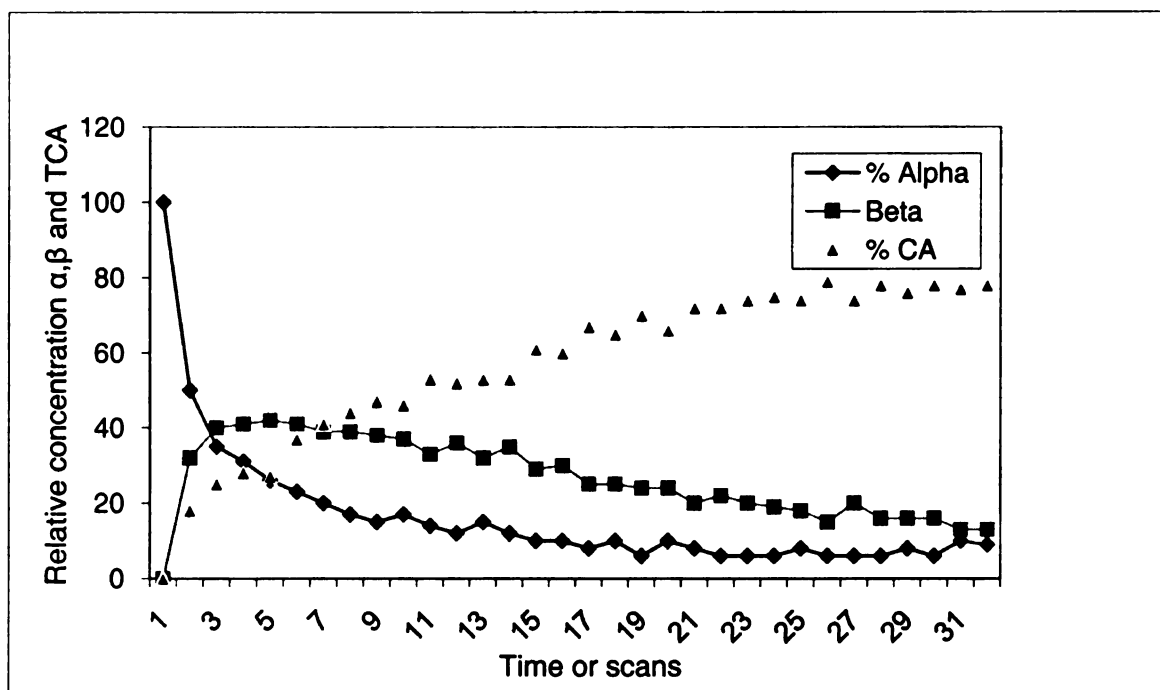
Figure 5.14 The plot of relative rates of formation of the substrate, β-phenylalanine and *trans-*cinnamic acid. The mass balance is referenced to the substrate (5 mM). At equilibrium the α and β phenylalanines have the same (~10 % each).

5.2.2 DISCUSSION

The equilibrium of the PAM reaction is 52% in favor of the product.[36-38]

The stereochemistry of the product has been established and partial mechanism

of the reaction has been proposed.[38] One of the mechanistic voids in the PAM

reaction and similar enzymes like HAL and PAL has been whether the aromatic

ring or the amino group of the substrate is the nucleophile which attacks the MIO.

A study carried out by Christenson[5] on SgTAM, which is mechanistically similar

to PAM, concludes that the amine is the nucleophile. In order to confirm this we

used an NMR technique, in which we monitor the change in the chemical shifts of

the ^{13}C and ^{15}N nuclei during the course of the reaction. A universally isotopically

labeled substrate (U-$^{13}C9$, ^{15}N-phenylalanine) was incubated with PAM (Figure

5.3) and the formation of intermediates was monitored overnight by taking scans

every 30 min at 31 °C. The isotopically enriched substrate presents challenges in

that the chemical shifts around the aromatic region are not clearly resolved. The

detection of intermediates required that they be in sufficient quantities to be

detected by NMR spectroscopy. Although the use of isotopically enriched

substrate gives distinct coupling pattern the disadvantage is the reduced signal to

noise ratio which makes the procedure less sensitive. The data presented in this

report seek to address the mechanistic questions of the PAM reaction as a

complimentary technique to crystal structure studies.

In PAL release of NH_3 is faster than release of cinnamate, whereas in

HAL, the release of NH_3 is slowest.[9,19,39] The mechanism involving the aromatic

238

ring as the nucleophile is doubtful considering the structure of PAL which Calabrese and co-workers proposed based on its crystal structure.[31] If six positively charged helices are pointing towards the aromatic ring of the substrate, it makes the phenyl ring a poor nucleophile. Furthermore creation of an ipso positive charge on the ring will be destabilizing and thermodynamically unfavorable because of the expected charge to charge repulsion.

^{15}N- NMR studies of the reaction of PAM with ^{15}N labeled phenylalanine demonstrated that the intermediates involve two species bearing ^{15}N, intimating that the amine could be the nucleophile (Figure 5.13). The ^{15}N chemical shift changes from 34 ppm in the free state to 36 ppm after 15 minutes of the reaction, other resonances are observed at -11, 10 and 80 ppm. The peak at 80 ppm signifies that the N is bound to an electron withdrawing group most likely an aromatic group, which in this case could be the MIO. The 80 ppm and -10 ppm peaks disappear after 30 minutes, as another peak at 44 ppm emerges Figure 5.13B, lower spectrum). After 2 hours, only three peaks are visible at 44, 36 and 11 ppm. The 36 ppm peak gradually diminishes in size over a period of 12 hours, a phenomena which is not clear, although it could arguably be due to nuclear overhauser effect (NOE). The signal at 36 ppm is the unused substrate, the one at 44 ppm is the β-product and the one at 11 ppm is likely to be NH_3. Based on this data and the information from the literature[5,31] we can conclude that the amine is the nucleophile although more evidence is required to confirm the identity of some of the compounds or intermediates formed during the reaction.

^{13}C NMR Spectra

239

The ^{13}C NMR collected in this work was not very useful in identifying the intermediates and transition states as originally designed. However the results were useful in confirming the product of the PAM reaction as β-phenylalanine and *trans*-cinnamic acid (Figure 5.11). At equilibrium (17 h) the α and β-phenylalanine were at 20% of the total mix with the *trans*-cinnamic acid making up 80% of the mixture. Perhaps the use of mono-labeled substrate will assist in increasing the sensitivity of the method by eliminating the carbon-carbon coupling. Sensitivity could also be enhanced by using at least 3 mM of enzyme.

In summary the NMR studies and other studies reported elsewhere in this report [40-43] demonstrate that PAM is a multifunctional enzyme that can participate in the following types of reactions; (1) reversible isomerization of α and β phenylalanine; (2) synthesis of cinnamic acids from either α or β phenylalanine; (3) synthesis of α and β phenylalanine from cinnamic acid and (4) *trans*-amination reaction (Figure 5.15).
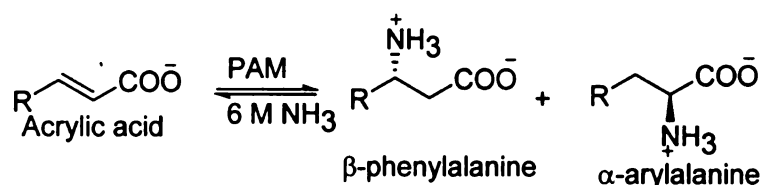

Figure 5.15 The role of PAM as an aminating enzyme. The α- and β-amino acids are formed from their corresponding cinnamates.
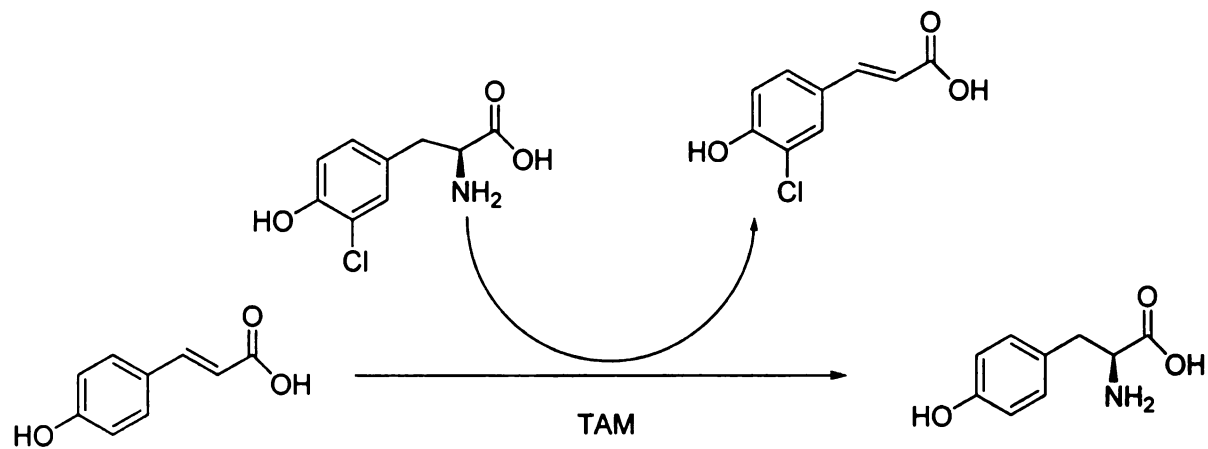
Figure 5.16 The potential function of PAM as a transaminase based on the functionality of TAM a mechanistically similar enzyme.

241

5.4 CONCLUSIONS AND RECOMMENDATIONS

The low enzyme concentration (only 0.13 mM) made it impossible to generate enough intermediate species for detection by ^{13}C NMR. The signal shifts (46 ppm) observed for ^{15}N strongly suggest the involvement of the amine of the substrate in the reaction. However, this conclusion is based on elimination rather than on direct evidence, since the ^{13}C chemical shifts for the transient states were below the detection limit. The formation of *trans*-cinnamic acid is very significant and it constitutes 80 % of the product mix at equilibrium as confirmed by both NMR and GC-MS analysis. The large pool of *trans*-cinnamic acid at equilibrium makes PAM a multifunctional enzyme which acts both as an ammonia lyase and aminomutase. This role makes PAM a versatile enzyme compared to ammonia lyases which only participate in non-oxidative elimination of ammonia from aromatic amino acids. Our results were confirmed by the Janssen group which published their work during the course of our study. They reported on the biosynthesis of both α- and β- amino acids from trans-cinnamates using PAM from *T. chinensis* an enzyme which is 99% identical to our PAM from *T. Canadensis*. Our method provides a method of synthesizing labeled α, β unsaturated phenylpropanoic acids and α- and β- aromatic amino acids capitalizing on the broad specificity of PAM.

Given the low solubility of PAM, we recommend carrying out the NMR experiment is whole cells. The major advantage of whole cell NMR is that no protein purification is required and the enzyme is in much higher concentration

and more substrate can be used. The disadvantages are the possible interferences from other cell components.

and more substrate can be used. The disadvantages are the possible interferences from other cell components.

5.3 MATERIALS AND METHODS

5.3.1 Materials

The ^{15}N and ^{13}C labeled substrate (U-$^{13}C_9$, 97-99%; ^{15}N 97-99% phenylalanine) was purchased from Cambridge Isotope Laboratories, Inc (Andover, MA, USA). All other reagents were obtained from Sigma-Aldrich and used without further purification.

5.3.2.1 *Enzyme purification*

Phenylalanine aminomutase (PAM) was purified to 95% homogeneity as previously described. The protein concentration was calculated based on the Bradford assay and the absorbance was measured on a DU 64 Coultier Beckmann Ultraviolet/visible spectrophotometer at a wavelength of 595 and the standard was constructed with a linear regression of $R^2 = 0.99$. The purified PAM was concentrated and buffer exchanged (50 mM, Phosphate, 300 mM NaCl and 250 mM Imidazole for 50 mM Phosphate, 5 % glycerol) by repeated ultra filtration over an Amicon 50 kDa cut off membrane.

5.3.2 *NMR*

NMR spectra were recorded with a Varian 500 MHz spectrometer in 5 mm NMR tubes at 30 °C. All ^{13}C and ^{15}N NMR experiments were performed in 50 mM Tris- or Phosphate buffer pH 8.0 with 10% D_2O for NMR signal lock. The ^{13}C NMR spectra were collected using the 500 MHz NMR spectrometer operating at frequency of 125.67 MHz with proton decoupling at 499.74 MHz. Spectra were

collected over a width of 33.9 kHz with 33-1024 transients. The pulse routine used included a 1.5 s delay and a signal acquisition time of 1s. 90° pulses were used. The spectral width was 33.3 kHz and all spectra were acquired with 88 000 data points. ^{13}C spectra were processed using 1 Hz line-broadening. All chemical shifts (δ) of ^{13}C were referenced against tetramethylsilane (δ =0) or CDCl$_3$ (77 ppm).

All ^{15}N-NMR experiments were performed in 50 mM Tris-HCl buffer pH 8.0 or 50 mM Phosphate buffer, pH 8.0 with 10% (v/v) D$_2$O for NMR signal lock. The Varian UnityPlus 500 operated at a frequency of 50.64 Hz for the ^{15}N nuclei. Inverse gated ^{1}H decoupling was applied only during signal acquisition. Spectral data were collected with a width of 10.0 kHz. All ^{15}N spectra were collected with 32-1024 transients with a 1 s pulse delay with signal acquisition times of 0.64 s. All samples were acquired with 45° and 90° pulses. Exponential multiplication and Fourier transform with 1, 5 or 10 Hz line broadening were utilized for data processing of ^{15}N spectra. All chemical shifts (δ) of ^{15}N were referenced to 110.0ppm for external ^{15}N-labelled formamide, but reported against liquid NH$_3$ (δ = 0 Hz). ^{15}N spectra were collected over a 480 ppm range to assure observation of all N species.

5.3.3 *Preparation of cis-CA crystals*

Approximately 1.5 g of *trans*-CA was dissolved in 96% ethanol and irradiated under ultraviolet-light for overnight. The mixture of *E* (*trans*-isoform) and *Z* (*cis*-isoform) isomers of cinnamic acid was re-dissolved in ethanol and separated on HPLC. Crystals of *cis*-CA were precipitated out of a *cis*-CA solution under vacuum. 1H nuclear magnetic resonance (NMR) was used to authenticate the structure of *cis*-CA and *trans*-CA as previously described.[44-59] Further qualitative assay were confirmed using GC-MS.

5.3.4 *High performance liquid chromatography.*

The high performance liquid chromatography (HPLC) used to purify *cis*-CA consists of Waters 600 controller, 600 pump, with a UV/visible detector. Separation of *cis*-CA from *trans*-cinnamic acid was achieved on a normal phase Astec Chirobiotic™ (25 cm x 4.6 mm, 5 µM). The mobile phase was a mixture of acetonitrile (buffer A) and acetic acid (buffer B). The ratio of buffer A to B was set to 3 : 7 at the initial stage and changed gradually to 4 : 6 by 8 min and finally to 4.5 5.5 by 30 min. The flow rate was set at 1.0 mL/min. The wavelength of UV-light detector was set at 261 nm because of the *cis*-CA absorption peaks at this wavelength. The retention time of authentic *cis*-CA standard on HPLC was determined to be 2.50 ± 0.25 min.

5.6 REFERENCES

1. Espin, J. C.; Varon, R.; Fenoll, L. G.; Gilabert, M. A.; Garcia-Ruiz, P. A.; Tudela, J.; Garcia-Canovas, F., Kinetic characterization of the substrate specificity and mechanism of mushroom tyrosinase. *Eur. J. Biochemistry* **2000**, *267*, (5), 1270-1279.

2. Merkel, D.; Retey, J., Further insight into the mechanism of the irreversible inhibition of histidine ammonia-lyase by L-cysteine and dioxygen. *Helv. Chim. Acta* **2000**, *83*, (6), 1151-1160.

3. Rettig, M.; Sigrist, A.; Rétey, J., Mimicking the reaction of phenylalanine ammonia lyase by a synthetic model. *Helv. Chim. Acta* **2000**, *83*, (9), 2246-2265.

4. Christianson, C. V.; Montavon, T. J.; Van Lanen, S. G.; Shen, B.; Bruner, S. D., The structure of L-tyrosine 2,3-aminomutase from the C-1027 enediyne antitumor antibiotic biosynthetic pathway. *Biochemistry* **2007**, *46*, (24), 7205-7214.

5. Montavon, T. J.; Christianson, C. V.; Festin, G. M.; Shen, B.; Bruner, S. D., Design and characterization of mechanism-based inhibitors for the tyrosine aminomutase SgTAM. *Bioorganic & Medicinal Chem. Lett.* **2008**, *18*, (10), 3099-3102.

6. Gloge, A.; Langer, B.; Poppe, L.; Rétey, J., The behavior of substrate analogs and secondary deuterium isotope effects in the phenylalanine ammonia-lyase reaction. *Arch. Biochem. Biophys.* **1998**, *359*, (1), 1-7.

7. Gloge, A.; Zon, J.; Kovari, A.; Poppe, L.; Retey, J., Phenylalanine ammonia-lyase: The use of its broad substrate specificity for mechanistic investigations and biocatalysis - Synthesis of L-arylalanines. *Chemistry-a Eur. J.* **2000**, *6*, (18), 3386-3390.

8. Katona, A.; Tosa, M. I.; Paizs, C.; Retey, J., Inhibition of histidine ammonia lyase by heteroaryl-alanines and acrylates. *Chemi. & Biodiversity* **2006**, *3*, (5), 502-508.

9. Langer, M.; Reck, G.; Reed, J.; Retey, J., Identification of Serine-143 as the Most Likely Precursor of Dehydroalanine in the Active-Site of Histidine Ammonia-Lyase - a Study of the Overexpressed Enzyme by Site-Directed Mutagenesis. *Biochemistry* **1994**, *33*, (21), 6462-6467.

10. Langer, M.; Pauling, A.; Retey, J., The Role of Dehydroalanine in Catalysis by Histidine Ammonia-Lyase. *Angewandte Chemie-International Edition in Eng.* **1995**, *34*, (13-14), 1464-1465.

11. Langer, B.; Starck, J.; Langer, M.; Retey, J., Formation of the Michaelis complex without involvement of the prosthetic group dehydroalanine of histidine ammonialyase. *Bioorganic & Medicinal Chemistry Letters* **1997**, *7*, (8), 1077-1082.

12. Langer, B.; Langer, M.; Retey, J., Methylidene-imidazolone (MIO) from histidine and phenylalanine ammonia-lyase. *Advances in Protein Chemistry*, *58* **2001**, 175-214.

13. Poppe, L.; Retey, J., [.omega.-(Adenosin-5'-O-yl)alkyl]cobalamins mimicking the posthomolysis intermediate of coenzyme B12-dependent rearrangements: kinetic investigations on methylmalonyl - CoA mutase. *Arch. Biochem. Biophys.* **1995**, *316*, (1), 541-6.

14. Rother, D.; Poppe, L.; Viergutz, S.; Langer, B.; Retey, J., Characterization of the active site of histidine ammonia-lyase from Pseudomonas putida. *Eur J Biochem* **2001**, *268*, (23), 6011-9.

15. Rother, D.; Poppe, L.; Morlock, G.; Viergutz, S.; Retey, J., An active site homology model of phenylalanine ammonia-lyase from Petroselinum crispum. *Eur. J. Biochem.* **2002**, *269*, (12), 3065-3075.

16. Schwede, T. F.; Badeker, M.; Langer, M.; Retey, J.; Schulz, G. E., Homogenization and crystallization of histidine ammonia-lyase by exchange of a surface cysteine residue. *Protein Engineer.* **1999**, *12*, (2), 151-153.

17. Schwede, T. F.; Retey, J.; Schulz, G. E., Crystal structure of histidine ammonia-lyase revealing a novel polypeptide modification as the catalytic electrophile. *Biochemistry* **1999**, *38*, (17), 5355-5361.

18. Viergutz, S.; Retey, J., Kinetic analysis of the reactions catalyzed by histidine and phenylalanine ammonia lyases. *Chem. & Biodiversity* **2004**, *1*, (2), 296-302.

19. Weber, K.; Retey, J., On the nature of the irreversible inhibition of histidine ammonia lyase by cysteine and dioxygen. *Bioorg. Med. Chem.* **1996**, *4*, (7), 1001-1006.

20. Cai, Z.-N.; Yu, Y.-N.; Chen, X.-X.; Yuan, L.-F., High-level expression of phenylalanine ammonia lyase with enzyme activity in *E. coli* by BL21DE3pET28C-rPAL-1-cDNA. *Zhongguo Yaolixue Yu Dulixue Zazhi* **2000**, *14*, (3), 211-215.

21. Chen, F. M. F.; Kuroda, K.; Benoiton, N. L., A simple preparation of symmetrical anhydrides of N-alkyloxycarbonylamino acids. *Synthesis* **1978**, (12), 928-9.

22. Chen, W. M.; Zhang, P. L.; Wu, B.; Zhang, Q. T., *Chin. Chem. Lett* **1991**, *2*, 441.

23. Chen, S. H.; Combs, C. M.; Hill, S. E.; Farina, V.; Doyle, T. W., *Tetrahedron Lett.* **1992**, 7679.

24. Chen, W. Z.; Zhou, J. Y.; Zhang, P. L.; Cheng, F. Q., *Chin. Chem. Lett.* **1993**, *4*, 699.

25. Chen, S.-H.; Farina, V.; Huang, S.; Gao, Q.; Golik, J.; Doyle, T. W., Studies on the photochemistry of taxol. *Tetrahedron* **1994**, *50*, (29), 8633-50.

26. Chen, H. P.; Wu, S. H.; Lin, Y. L.; Chen, C. M.; Tsay, S. S., Cloning, sequencing, heterologous expression, purification, and characterization of adenosylcobalamin-dependent D-ornithine aminomutase from *Clostridium sticklandii. J. biological chemistry* **2001**, *276*, (48), 44744-44750.

27. Chen, Y. F.; Raney, K. D., Cloning and overexpression of phenylalanine ammonia lyase from R. toruloides in E.Coli BL21(DE3). *Faseb J.***2002**, *16*, (5), A905-A905.

28. Chen, F.; Duran, A. L.; Blount, J. W.; Sumner, L. W.; Dixon, R. A., Profiling phenolic metabolites in transgenic alfalfa modified in lignin biosynthesis. *Phytochemistry (Elsevier)* **2003**, *64*, (5), 1013-1021.

29. Dryuchenko, E. A.; Berdyeva, G. T., Comparative Study of Histidine Ammonia Lyase Ec-4.3.1.3 from the Intestine of Pig Ascarids and Pig Liver. *Izvestiya Akademii Nauk Turkmenskoi SSR Seriya Biologicheskikh Nauk* **1976**, (3), 24-27.

30. Calabrese, J. C.; Jordan, D. B.; Boodhoo, A.; Sariaslani, S.; Vannelli, T., Crystal structure of phenylalanine ammonia lyase: Multiple helix dipoles implicated in catalysis. *Biochemistry* **2004**, *43*, (36), 11403-11416.

31. Shi Ru, J.; Jian Dong, C.; Yan, L.; Ai You, S., Production of L-phenylalanine from trans-cinnamic acids by high-level expression of phenylalanine ammonia lyase gene from Rhodosporidium toruloides in *Escherichia coli. Biochem. Eng. J.* **2008**, *42*, (3), 42 (3) 193-197.

32. Rother, R.; Poppe, L.; Viergutz, S.; Langer, B.; Retey, J., Characterization of the active site of histidine ammonia-lyase from Pseudomonas putida. *Eur. J. Biochem.* **2001**, *268*, (23), 6011-6019.

33. Röther, D.; Poppe, L.; Morlock, G.; Viergutz, S.; Rétey, J., An active site homology model of phenylalanine ammonia-lyase from Petroselinum crispum. *Eur. J. Biochem.* **2002,** *269*, (12), 3065-75.

34. Schroeder, A. C.; Kumaran, S.; Hicks, L. M.; Cahoon, R. E.; Halls, C.; Yu, O.; Jez, J. M., Contributions of conserved serine and tyrosine residues to catalysis, ligand binding, and cofactor processing in the active site of tyrosine ammonia lyase. *Phytochemistry* **2008,** *69*, (7), 1496-1506.

35. Klettke, K. L.; Sanyal, S.; Mutatu, W.; Walker, K. D., beta-styryl- and beta-aryl-beta-alanine products of phenylalanine aminomutase catalysis. *J. Am. Chem.Soc.* **2007,** *129*, (22), 6988-+.

36. Mutatu, W.; Klettke, K. L.; Foster, C.; Walker, K. D., Unusual Mechanism for an Aminomutase Rearrangement: Retention of Configuration at the Migration Termini. *Biochemistry* **2007,** *46*, (34), 9785-9794.

37. Burton, D. L.; McGill, W. B., Inductive and Repressive Effects of Carbon and Nitrogen on L-Histidine Ammonia-Lyase Activity in a Black Chernozemic Soil. *Soil Biology & Biochem.* **1991,** *23*, (10), 939-946.

38. Steele, C. L.; Chen, Y.; Dougherty, B. A.; Hofstead, S.; Lam, K. S.; Li, W.; Xing, Z. *Taxus* Phenylalanine Aminomutase and Methods to Improve Taxol Production. Patent: WO 03/066871 A2, February 10, 2003.

39. Steele, C. L.; Chen, Y.; Dougherty, B. A.; Li, W.; Hofstead, S.; Lam, K. S.; Xing, Z.; Chiang, S.-J., Purification, cloning, and functional expression of phenylalanine aminomutase: the first committed step in Taxol side-chain biosynthesis. *Arch. Biochem. Biophys.* **2005,** *438*, (1), 1-10.

40. Steele, C. L.; Chen, Y. J.; Dougherty, B. A.; Li, W. Y.; Hofstead, S.; Lam, K. S.; Xing, Z. H.; Chiang, S. J., Purification, cloning, and functional expression of phenylalanine aminomutase: The first committed step in Taxol side-chain biosynthesis. *Arch. Biochemistry and Biophysics* **2005,** *438*, (1), 1-10.

41. Walker, K. D.; Floss, H. G., Detection of a phenylalanine aminomutase in cell-free extracts of *Taxus brevifolia* and preliminary characterization of its reaction. *J. Am. Chem. Soc.* **1998,** *120*, (21), 5333-5334.

42. Allina, S. M.; Pri-Hadash, A.; Theilmann, D. A.; Ellis, B. E.; Douglas, C. J., 4-Coumarate:coenzyme A ligase in hybrid poplar. Properties of native enzymes, cDNA cloning, and analysis of recombinant enzymes. *Plant Physiology* **1998,** *116*, (2), 743-754.

43. Alunni, S.; Cipiciani, A.; Fioroni, G.; Ottavi, L., Mechanisms of inhibition of phenylalanine ammonia-lyase by phenol inhibitors and phenol/glycine synergistic inhibitors. *Arch. Biochem. Biophysics* **2003**, *412*, (2), 170-175.

44. Bjorklund, J. A.; Leete, E., Biosynthesis of the benzoyl moiety of cocaine from cinnamic acid via *R*-(+)-3-hydroxy-3-phenylpropanoic acid. *Phytochemistry* **1992**, *31*, 3883-3887.

45. Davin, L. B.; Lewis, N. G., An historical perspective on lignan biosynthesis: monolignol, allylphenol and hydroxycinnamic acid coupling and downstream metabolism. *Phytochemistry Reviews* **2004**, *2*, (3), 257-288.

46. Gloge, A.; Zon, J.; Kövári, Á.; Poppe, L.; Rétey, J., Phenylalanine ammonia-lyase: The use of its broad substrate specificity for mechanistic investigations and biocatalysis - synthesis of L-arylalanines. *Chemistry - A Eur. J.* **2000**, *6*, (18), 3386-3390.

47. Graf, E.; Boeddeker, H., The taxus alkaloids. III. The optical activity and configuration of the ?-aminohydrocinnamic acids and their N-methyl derivatives. *Ann* **1958**, *613*, 111-20.

48. Hashimoto, M.; Hatanaka, Y.; Nabeta, K., Novel photoreactive cinnamic acid analogues to elucidate phenylalanine ammonia-lyase. *Bioorg. Med. Chem. Lett.* **2000**, *10*, (21), 2481-2483.

49. Hocking, M. B., Photochemical and thermal isomerizations of *cis*- and *trans*-cinnamic acids, and their photostationary state. *Canadian J. Chem.* **1969**, *47*, (24), 4567-76.

50. MacDonald, M. J.; D'Cunha, G. B., A modern view of phenylalanine ammonia lyase. *Biochemistry and Cell Biology-Biochimie Et Biologie Cellulaire* **2007**, *85*, (3), 273-282.

51. Tan, C. Y. K.; Weaver, D. F., A one-pot synthesis of 3-amino-3-arylpropionic acids. *Tetrahedron* **2002**, *58*, (37), 7449-7461.

52. Wightman, R. H.; Staunton, J.; Battersby, A. R.; Hanson, K. R., Enzyme-mediated reactions. I. Syntheses of deuterium- or tritium-labeled (3S)- and (3R)-phenylalanines. Stereochemical course of the elimination catalyzed by L-phenylalanine ammonia-lyase. *J. Chem. Soc., Perkin Trans. 1* **1972**, (18), 2355-64.

53. Wu, B.; Szymanski, W.; Wietzes, P.; de Wildeman, S.; Poelarends, G. J.; Feringa, B. L.; Janssen, D. B., Enzymatic Synthesis of Enantiopure alpha- and beta-Amino Acids by Phenylalanine Aminomutase-Catalysed Amination of Cinnamic Acid Derivatives. *Chembiochem* **2009**, *10*, (2), 338-344.

54. Xue, Z.; McCluskey, M.; Cantera, K.; Ben-Bassat, A.; Sariaslani, R. S.; Huang, L., Improved production of p-hydroxycinnamic acid from tyrosine using a novel thermostable phenylalanine/tyrosine ammonia lyase enzyme. *Enzyme and Microbial Techn.* **2007**, *42*, 58-64.